The morphology of the cranium and the cervical vertebral column in patients with hypophosphatemic rickets

PhD dissertation

Hans Gjørup

Department of Dentistry
Health
Aarhus University
2014

The morphology of the cranium and the cervical vertebral column in patients with hypophosphatemic rickets

PhD dissertation

Hans Gjørup

Section of Pediatric Dentistry
Department of Dentistry
Health
Aarhus University
2014

Content

Preface

The studies of the present thesis were conducted from February 2009 to June 2013 at the Section of Paediatric Dentistry, Health, Aarhus University and the Section of Oral Health in Rare Diseases, Department of Oral & Maxillofacial Surgery, Aarhus University Hospital, Denmark.

The studies were performed under the guidance of my main supervisor Professor Dorte Haubek, Dr. Odont., PhD, DDS (Section of Pediatric Dentistry; Health, Aarhus University) and the co-supervisor Associate Professor Liselotte Sonnesen, Dr. Odont, PhD, DDS (Department of Orthodontics, Institute of Odontology, Faculty of Health Sciences, University of Copenhagen). During the initial stages of the project period, the main supervisor was Professor Sven Poulsen, Dr. Odont., Lic. Odont., DDS (Section of Pediatric Dentistry; Health, Aarhus University). During this period, Professor Inger Kjær, Dr. Med., Dr. Odont., DDS (Department of Orthodontics, Institute of Odontology, Faculty of Health Sciences, University of Copenhagen) was the co-supervisor in addition to Professor Dorte Haubek and Associate Professor Liselotte Sonnesen.

I have been a part-time PhD student during the entire study period. I was full-time employed at the Department of Oral & Maxillofacial Surgery as the Head of Centre of Oral Health in Rare Diseases, Aarhus University Hospital. The PhD project has been completed by the assistance and guidance from a lot of people.

First, my main supervisor, Professor Dorte Haubek, is sincerely acknowledged for her enthusiastic engagement in the project. Although the issue of the project was not an established part of Dorte`s former research areas, I have experienced Dorte`s great commitment in all processes of the project and Dorte as seriously dedicated to guide and help in all its phases. I have been impressed by Dorte`s abillity to use her general knowledge and experience in research to raise so many serious and relevant questions related to both the methods of the study and to the theme of the research. Dorte taught me how research is a composition of both the major things and the small details and that the researcher has to address all of it with the highest degree of seriousness. I am indeed grateful for Dorte`s guidance in this PhD project and for my collaboration and friendship with Dorte.

Associated Professor Liselotte Sonnesen is very much acknowledged for her willingness to participate as a co-supervisor throughout the whole project period. Liselotte, whom I on beforehand mostly knew as a good orthodontic colleague, has with great eager implemented her research knowledge and experiences in the discussions and the work with my project, and Liselotte has introduced me to the interesting aspects of the important structures just below foramen magnum.

In spite of a lot of duties in Liselotte`s local environment, she never hesitated to send me immediate feedback on manuscripts and questions. I would like to express my thanks.

Professor emeritus Sven Poulsen is gratefully acknowledged for his role as the initial main-supervisor of my PhD project as well as the other important roles Sven has had in relation to my professional life. Early in my carrier at "Center of Oral Health in Rare Diseases", Sven, in the role as my informal mentor, introduced me to the excitement and the great amount of work in collecting and analyzing data and to transform them into a research report. Sven immediately accepted to take part in my PhD project when I asked for that, and Sven did a tremendous work in the preparation of the protocol, the arrangement of the practical procedures, and in the guidance of my writing of the first scientific manuscript. For all the support and guidance I received from Sven, I am so grateful.

Next, I would like to express my sincere gratitude to Professor Inger Kjær, who created the overall idea of the project and was the person who encouraged me to start the PhD project based on the radiographs obtained in the "rickets project" of Odense and Aarhus. With great patience, Inger has introduced me to the results of her own tremendous research and has guided me to use this knowledge in the interpretation of data from the present project. With great commitment, Inger has joined the project to the very last end although she some time ago asked to finalize the formal role as co-supervisor. For all the inspiration, guidance, and help from Inger, I am very grateful.

I would also like to express my gratitude to my chief, John Jensen, PhD, DDS, Head of Department of Maxillofacial Surgery, Aarhus University Hospital, who on behalf of the department and Aarhus University Hospital gave me the opportunity to spend the many hours and days on this project. Not for more than a second, John hesitated when I asked him to initiate as a PhD-student five years ago. Certainly, this has been a privilege. I would like to express my thanks to John and Aarhus University Hospital.

If not for Signe Beck-Nielsen, PhD, MD (Department of Pediatrics, Hospital of Southwest Denmark, Esbjerg), this project had never been. Signe has recruited the rickets patients and initiated the collaboration between "the dentists in Aarhus" and the research group to which she belongs. I am very grateful that Signe did so, and in addition, Signe has been very active in the preparation of the manuscripts of the papers of the thesis. I would like to send a lot of thanks and my best wishes to Signe.

Former research year student, Mette Guldbæk DDS, is acknowledged for her enthusiastic participation in the examination of the rickets patients which took place back in 2007-2008.

List of original papers

The dissertation is based on the following papers which will be referred to in the text by their Roman numerals.

I. Gjørup H, Kjaer I, Sonnesen L, Haubek D, Beck-Nielsen SS, Hintze,H, Poulsen S; 2011. Craniofacial morphology in patients with hypophosphatemic rickets: A cephalometric study focusing on differences between bone of cartilaginous and intramembranous origin. Am J Med Genet A 155A: 2654-2660

II. Gjørup H, Kjaer I, Sonnesen L, Beck-Nielsen SS, Haubek D, 2013. Morphological characteristics of frontal sinus and nasal bone focusing on bone resorption and apposition in hypophosphatemic rickets. J Orthod Craniofac Research 16:246-55

III. Gjørup H, Sonnesen L, Beck-Nielsen SS, Haubek D. 2013. Upper spine morphology in hypophosphatemic rickets and healthy controls: A radiographic study. Eur J Orthod [Epub ahead of print]

IV. Gjørup H, Kjaer I, Beck-Nielsen SS, Poulsen MR, Haubek D, 2014. A radiological study on intra- and extra-cranial calcifications in adults with X-linked hypophosphatemic rickets and associations with other enthesopathies and childhood medical treatment. Orthod Craniofac Research [Submitted]

List of abbreviations

1,25(OH)2D	1,25 dihydroxy vitamin D or calcitriol
25(OH)D	25-hydroxyvitamin D
2D	2-dimensional
ADHR	Autosomal dominant hypophosphatemic rickets
ARHR	Autosomal recessive hypophosphatemic rickets
BMU	Basic multinuclear remodeling unit
C1	Atlas or cervical vertebra no. 1
C1-C5	Cervical vertebrae no. 1-5
C2	Axis or cervical vertebra no. 2
CBCT	Cone-beam computerized tomography
CI III	Class III malocclusion (mesial molar relationship & mandibular overjet)
CLCN5	Cloride chanel 5 gene
CMA	Conventional metrical approach
CMI	Chiari I malformation
CT	Computerized tomography
CVA	Cervical vertebral anomalies
DIFF	Mean-difference
DMP1	Dentine matrix protein 1 gene
EFF	Eliptical Fourier function
ENPP1	Ectonucleotide pyrophosphatase/phosphodiesterase 1 gene
FESA	Finite element scale analysis
FGF23	Fibroblast growth factor 23
FGFR	Fibroblast growth factor receptor
FUS	Fusions of the vertebrae
GA	Gestational age
HHRH	Hypophosphatemic rickets with hypercalcuria
HR	Hypophosphatemic rickets
HYP mice	Murine model of XLHR
MIM	Online Mendelian Inheritance in Man
MRI	Magnetic resonance imaging
NaPi-2a	Renal sodium/phosphate transport protein 2
NaPi-2c	Natrium/inorganic phosphate co-tranporter, type IIc
OI	Osteogenesis imperfecta
OPG	Osteoprotegerin
OSA	Obstructive sleep apnea
PA	Postero-anterior
PAD	Posterior arch deficiencies
PCA	Principal component analysis
PHEX	Phosphate regulating endopeptidase homolog, X-linked, gene
PiT-2	Phosphate transporter, sodium-dependent, 2
PTH	Parathyroid hormon
R	Houston`s coefficient of reliability
RANK	Receptor activator of nuclear factor kB
RANKL	Receptor activator of nuclear factor kB ligand

S-Ca	Serum level of calcium
S-Calcitriol	Serum level of calcitriol
S-CR	Serum level of creatinin
SD	Standard deviation
S-FGF23	Serum level of fibroblast-growth-factor 23
SLS34A3	Sodium/inorganic phosphate co-transporter, type IIc gene
S-PO4	Serum level of phosphate
S-PTH	Serum level of parathormon
ST	Sella turcica
TIO	Tumor induced osteomalacia
TPO4/GFR	S-PO4 - (U-PO4 x S-CR) / U-CR (renal reabsorption of phosphate)
U-Ca	Urinary level of calcium
U-CR	Urinary level of creatinin
U-PO4	Urinary level of phosphate
XLH	X-linked hypophosphatemia (adults)
XLHR	X-linked hypophosphatemic rickets (children)
XLHR	X-linked recessive hypophosphatemic rickets
K	Kappa coefficient

1. Background

1.1. Rickets

1.1.1. Mineral metabolism and vitamin D

Mineral homeostasis and the mineralization of bone are regulated by complicated mechanisms, in which the parathyroid hormone (PTH) and vitamin D play a key role. The regulatory mechanisms of the mineral homeostasis are monitored by the calcium and phosphate levels in the plasma.

PTH is produced in the parathyroid glands and the secretion of PTH is inversely related to the calcium level of the blood. PTH acts directly on the bone cells promoting release of calcium. In the kidneys, PTH increases the reabsorption of calcium, decreases the reabsorption of phosphate, and stimulates the hydroxylation of 25-hydroxyvitamin D (25(OH)D) into the active dihydroxyvitamin D (1,25(OH)2D, i.e., calcitriol). In addition, the PTH-stimulated calcitriol production increases the intestinal reabsorption of both calcium and phosphate (Levine, 2003).

Vitamin D (i.e., vitamin D3: cholcalciferol; vitamin D2: ergocalciferol) is obtained from the diet. In addition, vitamin D3 is synthesized in the skin when exposed to the sun. To become an active agent, vitamin D has to be hydroxylated, initally in the liver and thereafter in the kidneys. In bone, the di-hydroxylated vitamin D (i.e., calcitriol) activates the osteoclastogenesis by induction of the pre-osteoblast`s production of the receptor activator of nuclear factor kB ligand (RANKL), which interacts with the receptor RANK of the monocytic osteoclast-precursors enhancing the formation of the mature bone resorbing osteoclast. Furthermore, calcitriol, in addition to the activation of intestinal absorption of calcium and phosphate, induces an increased renal reabsorption of calcium (Levine, 2003).

1.1.2. Phosphate homeostasis and FGF23

In addition to PTH and vitamin D, the hormone fibroblast growth factor 23 (FGF23) is of importance in the regulation of bone mineralization. FGF23 is a potent phosphaturetic factor, being the principal regulatory hormone of the phosphate homeostasis (Shimada *et al.*, 2004). The hormone targets organs, particularly the kidney, via an fibroblast growth factor receptor (FGFR), whereby the renal phosphate reabsorption is decreased and the final hydroxylation of hydroxy-vitamin D (25(OH)D) into calcitriol (1,25(OH)2D) is down-regulated. The affinity of FGF23 to FGFR depends on the formation of a binding between Klotho and FGF23 into a complex (Kuro-o, 2010). The FGF23 secretion by osteocytes is regulated by mechanisms not fully revealed. The genes *PHEX, DMP1*, and *ENPP1* are suggested to play a modifying role in the FGF23 production (Quarles,

2012a; Quarles, 2012b). Remarkably, FGF23 has the direct effect on bone cells despite of the fact that the gene coding for Klotho (a co-receptor to the FGF-receptor) has not been detected in bone (Kuro-o *et al.*, 1997; Kuro-o, 2010). High levels of FGF23 are associated with hypophosphatemia, phosphaturia and decreased renal formation of calcitriol (Liu *et al.*, 2006a; Martin *et al.*, 2011). Without pathology, the level of serum phosphate (S-PO4) is maintained at the normal level by feedback-mechanisms, which include PTH, FGF23, and vitamin D (Fig. 1). PTH and FGF23 have been suggested to influence each other directly, whereby PTH induces the secretion of FGF23 and FGF23 reduces the secretion of PTH. In addition, the hormones interact indirectly through renal and intestinal phosphate-co-transporters, and 1α-hydroxylase. Both hormones cause a decrease in the activity of the renal phosphate-co-transporters, which leads to a decrease in the renal phosphate-reabsorption. Of the two hormones, only PTH enhances the formation of active vitamin D (calcitriol) by theactivation of the 1α-hydroxylase as opposed to the inhibitory effect by FGF23. The activated vitamin D (calcitriol) stimulates the intestinal reabsorption of phosphate by activation of the intestinal phosphate co-transporters. Thus, the effect of FGF23 is reduced intestinal phosphate absorption, and the effect of PTH is increased phosphate absorption. In addition, the circulating calcitriol have opposite effects on PTH and FGF23 by negative feed-back mechanisms: Calcitriol induces the FGF23 formation in the bone and suppresses the PTH production in the parathyroid glands (Bergwitz & Juppner, 2010; Pettifor & Thandrayen, 2012; Bergwitz & Juppner, 2012).
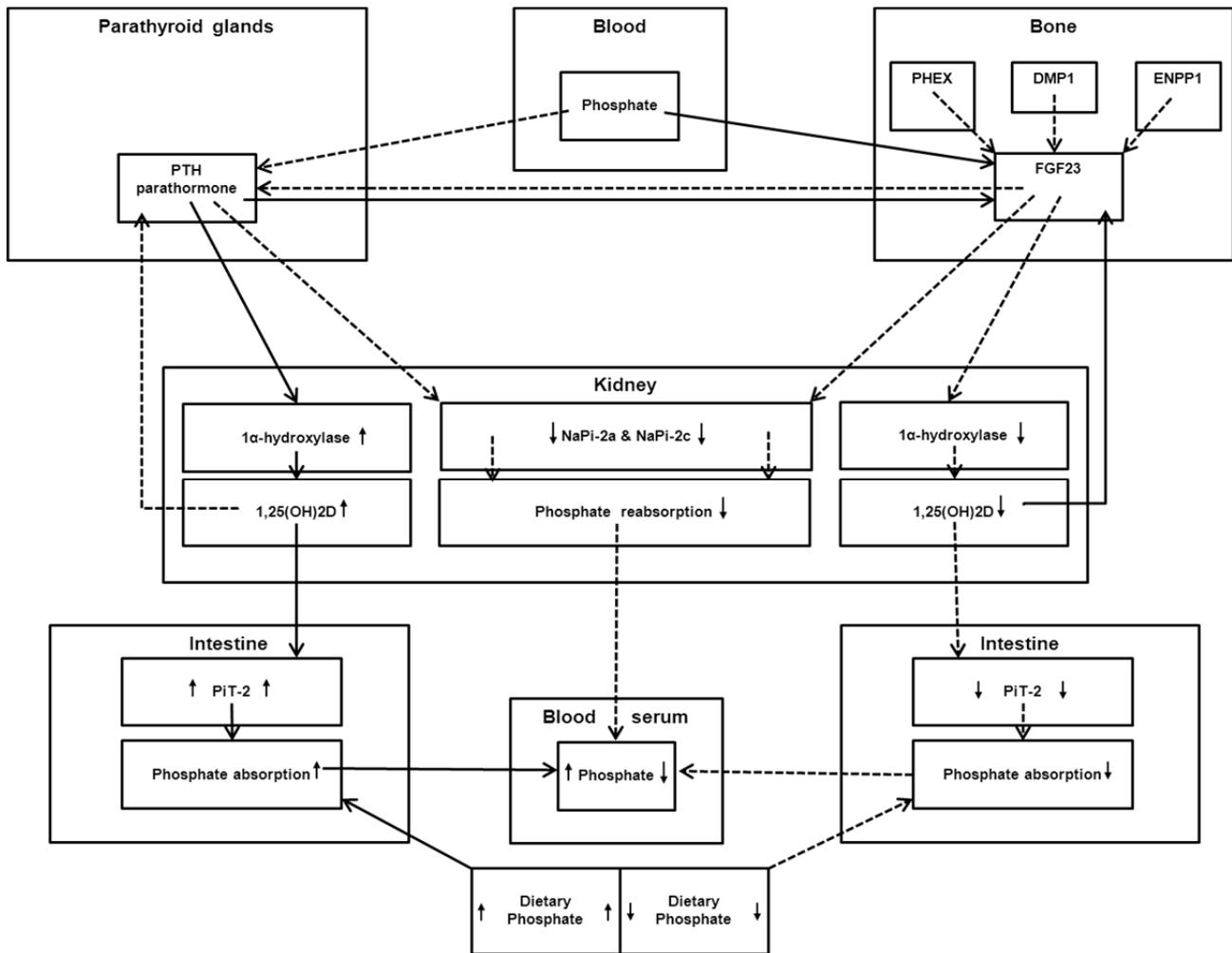
Fig 1. The regulation of phosphate metabolism by PTH and FGF23. A modification of the figures by Bergwitz and Jüppner (Bergwitz & Juppner, 2012) and Baroncelli et al.(Baroncelli et al., 2012).
The broken lines between boxes show pathways with down-regulation and solid lines show pathways with up-regulation.
The small arrows indicate increased (↑) or decreased (↓) level/absorption)
NaPi-2a and NaPi-2c are renal phosphate co-transporters; and PiT-2 are instestinal phosphate co-transporters

1.1.3. Definition and classification

Traditionally, rickets is defined as a disease of children caused by vitamin D deficiency, which results in abnormal calcium and phosphorus metabolism and deficient mineralization of bone with skeletal deformities (Simpson, 2013). The term "rickets" originates from the Old English "wrickken", to twist, but also refers to "rhachitis", the Greek term for "spine" (Hochberg, 2003) . In Danish, the disease is called "engelsk syge". Osteomalacia is defined as a generally impaired mineralization of the bone matrix and includes an increased bone mass opposed to, e.g., osteoporosis (Hochberg, 2003). Rickets refers specifically to changes in the mineralization of the bony growth plates, which

widen and become disorganized and wrecked. Usually, rickets and osteomalacia occur together as long as the growth plates are open, meaning that rickets is a disease of children and adolescents (Rauch, 2003; Hochberg, 2003).

Due to hypertrophy of the chondrocytes and in addition a decreased apoptosis, the growth plate cartilage forms a cup-shaped metaphysis, which results in the characteristic swelling around the joints (e.g., the knees). In addition, a decreased growth rate and bowing of the weight-bearing extremities are characteristics (Hochberg, 2003).

Rickets is closely linked to the vitamin D metabolism, but additional etiological factors have been described, and according to the etiology of the disease, rickets has been classified in: I) nutritional rickets (e.g., vitamin D deficiency), II) absorptive rickets (e.g., malabsorption diseases), III renal rickets (e.g., renal insufficiency), and IV) metabolic rickets (e.g., hypophosphatemic rickets (HR)) (Hochberg, 2003).

Recently, a classification according to pathophysiology has been proposed (Table I): I) vitamin D deficiency rickets (e.g., lack of sun exposure or inadequate D vitamin intake), II) vitamin D synthesis disturbances (e.g., 1-alfa-hydroxylase deficiency), III) calcium deficiency rickets (i.e., inadequate calcium intake), IV) FGF23-associated hypophosphatemic rickets (e.g., X-linked and autosomal dominant hypophosphatemic rickets), V) non-FGF23-associated hypophosphatemic rickets (e.g., X-linked recessive hypophosphatemic rickets). Vitamin D deficiency rickets and calcium deficiency rickets are all acquired rickets types. FGF23-associated HR is divided into hereditary and acquired sub-types. Non-FGF23 HR and vitamin D synthesis disturbances are hereditary types of rickets (Beck-Nielsen, 2012).

	FGF23-associated HR					Non-FGF23-associated HR	
	Hereditary				Acquired	Hereditary	
	Autosomal dominant (ADHR)	X-linked dominant (XLHR)	Autosomal recessive (ARHR1)	Autosomal recessive (ARHR2)	Tumor-induced osteomalacia (TIO)	HR with hypercalcuria (HHRH)	X-linked recessive HR (XLHR)
Gene involved	*FGF23*	*PHEX*	*DMP1*	*ENPP1*	-	*SLC34A3*	*CLCN5*
Function of gene product	Suppresses activation of renal phosphate co-transporters (NaPi-2a and NaPi-2c ↓) and 1α-hydroxylase (calcitriol ↓)	Reduces FGF23-expression in the bone	Reduces FGF23-expression in the bone	Reduces FGF23-expression in the bone	-	Activates renal phosphate co-transporters (NaPi-2c ↑).	Codes for the chloride channel 5
Effect of mutation in the gene involved	Activating mutation in *FGF23*	Inactivating mutation in *PHEX*	Inactivating mutation in *DMP1*	Inactivating mutation in *ENPP1*	-	Inactivating mutation in *SLC34A3*	Inactivating mutation in *CLCN5*
Pathogenesis	Enhanced biological FGF23-activity by preventing proteolytic cleavage of FGF23	Loss of PHEX function induces increased FGF23 expression	Loss of DMP1-function induces increased FGF23 expression	Loss of ENPP1-function induces increased FGF23 expression	Tumor-induced excessive secretion of FGF23	Suppressed FGF23 levels induces increased S-calcitriol with hypercalciuria	Proximal renal tubolopathy and Fanconi syndrome
S-PO$_4$	↓	↓	↓	↓	↓	↓	↓
S-Ca	N	N	N	N	N	N	N ↑
S-FGF23	N ↑	N ↑	N ↑	N ↑	N ↑	N ↓	-
S-PTH	N	N ↑	N ↑	N	N ↓↑	N ↓	N ↓↑
S-Calcitriol	N (↓)	N (↓)	N (↓)	N (↓)	N ↓	↑	↑
U-Ca	N ↓	N ↓	N ↓	N ↓	N ↓	↑	↑

Table I. Classification of hypophosphatemic rickets according to pathophysiology. Genetic and biochemical characteristics. A modification of tables by Baroncelli et al. and Carpenter (Carpenter, 2012; Baroncelli et al., 2012).

N Normal; ↑ increased; ↓ decreased; (↓) decreased relative to S-PO$_4$

NaPi-2a and NaPi-2c are renal phosphate co-transporters.

1.1.4. Hypophosphatemic rickets

Hypophosphatemic rickets are rare diseases with an incidence of 3.9 per 100.000 live births and a prevalence of 1:21.000 in Denmark (Beck-Nielsen *et al.*, 2009). HR is divided into different sub-types, based on different genetic origin, each of which is characterized by specific disturbances in the phosphate handling (Table I) (Drezner, 2003). A shared trait of all types is the presentation of hypophosphatemia caused by abnormalities in the renal reabsorption of phosphate. The phosphate depletion causes hypomineralization, softening of bone, and growth retardation. The clinical symptoms in untreated young HR patients include enlargement of the growth plates of the long bones, particularly wrists, knees, ankles, and the costochondral junctions of the ribs ("rachitic rosary"), and if severe, also development of a Harrison`s sulcus (i.e., inward pull of the diaphragm on the softened ribs). Subsequently, the legs become bowed and the physical stature becomes disproportionately reduced (Drezner, 2003; Beck-Nielsen *et al.*, 2010). Surgical correction of the leg deformities is a predominant incident in HR patients. In contrast, the risk of bone fractures is reported to be low (Beck-Nielsen *et al.*, 2010). In HR patients, the presence of a frontal bossing is described as another skeletal deformity (Marks *et al.*, 1965; Drezner, 2003). The experience of joint pain is common in adult HR patients (Beck-Nielsen *et al.*, 2010). In addition, muscular weakness, hypotonia, and a waddling gait are common clinical signs of HR. Despite the deficits in muscle function and a low muscle density, younger adults with HR (age < 50 years) demonstrate only a moderate physical impairment in everyday life (Veilleux *et al.*, 2012). Additional symptoms in adult HR patients are the development of mineralizing enthesopathies (i.e., calcification of the ligaments and their attachment to the bone) (Drezner, 2003; Beck-Nielsen *et al.*, 2010). Furthermore, the dentition may be characterized by a high number of teeth with endodontic complications in terms of pulpal necrosis, periapical infections, and root-fillings (Chaussain-Miller *et al.*, 2003; Andersen *et al.*, 2012). Apparently, that kind of dental aberration has been reported in only the X-linked type of HR.

The most predominant type of HR is inherited in a dominant X-linked fashion, caused by mutations in the gene encoding for the phosphate regulating endopeptidase homolog, X-linked (*PHEX* , MIM 300550) (XLHR, MIM 307800) (Hyp Consortium, 1995). XLHR is characterized by decreased inhibition of the formation of FGF23 indirectly mediated by the mutated PHEX gene product. FGF23 down regulates $S-PO_4$ by its phosphaturetic effect and thereby, FGF23 is associated with hypophosphatemia (Shimada *et al.*, 2004; Liu & Quarles, 2007).

The less predominant types of HR are either FGF23-related or non-FGF23-related (Table I) (Beck-Nielsen, 2012). The FGF23-related HR are 1) autosomal dominant HR (ADHR, MIM 193199) with a mutation in *FGF23* (MIM 605380) (ADHR Consortium, 2000), 2) autosomal recessive HR

(ARHR1, MIM 241520) with a mutation in the gene coding for the dentine matrix protein (*DMP1*, MIM600980) (Lorenz-Depiereux *et al.*, 2006a), and 3) another form of autosomal recessive HR (ARHR2, MIM 613312) with a mutation in ectonucleotide pyrophosphatase/phosphodiesterase 1 (*ENPP1*, MIM 173335) (Levy-Litan *et al.*, 2010; Lorenz-Depiereux *et al.*, 2010). The non-FGF23-related HR types are characterized by hypercalciuria: 1) hereditary HR with hypercalciuria (HHRH, MIM 241530) with mutation in the sodium-co-transporter gene (*SLS34A3*, MIM 609826) (Bergwitz *et al.*, 2006; Lorenz-Depiereux *et al.*, 2006b) and 2) X-linked recessive HR (XLHR, MIM 300554) with mutation in the gene coding for the chloride channel 5 (CLCN5, MIM 300008) (Brakemeier *et al.*, 2004; Cho *et al.*, 2008).

The biochemical effects of all types of FGF23-associated HR are the same despite the different genetic background, and they are all related to an increased action of FGF23: In the kidney, the increased level suppresses the activation of the phosphate co-transporter as well as the 1α-hydroxylase. The former leads to a decreased phosphate reabsorption in the proximal renal tubules and a renal waste of phosphate, and the latter leads to a reduced formation of the activated vitamin D (calcitriol). The reduced S-calcitriol reduces the intestinal reabsorption of phosphate, which adds to the hypophosphatemia. The S-PTH and S-Ca as well as the U-Ca remain normal in the FGF23-associated HR types (Baroncelli *et al.*, 2012).

The non-FGF23-associated HR shares the characteristic low $S-PO_4$ with the other types of HR, but shows low to normal S-FGF23. HHRH affects directly the renal phosphate co-transporters and leads to a reduced reabsorption of phosphate. The low $S-PO_4$ and S-FGF23 lead to a compensatory increase in plasma level of calcitriol, which causes release of minerals from bone and the concomitant renal depletion of calcium (i.e., hypercalciuria). In most cases, skeletal symptoms are mild and dental symptoms are absent. On the other hand, patients with HHRH may be at the risk of renal stones or nephro-calcinosis (Lorenz-Depiereux *et al.*, 2006b; Bergwitz & Juppner, 2012).

1.1.5. Treatment of hypophosphatemic rickets

The current medical treatment of the X-linked dominant HR addresses the hypophosphatemia and the decreased level of activated vitamin D (calcitriol). According to the recommendations by Carpenter and coworkers (Carpenter *et al.*, 2011), most children with XLHR have to be treated with phosphate-salts and vitamin-D-derivates (i.e., calcitriol or alfacalcidol). The aim of the treatment is to minimize skeletal deformities, improve the height, and avoid osteomalacia. Early start of treatment is advocated. The medication needs careful biochemical monitoring because of the risk of iatrogenic effects related to the phosphate treatment, which in high doses or not accompanied

by additional calcitriol treatment may induce hyperparathyroidism, nephrocalcinosis and hypercalciuria. Additional treatment with growth hormone is not recommended as a part of the standard treatment. If severe bowing of legs persists in spite of the medical treatment, orthopedic corrections may be indicated (Carpenter *et al.*, 2011).

The adults with XLH are treated according to the same principle as the children with XLHR. However, Carpenter and coworkers recommend restricting the treatment to the symptomatic adults. The aim of the treatment is to reduce skeletal pain and to reduce the osteomalacia, and the treatment need careful monitoring to prevent side effects (Carpenter *et al.*, 2011).

The other and rarer types of FGF23-associated HR are on an individualized basis treated according to the same protocol as patients with XLHR. Patients with the non-FGF23-associated HR are treated with phosphate-salts, only, and treatment with calcitriol is contraindicated (Bergwitz & Juppner, 2012).

The newly recognition of the central role of FGF23 in the pathogenesis of FGF23-associated HR raises the question of a future HR-treatment with anti-FGF23 antibodies or other ways to modify FGF23 activity. Promising treatment-studies on animals and humans are in progress (Pettifor & Thandrayen, 2012; Baroncelli *et al.*, 2012; Bergwitz & Juppner, 2012). In addition, future treatment strategies may include the utilization of calcimimetics (drugs which mimics calcium and inhibits hyperparathyroidism) or calcitonin (a thyroid hormone which stimulates calcitriol production and lower S-FGF23) (Lee & Imel, 2013).

1.2. Bone

Bone is a specialized connective tissue, which is highly mineralized. Macroscopically, the bony structures are divided into 1) the dense cortical bone, which forms the outer contour of the bone, and 2) the trabecular bone, which is a sponge-like network of many highly interconnected trabeculae. Both types of bone consist of cells and extracellular matrix. Collagen type one is the key protein of the bone matrix. Collagen is organized in a lamellar fashion, either parallel (e.g., along cortical bone surfaces or inside the bony trabeculae) or concentrically around the blood vessels embedded in the Haversian channels of the cortical bone. Hydroxyapatite crystals of matrix is the mineralized part of the bone, with the highest proportion of mineral in the cortical bone (90%) compared with the trabecular bone (20%) (Schett, 2012). Cells of the bone are osteoblasts, osteocytes, and osteoclasts. Osteoblasts are the boneforming cells developed by differentiation of the mesenchymal stem cells derived from the bone marrow (Karsenty *et al.*, 2009). Osteocytes are the most abundant cell type of the bone. They are derived from osteoblasts, which are entrapped

in the bone matrix. The osteocytes form a network through filamentary interconnections, which are located in the small canals (i.e., canaliculi) of the bone, and they have a specific function in the inhibition of a continuous bone formation by the excretion of sclerotin (i.e., an inhibitor of bone formation) (Knothe Tate *et al.*, 2004; Poole *et al.*, 2005). Osteoclasts are multi-nucleated cells, which are capable of bone resorption. They are derived from the hematopoietic monocytic precursor cells, and in the final stage, they become polarized and develop a ruffled border (i.e., a highly folded plasma membrane facing the bone matrix) designed to secret proteins and ions into the space between the osteoclast and the bone surface (Teitelbaum & Ross, 2003; Boyle *et al.*, 2003).

1.2.1. Bone formation

The bone formation (i.e., osteogenesis) is basically a replacement of a pre-existing connective tissue. Two different processes of osteogenesis are observed in the embryo: 1) The intramembraneous bone formation, in which bone tissue is laid down directly in the connective tissue or the mesenchyme, and 2) the endochondral bone formation (i.e., cartilaginous bone formation), in which bone tissue replaces a pre-existing cartilaginous template of the future bone. The flat bones of the skull are examples of intramembranous bone formation, and the long bones of the extremities are examples of endochondral ossification (Schoenwolf, 2009a).

The intramembraneous bone formation is initiated in the primitive mesenchyme, which becomes highly vascularized and initiates an aggregation of fibroblast-like cells. The osteoblasts begin to secret a bone matrix in numerous ossification centers, which fuse into a network forming the sponge bone (i.e., primary spongiosa). The collagen fibers of the newly formed bone are randomly oriented and this immature bone is described as woven bone. Later in the development, the woven bone converts into lamellar bone with the collagen fibers organized in parallel or concentric arrangements. The external and internal connective tissue layers of the future bone condense into the periosteum and the endosteum, respectively (Kierszenbaum & Tres, 2011).

The endochondral bone formation is initiated by the formation of a primary ossification center at the middle of the cartilaginous bone template (i.e., the diaphysis of the long bone). Internally, the ossification center is characterized by chondrocyte proliferation and hypertrophy, in-growth of blood vessels and osteo-progenitor cells from the perichondrium followed by apoptosis of the chondrocytes and a mineralization of the matrix. The primary ossification center also includes a periosteal collar, which is developed by the inner perichondral cells (by intramembranous bone formation). The primary ossification center is established prenatally (i.e., in the third month of fetal life) (Kierszenbaum & Tres, 2011).

Postnatal, secondary centers of ossification develop in the epiphyses. Centrally in the two epiphyses, the chondrocytes proliferate and become hypertrophic, and vessels and osteo-progenitor cells invade from the perichondrium. In the epiphysis, the cartilage is transformed into a sponge bone, except for the articular cartilage and a thin plate between the epiphysis and the diaphysis (i.e., the growth plate). The osteo-progenitor cells give rise to the osteoblasts, which initiate deposition of an osteoid layer along the cores of the calcified cartilage. Gradually, the cartilage is replaced by bone. The growth plate retains the capacity of chondrogenesis until after puberty and at the cessation of growth, where it ends up as the epiphyseal line (Karsenty *et al.*, 2009; Kierszenbaum & Tres, 2011).

In the cranium, both types of bone formation are present (Fig. 2). The cranial base (i.e., the major part of the occipital bone, the petrous part of the temporal bone, the wings and body of the sphenoid bone, and the ethmoid bone), a minor part of the mandible (i.e., the superior part of the condyles and the midline symphysis area), and the small bones of the ear (i.e., stapes, malleus, and incus) are structures of endochondral origin. All other bony structures of the cranium are of intramembranous origin. The spine, inclusive the upper cervical column, is a structure of endochondral origin (Moore *et al.*, 2013).

The osteogenesis is characterized by the deposition of minerals in the bony structures (Schett, 2012). A mineral deposition may also happen in the soft tissues often as a consequence of a tissue damage and of a local elevation of the extracellular calcium-phosphate product (Lorenzo *et al.*, 2011). Occasionally, the deposition is characterized as an extra-skeletal ossification, which in some pathologies (e.g., fibrodysplasia ossificans progresiva) can be extensive (McCarthy & Sundaram, 2005). Intracranial calcifications visible on a radiograph have been reported as an incidental finding, which normally is described as a physiological phenomenon (Daghighi et al., 2007; Kieffer and Gold, 1974; Saldino and Di, 1974). The ossification of the falx cerebri is, however, a rare condition, which in some cases has been associated with pathology (Debnath et al., 2009; Dorenbeck et al., 2002; Tubbs et al., 2006).

Fig 2. Schematic drawing of the origin of osseous structures of the cranium and the cervical vertical column.
Green: the structures of endochondral origin; Red: the structures of intramembraneous origin; Red/green: the nasal bone, the mandible, and the vomer are of intramembranous origin developed upon a scaffold of cartilage (i.e., Meckel`s cartilage, the cartilaginous nasal capsule and the nasal septum) (red/green). Illustration from Gjørup and coworkers (Gjørup et al., 2011).

1.2.2. Bone remodeling

Bone remodeling is the replacement of newly formed and old bone by a resorption-production sequence with the participation of the osteoclasts and the osteoblasts (Kierszenbaum & Tres, 2011; Lorenzo *et al*., 2011). It is a continuous process throughout the life with the purpose to keep optimum bone strength and to keep the calcium homeostasis. In the remodeling process, the osteoclasts are mobilized to resorb bone followed by the recruitment of osteoblasts, which lay down the new bone (i.e., osteoid). In the cortical bone, it is a process starting inside from the center of the old Haversian system, and in the trabecular bone, it is a process starting outside at the surface of the bone (Kierszenbaum & Tres, 2011). Normally, the bone formation and the resorption are coupled in a balanced situation regulated by local as well as systemic factors. One local factor is the direct osteoblast-osteoclast interaction: The pre-osteoblasts produce both osteo-protegerin (OPG), which has RANK receptor affinity and is an inhibitor of osteoclastogenesis, and RANKL, which stimulates osteoclast formation. If the cells produce more OPG than RANKL, OPG binds the available RANKL and the osteoclastogenesis is prevented causing dense bones as seen in, i.e., osteopetrosis (Helfrich, 2003). Contrarily, if the cells produce more RANKL than OPG, the

osteoclasts are formed and activated causing excessive bone resorption as seen, in i.e., Paget's disease of bone (Helfrich, 2003). Another local factor includes the immune system, in which the different subsets of T-lymphocytes can either enhance or inhibit osteoclastogenesis. The systemic neuro-endocrine control of bone homeostasis includes various hormonal pathways (i.e., PTH and calcitriol, and the insulin-like growth factor (IGF)). In addition, the two systemic regulators osteocalcin, which is produced by the osteoblasts, and the hormone leptin, produced by adipocytes, play major roles of the bone homeostasis in the co-regulation of bone, fat, and energy metabolism. Presumably, disturbances in the link between the adipogenesis and the osteogenesis heavily influence the bone homeostasis (Lorenzo et al., 2011; Schett, 2012).

Bone modeling is a process of the cortical bone carried out by uncoupled osteoblasts and osteoclasts with the purpose of creating the shape of bone during the growth (Lorenzo et al., 2011). This is opposed to the remodeling of bone, which is a temporarily regulated process, which throughout life, by coupling between the activations of bone resorbing and bone formation cells, results in the balanced renewal of bone by resorption and apposition. In addition, remodeling as opposed to modeling is more active in the trabecular bone compared to the cortical bone. The modeling is influenced by mechanical forces, increases during the growth spurt, and ceases at the end of the adolescent growth (Canalis, 2005; Lorenzo et al., 2011). Synonyms for the growth dependent modeling of facial bone are "growth remodeling" (Enlow & Hans, 1996), "surface remodeling" or simply "remodeling" of the external surfaces of the facial bones as a reaction to the concomitant displacement of craniofacial structures (Solow, 1980). The latter is a common terminology among Scandinavian orthodontic professionals. For example, facial growth studies using implants have described a differentiated "remodeling" of the mandibular lower border according to the type of mandibular rotation during growth (i.e., neutral, clockwise or counter clockwise rotation) (Bjørk, 1955; Bjørk & Skieller, 1983).

In HR, disturbances in the remodeling processes have been studied in both humans and in animal models of HR: Decades ago, histomorphometric studies in bone biopsies from children with HR showed a decreased osteoblastic function because of a low birth rate of the basic multinuclear remodeling unit (BMU) and a prolonged formation period of the units (Marie & Glorieux, 1981a). In addition, an enhancement of the BMU birth rate was demonstrated when the children were treated with phosphate and calcitriol (Marie & Glorieux, 1981b). Thus, osteoblast defects were suggested to be of primary importance to disturbances in bone remodeling in HR patients. Later, animal studies on HYP mice revealed impaired osteoclasts differentiation and function to impact the bone remodeling with an increased trabecular bone volume as the result (Hayashibara et al., 2007). Additional animal studies performed on DMP1-null mice showed that the disturbances in bone

21

remodeling are related to both an altered osteoblast function and a decrease in the number of osteoclasts (Zhang *et al.*, 2011). In the animal models of HR, the disturbances in the bone remodeling appear to be closely related to the low level of phosphate and the high level of FGF23 in serum. In these studies, a positive effect on bone phenotype by treating with phosphate has been demonstrated (Lu & Feng, 2011). The current treatment strategy in HR patients (administration of phosphate and calcitriol) does not fully normalize bone density (Cheung *et al.*, 2013). Treatment strategies including the use of FGF23 antagonists or antibodies might in the future normalize bone remodeling and bone mineralization HR patients (Lee & Imel, 2013).

1.3. Craniofacial growth and development

1.3.1. Normal versus pathologic development

Growth and development are complex biologic phenomenon starting at conception and continuing in postnatal life until the end of puberty. Prenatally, the maternal factors are dominant in regulating the growth of the fetus. In postnatal life, a complexity of genetic, hormonal, nutritional and other factors regulate the continuing growth and development (Westphal, 1995). The normal development can be interrupted and lead to disorders in the morphogenesis, i.e., processes leading to an abnormal form and/or structure of an organism or its parts (Spranger *et al.*, 1982). According to Spranger and coworkers (Spranger *et al.*, 1982) and Cohen (Cohen, 1990), the disorders of the morphogenesis are classified into four types: malformation (i.e., a defect as the result of an intrinsically abnormal developmental process), disruption (i.e., a defect as the result of an extrinsic breakdown of, or an interference with an originally normal developmental process), deformation (i.e., an abnormal form, shape or position caused by mechanical forces), and dysplasia (i.e., an abnormal organization of cells into tissue and its morphological results). The malformations arise in the embryonic period (i.e., gestational age (GA) 0-8 weeks) at the time of organogenesis. The deformations arise primarily in the fetal period (i.e., GA 8-38 weeks) affecting intact structures. However, the deformations may also occur postnatal, e.g., the bowlegs in patients with rickets. Examples of the dysplasias are osteogenesis imperfecta and Marfan syndrome, which basically are abnormalities of the connective tissue (Spranger *et al.*, 1982; Cohen, 1990).

1.3.2. Prenatal development

The development of the skeletal structures is preceded by the initiation of the development of other structures, e.g., the central nervous system (Kjaer, 1998a; Schoenwolf, 2009c). In the embryo, the formation of the central nervous system starts with the formation of the neural plate, which at GA 18 days arises by differentiation of the ectoderm into the neuro-ectoderm and the surface

ectoderm. Around the gestational age of four weeks, the neural plate changes into the neural tube by a folding around the long axis (neural groove) of the germ disc. The tube closes in a "zip-like" fashion starting in the cervico-occipital region and gradually extending cranially and caudally. The neural crest cells are formed in-between the layer of dorsal surface ectoderm and the edges of the neuro-ectoderm of the folded neural tube. In the mesenchyme ventral of the neural plate and tube, the notochord develops. The formation of the notochord begins at the primitive node of the germ disc and develops into a solid rod which grows in cranial direction defining the position of the future vertebral bodies. The notochord plays a role in induction and patterning of early development of structures, e.g., the vertebral bodies (Schoenwolf, 2009c; Schoenwolf, 2009d).

The notochord and the neural tube define the initial axis of the body. In the paraxial mesenchyme, the somites develop as transient segmented structures, which increase in number during the early phases of the embryonic life. The somite differentiates into the myotome, the dermatome, and the sclerotome. The sclerotomes develop into the vertebrae and the ribs: The ventral part of the sclerotome encloses the notochord and forms the vertebral corpora, and other parts of the sclerotome surround the neural tube initiating the formation of the later posterior arch of the vertebrae (Schoenwolf, 2009a; Schoenwolf, 2009c).

The sclerotomes of the four most cranial somites fuse into the occipital bone of the skull. The sclerotomes of all other somites resegmentate into two parts of, which the caudal part of one unit fuses with the cranial part of the next unit. At the line of segmentation, nerves can pass for innervation of the musculature, and further, the intervertebral disc develops in this area. By time, the notochord disappears in the vertebral corpora, but remnants of the notochord differentiate into the nucleus pulposus of the intervertebral disc (Schoenwolf, 2009a).

The notochord extends cranially in the posterior cranial base to the sella turcica region. Like the the caudal part of the vertebral column, the development of the posterior cranial base (i.e., the postsphenoid part of the sphenoid bone and the basilar part of the occipital bone) depends on signaling from the notochord (Kjaer, 1998a; Lomholt *et al.*, 2003).

In the hypophyseal placode anteriorly of the cranial end of the notochord, an adhesion evolves between the neuro-ectoderm and the pharyngeal ectoderm. Thus, the pituary gland, which becomes located in the sella turcica (ST), is composed of two components with different origin: the anteriorly located adenohypophysis developed from the pharyngeal ectoderm and the posteriorly located neurohypophysis developed from the neuro-ectoderm. In the fetal life, the region of the developing ST is a boundary area between structures developed by notochordal induction, which

has been described above, and structures of the face developed by anterior migration of neural crest cells (Kjaer, 1998a; Kjaer, 2010).

From the closed neural tube, an outgrowth bilaterally of the hemispheres begins approximately on day 35 and later on, an outgrowth dorsally of cerebellum appears in the region of rhombencephalon. The development of the hemispheres is necessary for the formation of theca, is illustrated by the absence of theca in fetuses with anencephaly (Kjaer *et al.*, 1994; Kjaer, 1998a).

The basic morphology of the face is established between the 4th and 10th weeks by the development and the fusion of five prominences: the frontonasal prominence, the two maxillary prominences, and the two mandibular prominences associated with the first pharyngeal arches. The mesenchyme of the prominences arises from the neural crest cells derived from the neural crest at the cranial end of the neural tube (Schoenwolf, 2009b). The neural crest cells migrate from different sites of the crest to specified regions or fields of the viscero-cranium and force forward the ectoderm of the face. The process resembles the act of inflating a balloon. The expanding regions get filled with mesenchyme and neural crest cells, which differentiate into nerves, muscles, vessels, cartilage, and bone. Each region or field supposedly has a common genetic background according to the starting crest site of the migrating neural crest cells The borders between the fields have been determined in studies of a number of pathologic conditions (Kjaer, 2010).

The main fields of the cranial development are the following: 1) the cerebellar and cervical spine field (i.e., the notochordal field), which develop by notochordal induction, 2) the theca field (i.e., antero-neural crest field), which depends on the development of the cerebrum (i.e., the two hemispheres), 3) the central frontonasal field, which is developed by migration of the neural crest cells and includes the nasal structures and the maxillary incisors, 4) the bilateral maxillary fields (i.e., antero-median neural crest field), which are developed by the neural crest cell migration and include the orbital structures and the maxillary premolars and canines, 5) the bilateral palatine fields (i.e., postero-median neural crest field), which are developed by the neural crest cell migration and include the posterior maxillary structures and the maxillary molars, and 6) the bilateral mandibular fields (i.e., posterior neural crest field), which are developed by the neural crest migration and include the mandibular structures and teeth (Kjaer, 1998a; Kjaer *et al.*, 1999; Kjaer, 2010).

In the nasofrontal field, the nasal bones develop bilaterally in the mesenchyme in close relation to the chondral nasal capsule. The osseous structure develops directly from the mesenchymal cells using the chondral nasal capsule as a scaffold (Sandikcioglu *et al.*, 1994a). In the mandibular field, Meckel´s cartilage is the initial solid structure of the field. The ossification of the mandible starts in

the mesenchyme buccal to Meckel´s cartilage. Except for the symphysis region, the development of the mandible is characterized by the intramembraneous ossification, which use the Meckel`s cartilage only as a scaffold. The mandibular condyle develops as a cartilagineous extension at the posterior end of the primitive osseous mandible. The condyle grows by apposition of cartilage distally and a concomitant endochondral bone formation at the interphase between the proximal mandibular bone and the distal condylar cartilage (Kjaer *et al.*, 1999).

1.3.3. Postnatal development

According to the functional matrix theory formulated by Moss (Moss & Salentijn, 1969), the postnatal craniofacial growth is dictated by the functional demands. The enlargement of bones of the cranium occurs in response to the increasing size of, e.g., the brain and orbit. In addition, the growth of bones around the oro-naso-pharyngeal spaces is regarded as an adaptation to the need of more space in the cavities for the breathing, the digestion, and other essential functions (Moss & Salentijn, 1969).

The cranial base lengthens by sutural growth anteriorly and by growth of the spheno-occipital synchondrosis posteriorly. At the age of 6-7 years, the sutures close, and the anterior cranial base becomes a relatively stable structure (Melsen, 1974). During further growth, the increasing prominence of the frontal bone in the glabella area mainly is related to appositional surface remodeling (i.e., modeling) of the external surfaces of the frontal bone. The spheno-occipital synchondrosis is active until the age of 12-15 years (i.e., 12-13 years in girls and 14-15 years in boys). The osseous closure starts in the cerebral region of the synchondrosis. The basilar part of the occipital bone (i.e., the clivus) is subject to a displacement upward and backward in relation to the sphenoid bone because of the differentiated closure of the spheno-occipital synchondrosis. The displacement is compensated by relocation down because of a surface remodeling (i.e., a modeling with an apposition of bone at the inferior surface and a resorption at the cranial surface of the clivus) (Melsen, 1974). The ST lies centrally in the medial cranial fossa containing the pituary gland. The depth and diameter of ST increases in the period of growth (Axelsson *et al.*, 2004b). The initial apposition of bone on the anterior internal wall of ST ceases around the age of 5-7 years (i.e., 6-7 years in boys and five years in girls). In contrast, the resorption on the distal part of the floor and the posterior wall continue in most of the growth period (Melsen, 1974; Bjørk & Skieller, 1983). A variation of the morphology of the ST is normal in groups of healthy persons with normal craniofacial morphology, and a classification system, which describe the deviations from the standard type has been proposed (Axelsson *et al.*, 2004b). The deviations are extraordinary frequent in some pathological conditions: cleft lip and palate (Nielsen *et al.*, 2005a; Alkofide, 2008), Rieger syndrome (Meyer-Marcotty *et al.*, 2008), Williams syndrome (Axelsson *et al.*, 2004a),

trisomy 21 (Russell & Kjaer, 1995), and solitary median maxillary central incisor (Tabatabaie *et al.*, 2008). A recent review has demonstrated a connection between the prenatal and postnatal deviations in ST morphology in pathological conditions. The author states that deviations in the anterior ST wall are associated with deviations in the frontonasal developmental field, while deviations in the posterior wall are associated with malformations in the posterior structures, e.g., cerebellum (Kjaer, 2012).

The flat bones of the skull (i.e., os frontale, os parietale, os occipital, and the squamous part of os temporale) are separated by sutures, and the skull increases in size by sutural growth. During the normal development, the sutural growth of the flat bones is combined with an internal (i.e., endosteal) resorption and an external (i.e., ectocranial and endocranial) apposition of bone. This is a bone modeling, which acts as a morphological adaptation to the displacement of the bones during growth (Enlow & Hans, 1996), and the curvature of the bones decline (Axelsson *et al.*, 2003). In comparison with the growth of the viscerocranium, the postnatal growth of the skull is limited, but the length and the diameter of the skull as well as the theca thickness increase until the end of puberty (Axelsson *et al.*, 2003).

The development of the maxilla is characterized by sutural growth, which lengthens, widens, and in relation to the anterior cranial base, lowers and advances the maxilla. In addition, a modeling resorption of the nasal floor and apposition on the palate take place. The maxillary growth ceases around the age of 17, which is 1-2 years before the end of mandibular growth (Bjørk, 1955; Bjørk, 1966). The mandible develops by condylar growth, which moves the bone downwards and more or less forward. The direction and amount of the condylar growth dictates the concomitant rotation of the mandible (i.e., a clockwise or anti-clockwise rotation of the mandibular corpus in relation to the anterior cranial base). The surfaces of the mandible undergo marked modeling (i.e., surface remodeling), which is differentiated according to the type of the mandibular rotation (Bjørk, 1955; Bjørk & Skieller, 1983).

The frontal sinus develops by the resorption of bone and appears radiological around the age of five years (Brown *et al.*, 1984). The final size of the frontal sinus varies considerably (Ruf & Pancherz, 1996). The growth of the nasal bone is extensive from 2-17 years of age, and the growth occurs both in the nasofrontal suture and appositional at the nasal tip along with a bone modeling occurring at the superior and inferior borders (Lestrel *et al.*, 1991).

1.4. Craniofacial and cervical vertebral column morphology

1.4.1. Craniofacial morphology

In almost a century, standardized profile radiographs have been used for the study of craniofacial morphology, including the study of the postnatal development of the craniofacial structures (Bjørk, 1955; Solow, 1966; Bjørk & Skieller, 1972; Bjørk & Skieller, 1974; Ingerslev & Solow, 1975; Wahl, 2006; Kjaer, 2010). The use of a rigid cephalostat during radiographic exposure has become a routine in the research clinics as well as in the orthodontic clinics. A number of different morphological analyses have been developed for a characterization of the craniofacial morphology and to act as a tool in the orthodontic treatment planning (Bjørk, 1975; McNamara, 1984; Wahl, 2006). In addition, cephalometric radiographs have been used in the study of severe maxillofacial growth anomalies often focusing on the effect of treatment, e.g., increased mandibular prognathia with mandibular overjet or posterior inclined mandible with anterior open bite (Ellis & McNamara, 1984; Ellis *et al.*, 1985; Nanda *et al.*, 1987; Basciftci *et al.*, 2003; Ruf & Pancherz, 2004; Wigal *et al.*, 2011; Joss *et al.*, 2012). Further, the craniofacial morphology in pathologic conditions and craniofacial anomalies have been analyzed using the cephalometric radiograph, e.g., in patients with osteogenesis imperfecta (Stenvik *et al.*, 1985; Jensen & Lund, 1997; Waltimo-Siren *et al.*, 2005), ectodermal dysplasia (Lexner *et al.*, 2007), achondroplasia (Cohen *et al.*, 1985), cleidocranial dysplasia (Jensen & Kreiborg, 1995), Williams syndrome (Axelsson *et al.*, 2005), or Seckel syndrome (Kjaer *et al.*, 2001b).

The cephalometric radiograph has also been used for the morphological as well as the metric analysis of minor structures of the craniofacial bones: the size of the frontal sinus (Erturk, 1968; Brown *et al.*, 1984), the size and the morphological characteristics of ST (Kjaer *et al.*, 1998; Russell & Kjaer, 1999; Axelsson *et al.*, 2004a; Axelsson *et al.*, 2004b; Nielsen *et al.*, 2005a; Alkofide, 2007; Brock-Jacobsen *et al.*, 2009), the thickness of the skull (Jacobsen *et al.*, 2008; Arntsen *et al.*, 2010), the nasal bone length (Nielsen *et al.*, 2005b; Lexner *et al.*, 2007; Meyer-Marcotty *et al.*, 2008; Arntsen *et al.*, 2009), and the dimensions of the posterior cranial fossa (Kjaer, 1998a; Caspersen *et al.*, 2010).

1.4.2. Craniofacial morphology in HR patients

In HR patients, previous cephalometric studies have described a number of skull abnormalities (Appendix; Table Z). One study of eight patients reported an increased skull length, an increased skull thickness, and an appearance with frontal bossing (Marks *et al.*, 1965). In another study, was published in the same period, nine HR patients showed less maxillofacial growth retardation than retardation of stature growth. In addition, they had less retardation of the mandibular growth than of

the maxillary growth (Tracy & Campbell, 1968) . Later, a cephalometric study of 22 Jordanian patients with HR has reported a shortened anterior cranial base and maxilla as well as reduced mandibular dimensions compared to a healthy age- and gender-matched control group (Al-Jundi *et al.*, 2009). In the same study, the cranial base was flattened and HR patients had a skeletal Class III malocclusion. In addition, anthropometric studies have described an increased cranial length, decreased occipital width, and an increased head circumference in HR patients (Pronicka *et al.*, 2004; Beck-Nielsen *et al.*, 2010).

Craniotabes (i.e., localized thinning of the skull) is a symptom of the vitamin D deficiency rickets and of an increased intracranial pressure (Shaw, 2003). Except for one study (imerslund, 1951), that symptom has not been reported in the cephalometric studies on HR patients (Appendix; Table ZZ). Occasionally, a premature synostosis of cranial sutures has been observed in HR patients (Imerslund, 1951; Reilly *et al.*, 1964; Carlsen *et al.*, 1984; Willis & Beattie, 1997; Currarino, 2007; Murthy, 2009). Most of the observed cases had synostosis of the sagittal suture, thus, the skull was reported as dolichocephalic (i.e., a relatively long skull). Synostosis of more than one suture has been reported in two HR cases (Imerslund, 1951; Willis & Beattie, 1997). The premature closing of sutures may induce an increase of the intracranial pressure, which is a common symptom in patients with syndromic craniosynostosis, e.g., Crouzon syndrome (de-Jong T. *et al.*, 2010). According to the review by de-Jong *et al* (de-Jong T. *et al.*, 2010), the majority of reported cases with syndromic craniosynostosis undergo a surgical expansion of the cranial vault at least one time. In contrast, only seven previously reported HR cases had an increased intracranial pressure with headache and/or neurological symptoms, which required a surgical expansion of the cranial vault (IMERSLUND, 1951; Carlsen *et al.*, 1984; Willis & Beattie, 1997; Currarino, 2007; Murthy, 2009). In studies on HR patients, the limited number of cases with symptoms related to cranial synostosis has been explained by a relatively late premature fusion of the sutures compared to the time of fusion in other conditions with premature craniosynostosis (Currarino, 2007). This is supported by the results of histological studies on HYP mice (Roy *et al.*, 1981). Further on, Currarino (Currarino, 2007) discussed the psychosocial need for surgical correction of craniosynostosis to improve the cranial appearance in the scaphocephalic HR patients. According to the author, surgical expansion of the cranial vault for aesthetic reasons was not relevant in any of the reported cases (Currarino, 2007).

The size of the posterior cranial fossa has been reported to be reduced in HR patients in comparison with controls (Caldemeyer *et al.*, 1995; Tubbs *et al.*, 2004). According to previous studies, the reduced volume of the posterior cranial fossa is related to an increased calvarial thickness, and it might be the reason for the presence of a Chiari I malformation (CMI: an

extension of cerebellar tissue into the spinal canal) seen in some few reported HR cases (Caldemeyer *et al.*, 1995; Kuether & Piatt, 1998; Tubbs *et al.*, 2004; Currarino, 2007) (Appendix; Table ZZ). According to a previous study on 16 HR patients (Caldemeyer *et al.*, 1995), two of seven patients with CMI were asymptomatic, four had headache or other unspecific subjective symptoms, and one was objectively diagnosed with neurological symptoms. Furthermore, two of the patients had syringomyelia (i.e., the development of a fluid-filled cyst (syrinx) within the spinal cord), which called for a surgical intervention. However, the total number of reported HR cases with surgical treatment in relation to CMI is limited to three (Caldemeyer *et al.*, 1995; Kuether & Piatt, 1998) (Appendix; Table ZZ).

Studies on HYP mice (the murine model of XLHR) report cranial malformation, which include an underdevelopment of the nasal bone (Iorio *et al.*, 1980; Mostafa *et al.*, 1982) (Appendix; Table ZZZ). In contrast to the reporting of an increased cranial length in human XLHR patients, the cranial length of the HYP mice was reduced (Iorio *et al.*, 1980; Mostafa *et al.*, 1982; Gonzalez *et al.*, 1992; Lorenz-Depiereux *et al.*, 2004). In HYP mice, the growth of the upper jaw is reported to be more restricted than the growth of the lower jaw (Iorio *et al.*, 1979; Iorio *et al.*, 1980; Gonzalez *et al.*, 1992; Lorenz-Depiereux *et al.*, 2004), which is in accordance with the findings in human studies on HR (Tracy & Campbell, 1968; Al-Jundi *et al.*, 2009).

1.4.3. Cervical vertebral column morphology

In most cases, the standardized profile radiograph of the skull (cephalogram) shows the upper cervical vertebral column, which enables radiographic analyses of both cranial and cervical (C1 – C5) structures on one radiograph. The proximity of the upper cervical column and the cranial base is the background for the studies of the cranio-cervical junction in relation to the basilar pathology (e.g., basilar impression) (Arponen *et al.*, 2010; Arponen *et al.*, 2012), as well as the posture of the head and neck and its association with the craniofacial morphology (Solow & Tallgren, 1976; Pirttiniemi *et al.*, 1989; Huggare *et al.*, 1991; Huggare & Cooke, 1994; Sandikcioglu *et al.*, 1994b; Huggare, 1998; Solow & Sonnesen, 1998; Sonnesen *et al.*, 2007). The dimensions of the atlas and their association with the craniofacial morphology have been analyzed in several studies (Huggare, 1989; Sandikcioglu *et al.*, 1994b; Huggare, 1995; Huggare & Houghton, 1996). For example, the vertical dimension of the atlas dorsal arch is associated with the growth direction of the mandible, which is a factor influencing the maxillo-facial morphology and the dental occlusion (Huggare, 1989). In addition to the analyses of the dimensions and the angulation of the vertebrae, the morphological deviations of the vertebrae (e.g., cervical vertebral anomalies (CVA)) can be visually assessed on the cephalograms (Farman *et al.*, 1979; Sandham, 1986). The cervical vertebral anomalies include the posterior arch deficiencies (PAD) and the fusions (FUS), which have been

divided into two and three subtypes, respectively (Sandham, 1986). The posterior arch deficiencies are relatively common (Currarino *et al.*, 1994; Sabuncuoglu *et al.*, 2011) and it is considered a normal variation to have FUS between C2 and C3 (14%) and PAD of C1 (5%) (Sonnesen & Kjaer, 2007b). In comparison with controls, the occurrence of CVA is a more frequent finding in a number of syndromes and pathological conditions: craniosynostosis syndromes (e.g., Crouzon and Apert syndrome) (Anderson *et al.*, 1976; Hemmer *et al.*, 1987; Moore *et al.*, 1995; Anderson *et al.*, 1996; Anderson *et al.*, 1997), Klippel Feil syndrome (Naikmasur *et al.*, 2011), 22q11deletion syndrome (Hultman *et al.*, 2000; Heliovaara & Hurmerinta, 2006), cleft lip and palate (Sandham, 1986; Ugar & Semb, 2001), mandibular hypoplasia (Sonnesen *et al.*, 2007), and obstructive sleep apnea (OSA) (Sonnesen *et al.*, 2008b). In addition, the occurrence of CVA is frequent in non-syndromic individuals with extreme skeletal malocclusions: deep bite, mandibular overjet, maxillary overjet, and open bite (Sonnesen & Kjaer, 2007a; Sonnesen & Kjaer, 2007b; Sonnesen & Kjaer, 2008a; Sonnesen & Kjaer, 2008b).

In HR patients, the overall growth of the vertebral column is less affected than the growth of the legs, which results in a disproportionate stature because of a relatively normal sitting height and a reduced length of the legs (Beck-Nielsen *et al.*, 2010). However, enthesopathies and calcification of the paravertebral ligaments are common in grown-up HR patients (Polisson *et al.*, 1985; Beck-Nielsen *et al.*, 2010). The calcification of the paravertebral ligament has been reported in HR patients to be the reason for a spinal cord compression, occasionally including the cervical area (Velan *et al.*, 2001; Soehle & Casey, 2002; Lee *et al.*, 2012). According to our knowledge, studies focusing the morphology of the upper cervical column in HR patients have not previously been performed.

1.5. Summary of introduction

- Hypophosphatemic rickets (HR) is a group of inherited bone diseases, characterized by abnormal mineralization of the osseous structures because of renal waste of phosphate. The most common type is inherited in an X-linked fashion and is associated with a *PHEX* mutation.

- A dominant skeletal symptom is the short lower legs, which are affected by severe deformity. The lower legs are bony structures of endochondral origin.

- Childhood treatment with phosphate-salts and calcitriol limits the skeletal HR symptoms. New treatment strategies are under development.

- In the cranium, osseous structures of different origin are present: osseous structures of endochondral origin, osseous structures of an intramembraneous origin, and osseous structures of an intramembraneous origin developed upon a cartilaginous scaffold.

- Extra-skeletal calcifications occur physiological or as the consequence of a pathology.

- The prenatal development of the cranium is conducted differently according to the location of the cranial structures in relation to the ST. Posterior or caudal of ST, the cranium (the cerebellar and the spine field) is developed by the notochordal induction similar to the development of other parts of the axial skeleton. Anterior of the ST, the cranial structures develop by forward migration of the neural crest cells.

- The postnatal development of the neurocranium ceases early and is limited compared to the development of the viscerocranium. By differentiated sutural and synchondrosal mechanisms and by modeling (i.e., displacement and surface remodeling), the morphology of the individual osseous structure adapts to the spatial rearrangements during the cranial growth.

- In patients with HR, aberrations in the craniofacial morphology have been described. However, the studies have been characterized by a limited sample size as well as an inaccuracy in the diagnostic criteria of HR.

- According to our knowledge, studies focusing on the morphology of the upper cervical column in HR patients have not been performed previously.

2. Aims and hypotheses

2.1. Aims

The overall purpose of the present study was to analyze the morphology of the osseous structures of the craniofacial region as well as the upper cervical column in patients with XLHR or XLH. Irrespectively of age, the diseased study population (XLHR or XLH) is mentioned HR patients or HR group.

The study was conducted with a focus on:
- The origin of the bone development, which is divided into the intramembranous and the endochondral (i.e., cartilaginous) bone formation
- The developmental fields of the head and the upper spine
- The skeletal severity of HR and its impact on the morphology

The papers I – IV were carried out with the following main aims:

I. To characterize the craniofacial morphology in patients with HR compared with healthy controls. Furthermore, we assessed the possible differences in the craniofacial morphology according to the bony origin of the cranial structures.

II. To characterize the size and the morphology of the frontal sinus and the nasal bone in adult HR patients compared with adult controls, and in the comparison to focus on the bone resorption and apposition. Furthermore, the aim was to examine the interrelationship between the nasal bone morphology and the severity of general skeletal impact of HR.

III. To characterize the upper spine morphology in adult patients with HR compared with adult controls and to study the associations between the upper spine morphology and the craniofacial morphology. Furthermore, the aim was to assess the differences in the upper spine morphology according to the severity of the skeletal impact of HR.

IV. To reveal the presence of intracranial and extra-cranial calcifications on cephalograms in adult HR patients compared with adult controls. Furthermore, the purpose was to assess the association between the presence of cranial calcifications and a) the presence of mineralizing enthesopathy at other extra-skeletal sites, b) the severity of the skeletal HR impact, and c) the medical treatment during childhood.

In addition, the morphology of the ST in adult HR patients compared with controls was studied.

2.2. Hypotheses

The overall null-hypothesis was that in the comparison between HR patients and controls, there was no difference in the cranial or cervical morphology.

In addition, it was hypothesized that:

- In HR patients, deviations in craniofacial morphology are dominant in structures of endonchondral bone origin opposed to structures of intramembranous bone origin;
- In HR patients, deviations in the craniofacial and cervical morphology are related to the severity of skeletal HR impact;
- In HR patients, disturbances in the remodeling of bone (bone-apposition and bone-resorption) are demonstrated by deviations in craniofacial and cervical column morphology;
- A general inborn interrelationship exists between the cervical column morphology and the craniofacial morphology;
- In HR patients, extra-skeletal calcifications are visible on cephalograms in line with findings on radiographs of other skeletal structures;
- The childhood medical treatment prevents the occurrence of extra-skeletal calcifications in HR patients.

3. Study population

3.1. Rickets patients

A medical survey of patients with rickets was conducted during 2006-2008, thus approved by the The Regional Scientific Ethical Committee for Vejle and Fuhnen County, now The Regional Scientific Ethical Committee for Southern Denmark (ID: M-2678-05). The approval was extended to include supplementary data for the present study, an investigation of the craniofacial morphology in patients with HR compared with healthy controls. The study, on which the present thesis is based, has been notified to The Danish Data Protection Agency, which granted the author of the thesis an authorization for the data collection of the study (ID: 2009-41-3613).

The recruitment of patients for the medical cross-sectional study on hereditary rickets previously has been described in detail (Beck-Nielsen *et al.*, 2010). Briefly, the method of the original patient inclusion was as follows: The patients were identified in the Danish National Patient Registry by a search based on the diagnosis codes of vitamin D-resistant rickets. The patients were recruited from Jutland and Funen. The diagnosis was confirmed by a review of the patients' medical files. By contacting the treating doctors, the patients with HR, who did not appear in the register, were identified. Finally, a family screening added additional cases.

The inclusion criteria were biochemical and/or genetic verification of HR. The biochemical criteria were one or more of the following: S-PO$_4$ below normal range, low renal threshold value for reabsorption of phosphate in urine (TPO$_4$/GFR), or elevated S-FGF23. In all cases except three, the diagnosis was genetically verified. In one family, the disease-causing *DMP1* mutation was identified, and in the other families and cases a number of different *PHEX* mutations were identified as disease-causing (Beck-Nielsen *et al.*, 2012). The patients with secondary rickets due to malabsorption or tumor-induced osteomalacia (TIO), or patients with hereditary vitamin D-dependent rickets type one (VDDR1A) were excluded.
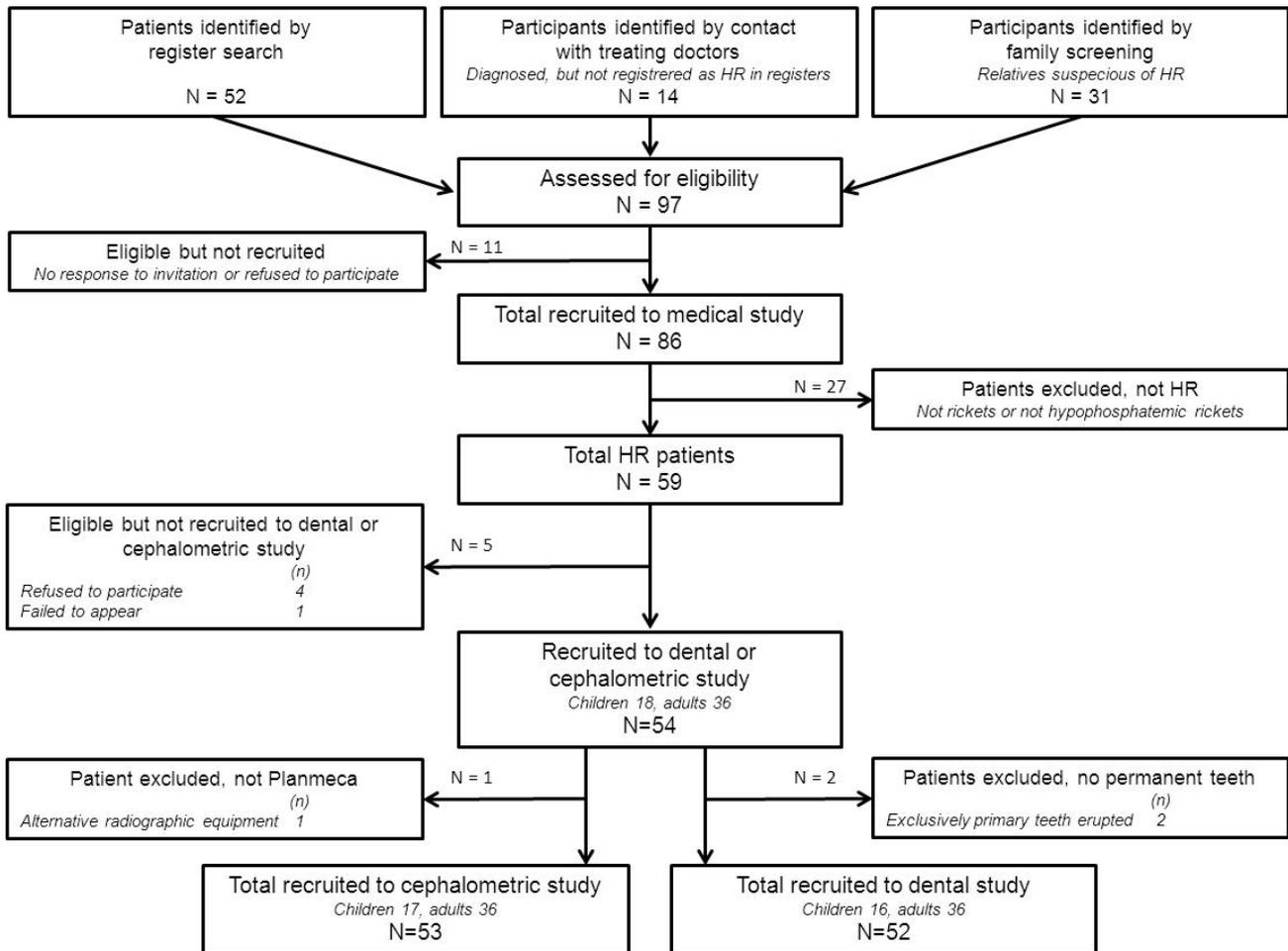
Fig. 3. Flow chart of the recruitment of the HR patients

All patients recruited for the medical survey were invited to join a clinical dental examination at The Dental Department of Health, Aarhus University. The examination included radiographs of the dentition as well as of the cranium. Five patients did not accept the invitation. Two patients had no erupted permanent teeth and were excluded from a previously reported study of the permanent dentition in HR patients, but they were included the present study (Andersen *et al.*, 2012). One patient was not able to show up at Aarhus University and was exposed by a radiographic equipment not specified for the present study of the craniofacial morphology in HR patients (Planmeca Promax[©], Planmeca Oy, Helsinki, Finland). A flow chart of the recruitment procedure of the HR patients is shown in Fig. 3. Conclusively, the HR population for the present study on the craniofacial morphology comprised 17 males and 36 females (age range: 3–75 years) (Table II).

The first HR patient underwent the radiographic examination the 12th of January 2007, and the examinations related to the studies described in the present thesis were finalized the 22th of September 2009.

	HR patients		Controls	
	Male	**Female**	**Male**	**Female**
< 18 yrs	5	12	14	16
≥ 18 yrs	12	24	23	26
Mean age (SD)[*]	32.8 (21.9)	30.8 (19.2)	29.2 (18.3)	30.9 (19.0)
Age range[*]	4.3–73.2	2.8–74.5	8.6-72.6	9.3–78.5

Table II. Distribution of 53 HR patients and 79 controls according to gender and age.
* Age in years

3.2. Control group

The size of the control group was based on power calculations, carried out after the recruitment of 51 HR patients (the final two HR patients were included at a later stage). The size of the control group was determined to ensure a sufficient power (80%) to identify differences between HR patients and controls at the 5% level of significance. The calculations were performed for six selected measurements of the cranium. Both linear and angular measurements were chosen and the variables were assumed to be representative for all parts of the cranium. The linear variables were: thi-fr, the thickness of the frontal skull; thi-oc, the thickness of the occipital skull; n-opi, the length nasion-opisthocranium, and n-na, the nasal bone length. The angular variables were: s-n-pg, the mandibular prognathism, and s-n/tgo-gn, the mandibular inclination. The mean and the standard deviation (SD) were calculated for each of the selected variables in the HR group. For each variable the SD in the control group was assumed to be equal to the SD in the HR group and an expected mean-difference (DIFF) was identified between the mean of the HR group and the mean of the control group. The DIFF were chosen according to a subjective judgment of the expected clinical deviations in the HR group compared with healthy controls. The results of the power calculations are shown in Table III together with the values used for SD, the DIFF, and the corresponding effect size (DIFF/SD). Power calculations according to the categorical variables were not used to determine the size of the control group.

| Variable | HR patients | | | Controls | | |
	Mean[*]	SD	Expected difference[#]	Effect size	N[§]	Power
thi-oc (mm)	9.1	2.9	2	0.61	60	0.88
thi-fr (mm)	9.2	3.3	2	0.69	60	0.96
n-opi (mm)	183	13	7	0.54	60	0.82
n-na (mm)	19	4.1	3	0.73	50	0.94
n-s-pg (degree)	79	5.1	3	0.59	50	0.85
s-n/tgo-gn (degree)	26	9.2	5	0.54	60	0.82

Table III. *Calculation of the size of the control group.*

[*] *Mean of the specified variable in 51 HR patients*

[#] *The expected difference in mean between HR patients and controls for the specified variable*

[§] *The calculated number of controls to achieve the power indicated at the variable*

Based on the power calculations, a control group of 60–70 individuals was estimated to give sufficient power (power > 80%) to identify relevant differences at the 5% level of significance.

Members of the control group were recruited among the patients, the students, and the employees at the Department of Dentistry, Aarhus University, and among the employees at the Department of Maxillofacial Surgery, Aarhus University Hospital. In addition, already existing profile radiographs of 30 children (age < 18 years) from two large municipal dental services (Aarhus and Odense) were included in the control group. In adults (age ≥ 18 years), the inclusion criteria for the control group were: 1) Scandinavian ethnicity, 2) no chronic diseases, except for allergies, 3) a minimum of 24 permanent teeth 4) normal, or only minor deviations from normal occlusion, 5) no history of orthodontic treatment, and 6) no craniofacial anomaly. In children, the inclusion criteria for the control group were: 1) Scandinavian ethnicity, 2) no chronic diseases, except for allergies, 3) no dental agenesis or former extraction of permanent teeth 4) normal, or only minor deviations from normal occlusion, 5) no history of orthodontic treatment, and 6) no craniofacial anomaly. PlanMeca Promax was obligatory as the X-ray equipment and with only minor absences, the whole skull should be visualized. In total, the control group consisted of 79 participants (Table II).

For the adult controls, the radiographic examinations were performed in the period from the 12th of March until the 23th of October 2009.

4. Methods

4.1. Radiological method

Profile radiographs (lateral cephalograms) and postero-anterior radiographs (PA cephalograms) were obtained in a standardized fashion as described by Bjørk (Bjørk, 1968) and Solow (Solow, 1966). Planmeca Promax$^©$ (Planmeca Oy, Helsinki, Finland) was used as the radiographic equipment. The sensor-focus distance was 1.50 meter and the enlargement factor was 1.13. During the exposure, the head of the patient was fixed in a rigid cephalostat, and the patients were instructed to keep their teeth in occlusion. The head posture was adjusted to the best fit of the borders of the sensor, and the head was not intended to be in the "natural head position", which is the position normally used for the study of the relationship between the facial morphology and the head position (Solow & Tallgren, 1971; Siersbaek-Nielsen & Solow, 1982). During the exposure for the PA cephalogram, the head was postured with the Frankfort plane horizontal. The radiographs were taken by skilled staff-members at Section of Radiology, Department of Odontology, Health, Aarhus University or Department of Maxillofacial Surgery, Aarhus University Hospital. It was intended to include the whole skull of the cranium as well as the upper cervical spine (C1-C5). In some patients, more than one radiograph was necessary to include all structures.

4.2. Analyses of the cephalograms

The analyses of the cephalograms were divided into two main groups: 1) the profile cephalometric analyses, which included the dimensions and the angles of the craniofacial profile and the cervical vertebral column, and 2) a visual assessment of the anatomical structures. The later included a classification of the structures according to established standards of the morphology of ST and the cervical vertebrae, and an assessment of the occurrence of intra- and extra-cranial calcifications.

4.2.1. Cephalometric analyses

Overall cephalometric analysis

The metric analyses of the radiographs were performed using the software for cephalometric analysis, Pordios$^®$ (Institute of Orthodontic Computer Science, Aarhus, Denmark). For the overall analysis of the craniofacial structures, 25 cephalometric landmarks were digitized (Fig. 4). Twenty-seven linear and 10 angular variables were calculated by the software. The variables of the cranial base and the facial skeleton were defined according to definitions by Bjørk (Bjørk, 1975), Solow (Solow, 1966), and McNamara (McNamara, 1984). The variables of the neurocranium were defined as described by Axelsson and coworkers (Axelsson *et al.*, 2003). Furthermore, variables describing the size and the morphology of the posterior cranial fossa were included (Caspersen *et al.*, 2010) (Fig. 4).
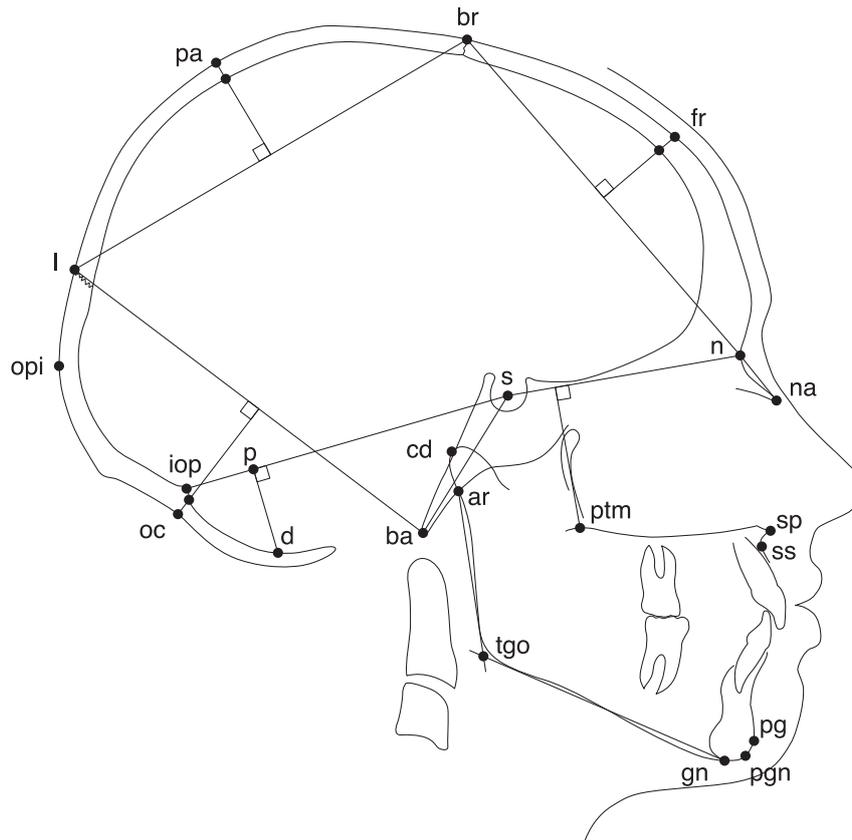
Fig. 4. Schematic drawing of the skull with the 25 landmarks used for measuring the cephalometric variables. *At the landmarks oc, pa, and fr, both the inner and the outer contour of the theca are marked.*

Cranial base		Theca	
n-s-ba	cranial base angle to basion	thi-fr	theca-thickness at frontale
n-s-ar	cranial base angle to articulare	thi-pa	theca-thickness at parietale
s-n	length of anterior cranial base	thi-oc	theca-thickness at occipitale
s-ba	length of posterior cranial base	s-n-fr	angle sella-nasion-frontale
Posterior cranial fossa		**Maxilla**	
d-p	height point d to point p	ptm-sp	length pterygomaxillare-anterior nasal spine
thi-iop	theca-thickness at int. occipital protuberance	n-sp	height nasion-anterior nasal spine
d-s-iop	angle point d-sella-int. occipital protuberance	ptm/s-n	heigth pterygomaxillare to nasion-sella line
s-iop	length sella-int. occipital protuberance	cd-ss	length condylion-subspinale
s-d	length sella to point d	s-n-ss	angle sella-nasion-subspinale
		s-n/ptm-sp	angle sella-nasion / pterygomaxillare-ant. nasal spine
Neurocranium		**Nasal bone & mandible**	
n-br	length nasion- bregma	n-na	length of nasal bone
n-l	length nasion-bregma	tgo-gn	length gonion-gnathion
n-opi	length nasion-opisthocranion	cd-tgo	height condylion-gonion
ba-br	length basion-bregma	n-gn	height nasion-gnathion
ba-l	length basion-lambda	cd-pgn	length condylion-prognathion
br-l	length bregma-lambda	s-n-pg	angle sella-nasion-pogonion
s-fr	length sella-frontale	s-n/tgo-gn	angle sella-nasion/gonion-gnathion
s-br	length sella bregma	ar-tgo-gn	jaw angle articulare-gonion-gnathion
s-l	length sella-lambda	tgo-gn-ar	beta angle gonion-gnathion-articulare

Measurements of minor cranial structures

Selected craniofacial structures were subjected to detailed analyses. The height and the width of the frontal sinus were measured by the software, according to the definitions by Brown and coworkers. (Brown *et al.*, 1984), Ertürk (Erturk, 1968), and Dostalova and coworkers (Dostalova *et al.*, 2003) (Fig. 5A). The length of the nasal bone and the angulation of the nasal bone in relation to the cranial base (S-N) were measured in accordance with the definition by Solow (Solow, 1966). In addition, the size of ST was measured according to definitions by Silverman (Silverman, 1957) (Fig. 5B).
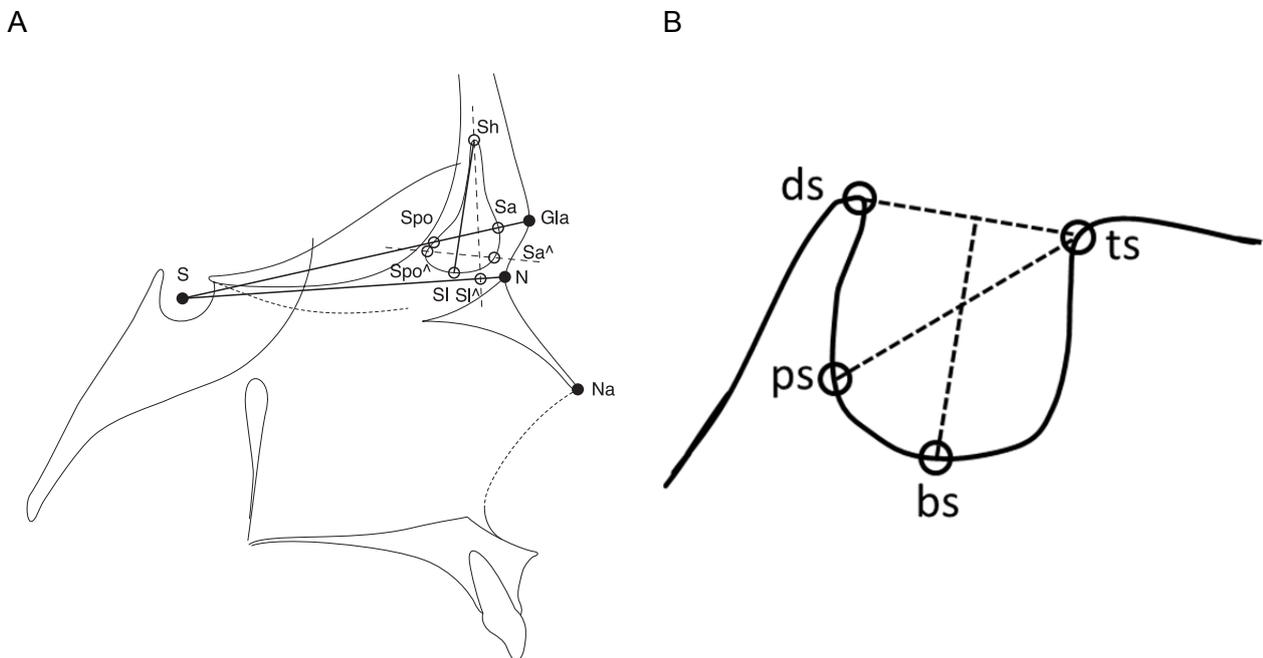
Fig. 5. Landmarks and cephalometric variables of the frontal sinus, the nasal bone, and ST. *A: 1) The frontal sinus: Sh-Sl: the absolute height of the sinus; Spo^-Sa^: the greatest anterior-posterior width perpendicular to the axis (Sh-Sl); Spo-Sa: the anterior-posterior width at the line S-Gla; Sh-Sl^: the projection height, i.e. the distance between Sh and Sl^ (i.e. the projection of Sh on S-N line). 2) The nasal bone: N-Na: the length of the bone; S-N-Na: the inclination (degree) of the nasal bone (N-Na) in relation to the anterior cranial base (S-N). B: ST dimensions: the length ts-ds (tuberculum sella - dorsum sella), the diameter ts-ps (the largest distance from the tuberculum sella to the posterior wall), and the depth bs-ts/ds (the perpendicular distance from the bottom of ST to the line ts-ds)*

Morphometric measurements of the nasal bone

As a separate part of the cephalometric analyses, the nasal bone morphology was assessed by measuring the nasal bone dimensions at lines perpendicular to the axis of the nasal bone (Fig. 6). The axis of the nasal bone was defined by the midpoint of a line N-N^ (Nmi) and Na. The point N^

was defined as the intersection of the lower border of the nasal bone and a perpendicular line to the line N-Na through N. N-N^ was regarded as a constructed fronto-nasal suture. Perpendicular to the nasal axis, multiple lines were constructed with a distance of three mm between the lines. The lines were numbered 0-11: proximally, line "0" was the base line passing through N (L0-N), line "11" was the most distal line. The intersections between the perpendicular lines and the upper and the lower border were used as the landmarks (U1-U11 and L0-L11, respectively). The distances from the N-Na line to the upper and the lower border, and the distances between the borders (L0-N, L1-U1, L2-U2, etc.) were calculated by the software. In addition, the ratio between the length of the basal line and the length of the nasal axis was calculated (base/axis: L0-N/Nmi-Na), and the area of the polygon defined by the landmarks on the upper and the lower borders of the nasal bone was calculated. A morphometric assessment of the nasal bone was obtained by the ratio between the dimension of the baseline and the axis of the nasal bone (L0-N/Nmi-Na). The ratio was defined as "low" when below 0.5 (i.e., a short and robust appearance of the nasal bone) and "high" when above 0.5 (i.e., a long and slender appearance of the nasal bone).
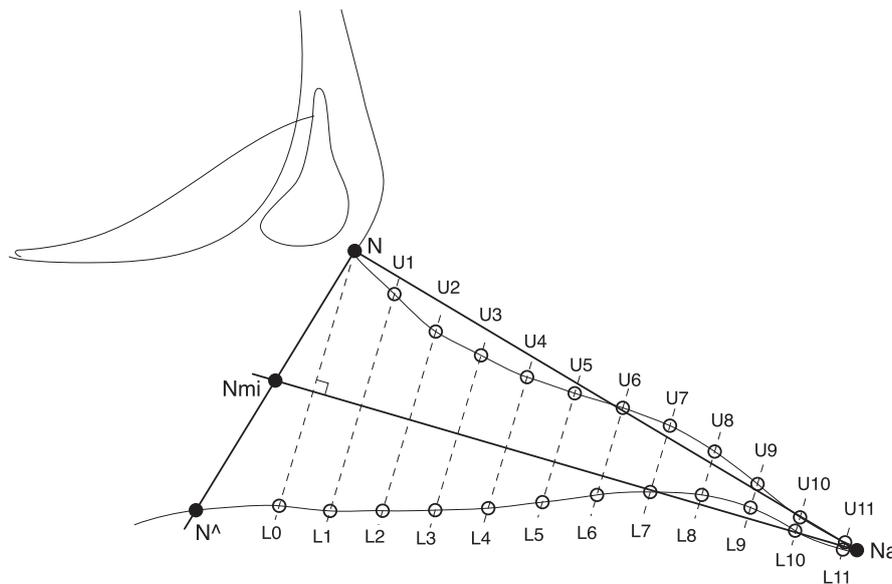
Fig. 6. Analysis of the morphology of the nasal bone. *N-N^: line perpendicular to line N-Na. Nmi: the midpoint of the line N-N^; Nmi-Na: the axis of the nasal bone; N-L0: the base of the nasal bone perpendicular to the axis (Nmi-Na). Lines number 1-11 are perpendicular to the axis (Nmi-Na), with three mm interline distance, and crossing the upper and lower border of the nasal bone in U1-U11 and L1-L11, respectively.*

Measurements of atlas and axis

The dimensions of the atlas and the axis were measured according to Huggare (Huggare, 1991) (Fig. 7).The landmarks were digitized directly on the cephalograms, and the dimensions of the atlas and the axis were calculated by the software (Huggare, 1991).
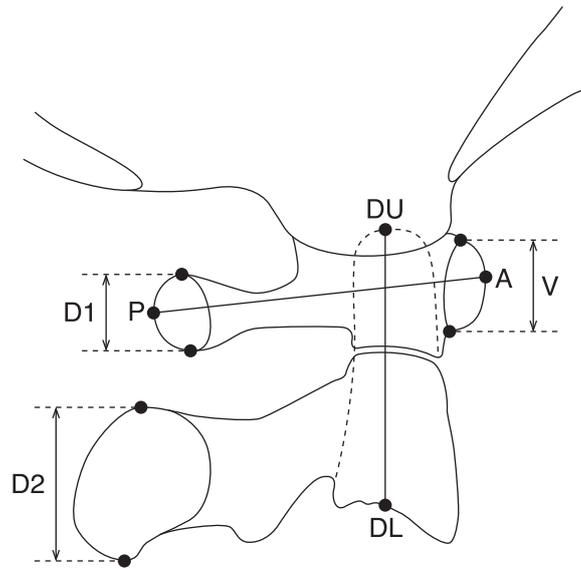
***Fig. 7. The reference points and variables used for the analyses of the dimensions of the atlas and the axis**. Atlas: **V**, the height of the anterior tubercle; **D1**, the height of the dorsal arch; **A-P**, the length between the most anterior point **(A)** of the tubercle and the most posterior point **(P)** on the dorsal arch. Axis: **D2**, the height of the dorsal arch; **Dens**, the height of the dens from midpoint of the lower border **(DL)** to the uppermost point **(DU)**. The height measurements are perpendicular to the line A-P.*

4.2.2. Visual assessment of anatomical structures

Upper cervical vertebrae

The morphology of the upper cervical vertebrae (C1 – C5) was visually assessed according to the classification proposed by Sandham (Sandham, 1986) as PAD or FUS. PAD was subdivided into the partial cleft (i.e., a failure of the posterior part of the neural arch to fuse) and the dehiscence (i.e., a failure of a part of the vertebral unit to develop) (Fig. 9, A-B). FUS was subdivided into the fusion (i.e., a fusion of one unit with another), the block fusion (i.e., a fusion of one unit with another, including the vertebral bodies), and the occipitalization (i.e., a assimilation of the atlas and the occipital bone) (Fig. 9, C-D-E) (Sandham, 1986). The assessment was performed by the author of the dissertation, and all the assessments were checked by one of the supervisors (LS) in a blinded fashion. If any doubt regarding the assessment of the cervical vertebral column, the vertebral column was registered as "no morphological deviations".
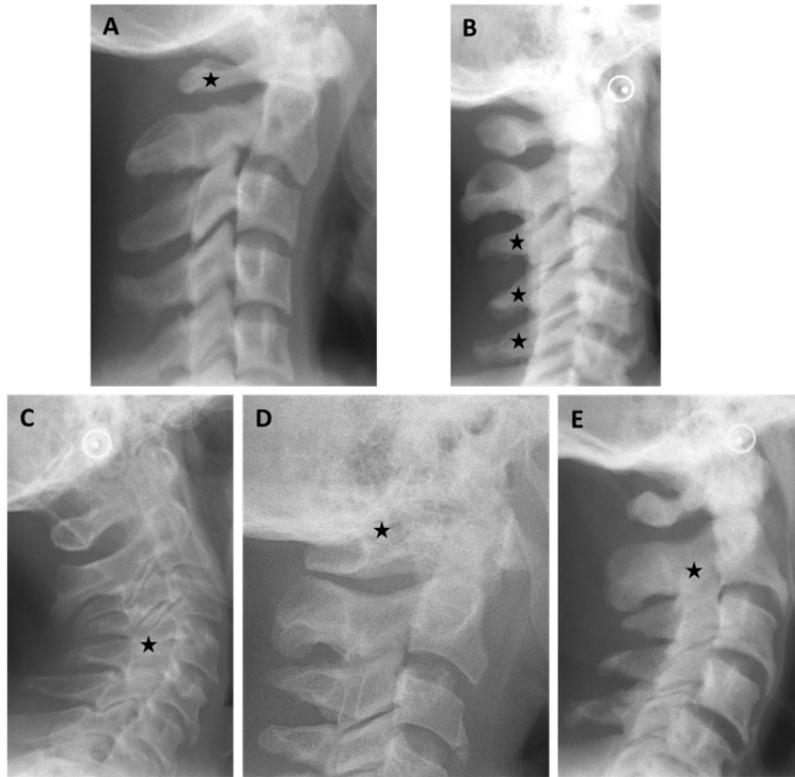
Fig. 9. Classification of the cervical vertebral anomalies (CVA). *The posterior arch deficiencies (PAD) and the fusions (FUS) of the cervical vertebrae in HR patients illustrated on radiographs: A, a partial cleft C1; B, a dehiscence of the posterior neural arch of C3-4-5; C, a fusion of C3-4-5; D, an occipitalization; E, a fusion of C2-3. Stars indicate the locations of PAD or FUS.*

ST morphology

The morphology of ST was visually assessed and classified according to the definitions by Axelsson and coworkers (Axelsson *et al*., 2004b). The contour of the ST was described as a standard ST type according the schematic drawing reported previously (Bjørk & Skieller, 1983). In addition to the standard ST type, five variations of normal morphology have been defined: an oblique anterior ST wall, a ST bridging, a double contour of the ST floor, irregularities (notching) of the posterior wall of the ST, and a pyramidal shape of the dorsum sella (Axelsson *et al.*, 2004b) (Fig. 8). If the ST morphology could not be categorized according to the definitions, the ST was categorized as "unclassified".
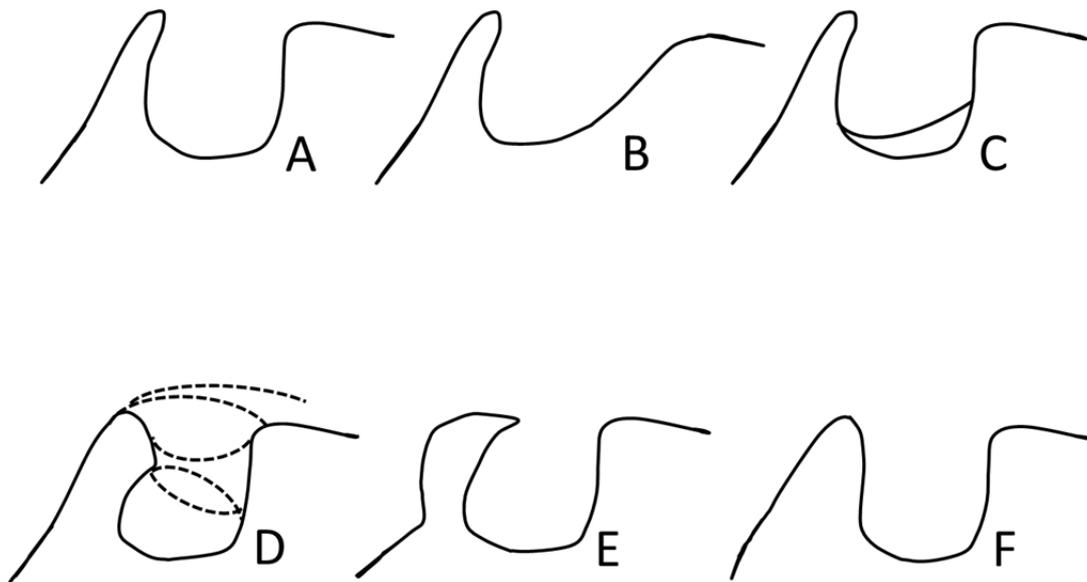
Fig. 8. Classification of ST morphology according to Axelsson and coworkers (Axelsson et al., 2004b). *A: the standard ST type: B: oblique anterior ST wall; C: double contour of the ST floor; D: ST bridge; E: irregularity (notching) in the posterior part of the ST; F: pyramidal shape of the dorsum sella.*

4.2.3. Intra- and extra-cranial calcifications

The presence of diffuse and indistinct radiopacities in relation to the intracranial surface of the frontal theca was described as intracranial calcifications. By the visual assessment of the lateral cephalograms, the calcifications were assessed as present or absent. The localization of the radiopacities in the transverse plane was assessed on the PA cephalogram. The nuchal ligament attaches to the posterior surface of the occipital bone at the external occipital prominence and at the occipital crest. By visual assessment of the cephalograms, the radiographic sign of calcifications at the cranial end of the ligament was recorded as present or absent.

4.2.4. Reliability

The digitizing of all radiographs (N = 132) was performed by one person (the author of the thesis) after a randomization of the radiographs in order to blind the observer to the health status (HR patient or control) of the individuals. By random, 22 radiographs were selected for the assessment of the intra-examiner reliability. The radiographs selected for the re-digitizing were included in the overall randomization of the radiographs in order to blind the observer to whether the radiographs were read before. The systematic error was estimated by calculating the differences between the

two sets of recording, and the differences for none of the variables were significantly different from zero ($p > 0.05$). For each of the cephalometric variables, the method error was calculated as described by Dahlberg (Dahlberg, 1940), and the coefficient of reliability (R) was estimated according to Houston (Houston, 1983). According to the overall craniofacial variables, the method error ranged from 0.08 to 2.39 and the reliability coefficient ranged from 0.91 to 1.00. According to the variables of the nasal bone and the frontal sinus, the method error ranged from 0.01 to 2.29 (the nasal bone) and from 0.64 to 4.38 (the frontal sinus). With the exception of the width measurements of the nasal bone (L0-L11: $0.74 < R < 0.99$), the reliability coefficient ranged from 0.92 to 0.99. According to the linear variables of the atlas and the axis, the method error ranged from 0.17 to 0.65 and the reliability coefficient ranged from 0.82 to 0.95.

To examine the reliability of the visual assessment of the morphological characteristics of ST, twenty-one radiographs were randomly selected. Independently, ST was classified by two examiners and the reliability was analyzed by kappa test ($K = 0.69$).

The reliability of the visual assessment of the morphological characteristics of the cervical vertebrae units has been reported previously ($K = 0.82$) (Sonnesen *et al.*, 2007).

4.3. Mineralizing enthesopathies

The presence of mineralizing enthesopathy of ligaments and tendons in relation to the vertebral column, ankles, knees, and hips was assessed from the evaluation of X-rays of the ankles, knees, pelvis including hips and lumbar spine in 31 of the 36 HR patients by a radiologist (Dr. M.R. Poulsen, Odense University Hospital). Similar X-rays were not available in the control group. Mineralizing enthesopathies were defined as bone proliferation at sites of ligament attachments or as calcification of ligaments. The total number of sites with mineralizing enthesopathy and a grouping according to the number of sites (0-1; 2-6, and ≥ 7) was recorded. In addition, vertebral enthesopathy (i.e., a mineralizing enthesopathy at the collateral ligaments of the vertebral column) was recorded as present or absent.

4.4. Medical treatment during childhood

The medical treatment history during childhood (age 0-18 years) was obtained by a review of the medical files and confirmed by interview (Beck-Nielsen, 2012). "Continued treatment" was defined as treatment with both calcitriol and phosphate initiated at least from age 4 years and continued without significant interruptions until 18 years of age. "Periodical treatment" was defined as treatment with a total duration of less than 10 years. "No treatment" was defined as treatment with a total duration of less than one year.

4.5. Data management

In all papers, the data were analyzed using Stata® 11.0 (StataCorp, College Station, TX). *P*-values equal to or below 0.05 were considered statistically significant.

4.5.1. Paper I. Craniofacial morphology

The study included all 132 participants, and a two-sided chi-squared test was used to compare the gender distribution in the HR group and in the control group. For each gender, the age distributions in the two groups were compared with an unpaired *t*-test.

The comparison of the cephalometric measurements between the HR patients and the controls was assessed by regression analysis. In the HR group as well as in the control group, the cephalometric measurements were examined visually for normality using Q-Q plots and histograms, and in both groups they were all found to be normally distributed. The cephalometric measurements were numeric outcome variables (linear or angular measurements), and the effect of health-status (i.e., HR or control), age and gender upon the cephalometric measurements were assessed by linear regression analysis. The patients of the study belonged to 21 different families with 1–13 participants in each family (1-2 in 15 families; 3-5 in four families; 7-13 in two families). With the purpose to allow for familiar dependence, the regression estimates were adjusted for the clustering. The analysis revealed an effect of the age, the gender, and the health-status. The potential interactions between the effect of the age and the health-status and between the effect of the gender and the health-status were assessed in the regression analysis.

In the presentation of the results, the cephalometric variables were grouped according to the bony origin of the structures (Fig. 2). The means and the standard deviations were used as the descriptive statistics.

4.5.2. Paper II. Nasal bone and frontal sinus

Paper II excluded children (age < 18 years), in whom the structures under investigation (the frontal sinus and the nasal bone) develop dramatically during the growth and keep a more constant size in the adulthood (Lestrel *et al.*, 1991; Ruf & Pancherz, 1996). Thus, the interrelationship between the age and the dimension in the childhood was not expected to be the same as in the adulthood, and only adults were included in the analyses.

The gender differences between the adult HR group and the adult control group were assessed by the two-sided chi-squared test. For each gender, the age distributions in the two groups were compared with the unpaired *t*-test.

Dimensions of the nasal bone and the frontal sinus

The comparison of the cephalometric measurements between the HR patients and the controls was assessed by a regression analysis. In both groups, the normality of the distribution of measurements was assessed as in paper I. The linear measurements of the nasal bone and the frontal sinus were the outcome variables. The effect of health-status, age, and gender upon the cephalometric measurements was assessed by linear regression analysis. To allow for familiar dependence, the regression estimates were adjusted for clustering. The potential interactions between the effect of the age and the health-status and between the effect of the gender and the health-status were assessed in the regression analysis.

Morphology of the nasal bone

The morphology of the nasal bone was visualized graphically by plotting the mean distances from the line N-Na to the nasal bone, i.e., the upper and lower border, respectively. In addition, the morphology was expressed as the proximal width divided by the length of the nasal bone.

Correlation with the HR severity

In the group of adult HR patients, it was intended to analyze if the potential morphological deviation of the nasal bone was correlated with the severity of the disease (i.e., the skeletal impact of HR). Therefore, the morphometric variable of the nasal bone (ratio base/axis; L0-N/Nmi-Na) was converted into a categorical variable by defining a low and a high ratio, ratio < 0.5 and ratio > 0.5, respectively. Accordingly to the medical criteria, the HR patients have been classified with either severely or mildly affected (Beck-Nielsen *et al.*, 2010). For the present analysis, the variable was dichotomized, i.e, the severe skeletal impact of HR was present or absent. In the group of adult HR patients, the proportion of the high-ratio base/axis (L0-N/Nmi-Na) according to the presence of a severe skeletal impact was compared by a two-sided chi-squared test.

4.5.3. Paper III. Cervical spine

Dimensions of the cervical vertebrae

The linear measurements of the atlas and the axis in the adult HR patients compared with the controls were assessed by the regression analysis. In both groups of adults, the normality of the distribution of the measurements was assessed as in paper I. Linear measurements of the atlas and the axis were the outcome variables. The effect of the health status (i.e., HR patient or

control), the age, and the gender upon the linear measurements of the atlas and the axis were assessed by linear regression analysis. To allow for the familiar dependence, the regression estimates were adjusted for the clustering. The potential interactions between the effect of the age and the health-status and between the effect of the gender and the health-status were assessed in the regression analysis.

Morphology of the cervical vertebrae

The morphological deviations of the vertebrae were analyzed by assessing the presence of FUS and PAD in the adult participants with and without HR. The presence of FUS and PAD in the HR patients in comparison with the controls was evaluated by the chi-squared test

Associations between the cervical column and the craniofacial structures

Associations between the upper cervical column and the craniofacial structures were assessed in the whole group of adults (HR patients and controls). The associations between the linear measurements of the cervical column and the cephalometric variables of the craniofacial structures were assessed by linear regression analysis, adjusting for the effect of the health status (i.e., HR or control), the gender, and the clustering. The association between CVA (i.e., PAD and FUS) and the cephalometric variables of the craniofacial structures were evaluated by logistic regression analysis, adjusting for the effect of health status (i.e., HR or control), the gender, the age, and clustering. The potential interactions between the effect of the cephalometric variable and the health status and the gender were assessed, respectively.

Correlation with the HR severity

It was intended to analyze if the dimensional deviations of the atlas and the axis as well as the presence of CVA (i.e., FUS or PAD) were correlated with the severity of the disease (i.e., the skeletal impact of HR). The variable of the skeletal severity was dichotomized, i.e., the severe skeletal impact was present or absent. Thus, in the group of adult HR patients, the associations between the linear variables of the cervical column and the presence of severe skeletal impact were assessed by linear regression analysis, adjusting for the effect of the age, the gender, and the clustering. In the group of adult HR patients, the association between the presence of CVA (i.e., FUS or PAD) and the presence of severe skeletal impact was evaluated by the chi-squared test.

4.5.4. Paper IV. Intra- and extra-cranial calcifications

Prevalence of calcifications

The prevalence of HR patients with diffuse and indistinct radiopacities in relation to the intracranial surface of the frontal theca and the prevalence of HR patients with a calcification of the nuchal ligament were compared with the controls by the Fischer`s exact test. In addition, the presence of nuchal ligament calcifications was assessed by logistic regression analysis, adjusting for the effect of the age, the gender, and the family clustering.

Correlation with mineralizing enthesopathy

In the group of HR patients, the associations between the presence of vertebral enthesopathies and intracranial calcifications respectively nuchal ligament calcifications were assessed by the Fischer`s exact test. The associations between the enthesopathy grouping (total sites: 0-1, 2-6, and ≥ 7) and intracranial calcifications respectively nuchal ligament calcifications were assessed by the Fischer`s exact test. Furthermore, the association between intracranial or nuchal ligament calcifications and the total number of sites with mineralizing enthesopathy was assessed by logistic regression analysis adjusted for the effect of age, gender, and family clustering.

Correlation with the HR severity

In the group of HR patients, the prevalence of patients with intracranial calcifications was compared in terms of the severity of the skeletal HR impact by the Fischer's exact test. The prevalence of the patients with calcification of the nuchal ligament was compared in terms of the severity of the skeletal HR impact by the two-sided chi-squared test.

Correlation with medical treatment

In the group of HR patients, the prevalence of the patients with signs of intracranial calcifications and the prevalence of the patients with signs of calcification of the nuchal ligament were compared in terms of the childhood medical treatment by Fischer's exact test.

4.5.5. Morphology of the ST

The prevalence of each of the specified types of ST morphology (the standard ST type and the five normal deviations) (Axelsson *et al.*, 2004b) in the adult HR patients was compared with the controls by the Fischer`s exact test. In addition, the presence of the standard types of ST morphology was evaluated by logistic regression analysis, adjusting for the effect of the health status (HR patient or control), the age, the gender, and the family clustering.

The ST dimensions in the adult HR patients compared with the controls were assessed by linear regression analysis adjusting for the effect of the age, the gender, and the family clustering. In the

regression analysis, the potential interactions between the effect of the age and the health status and between the effect of the gender and the health-status were assessed. According to the gender, the means and the standard deviation of the cephalometric variables were used as the descriptive statistics.

5. Results

The main results of the four papers, on which the thesis is based, are presented in this chapter. A more detailed description of the results can be found in the four papers, which also are included as a part of the thesis.

5.1. Paper I. Craniofacial morphology

The proportion of females in the whole HR group (i.e., the female children and adults) (68%) was not significantly higher than in the control group (53%) (p = 0.091). Furthermore, the differences in the mean age between the HR group and the controls were not statistically significant, irrespectively of gender (Table II).

Tables with the cephalometric data can be viewed in the appendix of the thesis (Appendix; E-Table I–VI). The individual table is characterized by the bony origin of the structures represented by the cephalometric data of the table. The data are presented according to the gender and the age categories (age < 18 years, age ≥ 18 years). In addition, p-values from the regression analysis are included as well as the information on significant interactions between the health status (i.e., HR patients or controls) and the age, or between the health status and the gender. A graphic summary of the differences between the HR patients and the controls is presented in Fig. 10.
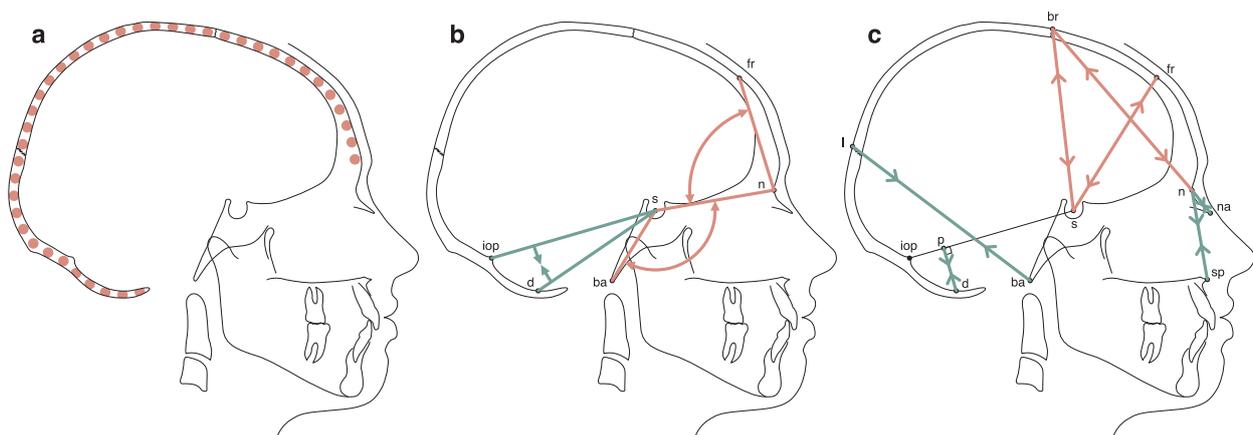
Fig. 10. Cranial morphology of the HR patients compared with the controls. A graphic summary of the significant differences.
a. Red dotted line: an increased thickness of the theca
b. Red lines: increased angles (n-s-ba, s-n-fr); green lines: decreased angle (d-s-iop
c. Red arrows: increased dimensions (s-br, s-fr, n-br); green arrows: decreased dimensions (ba-l, d-p, n-na, n-sp)

5.1.1. Endochondral-developed bone

The cranial base angle (n-s-ba and n-s-ar) was significantly increased in the HR patients compared with the controls (p = 0.001) (Appendix; E-Table I), which indicated a platybasia (i.e., a flat cranial base) (Fig. 10). In contrast, no significant difference in the dimensions of the structures of the cranial base was found.

In the posterior cranial fossa, the angle, d-s-iop, the depth, d-p, and the length, p-iop were all significantly reduced in the HR patients, which indicated a short and a flattened posterior cranial fossa. The thickness of the skull at the cephalometric landmark iop was significantly increased (Appendix; E-Table II) (Fig. 10).

5.1.2. Intramembraneous-developed bone

The dimensions of the anterior part of the neurocranium were significantly increased in the HR patients compared with the controls. In contrast, the length of the linear variable, ba-l was significantly reduced (Appendix; E-Table III) (Fig. 10).

The thickness of the theca and the frontal prominence were significantly increased in HR patients (Appendix; E-Table IV) (Fig. 10). The difference of the parietal thickness between the HR patients and the controls was much larger for the males than for the females, and the difference according to gender was significant (p = 0.020). In addition, the frontal prominence (s-n-fr) was affected by a significant interaction between the effect of health-status and the effect of age. The prominence decreased with increasing age in both the HR group and the control group, but the age dependence was significantly stronger in the HR patients (p = 0.029).

The anterior maxillary height (n-sp) was significantly reduced in the HR patients (Appendix; E-Table V) (Fig. 10). The posterior maxillary height (ptm-NL) was affected by interaction between the effect of the health-status and the effect of age. The height increased with increasing age in both groups, but the age dependence of the posterior maxillary height was significantly stronger in the HR group compared to the control group (p = 0.026).

The length of the nasal bone (n-na) was significantly reduced in the HR group, but none of the mandibular variables were significantly affected by the health-status (Appendix; E-Table VI) (Fig. 10).

5.2. Paper II. Nasal bone and frontal sinus

The proportion of females in the adult HR group (67%) did not significantly exceed the proportion of females in the adult control group (53%) (p = 0.208). Irrespectively of the gender, the mean age of the adult HR group and the adult control group was not significantly different (Table II).

5.2.1. Morphology and dimensions

Morphology of the nasal bone

The morphology of the nasal bone was illustrated by the mean distances from the line N-Na to the upper and the lower border of the nasal bone (Fig. 11).

Females   **Males**
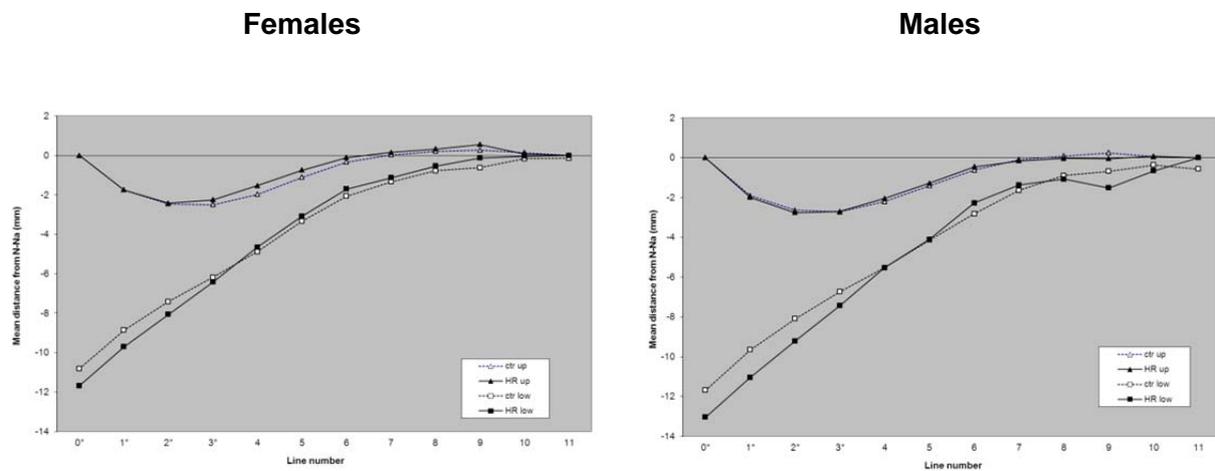
Fig. 11. The morphology of the nasal bone in the HR patients and the controls according to the gender. The mean distances from the line N-Na to the upper (up) and the lower (low) border of the nasal bone measured at the perpendicular lines (No. 0-11) to the axis of the nasal bone.
* The line numbers with a significant difference in the width of the nasal bone, the HR patients in comparison with the controls after adjustment for the effect of the gender, the age, and clustering.

In addition, the morphology of the nasal bone was expressed by the ratio base/axis. This ratio was significantly increased in the HR patients compared with the controls (Table IV).

Dimensions of the nasal bone and the frontal sinus

The height and the width of the frontal sinus were not significantly different in the adult HR patients and the controls ($p \geq 0.406$) (Table IV).

Variable	Males				Females				Adjusted comparison HR and control
	Control		HR		Control		HR		
	N = 23		N = 12		N = 26		N = 24		
Frontal sinus	mean	SD	mean	SD	mean	SD	mean	SD	*p*-value
Spo^-Sa^	12.67	4.42	13.16	5.17	9.96	3.36	10.07	5.52	0.815
Sh-Sl^	27.12	8.50	23.94	10.42	26.02	9.47	23.63	13.60	0.406
Sh-Sl	28.16	8.71	27.21	11.56	28.90	10.67	25.59	13.94	0.517
Spo-Sa	13.89	4.94	15.18	7.11	10.49	4.96	10.09	6.21	0.863
Nasal bone									
N-Na	27.12	3.97	24.37	4.90	25.24	4.14	24.15	3.39	0.122
NNa-NS	117.72	6.08	117.03	4.57	114.97	5.75	114.23	6.33	0.543
base/axis	0.45	0.07	0.58	0.12	0.45	0.09	0.52	0.12	0.010
area	98.94	27.06	103.97	25.05	90.29	26.38	94.76	25.68	0.440

Table IV. Descriptive statistics (means and standard deviations) of the cephalometric measurements in the fronto-nasal field of HR patients according to the gender and compared to the healthy controls.
p-values are from the regression analysis after adjustment for the effect of the gender, the age, and clustering

The regression analysis with the nasal bone length (N – Na) as the outcome variable, revealed a negative regression-coefficient (β) for the effect of HR (β = -1.73; 95% CI: -4.94, 0.48), which indicated a reduced nasal bone length in the adult HR patients. However, the coefficient did not reach the level of statistical significance ($p = 0.122$) (Table IV). Proximally, the width of the nasal bone was greater in the HR patients compared with the controls. The significant differences were restricted to the four proximal lines, the differences in the width being: L0: 1.06 ($p = 0.014$), L1: 1.04 ($p = 0.005$), L2: 0.08 ($p = 0.002$), and L3: 0.59 ($p = 0.007$).

5.2.2. Nasal bone morphology and HR severity

In HR patients with a severe skeletal impact of HR, the percentage of "high" ratio base/axis was almost twice that in the group of the mildly affected patients (Table V).

Nasal base/axis	N	Skeletal severity		p-value
		Mild	Severe	
Low	16	9 (56%)	7 (44%)	0.056
High	20	5 (25%)	15 (75%)	

Table V. Relation between the skeletal severity and the ratio nasal-base/nasal-axis (N-L0/Nmi-Na) in 36 HR-patients. *The numbers and percentages in the low-ratio group compared with the high-ratio group according to the skeletal severity.*

Low: the ratio nasal base/axis < 0.5; High: the ratio nasal base/axis > 0.5

p-value are from the chi-squared test

5.3. Paper III. Cervical spine

5.3.1. Cervical vertebrae morphology and dimensions

Morphology of the cervical vertebrae

In the adult group of HR patients, the prevalence of FUS was large compared with the controls ($p < 0.001$, Table VI), and the occipitalization of axis was the dominant finding ($p < 0.001$) (Table VI).

	HR patients		Controls		p-value
	n	%[*]	n	%[*]	
PAD	6	16.7	9	18.4	NS
Partial[a]	2	5.6	4	8.2	NS
Dehis[b]	4	11.1	5	10.2	NS
FUS	14	38.9	3	6.1	< 0.001
Fus[c]	1	2.8	3	6.1	NS
Blo[d]	1	2.8	0	0	NS
Occ[e]	13	36.1	0	0	< 0.001

Table VI. Comparison of the cervical vertebral anomalies (CVA) in 36 HR patients and 49 healthy controls according to the type of PAD and FUS.

p-value are from the chi-squared analysis; NS: p-value > 0.05

* percentage of the total number in the group

a) a partial cleft of the posterior arch; b) a dehiscence of the posterior arch; c) a fusion between C2-C3; d) a block fusion of C3-C4-C5; e) a occipitalization, i.e. a fusion of the atlas and the cranial base

One HR patient had both a fusion of C2-C3 and an occipitalization; two controls had both PAD and FUS

Dimensions of the cervical vertebrae

In the adult HR patients, the height and the length of the atlas and the height of the posterior arch of the axis were large compared with the controls ($p ≤ 0.001$, Table VII).

Axis (C1) & Atlas (C2)		HR patients			Controls			Adjusted comparison HR and control
		n	Mean	SD	n	Mean	SD	*p*-value
C1	Height V	36	12.10	1.38	48	11.43	1.17	< 0.001
C1	Height D1	36	13.27	1.96	49	11.70	1.94	< 0.001
C1	Length A-P	36	54.34	3.31	49	52.81	4.44	0.001
C2	Heigth D2	36	19.58	3.39	49	16.94	2.90	< 0.001
C2	Dens	36	38.12	2.65	49	38.96	3.09	0.392

Table VII. The dimensions (means and standard deviations (SD) in millimeters) of the atlas and the axis in 36 HR patients and 49 controls. A comparison between the groups adjusted for the effect of the gender, the age, and clustering.

p-values are from the linear regression analysis

5.3.2. Cervical vertebral column and craniofacial structures

In the whole study group of adults (i.e., HR patients and controls), the height of the posterior arch of the atlas (D1) and the length of the axis (A-P) were negatively correlated with the cranial base angle (N-S-Ba) (D1: $p = 0.017$; A-P: $p = 0.008$), D1 was positively correlated with the length of the posterior cranial base (s-ba: $p = 0.009$), and negatively correlated with the length of the posterior cranial fossa (s-iop).The anterior (V) and the posterior (D1) height of the atlas were positively correlated with the thickness of the occipital theca (V: $p = 0.015$; D1: $p = 0.001$). The height of the posterior arch of the axis (D2) was positively correlated with the depth of the posterior cranial base (d-s-iop: $p = 0.004$; p-d: $p = 0.013$). Furthermore, the length of the atlas was positively correlated with the degree of mandibular prognatism ($p = 0.042$). The height of the posterior arch of the axis (D2) was affected by an interaction between the effect of the sagittal jaw relation and the effect of the health status (ss-n-sm, $p = 0.003$; ss-n-pg, $p = 0.015$). No other significant interaction was identified.

In the whole group of adults, the only association identified between CVA (i.e., PAD or FUS) and the craniofacial structures was a positive association between FUS and the frontal and the parietal thickness ($p = 0.034$ and $p = 0.003$, respectively). In controls, in contrast to the HR patients, PAD

was associated with the length of the posterior cranial fossa (s-iop, *p* = 0.033). In the females in contrast to the males, FUS was associated with the occipital thickness (thi-oc, *p* = 0.001). But PAD and FUS were not significantly affected by an interaction between the effect of any other cephalometric variables and the health status or the gender, respectively.

5.3.3. Cervical vertebral column and HR severity

In the group of the adult HR patients, the length of the atlas correlated positively (*p* = 0.043) and the height of the dens negatively (*p* = 0.008) with the severity of the skeletal HR impact (Table VIII). In the group of the adult HR patients, the differences in the presence of CVA (i.e., PAD and FUS) depending on the severity of skeletal HR impact were not significant.

	Mild (n = 14)		**Severe** (n = 22)		Adjusted comparison mild vs. severe *p*-value
	Mean	SD	Mean	SD	
Height V	11.44	1.08	12.52	1.41	0.113
Height D1	12.69	1.18	13.63	2.28	0.384
Length A-P	52.74	2.53	55.36	3.39	0.043
Heigth D2	18.59	3.71	20.20	3.09	0.419
Dens	38.39	2.20	37.95	2.94	0.008

Table VIII. The length and height (in millimeters) of the atlas and the axis in 36 adult HR-patients according to the severity of skeletal as defined by Beck-Nielsen and coworkers (Beck-Nielsen et al., 2010).
p-values are from the linear regression analysis with adjustment for the effect of the gender, the age and clustering
n is the number of patients in the specified group

5.4. Paper IV. Intra- and extra-cranial calcifications

5.4.1. Cranial calcifications

The visual assessment of the whole cephalogram revealed six of 36 HR patients (16.7%) with major radiopaque irregularities and three controls with minor irregularities in relation to the inner contour of the frontal bone (Fig. 12, Table IX).

Calcification of the nuchal ligament was visible in 18 of 36 HR patients (50%) and in 10 of 44 assessed controls (23%) (p = 0.018, Table IX). According to the comparison adjusted for the effect of gender, age, and clustering, the difference was even more significant (p = 0.004).

Calcifications	HR patients N = 36		Controls N = 49		
	n	%	n	%	*p*-value
Intracranial major	6	16.7	0	0	0.159**
Intracranial minor	0	0	3	6.1	
Extra-cranial (the nuchal ligament)	18	50	10[a]	23	0.018

Table IX. The distribution of intra- and extra-cranial radiopacities on lateral cephalograms of 36 adult HR patients in comparison with 49 adult controls. The radiopacities indicate calcification of intracranial structures (major or minor) and of the nuchal ligament.

N is the total number in the group

n is the number of individuals with the specified type of radiopacity

p-values are from the Ficher's exact test

** comparison including all signs of intracranial calcifications (major or minor)

[a] *N = 44*
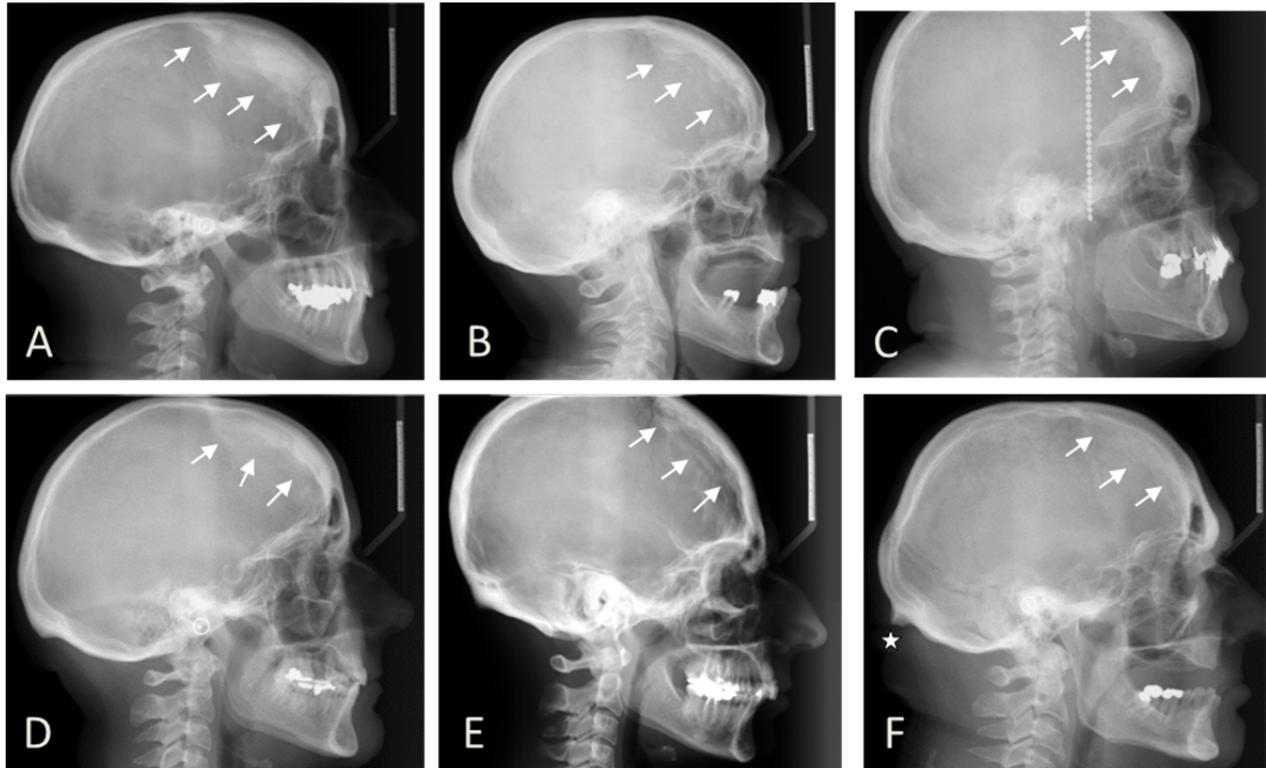
Fig. 12. Lateral cephalograms of the six HR patients with major radiopacities posterior to the frontal bone. The radiopacities are situated intra-cranially and represent supposedly calcifications of dura mater structures.

The arrows point at the radiopacities.

F: The star indicates an example of nuchal ligament calcification.

5.4.2. Cranial calcifications and HR severity

According to the severity of the skeletal impact of HR, the intracranial radiopaque irregularities was identified in four (29%) mildly affected HR patients and in two (9%) severely affected HR patients (p = 0.126). The calcification of the nuchal ligament was identified in four (29%) mildly affected HR patients and in 14 (64%) severely affected HR patients (p = 0.040).

5.4.3. Extra-skeletal calcifications and childhood treatment

The six HR patients with intracranial calcifications were all untreated during childhood. However, the occurrences of neither intracranial nor nuchal ligament calcifications were significantly associated with childhood treatment ($p \geq$ 0.226). Thirteen of 31 HR patients (42%) had at least one site with vertebral enthesopathy. The presence of vertebral enthesopathy correlated negatively with childhood treatment (p = 0.008).

5.5. Sella turcica

5.5.1. ST morphology and dimensions

Morphology of the ST

Few HR patients had the standard ST type compared with the controls (p ≤ 0.021; Table X). In six (16.7%) HR patients and one (2%) control, ST was unclassified without the characteristics of any of the six normal types (Axelsson *et al.*, 2004b). The six HR patients had severe deviations and irregularities of both the anterior and the posterior wall (Fig. 13). In two of them (Fig. 13, D & E), the contour of ST was hardly present.

ST type*	HR patients N = 36		Controls N = 49		
	n	**%**	**n**	**%**	*p-value*
Standard ST type	19	52.8	38	77.6	0.021
Oblique anterior wall	0	0[a]	0	0	-
ST bridge	0	0[a]	0	0	-
Double contour of floor	5	16.7[b]	5	10.2	0.492
Irregularities of post. part of dorsum sella	1	3.3[b]	3	6.4[c]	0.500
Pyramidal shape of dorsum sella	4	10.6[b]	0	0[c]	0.019
More than one type	1	2.8	2	4.1	0.615
Not classified	6	16.7	1	2.0	0.021

Table X. The distribution of the morphological types of ST in 36 HR patients in comparison with 49 controls.

N is the total number in the group

n is the number of individuals with the specified type of ST morphology

* The six normal types of ST morphology (Axelsson et al., 2004b)

p-values are from the Fischer`s exact test

[a] *N = 31,* [b] *N = 30, and* [c] *N = 48 for the specified variable in the group*
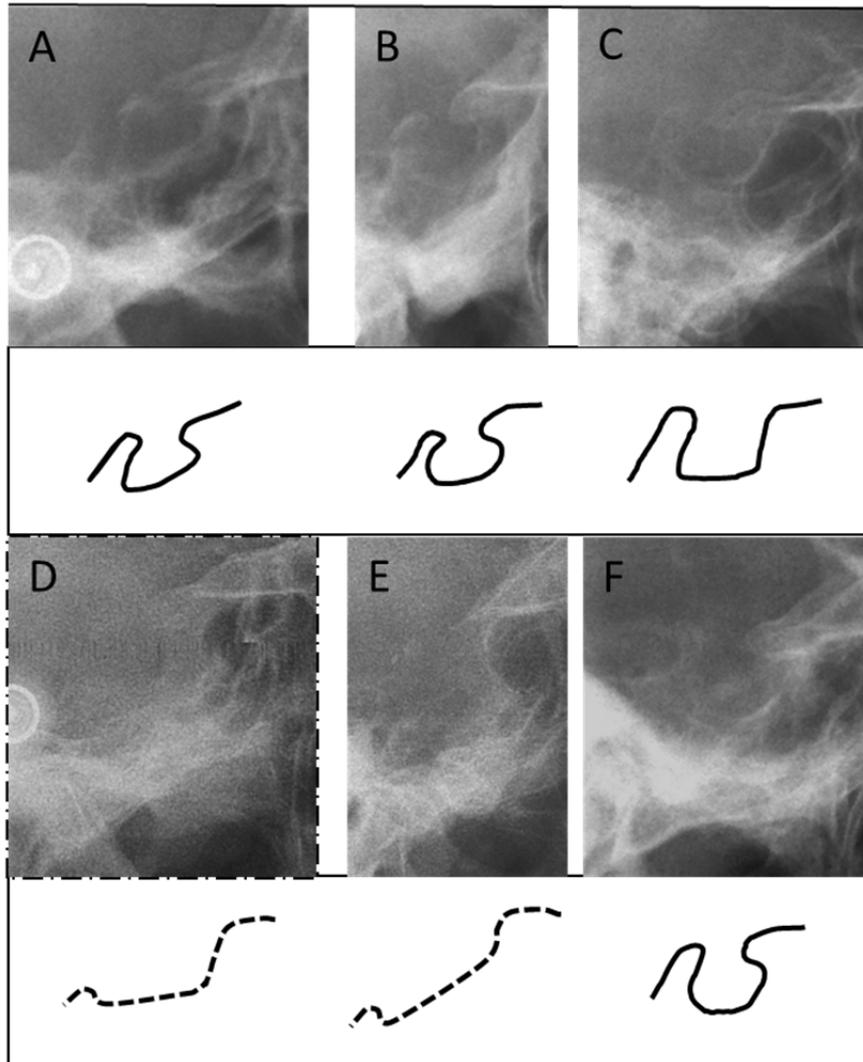
Fig. 13. Details of lateral cephalograms from the six HR patients with unclassified ST morphology. *The morphology fits hardly any of the normal ST types (Axelsson et al., 2004b). Totally or partly, the outlining of the ST is diffuse and irregular.*

Dimensions of the ST

The dimensions of ST in the HR patients did not significantly deviate from the dimensions of ST in the controls irrespective of whether the regression analysis included or excluded the individuals with the unclassified ST (Table XI). The diameter of the ST was affected negatively by the age in the control group, but positively in the HR group. This difference was significant (p = 0.037) however, the regression coefficients (β) of age were very close to zero (control group; β = -0.02; 95% CI: -0.04 to 0.01) (HR group; β = 0.05; 95% CI: -0.01 to 0.11). The depth and the length of the ST were not significantly affected by an interaction between the effect of health and age, and none of the ST dimensions were affected by an interaction between the effect of health and gender.

| | Males | | | | Females | | | | Adjusted comparison HR and control |
| | HR patients N = 12 | | Controls N = 23 | | HR patients N = 24 | | Controls N = 26 | | |
	mean	SD	mean	SD	mean	SD	mean	SD	p-value
Length	12.10[a]	1.52	12.41	1.89	11.99[b]	2.26	11.41	1.25	0.566
Diameter	13.33[b]	1.40	13.68[a]	1.23	13.94[d]	2.31	13.21[a]	1.24	0.463
Depth	10.08[a]	0.80	9.61	0.98	10.20[c]	1.36	9.59	1.11	0.13

*Table XI. **Comparison of the ST dimensions between the HR patients and the controls adjusted for the effect of the gender, the age, and the family clustering**. Means and standard deviations (SD) of the length, the diameter, and the depth of the ST according to the group (HR patients or controls) and the gender are given.*
p-values are from the linear regression analysis
[a] one missing value; [b] two missing values; [c] three missing values; [d] five missing values.

5.5.2. ST and HR severity

In the comparison according to the severity of the skeletal HR impact, four (29%) mildly affected HR patients and 15 (68%) severely affected HR patients had the standard type of ST morphology (p = 0.020), thus, the severity of skeletal HR impact was negatively correlated with deviations from the standard ST morphology. Three (21%) mildly affected HR patients and three (14%) severely affected HR patients were unclassified (p = 0.541), thus, the severity of skeletal HR impact was not associated with a diffuse and irregular outlining of ST.

6. Discussion

6.1. Overall scope of the study

The present dissertation is the presentation of the results from research projects carried out on the craniofacial and the spine morphology in patients with a rare disease, X-linked HR. The study period was the years from 2008 to 2013. The research on rare diseases calls for an interdisciplinary collaboration between different medical disciplines and in relation to some diseases includes also the dental profession. In addition, the networking between centers of expertise, occansionally across the national borders, is needed to raise the number of participant in the studies of rare diseases. This has previously been demonstrated in studies on, e.g., the patients with cleft lip and palate (Semb *et al.*, 2005; Shaw *et al.*, 2005). The present work is enabled by the collaboration between medical professionals in Southern Denmark, geneticists in Denmark and abroad, and dental professionals at Aarhus University and Copenhagen University. X-linked HR is an example of a rare congenital disease with documented consequences for the dentition, i.e., a high number of non-decayed teeth with endodontic affection or periapical infection (Andersen *et al.*, 2012). In the present dissertation, we have focused on the osseous structures of the cranium and the cervical spine in a population of patients with X-linked HR. The cranium and the spine are unique and composite structures, which develop by complicated mechanisms, not fully understood. The cranium and the spine contain the brain and other essential parts of the central-nervous system, and the neural and the osseous development are linked closely to each other (Kjaer, 1998a; Kjaer *et al.*, 1999). Additional vital functions are placed in the cranium, e.g., the visual, the auditory, and the stomatognatic functions, and it contains the entrance of the respiratory and the digestive system. Thus, a deviation in the morphology of the cranium or the spine may be associated with abnormalities in vital functions or in the developmental processes of the structures within the area or the connecting areas (Pruzansky, 1973; Cohen *et al.*, 1985).

6.1.1. Design and composition of the study

The dissertation is composed of four papers. Paper I is an overall cephalometric analysis of all parts of the cranium, which includes the traditional cephalometric measurements of the maxillofacial structures as well as newly developed methods for the assessment of the theca, the neurocranium, and the posterior cranial fossa. In the assessments, we have focused on the origin of the bony structures, i.e., the endochondral or the intramembraneous development. In paper II, detailed analyses of the morphology and the size of the frontal sinus and the nasal bone has been performed. The structures are located adjacent to the anterior cranial fossa. In the assessment, we have focused on the processes of bone resorption and apposition. In paper III, the morphology and

63

the dimensions of the upper cervical spine were evaluated. The associations between the cervical spine and the craniofacial structures were assessed with a special attention paid to the posterior cranial fossa, which belongs to the same developmental field as the cervical spine. In paper IV, the presence of extra-skeletal calcifications in relation to the cranium was studied. The associations between cranial calcifications and calcifications at other skeletal sites, severity of skeletal HR impact, or childhood treatment were explored. Furthermore, the dissertation has focused on the morphology and the dimensions of ST, a structure in the medial cranial fossa.

In general, the present study is a descriptive study of a patient group with a specific disease, i.e., X-linked HR. In a cross-sectional study design, the group of diseased patients was compared with a group of healthy individuals. The existing knowledge on bone origin and the developmental fields has been applied to the structuring of the study and to the description of the results. In addition to the descriptive parts of the study, a number of associations have been assessed. The assessments were addressed to the association between cervical and cranial morphology, to the association between the cranial or cervical morphology and the severity of skeletal HR impact, to the association between cranial and other extra-skeletal calcifications, and to the association between extra-skeletal calcifications and the childhood treatment. The purposes of these assessments have mainly had the character of hypothesis generation in contrast to hypothesis confirmation (Katz *et al.*, 2013). The assessment of the cranial and cervical morphology has had the purpose to discover new information within the data, either to generate new hypothesis or to comment on an existing hypothesis. Others have justified the usage of a "hunch" as the background for an exploration of morphometric data as opposed to the utilization of a clear hypothesis (Richtsmeier *et al.*, 2002). One of the "hunches" of the present study was the expectation of different deviations in the HR cranial morphology according to the bony origin of the structures. The bones of the lower extremities, which are impacted by a severe deformation in HR patients (Drezner, 2003; Beck-Nielsen *et al.*, 2010), are bones of endochondral origin, thus, the cranial bones of endochondral origin were expected to deviate more severely than cranial bone of intramembranous origin. However, the distinction between the structures according to bony origin might be unclear: Certain anatomical bones, e.g., the mandible and the occipital bone, are composed of subunits of different origin, and the borders between the different subunits are not visible at the postnatal stage (Kjaer *et al.*, 1999; Schoenwolf, 2009b). Furthermore, certain cephalometric variables are not restricted to one type of bony structure. For example, the angle "s-n-ss" describes the sagittal position of the maxilla, which is a structure of intramembranous origin, in relation to the anterior cranial base, which is a structure of endochondral origin. Furthermore, the lines "n-br" "n-pa", "n-l", and "n-opi" describe dimensions of the upper skull, which is composed of the intramembranous-developed calvarial bones, but the cephalometric measurements are partially

defined by a landmark located at the anterior end of the endochondral-developed cranial base. In contrast, the length of the maxilla (pns-ans) or the thickness of the parietal or frontal bone describe the dimension of structures with a purely intramembranous origin, and the dimensions and angulation of the cranial base describe a structure of purely endochondral origin. Significant deviations were found in variables describing structures of purely endochondral origin (e.g., ba-s-n) as well as in variables describing structures of purely intramembranous origin. Thus, it was justified to conclude that both types of bone were impacted in HR patients, which was in contrast to the initial "hunch". To fulfill the descriptive purpose of paper I, the inclusion of cephalometric variables assessing more than one type of bony structure was justified.

6.1.2. Assessment of morphology

The dissertation addresses the cranial and the cervical morphology. In general, morphology is defined as the study of the forms of things, which include the branch of biology that deals with the form of living organisms and their parts, and the relationships between their structures (Simpson, 2013). The form is understood as the combination of size and shape (Richtsmeier *et al.*, 2002), and the shape of a structure has been defined as the geometric information remaining after removal of any effect due to translation, rotation, or scale of the structure (Dryden & Mardia, 1998). In the orthodontic profession, it is a well-established tradition to assess the craniofacial and cervical morphology by linear and angular measurements between landmarks (Bjørk, 1975; McNamara, 1984; Wahl, 2006). This conventional metrical approach (CMA) has been applied to the present study in line with previous studies both within the orthodontic field (Wahl, 2006) and in a number of other biological disciplines, e.g., phylogenetics and anthropology (Wood *et al.*, 1991; Wood & Lieberman, 2001). Because of the irregular and not linear outlining of the cranial bones (and other bones), the CMA has some shortcomings in the assessment of cranial morphology, both in the study of morphological changes during growth and in the study of morphological deviations between groups. Thus, sophisticated morphometric alternatives have been proposed (Lestrel, 1997; Richtsmeier *et al.*, 2002). Relevant examples of the morphometric methods are the Eliptical Fourier function (EFF) (Kuhl & Giardina, 1982), Procrustes` superimposition and principal component analysis (PCA) (Halazonetis, 2004), and the finite element scale analysis (FESA) (Cheverud *et al.*, 1983; Richtsmeier & Cheverud, 1986). By EFF, the morphology of, e.g., the cranial vault (Lestrel *et al.*, 2010), the mandible (Schmittbuhl *et al.*, 2002; Lestrel *et al.*, 2013), and the nasal bone (Lestrel *et al.*, 1991) has previously been described. The PCA has been applied to the analysis of both the craniofacial complex as a whole (Halazonetis, 2004) and to minor cranial structures, e.g., ST (Andredaki *et al.*, 2007). The FESA has been applied to a number of studies on craniofacial morphology, e.g., in patients with syndromic craniosynostosis (Apert and Crouzon

syndrome) (Bookstein, 1987; Richtsmeier, 1987; Richtsmeier & Lele, 1990), in patients with cleft lip and palate (Lavelle, 1988; Hammond *et al.*, 1993; Sasaki *et al.*, 2004), and in patients with Class III malocclusion (Singh *et al.*, 1997; Singh & Hay, 1999). The advantage of the morphometric methods is the possibility to visualize the shape differences between groups and the possibility to quantify shape objectively. Thus, shape data is operationalized to be applied to, e.g., a statistical assessment of shape differences between groups (Lestrel, 1982; Lestrel, 1997; Richtsmeier *et al.*, 2002). Furthermore, the drawback of CMA in terms of many highly inter-correlated craniofacial measurements is minimized (Solow, 1966). However, morphometric methods also have their limitations. The data of the advanced morphometric methods are all derived statistically, and they do not necessarily have a clear biological interpretation. The methods are statistical models, which by different approaches describe the diversity in anatomical shape. They all represent a simplification of the "true" shape, and the result of the analysis might rely on the chosen method (Richtsmeier *et al.*, 2002; Rohlf, 2003; Halazonetis, 2004). In addition, the advanced morphometric methods demand special software.

In the present study, the morphology of cranial and cervical structures was primarily assessed by CMA as an alternative to the advanced morphometric methods. The angular measurement of the cranial base (ba-s-na) is independent of the dimension of the anatomic structure (the anterior and the posterioer cranial base) thus; the angle is a simple and valid expression of the morphology of the cranial base. In contrast, the angular measurements of the sagittal jaw relations (s-n-ss and s-n-pg), in addition to the spatial position of the jaw, is associated with the dimension of both the anterior cranial base (s-n) and the jaw itself (i.e., topographical inter-correlations) (Solow, 1966). Thus, this type of angular measurement is less valid in the expression of the maxillo-facial morphology, and it has to be interpreted in connection with an assessment of the linear dimension of the involved structures. The shape of the cranial vault has not been directly assessed in the study. However, the linear dimensions of the cranium (length and height) may be amalgamated into an impression of the shape and the differences in shape with the limitation given by the lack of a quantitative shape measurement. In addition to CMA, the morphology and characteristics of some few structures (i.e., ST and C1-C5) were visually assessed by subjective methods, which basically is a comparison to reference standards. The limitations by these subjective methods were minimized by the blinded approach during the assessment and by the use of two observers between whom the classification was discussed until agreement was achieved. If agreement could not be achieved or if there was other uncertainties in the assessment, the structure was assessed as "normal" or "standard". However, the blinded approach was compromised in few cases because some HR patients had many missing teeth in contrast to controls, which according to the inclusion criteria for the control group had to have at least 20 teeth. Because of the limited sample size,

recognition of some few cases with other special traits, e.g., a very thick skull was unavoidable during the repeated assessments in the study period.

6.1.3. Study population

The papers dealt with in the present dissertation are based on a relatively high number of HR patients compared with previous cephalometric studies on HR (Marks *et al.*, 1965; Tracy & Campbell, 1968; Al-Jundi *et al.*, 2009). Furthermore, the patients of the studies have been uniformly diagnosed, and except for three cases, the diagnosis was genetically verified (Beck-Nielsen *et al.*, 2010; Beck-Nielsen *et al.*, 2012). We have not investigated whether these three HR patients had autosomal recessive HR caused by the newly discovered mutation in *ENPP1* as this gene was not discovered at the time of the genetic evaluation. Two of the three patients were a mother and her son. Thus, only one patient with sporadic HR and no genetic diagnosis could be suspicious of an *ENPP1* mutation. The male:female ratio was not the same in the HR group (1:2.12) and the control group (1:1.14), however, the difference was not significant. This gender discrepancy was in accordance with the dominant X-linked inheritance of the disease, and a predominant female group is characteristic in the research regarding XLHR and XLH (Al-Jundi *et al.*, 2009; Gauche C *et al.*, 2009).

Individuals were included in the control group according to an objective estimation of the dental occlusion (close to normal occlusion), the number of teeth (n ≥ 24 teeth), and the facial appearance (no signs of craniofacial anomaly). In addition, the inclusion was based on the individual`s subjective information on their general health (no chronic diseases) and former dental treatment (no former orthodontic treatment). The potential failure of the inclusion according to the individuals` subjective information was judged to be minimal. The size of the control group was estimated by power calculations on six cephalometric variables which were assumed to be representative of the cranial dimensions and morphology. The final size of the control group (n = 79) exceeded the estimated minimum (60-70). The youngest age group (age < 7 years of age) was only present in the HR group. For ethical reasons, the children in the control group were only represented by profile radiographs taken for orthodontic treatment purposes. As such radiographs are rarely indicated in relation to the treatment of the very young children, this age group was not represented in the control group. The statistical models were designed to analyze the effect of the gender and the age on the influence of HR. This choice of the models aimed to compensate for the gender and age discrepancies between the HR group and the control group. Furthermore, the analyses in paper II-IV included adults, only. In children opposed to adults, the dimension of many cranial and vertebral structures increase with the age and consequently, children were excluded

from the analysis in paper II-IV (Bjørk & Skieller, 1983; Brown *et al.*, 1984; Lestrel *et al.*, 1991; Axelsson *et al.*, 2003).

6.1.4. Methods of the study

In diseases with bone pathology, it is common to assess the morphology of the osseous structures by radiographs. The use of the lateral cephalogram, i.e., the standardized profile radiograph, is usual in the orthodontic community in clinical settings as well as in the research of craniofacial and cervical spine morphology and growth (Wahl, 2006). In the present study, the analysis of 3-dimensional (3D) anatomical structures (the frontal sinus, the nasal bones, the cervical vertebrae, and the ST) was performed on 2-dimensional (2D) radiographs, which to some extent limits the interpretation of the results. The advantage of 2D-methods is the comparability with the previous cephalometric studies where 2D methods have been used in the assessment of the craniofacial structures, in example (Jensen & Kreiborg, 1995), (Ruf & Pancherz, 1996), (Lexner *et al.*, 2007), and (Al-Jundi *et al.*, 2009). The difficulty of determining the deviations in the upper spine morphology on a single lateral cephalogram has been discussed (Massengill *et al.*, 1997; Koletsis & Halazonetis, 2010; Bebnowski *et al.*, 2012). These studies found that some fusions observed on 2D radiographs were likely to be "pseudo-fusions", and a more valuable method, such as computerized tomography (CT) or cone-beam CT (CBCT), has been recommended. However, in a recent study of CVA in patients with obstructive sleep apnea, the agreement of the occurrence of CVA between the lateral cephalograms and the CBCTs showed good agreement (K = 0.64) (Sonnesen *et al.*, 2013). Furthermore, the lateral cephalograms of the present study were obtained before CBCT was generally used. In order to minimize false positive findings on 2D, clearly defined criteria were set up in the present study. Thus, we expect our results based on 2D to provide useful and reliable information regarding the morphological deviations.

The dissertation comprises radiological assessment of the bones of the cranium and the cervical column. The radiographic picture is impacted by potential errors in the acquisition of the picture: The positioning in the cephalostat affects not only the orientation of the structures, but also the distortion of the picture (Cooke & Wei, 1991). In the present study, it was aimed to visualize the whole skull. Furthermore, some of the HR patients had a very low body height (the youngest children) or a short neck, which made them unable to stand properly in the cephalostat. Because of the necessary positional adjustments according to these demands and circumstances, the correct positioning in the cephalostat was compromised in some of the participants. In addition, a number of different radiographers on different locations obtained the radiographs. However, in all participants (HR patients and controls) the same type of equipment (Planmeca©) was used to

obtain the radiographs, and the sources of the aquisitional errors were judged to be equal in the two groups.

In addition to the aquisitional errors, errors exist in relation to the cephalometric measurements (Kamoen *et al.*, 2001; Shaw *et al.*, 2013). The cephalometric errors are most importantly related to the errors in the landmark identification (Baumrind & Frantz, 1971; Houston *et al.*, 1986) The variance in the location of the landmarks are unequal depending on the character of the anatomical structure, at which the landmark is located, and on the quality of the radiograph at the specific location. Each landmark has a characteristic orientation of the variance: Some landmarks have a uniform variance in all directions (e.g., the point sella), and other landmarks vary more in one than in other directions (e.g., the B point, supramentale, has a relative large vertical variance opposed to horizontal variance) (Baumrind & Frantz, 1971; Broch *et al.*, 1981; Houston *et al.*, 1986). In the present study, the errors according to landmark identification were found to be acceptable; the issue is further discussed in the last paragraph of this section.

In general, landmarks on curved surfaces have a relatively great variance (Baumrind & Frantz, 1971), which in the present study might impact on the measurements of the skull. To minimize the errors in measurements of the skull thickness, the landmarks for measurement of the thickness was defined as the cross section between the skull contours and well-defined straight lines crossing the contours. The straight lines were defined by the anatomical points nasion, bregma, lambda, and basion (Axelsson *et al.*, 2003). In general, the nasion and the basion are points with a relatively low respectively high variance in the location of the landmark. In elder adults, the other two points often is difficult to identify because of the totally closed sutures. Thus, the landmarks of skull thickness measurements might be affected by a relatively high variance. However, the intra-examiner variability of the measurements was acceptable (the random error ranged from 0.11 to 0.21 (Dahlberg, 1940)) and in line with the reported errors in a previous study (Axelsson *et al.*, 2003).

As an integrated part of the present study, the intra-examiner errors in landmark identification and thereby in obtaining the cephalometric measurements were assessed on 22 radiographs, which were randomly selected for duplicate measurements: 1) An assessment of the potential systematic errors. Such errors were not identified, which indicated an adequate ability by the observer to reproduce the landmark identification. 2) An assessment of the random error was calculated by the method by Dahlberg (Dahlberg, 1940), and the errors ranged from 0.01 to 4.38, which for the majority of variables was in line with the random errors reported in other cephalometric studies (Kamoen *et al.*, 2001; Axelsson *et al.*, 2005; Sonnesen & Kjaer, 2007b). The errors of the frontal sinus measurements were relatively large (0.64-4.38), supposedly because of the irregular double

(or multiple) contours in the lateral aspect of this bilateral anatomical structure, which has the largest dimension in the frontal plane. 3) An assessment of the random error in relation to the total and biological variance by Houston`s coefficient of reliability (Houston, 1983). The magnitude of this coefficient was judged to be acceptable (0.91-1.00). In conclusion, the intra-examiner reproducibility of the majority of cephalometric measurements was acceptable.

6.1.5. Biases of the study

The statistical analysis of the study was constructed to minimize the confounding effect of age, gender, and family clustering. However, confounding effects in relation to the study population might exist e.g., 1) skewness according to the physical characteristcs of the participants, 2) skewness according to the gender, 3) differences according to childhood treatment of HR patients, and 4) undiagnosed diseases in the control group.

1) The body height, sitting height, arm span, and leg length are reduced in HR patients compared to standards (Drezner, 2003; Beck-Nielsen *et al.*, 2010). It could be speculated that the general physical measurements impact on some cranial measurements. In the present study, information on general physical measurements was available in the HR group, only. Thus, in the analysis it was not possible to adjust for the general physical measurements. Furthermore, previous forensic studies did not document a correlation between cranial thickness and the individual height and weight (Lynnerup, 2001). Thus, the biases according to physical measurements were judged to be minimal.

2) More women than men were represented in the HR group, and the skewness according to gender might impact on the means of the cephalometric variables, e.g., the skull thickness and the other dimensions of the skull. Previous studies on forensic samples have addressed the question on cranial sex dimorphism. >For example, a MRI study (i.e., a study based on Magnetic Resonance Imaging) revealed increased skull length and height in males compared to women (Hatipoglu *et al.*, 2008), which is in accordance with normative cephalometric standards (Axelsson *et al.*, 2003). The MRI study (Hatipoglu *et al.*, 2008) also concluded an increased calvarial diploe thickness (i.e., the thickness of the cortical bone in between the two cortical plates of the skull) in males compared to females. In contrast, other studies based on direct or radiographic measurements on skull biopsies concluded a lack of sex dimorphism in the total skull thickness and only a tendency towards increased diploetic thickness in males (Lynnerup, 2001; Lynnerup *et al.*, 2005). In the present study, the choice of a multiple regression in the statistical model made it feasible to adjust for the skewness according to gender.

3) Some patients have had medical treatment during their whole childhood, some few patients have had sporadic treatment, and others have had no treatment (Beck-Nielsen *et al.*, 2010). The goal of the treatment is to minimize the rachitic softening of bones, the radiological abnormalities, and the skeletal deformities (Carpenter *et al.*, 2011). The treatment impacts positively the skeletal growth and the final body height (Makitie *et al.*, 2003). Thus, there might be an effect of treatment also on the cranial bones and thereby the morphology of the cranium and the cervical column. In general, we did not adjust for the treatment in the analysis of the present study. The acceptance of this potential bias is justified by the limited sample size, which hardly could bear further stratifying in the analysis. In paper IV, a separate analysis of the association between childhood treatment and the occurrence of extra-skeletal calcifications has been performed.

4) In the control group, which according to the anamnestic information was healthy individuals, undiagnosed diseases might exist. Some diseases impact on cranial structures, e.g., pitutiary prolactinomas, which are relatively common, and which can remain asymptomatic for years (Buurman & Saeger, 2006; Melmed *et al.*, 2011). Pituary adenomas impacts on the size and the morphology of the ST (Alkofide, 2001). It would have been optimal to include an endocrine screening of all participants to exclude patients with previously undiagnosed chronic disease, e.g., a prolactinoma. If present, prolactinomas might have impacted on the ST morphology of the affected individual, thus, biased the ST results of the present study. However, the controls appeared to be healthy both objectively and subjectively, and the bias was judged to be minimal.

The present study, which is a radiological study on postnatal findings, addresses morphological deviations according to developmental fields. The definition of cranial and cervical developmental fields is raised in studies on foetal pathology, which is a discipline that relies on histologic studies (Kjaer, 1998b; Kjaer *et al.*, 1999; Kjaer, 2010). At the postnatal stage, the borders between the developmental fields have not been revealed in detail (Kjaer, 2010). The present study addresses potential associations between structures of the same field or between structures of different fields. This is in line with other radiological studies on postnatal cervical or cranial morphology (Kjaer *et al.*, 2001a; Tabatabaie *et al.*, 2008; Sonnesen, 2010; Molsted *et al.*, 2010). The biological interpretation of the associations might be uncertain, and other types of studies are needed to confirm the existence of a biological interrelationship, e.g., by immune-histochemical studies on mice (Sonnesen *et al.*, 2008a). However, the present study, which is in line with other radiographic studies on patients with a congenital disease or deformity (Axelsson *et al.*, 2004b; Axelsson *et al.*, 2005; Nielsen *et al.*, 2005a; Nielsen *et al.*, 2005b; Molsted *et al.*, 2010), is justified by its contribution to the ongoing process of an understanding of normal and abnormal development.

In the present study, the remodeling of bone as well as the mineralization of extra-skeletal structures has been addressed. This is processes, which are executed at a cellular level, and which only indirectly can be assessed on cranial radiographs. The interpretation of a morphological deviation, e.g., the increased thickness of the skull, is based on previously reported histological results on mice (Liu *et al.*, 2006b; Liu *et al.*, 2007; Liu *et al.*, 2008; Lu & Feng, 2011). Thus in terms of remodeling and modelling, the radiological results of the present study on HR have to be seen in connection with other types of research. This is in line with radiographic studies, on e.g., cleidocranial dysplasia or achondroplasia (Cohen *et al.*, 1985; Jensen & Kreiborg, 1993). In terms of extra-skeletal mineralization, the radiographic picture is well qualified for the assessment of such calcifications, and it has previously been applied to the diagnosis of mineralizing enthesopathies in HR studies (Polisson *et al.*, 1985; Carpenter *et al.*, 2011).

The assessment of potential associations between cranial or cervical morphology and the severity of skeletal HR impact is based on the severity definitions by Beck-Nielsen et al. (Beck-Nielsen *et al.*, 2010). According to the definition, a HR patient is severely impacted if the lower leg deformity index or the body height reduction equals or exceeds a certain limit (z-value = 2SD) or if a surgical correction of lower leg deformity have been performed. Thus, the severity assessment is equally impacted by naturally developed symptoms as by criteria, which depend on treatment decisions. However, it is common to demand the deviation in deformity to exceed 2SD before surgery (Beck-Nielsen *et al.*, 2010). In conclusion, the skeletal severity score is supposed to be valid.

6.2. Discussion paper I-IV

Selected topics from the individual papers are presented in this section. The more detailed discussions are available in the individual paper.

6.2.1. Paper I. Craniofacial morphology

Endochondral developed bone

According to paper I, the shape of the cranial base was affected by a flattening, while the size of the anterior as well as the posterior cranial base was unaffected. This is in agreement with earlier findings (Al-Jundi *et al.*, 2009). The depth of the posterior cranial fossa was reduced, but no significant difference of the length of the fossa was seen. The differences in shape of the posterior-inferior part of the cranium could be described as an upward compression of the structures around foramen magnum, including a more cranial position of the inferior part of clivus (basion), which would also add to the increased cranial base angle (n-s-ba). The reduced height of the posterior cranial fossa indicates a reduced volumen of the fossa, and this is in agreement with the results

from a study based on 3D imaging (computed tomographic or magnetic resonance imaging) (Tubbs *et al.*, 2004). A small posterior cranial fossa reduces the available room for the development of rhombencephalon. This might be related to the occurrence of hindbrain herniation (i.e., CMI) reported in some children with HR or the other types of rickets (Caldemeyer *et al.*, 1995; Tubbs *et al.*, 2004).

The increased cranial base angle (n-s-ba) and the reduced depth of the posterior cranial base in HR might be explained as a deformation of poorly mineralized bony structures caused by the weight of the brain and/or the weight of the thickened skull. This would be in line with the deformation of the lower legs in HR patients (Drezner, 2003; Beck-Nielsen *et al.*, 2010).

Intramembranous developed bone

In HR patients compared to controls, the morphology of the skull was abnormal as the result of an increased frontal bossing, an increased height of the anterior part of neurocranium, and a flattening of the parietal area. The finding of an increased frontal prominence is in agreement with former reports of frontal bossing (Marks *et al.*, 1965; Tracy & Campbell, 1968). In addition, a significant increase in the thickness of the skull was found; both in the parietal and the frontal part, which are of intramembraneous origin, and in the lower occipital part, which is of endochondral origin.

The reduced length of the nasal bone is in line with the findings in studies on HYP mice (Iorio *et al.*, 1980; Mostafa *et al.*, 1982). The reduced length of the nasal bone has also been reported in the patients with achondroplasia (Cohen *et al.*, 1985), cleft lip and palate (Nielsen *et al.*, 2005b), and hypohidrotic ectodermal dysplasia (Lexner *et al.*, 2007), which are inherited diseases with totally different backgrounds.

When comparing the HR patients and the healthy controls, no significant differences in the shape, the position, or the size of the mandible were found. This is in agreement with Tracy and Campbell (Tracy & Campbell, 1968), but is in contrast to the findings in Jordanian children with HR (2-16 years of age) in whom reduced mandibular dimensions and a relatively prognathic mandible were seen (Al-Jundi *et al.*, 2009). These discrepancies might be explained by the differences in the age range, the diagnostic criteria for inclusion of the diseased individuals, and the sample size.

6.2.2. Paper II. Nasal bone and frontal sinus

In paper II, certain structures, which were located in the same developmental field (i.e., the nasofrontal field) adjacent to the anterior cranial fossa, were selected for a morphological analysis focusing on the bone resorption and formation. The frontal sinus represents a structure, which

develops by the resorption of bone (Brown *et al.*, 1984), and the nasal bone represents a bony structure, which develops by the formation of bone (Lestrel *et al.*, 1991; Sandikcioglu *et al.*, 1994a).

Frontal sinus and the bone resorption

The size of the frontal sinus varied considerably in both groups (*i.e.,* HR patients and controls), but the differences between the groups were not statistically significant (Table IV). These findings of size variation are in accordance with a previous study regarding the variations in the sinus-development in healthy children (Brown *et al.*, 1984). In HR patients, the apparently unaffected resorption during the development of the frontal sinus may be a sign of normal osteoclastic activity within the frontal bone. Only three out 36 HR patients did not have a frontal sinus at all.

Nasal bone and the bone formation

The morphology of the nasal bone was abnormal because of a relative large proximal width of the bone (Table IV and Fig. 11). Furthermore, the degree of an abnormal morphology of the nasal bone seemed to be related to the severity of the general skeletal impact of HR (Table V). Prenatally, the nasal bone develops directly from the mesenchymal cells using the chondral nasal capsule as a scaffold (Sandikcioglu *et al.*, 1994a). In the postnatal development, the proximal part of the nasal bone is surrounded by bony structures developed by the endochondal ossification of the former nasal capsule (i.e., structures of the ethmoid bone), but the apical part of the nasal bone is supported by the cartilaginous nasal septum and the frontal processes of the maxilla, which is of intramembraneous origin (Fig. 2) (Drake *et al.*, 2013). In HR patients, the beak-like appearance of the nasal bone reflected increased bone formation in the proximal part, which was supported by osseous structures of endochondral origin. The morphological results might be interpreted as disturbances in the modeling with a net gain of bone in the proximal part. Apparently, the modeling of the apical part of the nasal bone, which is not supported by these structures, had another character. The mechanisms behind the increased width of the proximal part of the nasal bone might be identical with the mechanisms responsible for the increased thickness of theca, which develops with the meninges as a scaffold. The knowledge of impaired osteoclastogenesis in FGF23-associated HR (Lu & Feng, 2011) supports the suggestions of disturbances in the modeling of bone, although the reason for the apparent differences according to the presence respective absence of a supporting scaffold remains unclear.

The interpretation of the results of the paper is to some degree contradicting. In HR patients, the unaffected frontal sinus dimensions might be interpreted as the sign of a normal osteoclastic activity. Opposed to this, the deviation in nasal bone morphology might be the sign of disturbances in bone modelling, which imply abnormal osteoclastic or osteoblastic activity. Recent studies suggest primarily the osteoclastic activity as affected in HR (Lu & Feng, 2011). Some unknown

local factors might influence the apparent differentiated osteoclastic activity. For further elucidation of the issue, other types of studies are needed.

6.2.3. Paper III. Cervical spine

The focus of paper III was the structures of the cerebellar and cervical spine field. Primarily, the morphology and the size of the upper cervical vertebrae were analyzed and secondly, potential associations between the cervical and the craniofacial structures were assessed.

Morphology and dimensions of the cervical vertebrae

The increased dimensions of the atlas and the posterior arch of the axis (Table VII) may be associated with the increased thickness of the theca, which was reported in paper I (Appendix; E-Table IV). The increment in the dimensions of the atlas and the axis as well as the theca may reflect disturbances in the normal balance between the osteoclastic resorption and the osteoblastic formation of bone, which has been associated with the high levels of FGF23 in HR (Zhang *et al.*, 2011; Lu & Feng, 2011; Pettifor & Thandrayen, 2012).

According to the present paper, the atlas was longer and the dens were shorter in severely affected HR patients than in less severely affected HR patients (Table VIII). The differences in the severity of skeletal impact, depending on the subunits of the vertebral unit (e.g. vertebral body or posterior arch), might reflect the differentiated embryological development of the vertebrae. (Schoenwolf, 2009a). The cells of a specific region of the sclerotome (e.g., the future vertebral body) are controlled by distinct genes, which determine the characteristics of the region (Schoenwolf, 2009a), and it could be hypothesized, that the regional characteristics also determine the susceptibility and reaction to a pathological condition e.g., HR.

The CVA was a relatively frequent finding in HR patients, and the FUS (39%) was more common than the PAD (17%). Comparable differences have been reported in patients with severe skeletal malocclusions (FUS 42-61%; PAD 6-13%) (Sonnesen & Kjaer, 2007a; Sonnesen & Kjaer, 2007b; Sonnesen & Kjaer, 2008a; Sonnesen & Kjaer, 2008b). In the HR group, the FUS was mainly represented by occipitalizations. In patients with cleft deformities (cleft lip, cleft palate, or combined), CVA in total is common (22-39%) (Horswell, 1991; Lima *et al.*, 2009), and some studies report PAD (8-17-48%) as more frequent than FUS (0-12-38%) (Sandham, 1986; Ugar & Semb, 2001; Lima *et al.*, 2009). The differences in the prevalence and pattern of CVA between the various patients groups and controls may reflect the different pathogenesis of the conditions.

Associations between the cervical and the craniofacial structures

The finding of a significant correlation between the height of the dorsal arch of the atlas and the length of both the posterior cranial base and the posterior cranial fossa is in accordance with a previous study, which reported a significant correlation between the height of the dorsal arch of the atlas and the length of the posterior cranial base in healthy adults (Huggare, 1991). In addition, both the height of the arch and the length of the atlas correlated positively with the flexure of the cranial base (inversely related to the cranial base angle). The significant correlations indicate a close connection between the osseous structures of the cerebellar and the cervical spine field (Fig. 2). This finding supports the idea of a common embryological origin of the upper cervical spine and the basilar part of the occipital bone (Kjaer, 1998a; Schoenwolf, 2009a).

A previous report on the association between the height of the posterior arch of the atlas and the forward growth of the mandible (Huggare, 1989) is supported by the present finding of a positive correlation between the length of the atlas and the mandibular prognatism. In contrast, the present study found no association between FUS and the jaw relationship, which previously has been reported in patients with a severe skeletal malocclusion (Sonnesen & Kjaer, 2007a; Sonnesen & Kjaer, 2008a; Sonnesen & Kjaer, 2008b).The absence of an interrelationship between CVA and the maxillo-facial morphology may be related to the fact that the participants had a fairly normal maxillofacial morphology (Appendix; E-Table V-VI), thus, severe deviations in the maxillo-facial morphology were not present in the study population. Oppositely, the skull thickness was affected by severe deviations in the HR group, and a significant association was found between FUS and the thickness of the frontal and the occipital theca.

6.2.4. Paper IV. Extra-skeletal calcifications

In paper IV, extra-skeletal calcifications were assessed in terms of intracranial and extra-cranial calcifications in addition to mineralizing enthesopathies in relation to the ankles, the knees, the hips, and the collateral ligaments of the vertebral column.

Intracranial and extra-cranial calcifications

Extra-cranial calcifications in the nuchal ligament were frequent findings in HR patients (Table IX). The presence of nuchal ligament calcifications adjacent to the surface of the occipital bone adds information to the previous reporting of a high prevalence of mineralizing enthesopathy in HR patients (Liang et al., 2009; Polisson et al., 1985; Reid et al., 1989). However, the present study did not show a significant association between the presence of nuchal ligament calcifications and the presence of other sites with mineralizing enthesopathy. Previous histological examinations on entheses (i.e., ligaments and tendons) of HYP mice have revealed an expansion of mineralizing

fibrocartilage in the entheses, thus, rejected the idea of an osteogenic bone spur formation at the insertion sites (Liang et al., 2009). The mineralization of these entheses has been suggested to be due to a direct action of FGF23 on the fibrochondrocytes of the entheses (Karaplis *et al.*, 2012).

Severity of skeletal HR impact and childhood treatment

The presence of the extra-cranial calcifications in the nuchal ligament was correlated positively with the severity of skeletal HR impact (p = 0.040). In contrast, the intracranial calcifications and the vertebral enthesopathies were not associated with the severity, thus, indicating different mechanisms according to the site of the extra-skeletal calcifications. The presence of nuchal ligament calcifications was not associated with the medical treatment during childhood. This may be an indication of the unsufficiency in the present treatment strategy, which addresses the improvement of osteomalacia and rachitic bone deformation. Future treatment strategies based on a direct modification of the FGF23 activity are believed to be more effective, e.g., by restraining the presence of mineralizing enthesopathy (Lee & Imel, 2013). This effect might include a reduction in the atypical calcification of the nuchal ligament.

6.3. Discussion sella turcica

This part of the study focused the central part of the medial cranial fossa i.e., the ST.

Morphology of the ST

The prevalence of the standard ST type in the HR group was low compared with the control group (Table X), but higher than the reported prevalence of the normal standard ST type in the patients with Williams syndrome (32-42%) (Axelsson *et al.*, 2004a), with cleft lip and palate (37%) (Alkofide, 2008), or with 22q11 deletion syndrome (0-7%) (Molsted *et al.*, 2010). According to the present study, the prevalence of each of the other normal ST types was equal in the HR and the control group, except for the type characterized by a pyramidal shape of the dorsum sella (Table X). The prevalence of the five normal types ST types, which deviated from the standard ST type, was low in the HR group (31%) compared with the reported prevalence of these ST types in the patients with Williams syndrome (females: 59%; males: 50%; (Axelsson *et al.*, 2004a)), with 22q11 deletion syndrome (females: 60%; males: 61%; (Molsted *et al.*, 2010)), or with cleft lip and palate (63% (Alkofide, 2008)).

A number of the adult HR patients (17%) had unclassified ST, which represented deviations exceeding the normal morphological variation (Fig. 13). In two of them (a mother and her son, Fig. 13, D & F), whom also were severely HR impacted, the outlining of ST was totally absent. In HR patients, the poor outlining of the ST structures might to some extent be associated with a hypomineralization of the cranial base. The hypomineralization and softening of the bones are

some of the characteristics of HR (Hyp Consortium, 1995; Beck-Nielsen *et al.*, 2010). Since the hypomineralization reduces the radiopacity of the osseous structures, this might explain the absent outlining of the ST in patients with severe HR. Thus, the cephalogram may demonstrate a previously described paradox in the presence of both extra-skeletal calcifications (e.g., the nuchal ligament calcifications) and bone hypomineralization (e.g., the cranial base deformation and the poor ST outlining) in HR patients (Liang *et al.*, 2009; Karaplis *et al.*, 2012).

Dimensions of the ST

In the present study, the radiographic magnification (i.e., 113%) was not corrected in the results, which mainly explains the large values of ST dimensions in the control group compared with Norwegian standards (Axelsson *et al.*, 2004b). In comparison with our results, the standards in an adult Saudi population (15-26 years) were even larger, although the magnification was corrected in that study (Alkofide, 2007). Most likely, these discrepancies in the dimensions of ST were caused by differences in the definition of the ST landmarks by the examiners. In addition, some ethnic differences in the ST dimensions might exist. In the literature, only a few studies of ST dimension in patient groups with diseases or anomalies have been reported. Our finding of no significant difference of the ST dimension in HR patients is in contrast to the reporting of the reduced ST dimensions in the patients with Williams syndrome (Axelsson *et al.*, 2004a) and the patients with cleft lip and palate (Alkofide, 2008). In addition, the deviations in the ST size, depending on the type of malocclusion, have been reported (Alkofide, 2007). An increased dimension of ST has also been reported in four relatives with Rieger syndrome (Meyer-Marcotty *et al.*, 2008) and in patients with pituary adenoma or acromegaly (Alkofide, 2001; Chang *et al.*, 2005). In the HR group compared with the control group, more individuals had unclassified ST (p = 0.021) characterized by a diffuse and irregular outlining of the ST. This may explain the high number of missing measurements of ST dimension in the HR group. However, except for a tendency towards an increased depth of the ST in HR patients (p = 0.081), the exclusion of the individuals with unclassified ST did not reveal significant differences in the ST dimensions between the HR patients and the controls.

Severity of skeletal impact

According to the present study, the severely affected HR patients were more likely to have the standard ST type compared with the mildly affected HR patients (p = 0.020), but the presence of unclassified ST was not different in the two HR groups (p = 0.541). Thus, an increase in the severity of the skeletal HR impact is not necessarily reflected in the presence of deviations in the ST morphology.

7. Conclusions

7.1 Paper I

In HR patients in comparison with controls

- the cranial base was flattened and the depth of the posterior cranial fossa was reduced
- the thickness of the skull was increased
- the dimensions of the anterior part of the neurocranium were increased
- the nasal bone length and the anterior maxillary height were reduced
- the cranial structures of endochondral origin as well as the structures of intramembraneous origin were affected

7.2. Paper II

In adult HR patients in comparison with controls

- the size of the frontal sinus was unaffected, which might suggest a normal ability of bone resorption within the frontal bone
- the morphology of the nasal bone was abnormal, which might suggest a disturbance in the bone formation during the growth
- the disturbances in the nasal bone modeling were mainly expressed in the proximal part supported by osseous structures of endochondral origin

In adult HR patients

- the degree of an abnormal morphology of the nasal bone tended to correlate with the severity of the general skeletal impact of HR

7.3. Paper III

In adult HR patients in comparison with controls

- the dimensions of the atlas and the axis were increased
- the prevalence of fusions of the upper vertical vertebrae was increased

In the total study population of adults

- the upper spine dimensions were associated with the craniofacial dimensions, primarily in relation to the posterior cranial fossa, which indicated an association between the structures within the cerebellar and cervical spine field

In adult HR patients

- the dimensions of the atlas and the dens were associated with the severity of skeletal impact of HR

7.4. Paper IV

In adult HR patients in comparison with controls
- the calcifications in the extra-cranial nuchal ligament were prevalent
- the intracranial calcifications were more evident

In adult HR patients
- the nuchal ligament calcifications were not associated with mineralizing enthesopathy at other extra-skeletal sites
- the nuchal ligament calcifications were positively correlated with the severity of skeletal HR impact
- the medical treatment during childhood was negatively correlated with vertebral enthesopathies, but not associated with the presence of neither intracranial nor nuchal ligament calcifications

7.5. Sella turcica

In adult HR patients in comparison with controls
- the deviation from the standard ST morphology was prevalent
- the dimension of ST was unaffected

In adult HR patients
- the deviation from the standard ST morphology was negatively correlated with the severity of skeletal HR impact

8. Future perspectives

The present study was a study on the craniofacial and the cervical spine morphology in patients with a rare disease, X-linked HR. The characteristics of the cranium and the cervical spine reflected developmental disturbances and general pathological traits of HR, e.g., deviations in bone remodeling and the presence of extra-skeletal calcifications. The assessment of associations between the general disease and the craniofacial, cervical or dental characteristics implied collaboration between dental and medical professionals. Thus, the collaboration between researchers of the dental profession and researchers of the medical profession is beneficial in studies of rare diseases with potential impact on cranium or dentition. A continuation of such types of interdisciplinary collaboration is warranted also in future studies.

The present radiological study was based on 2D radiographic methods. In future radiological studies of the craniofacial morphology in rare diseases, an increased use of 3D radiographic methods (e.g., CBCT) is anticipated. The 3D imaging is based on volumetric data, and supposedly, CBCT may give additional information on the morphology of the osseous structures of the cranium and the cervical spine. On the other hand, 3D radiographic techniques are more "expensive" in terms of the potential radiation hazards as well as the financial costs. The benefits in comparison with the use of 2D imaging techniques should be considered carefully according to the purpose of the study.

The present finding of cranial calcifications in HR patients calls for supplementary studies, in which other diagnostic methods would be of relevance, e.g., MRI. In addition, the use of MRI could add to the information on the morphology of both the ST and the pituitary glands located in the ST. Furthermore, the present finding of morphological deviations in the posterior cranial fossa and previous reports on CMI in HR patients (Caldemeyer *et al*., 1995; Currarino, 2007) calls for further exploration, e.g., by MRI.

During the phase of recruitment of patients for the present study on XLHR and XLH, other types of hereditary rickets have been located. Thus, descriptive studies of craniofacial and dental characteristics of a very rare condition, 1-alfa-hydroxylase deficiency rickets (VDDR type 1) have been founded during the current study, and such studies are of our interest. The potential deviations in the craniofacial and the cervical spine morphology of VDDR1 patients might be different from those in HR patients or from other types of inherited rickets. Such differences have to be expected because of the differences in the genetic background and in the pathophysiology depending on the type of rickets. The analyses of VDDR1 patients, identified during the recruitment of the HR patients, are in progress.

The scientific discussions in relation to both the present study and the other rickets study of our research group have also increased our interest on the acquired types of rickets. The acquired types (vitamin D deficiency or the lack of sun exposure) are conditions, which usually are treated by the intake of vitamin D. Despite treatment, it has previously been described that dental aberration persists as enamel hypoplasia in individuals with a childhood history of vitamin D deficiency rickets (Pindborg, 1970). It could be of interest in future clinical studies to explore in detail the effect of vitamin D deficiency rickets on the dentition, and to reveal if additional aberrations are present in the craniofacial structures.

The present radiological study on HR patients suggests deviations in the formation or the function of the osteoclasts and thereby in the remodeling of bone. The morphological effect of remodeling processes of the osseous structures could be further elucidated in future radiological studies on patients with other congenital diseases, which impact on the bone formation and function. For example, osteopetrosis is a rare congenital disease, which is characterized by disturbances in the formation or the function of the osteoclasts. In contrast to HR, a general excess of bone formation is a characteristic of osteopetrosis. Thus, detailed analyses of the cranial morphology in osteopetrosis might provide additional information on the knowledge of bone remodeling processes.

The present study described the cerebellar and cervical spine field with a focus on the embryological development of the structures. Apparently, symptoms in relation to morphological deviations in the cervico-cranial junction were rare. Previous studies on patients with osteogenesis imperfecta (OI) have had a particular focus on this area and reported on basilar impression and various symptoms (e.g., CMI) (Arponen *et al*., 2012). OI is another rare disease, which affects the bone and the dentition. In OI, the mineralization of bone is basically normal, but the disease is characterized by structural deviations of the bone (i.e., bone dysplasia with collagen deficiencies). Thus, it could be of interest to compare HR and OI according to the cervico-cranial junction and to explore the presence or absence of symptoms in relation to the morphological deviations in the respective groups.

A metabolic bone disease might affect the patient`s quality of life, and it could be speculated, that craniofacial and oral symptoms may have an impact on quality of life. During the collection of data for the present study of HR patients, the patients have filled questionnaires on oral health related quality of life. Analysis and reporting of these data has been planned.

9. English summary

The present PhD dissertation is a radiological study of the cranial and the cervical spine morphology in patients with hypophophatemic rickets (HR) compared with healthy controls. HR is a rare congenital disease, which is characterized by a renal waste of phosphate and a hypomineralization of the bone.

The dissertation comprises four papers, and the papers had the following aims:

I. To characterize the overall craniofacial morphology in patients with HR compared with healthy controls and to assess the possible differences in the craniofacial morphology according to the bony origin of the craniofacial structures

II. To characterize the size and the morphology of the frontal sinus and the nasal bone in adult HR patients compared with healthy controls, and to focus on the processes of bone resorption and apposition

III. To characterize the upper spine morphology in HR patients compared with controls and to analyze the associations between the spine morphology and the craniofacial morphology. Furthermore, the aim was to assess differences in the spine morphology according to the severity of the skeletal impact of HR

IV. To reveal the presence of intracranial and extra-cranial calcifications on cephalograms in adult HR patients compared with adult controls. Furthermore, the purpose was to assess the association between the presence of cranial calcifications and a) the presence of mineralizing enthesopathy at other extra-skeletal sites, b) the severity of the skeletal HR impact, and c) the medical treatment during childhood.

In addition, the morphology of the ST in adult HR patients compared with controls was studied.

In total, 53 HR patients (mean age 31.5 (SD 19.9), range 3-75 years) and 79 healthy individuals (mean age 30.1 (SD 18.6), range 9-79 years) were included. Lateral cephalograms were obtained from all participants. The cephalograms underwent cephalometric analyses and a visual assessment of the cranial and the cervical structures of interest.

In paper I (n = 132), the cephalometric measurements of the cranial base, the posterior cranial fossa, the neurocranium, the theca, the maxilla, the mandible, and the nasal bone were obtained. In the HR patients, the cranial base was flattened ($p = 0.001$) and the depth of the posterior cranial fossa was decreased ($p < 0.001$). The anterior height of the cranium, the angle sella-nasion-frontale, and the thickness of theca were increased ($p \leq 0.05$, $p = 0.028$, $p \leq 0.25$, respectively). The length of the nasal bone and the height of the maxilla were reduced ($p = 0.023$ and $p = 0.003$,

respectively). The cranial structures of endochondral origin as well as the structures of intramembraneous origin were affected in the HR patients.

In paper II, adult HR patients (n = 36) and controls (n = 49) were included only. In HR patients, the size of the frontal sinus was unaffected ($p > 0.406$). The proximal width of the nasal bone, and the ratio between the proximal width and the axial length of the nasal bone was increased in HR-patients compared with controls ($p<0.05$), which indicated a deviation in the nasal bone morphology of HR patients.
The unaffected size of the frontal sinus indicated a normal ability of bone resorption within the bone. The morphology of the nasal bone was abnormal, which may indicate a disturbance in the bone formation during growth. The disturbances in the nasal bone modeling were mainly expressed in the proximal part supported by structures of endochondral origin. The degree of an abnormal morphology of the nasal bone tended to correlate positively with the severity of the general skeletal impact of HR.

In paper III, the radiographic dimensions of the atlas and the axis were measured and the cervical vertebral anomalies (posterior arch deficiencies or fusions) were visually assessed in the same study group as in paper II. The height and the length of the atlas and the height of the posterior arch of the axis were large in the HR patients compared with the controls ($p \leq 0.001$), and more HR patients had fusions (32%) compared with the controls (11%) ($p = 0.003$). In the whole group of adults (n = 85), the height of the posterior arch of the atlas and the length of the axis correlated negatively with the cranial base angle ($p = 0.017$ and $p = 0.008$, respectively), and the vertical dimensions of the atlas correlated positively with the thickness of the occipital skull ($p \leq 0.015$). The length of the atlas was positively correlated with the mandibular prognatism (s-n-pg) ($p = 0.042$). The presence of fusions was correlated positively with the frontal and parietal skull thickness ($p = 0.034$ and $p = 0.003$, respectively). In HR patients, the length of the atlas correlated positively ($p = 0.043$), and the height of the dens correlated negatively ($p = 0.008$) with the severe skeletal HR impact. In conclusion, the dimensions of the atlas and the axis and the prevalence of fusions were increased in the HR patients. In the total study group, the upper spine dimensions were associated with the craniofacial dimensions, primarily in relation to the posterior cranial fossa, which indicated an association between the structures within the cerebellar and cervical spine field.

In paper IV, The study population was the same as in paper II and III. A high number of HR patients (17%) had manifest radiological signs of intracranial calcifications, which to the same degree not was present in the controls. The nuchal ligament had radiological signs of calcifications in 50% of HR patients and in 27% of controls ($p = 0.009$). The presence calcifications in the nuchal ligament was correlated positively with a severe skeletal HR impact ($p = 0.006$). Forty-two percent

of HR patients had vertebral enthesopathies. The medical treatment during childhood was negatively correlated with vertebral enthesopathies ($p = 0.008$)

The morphology of the ST was visually assessed and classified according to six normal ST types (one standard type and five normal deviations). The prevalence of patients with the standard ST type was low in the HR group (53%) compared with the control group (78%) ($p = 0.021$). The size of ST was unaffected ($p \geq 0.13$). An increase in the severity of the skeletal impact of HR was not necessarily reflected in the presence of deviations in the ST morphology.

Final conclusion: In HR patients in comparison with healthy controls, certain differences in the cranial and the cervical spine morphology existed, and the differences were present in osseous structures of intramembranous origin as well as in structures of endochondral origin. In HR patients, the deviations in cranial and cervical spine morphology might have reflected irregularities in the bone remodeling. The dimensions of the atlas and the axis were associated with certain cranial measurements primarily of structures in the cerebellar and spine developmental field. Calcifications in the nuchal ligament were common in HR patients. The deviations in the cranial and the cervical spine morphology and the presence of nuchal ligament calcifications could to some extent be related to the severity of the general skeletal HR impact. The medical treatment during childhood was negatively correlated with vertebral enthesopathies.

10. Dansk sammenfatning

Denne ph.d.-afhandling er en radiologisk undersøgelse af kraniets og halshvirvelsøjlens morfologi på patienter med hypofosfatæmisk rakitis (HR) sammenlignet med raske kontrolpersoner (KTR). HR er en sjælden, medfødt sygdom, som er kendetegnet ved fosfattab via nyrerne og en deraf følgende hypomineralisering af knogle.

Afhandlinger er baseret på 4 artikler (I-IV), der havde til formål:

I. at karakterisere den overordnede kraniofaciale morfologi på HR patienter sammenlignet med KTR og at vurdere eventuelle forskelle i den kraniofaciale morfologi afhængigt at den enkelte knoglestrukturs ossøse oprindelse

II. at karakterisere pandehulens og næsebenets morfologi og størrelse hos voksne HR patienter sammenlignet med voksne KTR og i analysen at have et særligt fokus på resorptions- og appositions-processer i knoglen

III. at karakterisere halshvirvelsøjlens morfologi på voksne HR patienter sammenlignet med voksne KTR samt at analysere mulige sammenhænge mellem halshvirvelsøjlens og kraniets morfologi. Endvidere var det formålet at vurdere forskelle i halshvirvelsøjlens morfologi afhængigt af alvorlighedsgraden af den generelle skeletale påvirkning ved HR

IV. at påvise radiologiske tegn på intra- og ekstra-kranielle forkalkninger på kranierøntgen (cephalogrammer) af vokne HR patienter sammenlignet med voksne KTR. I HR gruppen, var det endvidere formålet at vurdere associationer mellem tilstedeværelsen af disse kranielle forkalkninger og 1) tilstedeværelsen af forkalket entesopati ved andre skelet-lokalisationer, 2) alvorlighedsgraden af den generelle skeletale påvirkning ved HR og 3) medicinsk behandling i barndommen.

Desuden blev sella turcicas (ST) morfologi og størrelse hos voksne HR patienter sammenlignet med voksne KTR studeret.

I undersøgelsen er inkluderet 53 HR patienter (gennemsnitsalder 31,5 (SD 19,9), range 3-75 år) og 79 KTR (gennemsnitsalder 30,1 (SD 18,6), range 9-79 år). På alle deltagerne er der optaget et profil røntgenbillede. Profilrøntgenbillederne blev gjort til genstand for cephalometriske analyser samt en visuel vurdering af specifikke kranie- og halshvirvel-strukturer.

I artikel I (n = 132) gennemførtes cephalometriske opmålinger på kraniebasis, den posteriore kraniefossa, neurokraniet, kranieskallen (theca), maxillen, mandiblen og næsebenet. Kraniebasis var affladet (*p* = 0,001) og dybden af den posteriore kraniefossa var reduceret (p<0.001) hos HR patienter i forhold KTR. Den anteriore højde af neurokranium, vinklen sella-nasion-frontale og

theca tykkelse var forøget (p < 0,05; *p* = 0,028; p ≤ 0,25). Længden af næsebenet (*p* = 0,023) og højde af maxillen (*p* = 0,003) var reduceret. Ossøse kraniestrukturer af såvel endochondral som af intramemembranøs oprindelse kan være påvirket hos patienter med HR.

I artikel II inkluderedes alene voksne HR patienter (n = 36) og voksne KTR (n = 49). Pandehulens størrelse var ikke påvirket hos HR patienter i forhold til KTR (*p* > 0,406). Næsebenets proksimale bredde og forholdet mellem denne bredde og længden på næsebenets akse var forøget hos HR patienter i forhold til KTR (*p* < 0.05), hvilket indikerede en afvigende næsebens-morfologi hos HR patienter. Den upåvirkede størrelse af pandehulen indikerede en normal evne til intern knogleresorption. Næsebenets morfologi var ikke normal, hvilket kunne indikere forstyrrelser i knogledannelsen under næsebenets vækst. Disse forstyrrelser manifesterede sig hovedsageligt i den proksimale del, der er støttet af strukturer af endochondral oprindelse. Graden af afvigende næsebensmorfologi synes at være positivt korreleret med alvorlighedsgraden af den generelle skeletale HR påvirkning.

I artikel III anvendtes den samme studiepopulation som i artikel II. På profilrøntgenbillederne opmåltes dimensionerne af atlas og axis og ved en visuel vurdering blev det afdækket, om der var radiologiske tegn på anomalier i relation til de øverste 5 halshvirvler (fusioner eller hvirvelbue dehiscencer). Atlas højde og længde samt højden på axis hvirvelbue var forøget hos HR patienter i forhold til KTR (p ≤ 0,001), og flere HR patienter (32%) end KTR (11%) havde fusioner (*p* = 0,003). I den samlede gruppe af voksne (n = 85) var højden af atlas hvirvelbue og længden af axis negativt korrelerede med kraniebasis vinklen (*p* = 0,017 hhv. *p* = 0,008), og atlas vertikale dimensioner var positivt korrelerede med den occipitale theca tykkelse (p ≤ 0,015). Atlas længde var positivt korreleret med den mandibulære prognati (angle s-n-pg) (*p* = 0,042). Forekomsten af fusioner var positivt korrelerede med tykkelsen af kranie theca frontalt og parietalt (hhv. *p* = 0.034 and *p* = 0.003). Hos HR patienter var atlas længde positivt korreleret (*p* = 0,043) og dens højde negativt korreleret (*p* = 0,008) med alvorlighedsgraden af den generelle skeletale HR påvirkning. Det konkluderedes, at atlas og axis dimensioner samt forekomsten af fusioner i halshvirvelsøjlen var forøget i gruppen af HR patienter. I den samlede gruppe var der en sammenhæng mellem hvirvellegemernes dimensioner og de kranio-faciale dimensioner, hvilket var tydeligst i forhold til den posteriore kraniefossa. Dette indikerer en særlig tæt sammenhæng mellem de ossøse strukturer indenfor det fælles cerebellare og spinale udviklingsfelt.

I artikel IV anvendtes den samme studiepopulation som i artikel II og III. Det blev vurderet, om der på røntgenbillederne var tegn på intra- eller extra-kranielle forkalkninger. I alt 17% af HR patienter havde radiologiske tegn på intrakranielle forkalkninger, hvilket ikke i samme grad var tilfældet hos KTR. I det nuchale ligament var der radiologiske tegn på forkalkninger hos 50% af HR patienterne

og 27% af KTR (p = 0,009). Tilstedeværelsen af forkalkninger i det nuchale ligament var positivt korreleret med alvorlighedsgraden af den generelle skeletale HR påvirkning (p = 0,006). I alt 42% af HR patienterne havde vertebrale entesopatier, Forekomsten af vertebrale entesopatier var negativt korreleret med medicinsk behandling i barndommen (p = 0.008).

ST morfologien blev visuelt vurderet og klassificeret i forhold til 6 normale ST typer (1 standard type og 5 normal-afvigelser fra standarden). Forekomsten af standard ST typen var lav i HR gruppen (53%) sammenlignet med KTR gruppen (78%) (p = 0,021). ST dimensionerne var upåvirkede hos HR patienter i forhold til KTR (p ≥ 0.13). Der var ikke en entydig sammenhæng mellem afvigelser i ST morfologi og alvorlighedsgraden af den generelle skeletale påvirkning ved HR.

Afsluttende konklusion. Ved en sammenligning af HR patienter i forhold til raske KTR kunne der konstateres visse afvigelser i såvel kraniets som halshvirvelsøjlens morfologi, og at disse afvigelser manifesterede sig uafhængigt af den ossøse oprindelse af en given struktur. Afvigelserne i kraniets og halshvirvelsøjlens morfologi antydede forstyrrelser i knogle-remodelerings-processer hos HR patienter. Atlas og axis dimensioner syntes at have en særlig sammenhæng med morfologien af de øvrige strukturer i den kranielle del af det cerebellare og spinale udviklingsfelt. Forkalkninger i det nuchale ligament var hyppigt forekommende hos HR patienter. Afvigelser i kraniets og halshvirvelsøjlens morfologi samt tilstedeværelsen af forkalkninger i det nuchale ligament korrelerer til en vis grad med alvorlighedsgraden af den generelle skeletale HR påvirkning. Medicinsk behandling i løbet af barndommen korrelerer negativt med forekomsten af vertebrale entesopatier.

11. References

ADHR Consortium 2000 Autosomal dominant hypophosphataemic rickets is associated with mutations in FGF23. Nat Genet 26: 345-348

Al-Jundi S H, Dabous I M, Al-Jamal G A 2009 Craniofacial morphology in patients with hypophosphataemic vitamin-D-resistant rickets: a cephalometric study. J Oral Rehabil 36: 483-490

Alkofide E 2001 Pituitary adenoma: a cephalometric finding. Am J Orthod Dentofacial Orthop 120: 559-562

Alkofide E A 2007 The shape and size of the sella turcica in skeletal Class I, Class II, and Class III Saudi subjects. Eur J Orthod 29: 457-463

Alkofide E A 2008 Sella turcica morphology and dimensions in cleft subjects. Cleft Palate Craniofac J 45: 647-653

Andersen M G, Beck-Nielsen S S, Haubek D, Hintze H, Gjorup H, Poulsen S 2012 Periapical and endodontic status of permanent teeth in patients with hypophosphatemic rickets. J Oral Rehabil 39: 144-150

Anderson P J, Hall C, Evans R D, Harkness W J, Hayward R D, Jones B M 1976 The cervical spine in Crouzon syndrome. Spine 22: 402-405

Anderson P J, Hall C M, Evans R D, Hayward R D, Harkness W J, Jones B M 1997 The cervical spine in Saethre-Chotzen syndrome. Cleft Palate Craniofac J 34: 79-82

Anderson P J, Hall C M, Evans R D, Jones B M, Harkness W, Hayward R D 1996 Cervical spine in Pfeiffer's syndrome. J Craniofac Surg 7: 275-279

Andredaki M, Koumantanou A, Dorotheou D, Halazonetis D J 2007 A cephalometric morphometric study of the sella turcica. Eur J Orthod 29: 449-456

Arntsen T, Kjaer I, Sonnesen L 2009 Lengths of the maxillary central incisor, the nasal bone, and the anterior cranial base in different skeletal malocclusions. Acta Odontol Scand 67: 1-6

Arntsen T, Kjaer I, Sonnesen L, Molsted K 2010 Skull thickness in patients with clefts. Orthod Craniofac Res 13: 75-81

Arponen H, Evalahti M, Waltimo-Siren J 2010 Dimensions of the craniocervical junction in longitudinal analysis of normal growth. Childs Nerv Syst 26: 763-769

Arponen H, Makitie O, Haukka J, Ranta H, Ekholm M, Mayranpaa M K, Kaitila I, Waltimo-Siren J 2012 Prevalence and natural course of craniocervical junction anomalies during growth in patients with osteogenesis imperfecta. J Bone Miner Res 27: 1142-1149

Axelsson S, Kjaer I, Bjornland T, Storhaug K 2003 Longitudinal cephalometric standards for the neurocranium in Norwegians from 6 to 21 years of age. Eur J Orthod 25: 185-198

Axelsson S, Kjaer I, Heiberg A, Bjornland T, Storhaug K 2005 Neurocranial morphology and growth in Williams syndrome. Eur J Orthod 27: 32-47

Axelsson S, Storhaug K, Kjaer I 2004a Post-natal size and morphology of the sella turcica in Williams syndrome. Eur J Orthod 26: 613-621

Axelsson S, Storhaug K, Kjaer I 2004b Post-natal size and morphology of the sella turcica. Longitudinal cephalometric standards for Norwegians between 6 and 21 years of age. Eur J Orthod 26: 597-604

Baroncelli G I, Toschi B, Bertelloni S 2012 Hypophosphatemic rickets. Curr Opin Endocrinol Diabetes Obes 19: 460-467

Basciftci F A, Uysal T, Buyukerkmen A, Sari Z 2003 The effects of activator treatment on the craniofacial structures of Class II division 1 patients. Eur J Orthod 25: 87-93

Baumrind S, Frantz R C 1971 The reliability of head film measurements. 1. Landmark identification. Am J Orthod 60: 111-127

Bebnowski D, Hanggi M P, Markic G, Roos M, Peltomaki T 2012 Cervical vertebrae anomalies in subjects with Class II malocclusion assessed by lateral cephalogram and cone beam computed tomography. Eur J Orthod 34: 226-231

Beck-Nielsen S S 2012 Rickets in Denmark. Dan Med J 59: B4384

Beck-Nielsen S S, Brixen K, Gram J, Brusgaard K 2012 Mutational analysis of PHEX, FGF23, DMP1, SLC34A3 and CLCN5 in patients with hypophosphatemic rickets. J Hum Genet 57: 453-458

Beck-Nielsen S S, Brock-Jacobsen B, Gram J, Brixen K, Jensen T K 2009 Incidence and prevalence of nutritional and hereditary rickets in southern Denmark. Eur J Endocrinol 160: 491-497

Beck-Nielsen S S, Brusgaard K, Rasmussen L M, Brixen K, Brock-Jacobsen B, Poulsen M R, Vestergaard P, Ralston S H, Albagha O M, Poulsen S *et al.* 2010 Phenotype presentation of hypophosphatemic rickets in adults. Calcif Tissue Int 87: 108-119

Bergwitz C, Juppner H 2010 Regulation of phosphate homeostasis by PTH, vitamin D, and FGF23. Annu Rev Med 61: 91-104

Bergwitz C, Juppner H 2012 FGF23 and syndromes of abnormal renal phosphate handling. Adv Exp Med Biol 728:41-64. doi: 10.1007/978-1-4614-0887-1_3.: 41-64

Bergwitz C, Roslin N M, Tieder M, Loredo-Osti J C, Bastepe M, bu-Zahra H, Frappier D, Burkett K, Carpenter T O, Anderson D *et al.* 2006 SLC34A3 mutations in patients with hereditary hypophosphatemic rickets with hypercalciuria predict a key role for the sodium-phosphate cotransporter NaPi-IIc in maintaining phosphate homeostasis. Am J Hum Genet 78: 179-192

Bjørk A 1955 Facial growth in man, studied with the aid of metallic implants. Acta Odontol Scand 13: 9-34

Bjørk A 1966 Sutural growth of the upper face studied by the implant method. Acta Odontol Scand 24: 109-127

Bjørk A 1968 The use of metallic implants in the study of facial growth in children: method and application. Am J Phys Anthropol 29: 243-254

Bjørk A 1975 Kæbernes relation til det øvrige kranium. In: Lundström I (ed.) Nordisk Lärobok i Ortodonti. Sveriges Tandläkarförbunds Förlagsförening, Stockholm

Bjørk A, Skieller V 1972 Facial development and tooth eruption. An implant study at the age of puberty. Am J Orthod 62: 339-383

Bjørk A, Skieller V 1974 Growth in width of the maxilla studied by the implant method. Scand J Plast Reconstr Surg 8: 26-33

Bjørk A, Skieller V 1983 Normal and abnormal growth of the mandible. A synthesis of longitudinal cephalometric implant studies over a period of 25 years. Eur J Orthod 5: 1-46

Bookstein F L 1987 Describing a craniofacial anomaly: finite elements and the biometrics of landmark locations. Am J Phys Anthropol 74: 495-509

Boyle W J, Simonet W S, Lacey D L 2003 Osteoclast differentiation and activation. Nature 423: 337-342

Brakemeier S, Si H, Gollasch M, Hoffler D, Buhl M, Kohler R, Hoyer J, Eichler I 2004 Dent's disease: identification of a novel mutation in the renal chloride channel CLCN5. Clin Nephrol 62: 387-390

Broch J, Slagsvold O, Rosler M 1981 Error in landmark identification in lateral radiographic headplates. Eur J Orthod 3: 9-13

Brock-Jacobsen M T, Pallisgaard C, Kjaer I 2009 The morphology of the sella turcica in monozygotic twins. Twin Res Hum Genet 12: 598-604

Brown W A, Molleson T I, Chinn S 1984 Enlargement of the frontal sinus. Ann Hum Biol 11: 221-226

Buurman H, Saeger W 2006 Subclinical adenomas in postmortem pituitaries: classification and correlations to clinical data. Eur J Endocrinol 154: 753-758

Caldemeyer K S, Boaz J C, Wappner R S, Moran C C, Smith R R, Quets J P 1995 Chiari I malformation: association with hypophosphatemic rickets and MR imaging appearance. Radiology 195: 733-738

Canalis E 2005 The fate of circulating osteoblasts. N Engl J Med 352: 2014-2016

Carlsen N L, Krasilnikoff P A, Eiken M 1984 Premature cranial synostosis in X-linked hypophosphatemic rickets: possible precipitation by 1-alpha-OH-cholecalciferol intoxication. Acta Paediatr Scand 73: 149-154

Carpenter T O 2012 The expanding family of hypophosphatemic syndromes. J Bone Miner Metab 30: 1-9

Carpenter T O, Imel E A, Holm I A, Jan de Beur S M, Insogna K L 2011 A clinician's guide to X-linked hypophosphatemia. J Bone Miner Res 26: 1381-1388

Caspersen L M, Kjaer I, Sonnesen L 2010 How does occipitalization influence the dimensions of the cranium? Orthod Craniofac Res 13: 162-168

Chang H P, Tseng Y C, Chou T M 2005 An enlarged sella turcica on cephalometric radiograph. Dentomaxillofac Radiol 34: 308-312

Chaussain-Miller C, Sinding C, Wolikow M, Lasfargues J J, Godeau G, Garabedian M 2003 Dental abnormalities in patients with familial hypophosphatemic vitamin D-resistant rickets: prevention by early treatment with 1-hydroxyvitamin D. J Pediatr 142: 324-331

Cheung M, Roschger P, Klaushofer K, Veilleux L N, Roughley P, Glorieux F H, Rauch F 2013 Cortical and trabecular bone density in X-linked hypophosphatemic rickets. J Clin Endocrinol Metab 98: E954-E961

Cheverud J, Lewis J L, Bachrach W, Lew W D 1983 The measurement of form and variation in form: an application of three-dimensional quantitative morphology by finite-element methods. Am J Phys Anthropol 62: 151-165

Cho H Y, Lee B H, Choi H J, Ha I S, Choi Y, Cheong H I 2008 Renal manifestations of Dent disease and Lowe syndrome. Pediatr Nephrol 23: 243-249

Cohen M M 1990 Syndromology: an updated conceptual overview. VIII. Deformations and disruptions. Int J Oral Maxillofac Surg 19: 33-37

Cohen M M, Walker G F, Phillips C 1985 A morphometric analysis of the craniofacial configuration in achondroplasia. J Craniofac Genet Dev Biol Suppl 1: 139-165

Cooke M S, Wei S H 1991 Cephalometric errors: a comparison between repeat measurements and retaken radiographs. Aust Dent J 36: 38-43

Currarino G 2007 Sagittal synostosis in X-linked hypophosphatemic rickets and related diseases. Pediatr Radiol 37: 805-812

Currarino G, Rollins N, Diehl J T 1994 Congenital defects of the posterior arch of the atlas: a report of seven cases including an affected mother and son. AJNR Am J Neuroradiol 15: 249-254

Dahlberg G 1940 Statistical methods for medical and biological students. Georges Allen and Unwin, London

de-Jong T., Bannink N, Bredero-Boelhouwer H H, van Veelen M L, Bartels M C, Hoeve L J, Hoogeboom A J, Wolvius E B, Lequin M H, van der Meulen J J *et al.* 2010 Long-term functional outcome in 167 patients with syndromic craniosynostosis; defining a syndrome-specific risk profile. J Plast Reconstr Aesthet Surg 63: 1635-1641

Dostalova S, Sonka K, Smahel Z, Weiss V, Marek J 2003 Cephalometric assessment of cranial abnormalities in patients with acromegaly. J Craniomaxillofac Surg 31: 80-87

Drake R L, Vogl A W, Mitchell T C 2013 Gray's Anatomy for Students. Churchil Livingstone, Elsevier Inc., Philadelphia PA

Drezner M K 2003 Hypophosphatemic Rickets. Endocr Dev 6: 126-155

Dryden I L, Mardia K V 1998 Statistical shape analysis. John Wiley and Sons, New York

Ellis E, McNamara J A 1984 Components of adult Class III open-bite malocclusion. Am J Orthod 86: 277-290

Ellis E, McNamara J A, Jr., Lawrence T M 1985 Components of adult Class II open-bite malocclusion. J Oral Maxillofac Surg 43: 92-105

Enlow D H, Hans M G 1996 The neurocranium. In: Enlow D H, Hans M G (eds.) Facial Growth. Handbook in Facial Growth. Saunders, Philadelphia, pp. 99-110

Erturk N 1968 [Teleroentgen studies on the development of the frontal sinus]. Fortschr Kieferorthop 29: 245-248

Farman A G, Nortje C J, Joubert J J 1979 Radiographic profile of the first cervical vertebra. J Anat 128: 595-600

Gauche C, Nguyen TM, Esterle L, Garabedian M, Jehan F, Walrant-Debray O 2009 PHEX analysis in 118 pedigrees reveals new genetic clues in hypophosphatemic rickets. Hum Genet 125: 401-411

Gjørup H, Kjaer I, Sonnesen L, Haubek D, Beck-Nielsen S S, Hintze H, Poulsen S 2011 Craniofacial morphology in patients with hypophosphatemic rickets: a cephalometric study focusing on differences between bone of cartilaginous and intramembranous origin. Am J Med Genet A 155A: 2654-2660

Gonzalez C D, Meyer R A, Jr., Iorio R J 1992 Craniometric measurements of craniofacial malformations in the X-linked hypophosphatemic (Hyp) mouse on two different genetic backgrounds: C57BL/6J and B6C3H. Teratology 46: 605-613

Halazonetis D J 2004 Morphometrics for cephalometric diagnosis. Am J Orthod Dentofacial Orthop 125: 571-581

Hammond A B, Smahel Z, Moss M L 1993 Finite element method analysis of craniofacial morphology in unilateral cleft lip and palate prior to palatoplasty. J Craniofac Genet Dev Biol 13: 47-56

Hatipoglu H G, Ozcan H N, Hatipoglu U S, Yuksel E 2008 Age, sex and body mass index in relation to calvarial diploe thickness and craniometric data on MRI. Forensic Sci Int 182: 46-51

Hayashibara T, Hiraga T, Sugita A, Wang L, Hata K, Ooshima T, Yoneda T 2007 Regulation of osteoclast differentiation and function by phosphate: potential role of osteoclasts in the skeletal abnormalities in hypophosphatemic conditions. J Bone Miner Res 22: 1743-1751

Helfrich M H 2003 Osteoclast diseases. Microsc Res Tech 61: 514-532

Heliovaara A, Hurmerinta K 2006 Craniofacial cephalometric morphology in children with CATCH 22 syndrome. Orthod Craniofac Res 9: 186-192

Hemmer K M, McAlister W H, Marsh J L 1987 Cervical spine anomalies in the craniosynostosis syndromes. Cleft Palate J 24: 328-333

Hochberg Z 2003 Rickets - past and present. Introduction. Endocr Dev 6: 1-13

Horswell B B 1991 The incidence and relationship of cervical spine anomalies in patients with cleft lip and/or palate. J Oral Maxillofac Surg 49: 693-697

Houston W J, Maher R E, McElroy D, Sherriff M 1986 Sources of error in measurements from cephalometric radiographs. Eur J Orthod 8: 149-151

Houston W J B 1983 The analysis of errors in orthodontic measurements. Am J Orthod 83: 382-390

Huggare J 1989 The first cervical vertebra as an indicator of mandibular growth. Eur J Orthod 11: 10-16

Huggare J 1991 Association between morphology of the first cervical vertebra, head posture, and craniofacial structures. Eur J Orthod 13: 435-440

Huggare J 1995 Craniocervical junction as a focus for craniofacial growth studies. Acta Odontol Scand 53: 186-191

Huggare J 1998 Postural disorders and dentofacial morphology. Acta Odontol Scand 56: 383-386

Huggare J, Houghton P 1996 Associations between atlantoaxial and craniomandibular anatomy. Growth Dev Aging 60: 21-30

Huggare J, Pirttiniemi P, Serlo W 1991 Head posture and dentofacial morphology in subjects treated for scoliosis. Proc Finn Dent Soc 87: 151-158

Huggare J A, Cooke M S 1994 Head posture and cervicovertebral anatomy as mandibular growth predictors. Eur J Orthod 16: 175-180

Hultman C S, Riski J E, Cohen S R, Burstein F D, Boydston W R, Hudgins R J, Grattan-Smith D, Uhas K, Simms C 2000 Chiari malformation, cervical spine anomalies, and neurologic deficits in velocardiofacial syndrome. Plast Reconstr Surg 106: 16-24

Hyp Consortium 1995 A gene (PEX) with homologies to endopeptidases is mutated in patients with X-linked hypophosphatemic rickets. The HYP Consortium. Nat Genet 11: 130-136

Imerslund O 1951 Craniostenosis and vitamin D resistant rickets. Acta Paediatr 40: 449-456

Ingerslev C H, Solow B 1975 Sex differences in craniofacial morphology. Acta Odontol Scand 33: 85-94

Iorio R J, Bell W A, Meyer M H, Meyer R A, Jr. 1979 Histologic evidence of calcification abnormalities in teeth and alveolar bone of mice with X-linked dominant hypophosphatemia (VDRR). Ann Dent 38: 38-44

Iorio R J, Murray G, Meyer R A, Jr. 1980 Craniometric measurements of craniofacial malformations in mice with X-linked, dominant hypophosphatemia (vitamin D-resistant rickets). Teratology 22: 291-298

Jacobsen P E, Kjaer I, Sonnesen L 2008 Skull thickness in patients with skeletal deep bite. Orthod Craniofac Res 11: 119-123

Jensen B L, Kreiborg S 1993 Craniofacial abnormalities in 52 school-age and adult patients with cleidocranial dysplasia. J Craniofac Genet Dev Biol 13: 98-108

Jensen B L, Kreiborg S 1995 Craniofacial growth in cleidocranial dysplasia - a roentgencephalometric study. J Craniofac Genet Dev Biol 15: 35-43

Jensen B L, Lund A M 1997 Osteogenesis imperfecta: clinical, cephalometric, and biochemical investigations of OI types I, III, and IV. J Craniofac Genet Dev Biol 17: 121-132

Joss C U, Triaca A, Antonini M, Kiliaridis S, Kuijpers-Jagtman A M 2012 Skeletal and dental stability of segmental distraction of the anterior mandibular alveolar process. A 2-year follow-up. Int J Oral Maxillofac Surg 41: 553-559

Kamoen A, Dermaut L, Verbeeck R 2001 The clinical significance of error measurement in the interpretation of treatment results. Eur J Orthod 23: 569-578

Karaplis A C, Bai X, Falet J P, Macica C M 2012 Mineralizing enthesopathy is a common feature of renal phosphate-wasting disorders attributed to FGF23 and is exacerbated by standard therapy in hyp mice. Endocrinology 153: 5906-5917

Karsenty G, Kronenberg H M, Settembre C 2009 Genetic control of bone formation. Annu Rev Cell Dev Biol 25:629-48. doi: 10.1146/annurev.cellbio.042308.113308.: 629-648

Katz L D, Elmore J G, Wild D M G, Lucan S C 2013 Common research designs and issues in epidemiology. In: Katz L D, Elmore J G, Wild D M G, Lucan S C (eds.) Jekel's Epidemiology, Biostatistics, Preventive Medicine, and Public Health. Saunders, Elsevier Inc., Philadelphia, Pa,

Kierszenbaum A l, Tres L L 2011 Osteogenesis. In: Kierszenbaum A l, Tres.L.L. (eds.) Histology and cell biology - An introduction to pathology. Saunders, Elsevier Inc., Philadelphia PA,

Kjaer I 1998a Neuro-osteology. Crit Rev Oral Biol Med 9: 224-244

Kjaer I 1998b Prenatal traces of aberrant neurofacial growth. Acta Odontol Scand 56: 326-330

Kjaer I 2010 Orthodontics and foetal pathology: a personal view on craniofacial patterning. Eur J Orthod 32: 140-147

Kjaer I 2012 Sella turcica morphology and the pituitary gland - a new contribution to craniofacial diagnostics based on histology and neuroradiology. Eur J Orthod [Epub ahead of print]

Kjaer I, Becktor K B, Lisson J, Gormsen C, Russell B G 2001a Face, palate, and craniofacial morphology in patients with a solitary median maxillary central incisor. Eur J Orthod 23: 63-73

Kjaer I, Hansen N, Becktor K B, Birkebaek N, Balslev T 2001b Craniofacial morphology, dentition, and skeletal maturity in four siblings with Seckel syndrome. Cleft Palate Craniofac J 38: 645-651

Kjaer I, Keeling J W, Graem N 1994 Cranial base and vertebral column in human anencephalic fetuses. J Craniofac Genet Dev Biol 14: 235-244

Kjaer I, Keeling J W, Hansen B F 1999 The Prenatal Human Cranium - normal and pathologic development. Munksgaard, Copenhagen

Kjaer I, Wagner A, Madsen P, Blichfeldt S, Rasmussen K, Russell B 1998 The sella turcica in children with lumbosacral myelomeningocele. Eur J Orthod 20: 443-448

Knothe Tate M L, Adamson J R, Tami A E, Bauer T W 2004 The osteocyte. Int J Biochem Cell Biol 36: 1-8

Koletsis D D, Halazonetis D J 2010 Cervical vertebrae anomalies in orthodontic patients: a growth-based superimpositional approach. Eur J Orthod 32: 36-42

Kuether T A, Piatt J H 1998 Chiari malformation associated with vitamin D-resistant rickets: case report. Neurosurgery 42: 1168-1171

Kuhl F P, Giardina C R 1982 Eliptical Fourier features of a closed contour. Computer graphics and image processing 18: 236-258

Kuro-o M 2010 Overview of the FGF23-Klotho axis. Pediatr Nephrol 25: 583-590

Kuro-o M, Matsumura Y, Aizawa H, Kawaguchi H, Suga T, Utsugi T, Ohyama Y, Kurabayashi M, Kaname T, Kume E *et al.* 1997 Mutation of the mouse klotho gene leads to a syndrome resembling ageing. Nature 390: 45-51

Lavelle C L 1988 An analysis of craniofacial form in cleft palate patients. Anat Anz 166: 157-163

Lee J Y, Imel E A 2013 The changing face of hypophosphatemic disorders in the FGF-23 era. Pediatr Endocrinol Rev 10 Suppl 2:367-79.: 367-379

Lee S H, Agashe M V, Suh S W, Yoon Y C, Song S H, Yang J H, Lee H, Song H R 2012 Paravertebral ligament ossification in vitamin D-resistant rickets: incidence, clinical significance, and genetic evaluation. Spine 37: E792-E796

Lestrel P E 1982 A Fourier analytic procedure to describe complex morphological shapes. Prog Clin Biol Res 101:393-409.: 393-409

Lestrel P E 1997 Morphometrics of craniofacial form: A Fourier analytic procedure to describe complex morphological shapes. In: Dixon A D, Hoyte D A N, Ronning O (eds.) Fundamentals of cranial facial growth. CRC Press, New York,

Lestrel P E, Engstrom C, Chaconas S J 1991 A longitudinal study of the human nasal bone in Norma Lateralis: size and shape considerations. In: Dixon A D, Sarnat B G, Hoyte D A N (eds.) Fundamentals of bone growth: Methodology and Applications. CRC Press. Inc., London, pp. 547-564

Lestrel P E, Ohtsuki F, Wolfe C A 2010 Cranial vault shape in fossil hominids: Fourier descriptors in norma lateralis. Homo 61: 287-313

Lestrel P E, Wolfe C A, Bodt A 2013 Mandibular shape analysis in fossil hominins: Fourier descriptors in norma lateralis. Homo 64: 247-272

Levine M A 2003 Normal mineral homeostasis. Interplay of parathyroid hormone and vitamin D. Endocr Dev 6: 14-33

Levy-Litan V, Hershkovitz E, Avizov L, Leventhal N, Bercovich D, Chalifa-Caspi V, Manor E, Buriakovsky S, Hadad Y, Goding J *et al.* 2010 Autosomal-recessive hypophosphatemic rickets is associated with an inactivation mutation in the ENPP1 gene. Am J Hum Genet 86: 273-278

Lexner M O, Bardow A, Bjorn-Jorgensen J, Hertz J M, Almer L, Kreiborg S 2007 Anthropometric and cephalometric measurements in X-linked hypohidrotic ectodermal dysplasia. Orthod Craniofac Res 10: 203-215

Liang G, Katz L D, Insogna K L, Carpenter T O, Macica C M 2009 Survey of the enthesopathy of X-linked hypophosphatemia and its characterization in Hyp mice. Calcif Tissue Int 85: 235-246

Lima M C, Franco E J, Janson G, Carvalho I M, Santos C F, Capelozza A L 2009 Prevalence of upper cervical vertebrae anomalies in patients with cleft lip and/or palate and noncleft patients. Cleft Palate Craniofac J 46: 481-486

Liu S, Quarles L D 2007 How fibroblast growth factor 23 works. J Am Soc Nephrol 18: 1637-1647

Liu S, Tang W, Zhou J, Stubbs J R, Luo Q, Pi M, Quarles L D 2006a Fibroblast growth factor 23 is a counter-regulatory phosphaturic hormone for vitamin D. J Am Soc Nephrol 17: 1305-1315

Liu S, Tang W, Zhou J, Vierthaler L, Quarles L D 2007 Distinct roles for intrinsic osteocyte abnormalities and systemic factors in regulation of FGF23 and bone mineralization in Hyp mice. Am J Physiol Endocrinol Metab 293: E1636-E1644

Liu S, Zhou J, Tang W, Jiang X, Rowe D W, Quarles L D 2006b Pathogenic role of Fgf23 in Hyp mice. Am J Physiol Endocrinol Metab 291: E38-E49

Liu S, Zhou J, Tang W, Menard R, Feng J Q, Quarles L D 2008 Pathogenic role of Fgf23 in Dmp1-null mice. Am J Physiol Endocrinol Metab 295: E254-E261

Lomholt J F, Nolting D, Hansen B F, Stoltze K, Kjaer I 2003 The pre-natal development and osseous growth of the human cerebellar field. Orthod Craniofac Res 6: 143-154

Lorenz-Depiereux B, Bastepe M, Benet-Pages A, Amyere M, Wagenstaller J, Muller-Barth U, Badenhoop K, Kaiser S M, Rittmaster R S, Shlossberg A H *et al.* 2006a DMP1 mutations in autosomal recessive hypophosphatemia implicate a bone matrix protein in the regulation of phosphate homeostasis. Nat Genet 38: 1248-1250

Lorenz-Depiereux B, Benet-Pages A, Eckstein G, Tenenbaum-Rakover Y, Wagenstaller J, Tiosano D, Gershoni-Baruch R, Albers N, Lichtner P, Schnabel D *et al.* 2006b Hereditary hypophosphatemic rickets with hypercalciuria is caused by mutations in the sodium-phosphate cotransporter gene SLC34A3. Am J Hum Genet 78: 193-201

Lorenz-Depiereux B, Guido V E, Johnson K R, Zheng Q Y, Gagnon L H, Bauschatz J D, Davisson M T, Washburn L L, Donahue L R, Strom T M *et al.* 2004 New intragenic deletions in the Phex gene clarify X-linked hypophosphatemia-related abnormalities in mice. Mamm Genome 15: 151-161

Lorenz-Depiereux B, Schnabel D, Tiosano D, Hausler G, Strom T M 2010 Loss-of-function ENPP1 mutations cause both generalized arterial calcification of infancy and autosomal-recessive hypophosphatemic rickets. Am J Hum Genet 86: 267-272

Lorenzo J A, Canalis E, Raisz L G 2011 Metabolic bone disease. In: Melmed S (ed.) Williams textbook of endocrinology. Saunders, Elsevier Inc., Philadelphia PA,

Lu Y, Feng J Q 2011 FGF23 in skeletal modeling and remodeling. Curr Osteoporos Rep 9: 103-108

Lynnerup N 2001 Cranial thickness in relation to age, sex and general body build in a Danish forensic sample. Forensic Sci Int 117: 45-51

Lynnerup N, Astrup J G, Sejrsen B 2005 Thickness of the human cranial diploe in relation to age, sex and general body build. Head Face Med 1:13.: 13

Makitie O, Doria A, Kooh S W, Cole W G, Daneman A, Sochett E 2003 Early treatment improves growth and biochemical and radiographic outcome in X-linked hypophosphatemic rickets. J Clin Endocrinol Metab 88: 3591-3597

Marie P J, Glorieux F H 1981a Histomorphometric study of bone remodeling in hypophosphatemic vitamin D-resistant rickets. Metab Bone Dis Relat Res 3: 31-38

Marie P J, Glorieux F H 1981b Stimulation of cortical bone mineralization and remodeling by phosphate and 1,25-dihydroxyvitamin D in vitamin D-resistant rickets. Metab Bone Dis Relat Res 3: 159-164

Marks S C, Lindahl R L, Bawden J W 1965 Dental and cephalometric findings in vitamin D resistant rickets. J Dent Child 32: 259-265

Martin A, Liu S, David V, Li H, Karydis A, Feng J Q, Quarles L D 2011 Bone proteins PHEX and DMP1 regulate fibroblastic growth factor FGF23 expression in osteocytes through a common pathway involving FGF receptor (FGFR) signaling. FASEB J 25: 2551-2562

Massengill A D, Huynh S L, Harris J H, Jr. 1997 C2-3 facet joint "pseudo-fusion": anatomic basis of a normal variant. Skeletal Radiol 26: 27-30

McCarthy E F, Sundaram M 2005 Heterotopic ossification: a review. Skeletal Radiol 34: 609-619

McNamara J A Jr 1984 A method of cephalometric evaluation. Am J Orthod 86: 449-469

Melmed S, Casanueva F F, Hoffman A R, Kleinberg D L, Montori V M, Schlechte J A, Wass J A 2011 Diagnosis and treatment of hyperprolactinemia: an Endocrine Society clinical practice guideline. J Clin Endocrinol Metab 96: 273-288

Melsen B 1974 The cranial base. Acta Odontol Scand 32 Supplement 62

Meyer-Marcotty P, Weisschuh N, Dressler P, Hartmann J, Stellzig-Eisenhauer A 2008 Morphology of the sella turcica in Axenfeld-Rieger syndrome with PITX2 mutation. J Oral Pathol Med 37: 504-510

Molsted K, Boers M, Kjaer I 2010 The morphology of the sella turcica in velocardiofacial syndrome suggests involvement of a neural crest developmental field. Am J Med Genet A 152A: 1450-1457

Moore K L, Persaud T V N, Torchia M G 2013 Skeletal System. In: Moore K L, Persaud T V N, Torchia M G (eds.) The Developing Human. Saunders, Elsevier Inc., Philadelphia PA, pp. 343-360

Moore M H, Lodge M L, Clark B E 1995 Spinal anomalies in Pfeiffer syndrome. Cleft Palate Craniofac J 32: 251-254

Moss M L, Salentijn L 1969 The primary role of functional matrices in facial growth. Am J Orthod 55: 566-577

Mostafa Y A, El-Mangoury N H, Meyer R A, Jr., Iorio R J 1982 Deficient nasal bone growth in the X-linked hypophosphataemic (HYP) mouse and its implication in craniofacial growth. Arch Oral Biol 27: 311-317

Murthy A S 2009 X-linked hypophosphatemic rickets and craniosynostosis. J Craniofac Surg 20: 439-442

Naikmasur V G, Sattur A P, Kirty R N, Thakur A R 2011 Type III Klippel-Feil syndrome: case report and review of associated craniofacial anomalies. Odontology 99: 197-202

Nanda R, Bouayad O, Topazian R G 1987 Facial growth subsequent to Le Fort I osteotomies in adolescent monkeys. J Oral Maxillofac Surg 45: 123-136

Nielsen B W, Molsted K, Kjaer I 2005a Maxillary and sella turcica morphology in newborns with cleft lip and palate. Cleft Palate Craniofac J 42: 610-617

Nielsen B W, Molsted K, Skovgaard L T, Kjaer I 2005b Cross-sectional study of the length of the nasal bone in cleft lip and palate subjects. Cleft Palate Craniofac J 42: 417-422

Pettifor J M, Thandrayen K 2012 Hypophosphatemic rickets: unraveling the role of FGF23. Calcif Tissue Int 91: 297-306

Pindborg J J 1970 The pathology of dental hard tissues. Saunders, Philadelphia

Pirttiniemi P, Lahtela P, Huggare J, Serlo W 1989 Head posture and dentofacial asymmetries in surgically treated muscular torticollis patients. Acta Odontol Scand 47: 193-197

Polisson R P, Martinez S, Khoury M, Harrell R M, Lyles K W, Friedman N, Harrelson J M, Reisner E, Drezner M K 1985 Calcification of entheses associated with X-linked hypophosphatemic osteomalacia. N Engl J Med 313: 1-6

Poole K E, van Bezooijen R L, Loveridge N, Hamersma H, Papapoulos S E, Lowik C W, Reeve J 2005 Sclerostin is a delayed secreted product of osteocytes that inhibits bone formation. FASEB J 19: 1842-1844

Pronicka E, Popowska E, Rowinska E, Arasimowicz E, Syczewska M, Jurkiewicz D, Lebiedowski M 2004 Anthropometric characteristics of X-linked hypophosphatemia. Am J Med Genet A 126A: 141-149

Pruzansky S 1973 Clinical investigation of the experiments of nature. Am Speech Hearing Assoc 8: 62-94

Quarles L D 2012a Role of FGF23 in vitamin D and phosphate metabolism: implications in chronic kidney disease. Exp Cell Res 318: 1040-1048

Quarles L D 2012b Skeletal secretion of FGF-23 regulates phosphate and vitamin D metabolism. Nat Rev Endocrinol 8: 276-286

Rauch F 2003 The rachitic bone. Endocr Dev 6: 69-79

Reilly B J, Leeming J M, Fraser D 1964 Craniosynostosis in the rachitic spectrum. J Pediatr 64:396-405.: 396-405

Richtsmeier J T 1987 Comparative study of normal, Crouzon, and Apert craniofacial morphology using finite element scaling analysis. Am J Phys Anthropol 74: 473-493

Richtsmeier J T, Cheverud J M 1986 Finite element scaling analysis of human craniofacial growth. J Craniofac Genet Dev Biol 6: 289-323

Richtsmeier J T, DeLeon V B, Lele S R 2002 The promise of geometric morphometrics. Am J Phys Anthropol Suppl 35:63-91.: 63-91

Richtsmeier J T, Lele S 1990 Analysis of craniofacial growth in Crouzon syndrome using landmark data. J Craniofac Genet Dev Biol 10: 39-62

Rohlf F J 2003 Bias and error in estimates of mean shape in geometric morphometrics. J Hum Evol 44: 665-683

Roy W A, Iorio R J, Meyer G A 1981 Craniosynostosis in vitamin D-resistant rickets. A mouse model. J Neurosurg 55: 265-271

Ruf S, Pancherz H 1996 Development of the frontal sinus in relation to somatic and skeletal maturity. A cephalometric roentgenographic study at puberty. Eur J Orthod 18: 491-497

Ruf S, Pancherz H 2004 Orthognathic surgery and dentofacial orthopedics in adult Class II Division 1 treatment: mandibular sagittal split osteotomy versus Herbst appliance. Am J Orthod Dentofacial Orthop 126: 140-152

Russell B G, Kjaer I 1995 Tooth agenesis in Down syndrome. Am J Med Genet 55: 466-471

Russell B G, Kjaer I 1999 Postnatal structure of the sella turcica in Down syndrome. Am J Med Genet 87: 183-188

Sabuncuoglu H, Ozdogan S, Karadag D, Kaynak E T 2011 Congenital hypoplasia of the posterior arch of the atlas: case report and extensive review of the literature. Turk Neurosurg 21: 97-103

Sandham A 1986 Cervical vertebral anomalies in cleft lip and palate. Cleft Palate J 23: 206-214

Sandikcioglu M, Molsted K, Kjaer I 1994a The prenatal development of the human nasal and vomeral bones. J Craniofac Genet Dev Biol 14: 124-134

Sandikcioglu M, Skov S, Solow B 1994b Atlas morphology in relation to craniofacial morphology and head posture. Eur J Orthod 16: 96-103

Sasaki A, Takeshita S, Publico A S, Moss M L, Tanaka E, Ishino Y, Watanabe M, Tanne K 2004 Finite element growth analysis for the craniofacial skeleton in patients with cleft lip and palate. Med Eng Phys 26: 109-118

Schett G 2012 Biology, physiology, and morphology of bone. In: Firestein G S, Budd R C, Gabriel S E, McInnes I B, O`Dell J R (eds.) Kelleys textbook of rheumatology. Saunders, Elsevier Inc., Philadelphia PA,

Schmittbuhl M, Le Minor J M, Schaaf A, Mangin P 2002 The human mandible in lateral view: elliptical fourier descriptors of the outline and their morphological analysis. Ann Anat 184: 199-207

Schoenwolf G C 2009a Development of the musculoskeletal system. In: Schoenwolf G C, Bleyl S B, Brauer P R, Francis-West P H (eds.) Larsen's human embryology. Churchill Livingstone, Elsevier Inc., Philadelphia PA,

Schoenwolf G C 2009b Development of the pharyngeal apparatus and the face. In: Schoenwolf G C, Bleyl S B, Brauer P R, Francis-West P H (eds.) Larsen's human embryology. Churchill Livingstone, Elsevier Inc., Philadelphia PA,

Schoenwolf G C 2009c Fourth week: Forming the embryo. In: Schoenwolf G C, Bleyl S B, Brauer P R, Francis-West P H (eds.) Larsen's human embryology. Churchill Livingstone, Elsevier Inc., Philadelphia PA,

Schoenwolf G C 2009d Third week: Becoming trilaminar and establishing body axes. In: Schoenwolf G C, Bleyl S B, Brauer P R, Francis-West P H (eds.) Larsen's human embryology. Churchill Livingstone, Elsevier Inc., Philadelphia PA,

Semb G, Brattstrom V, Molsted K, Prahl-Andersen B, Shaw W C 2005 The Eurocleft study: intercenter study of treatment outcome in patients with complete cleft lip and palate. Part 1: introduction and treatment experience. Cleft Palate Craniofac J 42: 64-68

Shaw K, McIntyre G, Mossey P, Menhinick A, Thomson D 2013 Validation of conventional 2D lateral cephalometry using 3D cone beam CT. J Orthod 40: 22-28

Shaw N J 2003 Vitamin D deficiency rickets. Endocr Dev 6:93-104.: 93-104

Shaw W C, Brattstrom V, Molsted K, Prahl-Andersen B, Roberts C T, Semb G 2005 The Eurocleft study: intercenter study of treatment outcome in patients with complete cleft lip and palate. Part 5: discussion and conclusions. Cleft Palate Craniofac J 42: 93-98

Shimada T, Kakitani M, Yamazaki Y, Hasegawa H, Takeuchi Y, Fujita T, Fukumoto S, Tomizuka K, Yamashita T 2004 Targeted ablation of FGF23 demonstrates an essential physiological role of FGF23 in phosphate and vitamin D metabolism. J Clin Invest 113: 561-568

Siersbaek-Nielsen S, Solow B 1982 Intra- and interexaminer variability in head posture recorded by dental auxiliaries. Am J Orthod 82: 50-57

Silverman F N 1957 Roentgen standards fo-size of the pituitary fossa from infancy through adolescence. Am J Roentgenol Radium Ther Nucl Med 78: 451-460

Simpson J 2013 Oxford Dictionary of English. Oxford University Press, Oxford

Singh G D, Hay A D 1999 Morphometry of the mandible in prepubertal craniofacial microsomia patients following an inverted L osteotomy. Int J Adult Orthodon Orthognath Surg 14: 229-235

Singh G D, McNamara J A, Jr., Lozanoff S 1997 Morphometry of the cranial base in subjects with Class III malocclusion. J Dent Res 76: 694-703

Soehle M, Casey A T 2002 Cervical spinal cord compression attributable to a calcified intervertebral disc in a patient with X-linked hypophosphatemic rickets: case report and review of the literature. Neurosurgery 51: 239-242

Solow B 1966 The pattern of craniofacial associations. Department of Orthodontics, The Royal Dental College, Copenhagen

Solow B 1980 The dentoalveolar compensatory mechanism: background and clinical implications. Br J Orthod 7: 145-161

Solow B, Sonnesen L 1998 Head posture and malocclusions. Eur J Orthod 20: 685-693

Solow B, Tallgren A 1971 Natural head position in standing subjects. Acta Odontol Scand 29: 591-607

Solow B, Tallgren A 1976 Head posture and craniofacial morphology. Am J Phys Anthropol 44: 417-435

Sonnesen L 2010 Associations between the Cervical Vertebral Column and Craniofacial Morphology. Int J Dent 2010: 295728

Sonnesen L, Jensen K E, Petersson A R, Petri N, Berg S, Svanholt P 2013 Cervical vertebral column morphology in patients with obstructive sleep apnoea assessed by lateral cephalogram and cone beam CT. A comparative study. Dentomaxillofac Radiol 42(6): 20130060

Sonnesen L, Kjaer I 2007a Cervical column morphology in patients with skeletal Class III malocclusion and mandibular overjet. Am J Orthod Dentofacial Orthop 132: 427

Sonnesen L, Kjaer I 2007b Cervical vertebral body fusions in patients with skeletal deep bite. Eur J Orthod 29: 464-470

Sonnesen L, Kjaer I 2008a Anomalies of the cervical vertebrae in patients with skeletal Class II malocclusion and horizontal maxillary overjet. Am J Orthod Dentofacial Orthop 133: 188

Sonnesen L, Kjaer I 2008b Cervical column morphology in patients with skeletal open bite. Orthod Craniofac Res 11: 17-23

Sonnesen L, Nolting D, Kjaer K W, Kjaer I 2008a Association between the development of the body axis and the craniofacial skeleton studied by immunohistochemical analyses using collagen II, Pax9, Pax1, and Noggin antibodies. Spine 33: 1622-1626

Sonnesen L, Pedersen C E, Kjaer I 2007 Cervical column morphology related to head posture, cranial base angle, and condylar malformation. Eur J Orthod 29: 398-403

Sonnesen L, Petri N, Kjaer I, Svanholt P 2008b Cervical column morphology in adult patients with obstructive sleep apnoea. Eur J Orthod 30: 521-526

Spranger J, Benirschke K, Hall J G, Lenz W, Lowry R B, Opitz J M, Pinsky L, Schwarzacher H G, Smith D W 1982 Errors of morphogenesis: concepts and terms. Recommendations of an international working group. J Pediatr 100: 160-165

Stenvik A, Larheim T A, Storhaug K 1985 Incisor and jaw relationship in 27 persons with osteogenesis imperfecta. Scand J Dent Res 93: 56-60

Tabatabaie F, Sonnesen L, Kjaer I 2008 The neurocranial and craniofacial morphology in children with solitary median maxillary central incisor (SMMCI). Orthod Craniofac Res 11: 96-104

Teitelbaum S L, Ross F P 2003 Genetic regulation of osteoclast development and function. Nat Rev Genet 4: 638-649

Tracy W E, Campbell R A 1968 Dentofacial development in children with vitamin D resistant rickets. J Am Dent Assoc 76: 1026-1031

Tubbs R S, Webb D, Abdullatif H, Conklin M, Doyle S, Oakes W J 2004 Posterior cranial fossa volume in patients with rickets: insights into the increased occurrence of Chiari I malformation in metabolic bone disease. Neurosurgery 55: 380-383

Ugar D A, Semb G 2001 The prevalence of anomalies of the upper cervical vertebrae in subjects with cleft lip, cleft palate, or both. Cleft Palate Craniofac J 38: 498-503

Veilleux L N, Cheung M, Ben A M, Rauch F 2012 Abnormalities in muscle density and muscle function in hypophosphatemic rickets. J Clin Endocrinol Metab 97: E1492-E1498

Velan G J, Currier B L, Clarke B L, Yaszemski M J 2001 Ossification of the posterior longitudinal ligament in vitamin D-resistant rickets: case report and review of the literature. Spine 26: 590-593

Wahl N 2006 Orthodontics in 3 millennia. Chapter 8: The cephalometer takes its place in the orthodontic armamentarium. Am J Orthod Dentofacial Orthop 129: 574-580

Waltimo-Siren J, Kolkka M, Pynnonen S, Kuurila K, Kaitila I, Kovero O 2005 Craniofacial features in osteogenesis imperfecta: a cephalometric study. Am J Med Genet A 133A: 142-150

Westphal O 1995 Normal growth and growth disorders in children. Acta Odontol Scand 53: 174-178

Wigal T G, Dischinger T, Martin C, Razmus T, Gunel E, Ngan P 2011 Stability of Class II treatment with an edgewise crowned Herbst appliance in the early mixed dentition: Skeletal and dental changes. Am J Orthod Dentofacial Orthop 140: 210-223

Willis F R, Beattie T J 1997 Craniosynostosis in X-linked hypophosphataemic rickets. J Paediatr Child Health 33: 78-79

Wood B, Lieberman D E 2001 Craniodental variation in Paranthropus boisei: a developmental and functional perspective. Am J Phys Anthropol 116: 13-25

Wood B A, Li Y, Willoughby C 1991 Intraspecific variation and sexual dimorphism in cranial and dental variables among higher primates and their bearing on the hominid fossil record. J Anat 174:185-205.: 185-205

Zhang R, Lu Y, Ye L, Yuan B, Yu S, Qin C, Xie Y, Gao T, Drezner M K, Bonewald L F *et al.* 2011 Unique roles of phosphorus in endochondral bone formation and osteocyte maturation. J Bone Miner Res 26: 1047-1056

Appendix

Tables on reviews of studies on cranial morphology in HR patients or in HYP mice:

- Table Z. A review of cephalometric and anthropometric studies on cranial morphology in HR patients
- Table ZZ. A review of studies on cranial synostosis and other cranial deviations in HR patients
- Table ZZZ. A review of studies on cranial morphology in HYP mice.

Tables on descriptive statistics of cephalometric variables in HR patients compared with healthy controls:

- E-TABLE I. Descriptive statistics (means and standard deviations) of cephalometric measurements of the cranial-base
- E-TABLE II. Descriptive statistics (means and standard deviations) of cephalometric measurements of the posterior cranial fossa
- E-TABLE III. Descriptive statistics (means and standard deviations) of cephalometric measurements of the neurocranium
- E-TABLE IV. Descriptive statistics (means and standard deviations) of cephalometric measurements of the cranial theca
- E-TABLE V. Descriptive statistics (means and standard deviations) of cephalometric measurements of the maxilla
- E-TABLE VI. Descriptive statistics (means and standard deviations) of cephalometric measurements of the nasal-bone and the mandible.

Tabel Z. A review of cephalometric and anthropometric studies on cranial morphology in HR patients, including study characteristics and main results.

	Study design[a]	Method & measurement type[b]	HR patients Female/Male[c]	Age group[d]	Comparison group[e]	Cranium or head[f]		Face height[g]		Jaw length/ sagital position[h]		Frontal bossing[i]	Theca thick.[j]	Cranial base angle[k]	Other findings
						Length	Circumference	Total	Upper	Maxilla	Mandible				
Albright *et al.* 1937	Case report	2 D ceph	1M	< 18	-	↑(1M)		-	-	-	-	-	-	↑	
Marks *et al.* 1965	Case series	2D ceph	9	< 18	Reference data	↑	-	-	-	-	-	x	↑	-	"Abnormal skull" (8 cases)
Tracy & Campbell, 1968	Case series	2D ceph	6F/3M	< 18	Reference data	-	-	-	↓	↓	(↓)	-		-	
O'Malley *et al.* 1988	Case series	Tomography of petrous bone & 2D ceph	11	?	11 Controls	↑ (2)	-	-	-	-	-	-	↑ (9)	↔	Thickening of petrous bone
Pronicka *et al.* 2004	Case-control	Anthropometric	57F/25M	< 18 ≥ 18	Family members	↑	F: ↑ M: ↔	↔	-	-	-	-			
Al-Jundi *et al.* 2009	Case-control	2D ceph	15F/7M	< 18	Matched controls	-	-	↔	↔	↓	↔	-		↑	
Beck-Nielsen *et al.* 2010	Case-control	Anthropometric	25F/13M	≥ 18	Reference data	-	↑	-	-	-	-	-	-	-	

Arrows indicate an increase (↑), a decrease (↓), or unaffected (↔) parameter in HR patients. "x" indicates a positive finding

[a] Design of the study: Case report, case series, or cross-sectional case-control studies

[b] Method of the study: 2D cephalometry/profile radiographs, 3D CT scanning, MRI scanning, clinical photos or anthropometric measurements.

[c] HR patients in the study: number of females/number of males

[d] Age group: below or above 18 years of age

[e] The comparison group: reference data (i.e., normative cephalometric or anthropometric data), age and gender matched control group, or another type of control group

[f] Length and circumference of the neurocranium/the head

[g] The total face height and the upper face height

[h] The length or the sagittal position of the maxilla and of the mandible

[i] Extraordinary prominence of the forehead

[j] Thickness of the theca/the cranial vault

[k] Deviations in the size of the cranial base angle (basion-sella-nasion)

Tabel ZZ. A review of studies on cranial synostosis and other cranial deviations in HR patients, including study characteristics and main results.

	Study design[a]	Method & measurement type[b]	HR patients Female/Male[c]	Age group[d]	Cranial length[e]	Frontal Bossing[f]	Cranial Synostosis[g]	CMI[h]	Theca thickness[i]	Posterior cranial fossa volumen[j]	Cranial base angle[k]	Other findings
Immerslund, 1951	Case report	2D ceph	1F/1M	< 18 ≥ 18	↑ (1F)	-	Sagittal (1F) Multiple(1M)	-	↓ local	-	↓ (1F)	Intracranial pressure ↑ (1 case)
Reilly et al. 1964	Case series	2D ceph	26	< 18	-	-	x (8)	-	-	-	-	
Stickler et al. 1970	Case series	Photos	27F/16M	< 18	↑ (3)	x (3)	Sagtittal (3)	-	-	-	-	
Carlsen et al. 1984	Case report	2D ceph	1M	< 18	-	-	Sagittal (1M)	-	↑ (1)	-	-	Intracranial pressure ↑ (1 case)
Caldemeyer et al. 1995a	Case series	MRI	10F/6M	< 18 ≥ 18	-	-	-	x (7)	↑ (9)	↓ (6)	-	Suboccipital craniectomy & laminectomy (2 cases)
Caldemeyer et al. 1995b	Case report	3D CT scan	1M	< 18	-	-	-	-			-	Optical canal narrowing. Extra-skeletal calcifications
Willis & Beattie, 1997	Case series	2D scan or 3D CT scan	8F/6M	< 18	-	-	Sagittal (2M) Multiple (1M)	-	-	-	-	Intracranial pressure ↑ (3 cases)
Kuther et al. 1998	Case report	MRI	1M	< 18				x (1)				Suboccipital craniectomy & laminectomy (1 cases)
Tubbs et al. 2004	Case-control	MRI or 3D CT scan	19*	< 18				x (2)		↓		
Currarino, 2007	Case series	2 D ceph (MRI)	28	< 18	↑ ** (10)	x (few)	Sagittal (7F) Sagittal (5M) Multiple (1M)	x (1)	-	-	-	Intracranial pressure ↑ (1 case)
Murthy, 2009	Case report	3D CT scan	1M	< 18	↑		Sagittal (1M)					Intracranial pressure ↑ (1 case)

Arrows indicate an increase (↑), a decrease (↓), or unaffected (↔) parameter in HR patients. "x" indicates a positive finding

[a] Design of the study: Case report, case series, or cross-sectional case-control studies

[b] Method of the study: 2D cephalometry/profile radiographs, 3D CT scanning, MRI scanning, clinical photos or anthropometric measurements.

[c] HR patients in the study: number of females/number of males.

[d] Age group: below or above 18 years of age

[e] Length of the neurocranium.

[f] Extraordinary prominence of the forehead.

[g] Premature cranial synostosis: the sagittal suture or other sutures

[h] Chiari Malformation type I, a tonsillar herniation of the cerebellum into the spinal canal.

[i] Thickness of the theca/the cranial vault

[j] The size of the posterior cranial fossa: Volumetric deviations or deviation in depth of the fossa

[k] Deviations in the size of the cranial base angle (basion-sella-nasion)

* Both vitamin-D-deficiency rickets and inherited types of rickets are included

** Cephalic index < 75, which indicate dolichocephaly. (cephalic index = (max internal width / max internal length) x 100)

Table ZZZ. A review of studies on cranial morphology in HYP mice, including study characteristics and main results.

	Study design[a]	Method & measurement type[b]	HYP mice Female/Male[c]	Age (weeks)[d]	Wild type Female/Male[e]	Cranium or head[f]				Jaw length/ sagittal position.[g]		Nose length[h]	Occipital bossing[i]	Cranial synostosis[j]	Other findings
						Length	Width	Total height	Upper height	Upper	Lower				
Iorio *et al.* 1979	Case control	2D ceph	7M*	13	7M	-	-	-	-	↓	(↓)	-	x	-	Hypocalcification of bone and teeth
Iorio *et al.* 1980	Case control	Direct	10F/10M *	13	10F/10M	↓	↔	↔	-	↓	↓	↓	-	-	
Roy *et al.* 1981	Case control longitudinal	Histological specimens	M *#	1-13	? M	-	-	-	-	-	-	-	-	Coronal	
Mostafa *et al.* 1982	Case control longitudinal	2D ceph	11M *	6, 9, and 12	20M	↓	-	-	↓	-	↓	↓	-	-	Deformation of frontonasal suture
Shetty & Meyer, 1991	Case control longitudinal	Direct	F* *hyp/+* # F* *hyp/hyp* #	10	? F	↓ ↓	↔ ↔	↔ ↓	-	↓ ↓	↔ ↓	↓ ↓	-	-	
Gonzales *et al.* 1992	Case control	Direct	11F/11M* 11 F/11M**	10	11F /11M	↓ ↓	↔ ↔	↔ ↑##	-	↓## ↓	↔ ↔	↓## ↓	-	-	
Lorenz-Depiereux *et al.* 2004	Case control	Direct	6M*** 6M****	12	6M	↓ ↓	↓ ↔	- 	-	↔ ↓	↔ ↔	↔ ↓	-	-	

Arrows indicate an increase (↑), a decrease (↓), or unaffected (↔) parameter in HYP mice. "x" indicates a positive finding

[a] Design of the study: Cross-sectional case-control study or a modified longitudinal study

[b] Method of the study: 2D cephalometry/profile radiographs, direct measurements on the cranium with a caliper, or histological assessment on specimens of the mice head.

[c] HYP mice in the study: number of females/number of males.

[d] Age in weeks at the time of sacrifice of the mice

[e] Wild type mice: the number of normal wild type mice, females and males.

[f] Length, width, total height, and the upper height of the cranium/the head

[g] The length or the sagittal position of the upper jaw and of the lower jaw.

[h] The length of the nose

[i] Extraordinary prominence of the occipital part of the cranium

[j] Premature cranial synostosis

*) HYP mice with genetic background *C57BL/6J* Females homozygotic *(hyp/hyp)* or heterozygotic *(hyp/+)*

**) HYP mice with genetic background *B6C3H*

***) HYP mice with *Hyp-2J*, an intrageneic deletions in the mouse *Phex* gene, hypophosphatemia-2 Jackson.

****) HYP mice with *Hyp-Duk*, an intrageneic deletions in the mouse *Phex* gene, hypophosphatemia-Duke

#) The number of HYP mice was not reported

##) Significant deviation only in males

?) The number not specified

E-TABLE I. Descriptive statistics (means and standard deviations) of cephalometric measurements of the cranial-base; bony structures of endochondral origin.

| | | Males | | | | | | Females | | | | | | Adjusted comparison of HR and control (*p*-value) |
| | | HR | | | Control | | | HR | | | Control | | | |
	Age in yrs	N	mean	SD	N	mean	SD	N	mean	SD	N	mean	SD	
n-s-ba	< 18	5	135.6	4.6	14	128.5	4.7	12	137.0	5.1	16	131.7	4.3	0.001*
	≥ 18	12	132.7	5.6	23	128.3	5.0	24	133.8	5.7	26	132.5	5.7	
n-s-ar	< 18	5	130.8	4.3	14	121.6	5.0	12	130.7	5.3	16	125.0	4.9	< 0.001*
	≥ 18	12	129.1	6.1	23	122.9	5.1	24	129.2	6.1	26	125.7	5.9	
s-n	< 18	5	74.0	7.9	14	75.3	4.1	12	69.4	4.4	16	71.9	2.5	0.111
	≥ 18	12	79.7	4.6	23	80.6	3.3	24	74.8	3.8	26	76.2	2.9	
s-ba	< 18	5	43.5	4.9	14	46.2	3.6	12	41.5	4.2	16	43.7	2.5	0.125
	≥ 18	12	48.8	3.6	23	49.5	2.8	24	45.5	2.8	26	45.7	2.7	

N: numbers of assessable measurements for the variable

P-values are from the regression analysis after adjustment for the effect of gender, age, and clustering, but with no interaction term

* Significant interaction between gender and health-status (*i.e.,* HR or control), (*p*-value ≤ 0.050)

E-TABLE II. Descriptive statistics (means and standard deviations) of cephalometric measurements of the posterior cranial fossa; bony structures of endochondral origin.

		Males						Females						Adjusted comparison of HR and control (*p*-value)
		HR			Control			HR			Control			
	Age in yr	N	mean	SD	N	mean	SD	N	mean	SD	N	mean	SD	
d-p	< 18	5	26.7	4.4	14	35.5	4.7	12	30.7	2.8	16	34.5	3.1	< 0.001
	≥ 18	12	30.4	5.9	20	36.8	3.4	24	30.0	3.5	25	35.3	3.6	
thi-iop	< 18	5	11.9	3.2	14	9.5	2.7	12	11.1	3.2	16	9.4	1.4	0.002
	≥ 18	12	16.4	3.9	20	12.7	2.3	24	13.6	3.1	25	12.3	2.5	
d-s-iop	< 18	5	18.0	3.9	14	25.1	3.9	12	23.4	3.5	16	25.7	3.4	< 0.001
	≥ 18	12	19.8	3.5	20	25.2	2.7	24	21.2	2.8	25	25.7	3.3	
s-iop	< 18	5	109.0	7.9	14	107.3	4.5	12	103.4	3.7	16	103.0	4.0	0.239
	≥ 18	12	110.4	7.2	20	108.2	5.2	24	106.6	4.8	25	105.6	4.8	
s-d	< 18	5	87.4	6.5	14	84.0	3.1	12	78.1	6.3	16	80.1	4.0	0.095
	≥ 18	12	89.6	5.8	23	86.4	3.3	24	83.5	4.6	26	81.7	3.5	

N: numbers of assessable measurements for the variable

P-values are from the regression analysis after adjustment for the effect of gender, age, and clustering, but with no interaction term

E-TABLE III. Descriptive statistics (means and standard deviations) of cephalometric measurements of the neurocranium; bony structures of intramembranous origin.

| | | Males | | | | | | Females | | | | | | Adjusted comparison of HR and control (*p*-value) |
| | | HR | | | Control | | | HR | | | Control | | | |
	Age in yr	N	mean	SD	N	mean	SD	N	mean	SD	N	mean	SD	
n-br	< 18	4	143.7	13.2	11	124.5	5.1	11	123.1	7.1	11	122.9	5.2	0.011
	≥ 18	8	137.2	11	23	134.5	5.7	18	128.4	3.9	25	126.4	3.6	
n-l	< 18	5	212.5	19.1	14	205.7	10.7	12	193.8	10.0	16	197.8	7.2	0.203
	≥ 18	12	217.0	11.2	19	210.5	5.7	24	204.7	8.0	25	203.2	5.2	
n-opi	< 18	5	214.3	19.5	14	208.3	11.1	12	196.4	10.9	16	200.7	6.3	0.255
	≥ 18	12	219.5	11.1	17	214.6	5.8	24	208.5	8.2	21	206.7	4.8	
ba-br	< 18	4	160.5	7.6	11	155.9	6.6	11	147.3	5.8	11	148.5	4.1	0.773
	≥ 18	8	160.3	5.0	23	162.3	7.2	18	155.8	3.3	25	153.9	6.5	
ba-l	< 18	5	132.3	6.5	14	137.7	8.7	12	125.2	8.3	16	132.1	5.1	0.003
	≥ 18	12	134.4	6.9	19	137.3	6.2	24	131.7	4.4	25	132.6	5.4	
br-l	< 18	4	152.0	17.9	11	143.0	8.6	11	136.5	9.6	11	135.5	8.4	0.089
	≥ 18	8	147.5	13.7	19	142.6	7.0	18	143.9	8.7	24	138.5	7.7	
s-fr	< 18	4	109.2	9.4	11	100.4	6.0	11	100.2	4.3	11	97.5	3.9	0.050
	≥ 18	8	105.3	5.9	23	104.8	4.4	18	102.8	3.4	25	101.4	3.9	
s-br	< 18	4	123.6	6.1	11	113.1	5.4	11	112.6	3.7	11	109.9	3.3	0.030
	≥ 18	8	118.1	6.2	23	117.5	6.3	18	114.7	3.5	25	112.6	4.4	
s-l	< 18	5	142.2	11.3	14	136.8	8.3	12	130.8	7.1	16	132.8	4.9	0.058
	≥ 18	12	142.1	9.1	19	135.6	5.2	24	136.0	6.1	25	133.7	5.2	

N: numbers of assessable measurements for the variable

P-values are from the regression analysis after adjustment for the effect of gender, age, and clustering, but with no interaction term

E-TABLE IV. Descriptive statistics (means and standard deviations) of cephalometric measurements of the cranial theca; bony structures of mainly intramembranous origin.

	Age in yr		Males						Females						Adjusted comparison of HR and control (*p*-value)
		HR			Control			HR			Control			
		N	mean	SD	N	mean	SD	N	mean	SD	N	mean	SD	
thi-fr	< 18	4	8.9	1.0	11	6.2	1.9	11	7.2	1.7	11	5.8	1.5	< 0.001
	≥ 18	8	11.3	1.6	23	7.8	1.6	18	10.8	2.8	25	8.3	1.5	
thi-pa	< 18	4	9.7	1.6	11	7.7	2.2	11	7.1	1.8	11	7.4	1.5	0.025**
	≥ 18	8	10.7	1.2	19	9.1	2.2	18	9.7	2.3	24	8.9	1.5	
thi-oc*	< 18	5	5.2	2.1	14	3.5	1.0	12	3.9	0.9	16	4.1	0.9	0.004
	≥ 18	12	7.3	4.1	19	4.6	0.9	24	6.2	2.0	25	4.6	1.5	
s-n-fr	< 18	4	88.1	6.2	11	87.8	2.4	11	92.7	4.6	11	88.1	3.1	0.028***
	≥ 18	8	85.6	3.6	23	85.0	3.0	18	88.9	2.2	25	87.4	3.3	

N: numbers of assessable measurements for the variable

P-values are from the regression analysis after adjustment for the effect of gender, age, and clustering, but with no interaction term

* The occipital theca is of endochondral origin

** Significant interaction between gender and health-status (*i.e.,* HR or control)

*** Significant interaction between age and health-status (*i.e.,* HR or control)

E-TABLE V. Descriptive statistics (means and standard deviations) of cephalometric measurements of the maxilla; bony structures of intramembranous origin.

| | | Males | | | | | | Females | | | | | | Adjusted comparison of HR and control (*p*-value) |
| | | HR | | | Control | | | HR | | | Control | | | |
	Age in yr	N	mean	SD	N	mean	SD	N	mean	SD	N	mean	SD	
ptm-sp	< 18	5	55.2	5.0	14	55.9	4.3	12	53.2	4.7	16	55.1	2.5	0.361
	≥ 18	12	62.7	4.1	23	62.2	3.4	24	58.1	2.5	26	59.4	2.6	
n-sp	< 18	5	49.1	5.8	14	53.9	5.7	12	46.4	6.7	16	51.0	3.3	0.003
	≥ 18	12	57.8	3.4	23	58.2	3.3	24	53.0	3.4	26	54.5	2.6	
ptm/s-n	< 18	5	42.8	6.5	14	48.9	3.0	12	42.0	5.4	16	45.5	2.9	0.177**
	≥ 18	12	53.2	3.3	23	53.2	3.0	24	48.8	2.5	26	48.9	2.5	
cd-ss	< 18	5	93.3	8.2	14	92.2	6.2	12	89.4	9.2	16	89.9	3.2	0.201
	≥ 18	12	104.9	6.4	23	101.8	5.0	24	97.9	4.6	26	96.9	3.4	
s-n-ss	< 18	5	78.9	3.2	14	81.2	3.8	12	82.1	3.8	16	81.5	3.8	0.966
	≥ 18	12	82.2	4.0	23	83.1	4.4	24	82.9	3.6	26	82.2	3.0	
s-n/ptm-sp	< 18	5	8.1	4.9	14	6.3	4.0	12	7.3	3.0	16	7.7	2.8	0.492
	≥ 18	12	5.6	3.0	23	6.0	3.0	24	5.7	4.1	26	7.0	2.7	

N: numbers of assessable measurements for the variable

P-values are from the regression analysis after adjustment for the effect of gender, age, and clustering, but with no interaction term

** Significant interaction between age and health-status (*i.e.,* HR or control)

E-TABLE VI. Descriptive statistics (means and standard deviations) of cephalometric measurements of the nasal-bone and the mandible;

bony structures of intramembranous origin developed upon a cartilaginous scaffold.

| | | Males | | | | | | Females | | | | | | Adjusted comparison of HR and control (*p*-value) |
| | | HR | | | Control | | | HR | | | Control | | | |
	Age in yr	N	mean	SD	N	mean	SD	N	mean	SD	N	mean	SD	
n-na	< 18	5	22.3	4.2	14	24.7	4.0	12	21.7	4.2	16	24.9	3.1	0.023
	≥ 18	12	23.3	5.2	23	26.2	3.8	24	23.3	3.5	26	24.3	4.2	
tgo-gn	< 18	5	71.9	12.5	14	75.3	4.6	12	66.2	9.8	16	72.8	3.6	0.236
	≥ 18	12	85.8	5.4	23	85.2	5.1	24	79.3	5.3	26	79.7	4.4	
cd-tgo	< 18	5	58.3	12.3	14	60.0	8.2	12	55.6	9.6	16	57.0	5.0	0.119
	≥ 18	12	77.2	5.9	23	74.8	5.1	24	70.2	6.0	26	65.8	4.6	
n-gn	< 18	5	123.9	11.9	14	126.0	10.7	12	116.2	13.0	16	117.7	6.0	0.118
	≥ 18	12	143.3	5.9	23	137.9	7.1	24	131.3	6.7	26	128.3	6.2	
cd-pgn	< 18	5	118.3	18.2	14	122.4	9.6	12	111.2	15.3	16	115.4	4.5	0.369
	≥ 18	12	142.0	7.5	23	136.5	5.8	24	130.0	5.9	26	127.6	4.9	
s-n-pg	< 18	5	74.9	7.1	14	78.5	2.3	12	75.5	5.6	16	78.2	2.9	0.293
	≥ 18	12	81.0	3.6	23	81.7	4.6	24	80.0	4.0	26	79.5	3.0	
s-n/tgo-gn	< 18	5	35.2	8.5	14	34.6	2.8	12	35.3	7.7	16	32.3	4.6	0.818
	≥ 18	12	27.7	5.4	23	26.2	7.2	24	29.3	7.1	26	30.6	6.4	
ar-tgo-gn	< 18	5	127.0	6.7	14	125.2	3.5	12	126.9	7.4	16	121.9	4.5	0.264
	≥ 18	12	118.4	4.6	23	116.3	7.9	24	119.4	8.8	26	119.8	6.7	
tgo-gn-ar	< 18	5	19.4	3.1	14	19.7	2.1	12	19.9	2.8	16	20.8	2.4	0.708
	≥ 18	12	24.6	2.6	23	25.2	3.3	24	23.6	4.0	26	22.5	3.1	

N: numbers of assessable measurements for the variable

P-values are from the regression analysis after adjustment for the effect of gender, age, and clustering, but with no interaction term

Craniofacial Morphology in Patients With Hypophosphatemic Rickets: A Cephalometric Study Focusing on Differences Between Bone of Cartilaginous and Intramembranous Origin

Hans Gjørup,[1,2]* Inger Kjær,[3] Liselotte Sonnesen,[3] Dorte Haubek,[2] Signe Sparre Beck-Nielsen,[4,5] Hanne Hintze,[6] and Sven Poulsen[2]

[1]Center for Oral Health in Rare Conditions, Aarhus University Hospital, Aarhus, Denmark

[2]Department of Pediatric Dentistry, School of Dentistry, University of Aarhus, Aarhus, Denmark

[3]Department of Orthodontics, School of Dentistry, University of Copenhagen, Copenhagen, Denmark

[4]Department of Pediatrics, H. C. Andersen Children's Hospital, Odense University Hospital, Odense, Denmark

[5]Institute of Clinical Research, University of Southern Denmark, Odense, Denmark

[6]Department of Oral Radiology, School of Dentistry, University of Aarhus, Aarhus, Denmark

Hypophosphatemic rickets (HR) are diseases characterized by deficient mineralization of bone due to abnormal renal wasting of phosphate. Deformation of bony structures of cartilaginous origin has been described as a major characteristic in patients with HR, but little is known about the impact on bony structures of intramembranous origin. The aim of the present study was to describe the osseous morphology of the craniofacial structures in patients with HR compared to healthy controls, and to investigate the impact of different bone origin on the osseous morphology. Fifty-three patients with HR (17 males, 36 females), aged 3–74 yrs, were included. Fifty HR patients had dominant X-linked disease, and in three patients no mutations were identified. A total of 79 healthy individuals (37 males, 42 females), aged 6–79 yrs, with normal occlusion served as controls. Significant cephalometric differences were found between HR patients and controls. In HR patients, the cranial base was flattened and the depth of the posterior cranial fossa was decreased. The anterior height of the cranium, the angle nasion-sella-frontale, and the thickness of theca were increased. The length of the nasal bone and the height of the maxilla were reduced. In contrast, the vertical as well as the sagittal relation between the jaws were unaffected in HR patients compared to controls. In conclusion, we found that the cranial structures of cartilaginous origin as well as the structures of intramembraneous origin were affected in patients with HR. © 2011 Wiley Periodicals, Inc.

Key words: hypophosphatemic rickets; skull; cephalometry; osteogenesis

INTRODUCTION

Hypophosphatemic rickets (HR) are rare diseases characterized by deficient mineralization of the bones due to abnormal renal wasting

of phosphate. Its prevalence has recently been estimated to 4.8 per 100,000 children in Denmark [Beck-Nielsen et al., 2009]. The most predominant type of HR is inherited in a dominant X-linked fashion, and caused by mutations in the gene encoding for the phosphate regulating endopeptidase homolog, X-linked (*PHEX*) [Hyp Consortium, 1995]. Less predominant types of HR include autosomal dominant HR, caused by a mutation in the gene encoding for fibroblast growth factor 23 (*FGF23*), autosomal recessive HR, caused by a mutation in the gene encoding for dentin matrix acidic phosphoprotein 1 (*DMP1*), or a mutation in the sodium–phosphate cotransporter gene (*SLC34A3*) [Gauche et al.,

2009], or by a mutation in the gene encoding for ecto-nucleotide pyrophosphatase/phosphodiesterase 1 (*ENPP1*) [Levy-Litan et al., 2010]. In addition, a recessive X-linked type, caused by a mutation in the gene encoding for chloride chanel 5 (*CLCN5*), has been described [Bolino et al., 1993].

The main clinical signs of HR are identical to the signs of nutritional rickets: General growth retardation and deformation of the extremities, e.g., bowing of the lower limbs [Winters et al., 1958; Beck-Nielsen et al., 2010], i.e., mainly affection of the bony structures of cartilaginous origin. In addition, dental symptoms with pulpal necrosis and periapical ostitis are frequent signs of HR [Seow, 2003; Pereira et al., 2004; Baroncelli et al., 2006; Beck-Nielsen et al., 2010].

Previous studies have described craniotabes, (i.e., presence of areas of thinning and softening of the skull bones) and frontal bossing in HR [Marks et al., 1965; Tracy and Campbell, 1968], as well as an increased risk of sagittal craniosynostosis with dolicho-cephaly [Currarino, 2007]. Recently, a cephalometric study of 22 Jordanian patients with HR described a shortened anterior cranial base and maxilla as well as reduced mandibular dimensions compared to a healthy age- and gender-matched control group. The cranial base was flattened and HR patients had a skeletal Class III malocclusion [Al-Jundi et al., 2009]. In addition, anthropometric studies have described an increased cranial length and occipital width as well as increased head circumference in HR patients [Pronicka et al., 2004; Beck-Nielsen et al., 2010]. Animal studies on mice with HR report malformation of the HR-affected cranium, as well as underdevelopment of the nasal bone [Iorio et al., 1980; Mostafa et al., 1982].

The previous cephalometric studies on HR patients are based on a limited numbers of individuals, e.g., nine rickets patients in the studies by Marks et al. [1965], and Tracy and Campbell [1968]. The HR diagnosis in these studies was not genetically verified as a genetic diagnosis was unavailable at that time. Furthermore, previous studies have not evaluated the affection of HR on the different origins of the craniofacial bone (i.e., cartilaginous versus intra-membraneous bone).

The aim of this study was to characterize the craniofacial morphology in patients with genetically or biochemically verified HR compared to healthy controls. Furthermore, we assessed the possible differences in the craniofacial morphology according to the bony origin of the cranial structures.

MATERIALS AND METHODS
Study Population

A total of 53 children and adults with HR participated in this study (Table I). One male and four females were under age seven. The HR patients were recruited from a cross-sectional study on HR patients of whom six refused to participate in the cephalometric examination. The patients in this study belonged to 21 different families with 1–13 participants from each family (1–2 in 15 families; 3–5 in 4 families; 7–13 in 2 families). A detailed description of patient recruitment has previously been published [Beck-Nielsen et al., 2010]. The HR diagnosis was determined by biochemical criteria and in all, except three cases, also genetically verified. In addition,

TABLE I. Distribution of 53 HR Patients and 79 Controls Accordingto Gender and Age

	HR		Control	
	Male	Female	Male	Female
<18 years	5	12	14	16
≥18 years	12	24	23	26
Mean age*	32.8	30.8	29.2	30.9
(SD) age*	(21.9)	(19.2)	(18.3)	(19.0)
Age range*	4.3–73.2	2.8–74.5	8.6–72.6	9.3–78.5

*Age in years.

a history of childhood rickets was required. The biochemical criteria were at least one of the following: (1) serum phosphate below normal range, (2) low renal threshold value for reabsorption of phosphate in the urine, or (3) elevated FGF23 in serum. The genetic criterion was detection of a disease-causing mutation in *PHEX*, *FGF23*, or *DMP1*. All participants (except the three cases without genetical verification) had a *PHEX* mutation (37 cases) or had strong evidence of linkage to *PHEX* (one family with 13 participants). Details of the genetic and the biochemical analyses have been reported earlier [Beck-Nielsen et al., 2010].

Based on power calculations, a control group of 60–70 individuals was estimated to give sufficient power (80%) to identify relevant differences at the 5% level of significance. The calculations were performed on six selected cephalometric variables, which were assumed to be representative of all parts of the cranium. All recruited HR patients (53 individuals) provided the basis for the power calculations.

The control group consisted of 49 healthy adults (≥18 years), recruited among patients, students, and employees at the School of Dentistry, Aarhus University, and among employees at Department of Maxillofacial Surgery, Aarhus University Hospital. In addition, already existing profile radiographs of 30 children (<18 years) from two large municipal dental services (Aarhus and Odense) were included as controls. The inclusion criteria for the control group were: (1) Scandinavian ethnicity, (2) no chronic diseases except for allergies, (3) for adults: A minimum of 24 permanent teeth; for children: No dental agenesis or extractions of permanent teeth, (4) normal, or only minor deviations from normal occlusion, (5) no history of orthodontic treatment, and (6) no craniofacial anomaly. In Table I, the distribution of the 79 healthy individuals according to age and gender is reported. In the control group, children under 7 years of age were excluded.

METHODS

Standardized profile radiographs were obtained as described by Solow [1966], using the digital radiographic equipment Planmeca Promax© (Planmeca Oy, Helsinki, Finland). The sensor-focus distance was 1.50 m and the enlargement factor 1.13. During exposure, the head of the patient was fixed in a rigid cephalostat, and the patients were instructed to keep the teeth in occlusion.

The head posture was adjusted to the best fit of the borders of the sensor.

The analysis of the radiographs was performed using software for cephalometric analysis, Pordios® (Institute of Orthodontic Computer Science, Aarhus, Denmark). Twenty-five cephalometric landmarks were digitized (Fig. 1). The digitizing of all radiographs was performed by the first author after randomization of the radiographs in order to blind the observer to the health status of the individuals. Twenty-seven linear and 10 angular variables were calculated by the software (Table II). The variables of the cranial base and the facial skeleton were defined according to definitions by Bjørk [1975], Solow [1966], and McNamara [1984]. The variables of the neurocranium were defined as described by Axelsson et al. [2003]. In addition, recently defined variables describing the size and morphology of the posterior cranial fossa were included [Caspersen et al., 2010].

Reliability

In order to test the intra-examiner reliability, 22 randomly selected radiographs were digitized twice by the first author. The radiographs selected for re-digitizing were included in the overall randomization of radiographs in order to blind the observer to whether the radiographs were read before. The systematic error was estimated by calculating the differences between the two sets of recording, and the differences for none of the variables were significantly different from zero ($P > 0.1$). For each of the cephalometric variables, the random error was calculated as described by
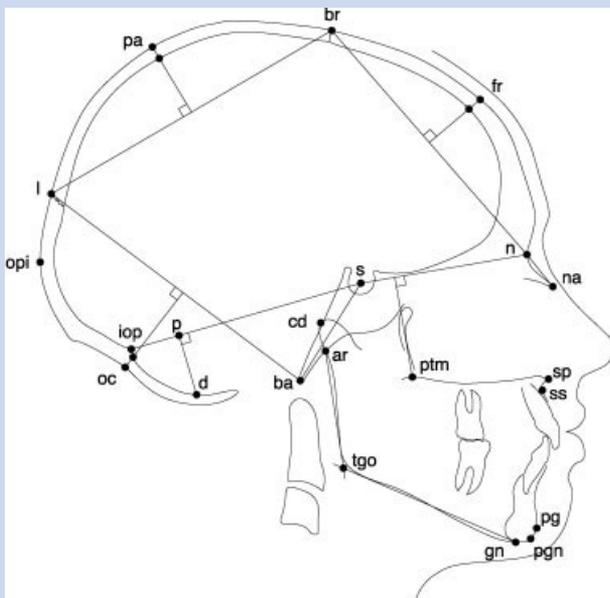
FIG. 1. Schematic drawing of the skull with the 25 landmarks used for measuring the cephalometric variables. At the landmarks oc, pa, and fr, both the inner and the outer contour of the theca are marked. The landmarks and the variables are defined according to Bjørk [1975], Axelsson et al. [2003], and Caspersen et al. [2010]. The cephalometric variables are described in Table II.

TABLE II. Description of the Cephalometric Variables, Landmarks Shown in Figure 1

Cranial base	
n-s-ba	cranial base angle to basion
n-s-ar	cranial base angle to articulare
s-n	length of anterior cranial base
s-ba	length of posterior cranial base
Posterior cranial fossa	
d-p	height point d to point p
thi-iop	theca-thickness at internal occipital protuberance
d-s-iop	angle point d-sella to internal occipital protuberance
s-iop	length sella to internal occipital protuberance
s-d	length sella to point d
Neurocranium	
n-br	length nasion-bregma
n-l	length nasion-bregma
n-opi	length nasion-opisthocranion
ba-br	length basion-bregma
ba-l	length basion-lambda
br-l	length bregma-lambda
s-fr	length sella-frontale
s-br	length sella bregma
s-l	length sella-lambda
Theca	
thi-fr	theca-thickness at frontale
thi-pa	theca-thickness at parietale
thi-oc	theca-thickness at occipitale
s-n-fr	angle sella-nasion-frontale
Maxilla	
ptm-sp	length pterygomaxillare to anterior nasal spine
n-sp	height nasion to anterior nasal spine
ptm/s-n	heigth pterygomaxillare to nasion-sella line
cd-ss	length condylion to subspinale
s-n-ss	angle sella-nasion-subspinale
s-n/ptm-sp	Angle selle-nasion/pterygomaxillare-anterior nasal spine
Nasal bone & mandible	
n-na	length of nasal bone
tgo-gn	length gonion to gnathion
cd-tgo	height condylion to gonion
n-gn	height nasion to gnathion
cd-pgn	length condylion to prognathion
s-n-pg	angle sella-nasion-pogonion
s-n/tgo-gn	angle sella-nasion/gonion-gnathion
ar-tgo-gn	jaw angle articulare-gonion-gnathion
tgo-gn-ar	beta angle gonion-gnathion-articulare

Dahlberg [1940] and ranged from 0.08 to 2.39. The coefficient of reliability was estimated according to Houston [1983] and ranged from 0.91 in the case of the angular variable, d-s-iop, and to 1.00 in case of the length of the linear variables, n-gn, s-fr, s-br, n-opi, and n-l.

Statistical Analyses

Irrespective of age, the gender distribution in HR group and in control group was compared by two-sided chi-square test. For each gender, the age distributions in the two groups were compared with unpaired t-test. In both the HR group and the control group, the cephalometric measurements were examined visually for normality using Q–Q plots and histograms, and in both groups they were all found to be normally distributed. The effect of health-status (i.e., HR or control), age and gender upon the cephalometric measurements was assessed by linear regression analyses. To allow for familiar dependence, the regression estimates were adjusted for clustering. The analyses revealed an effect of age, gender, and health-status. Thus, the cephalometric data are presented according to gender and age categories (<18 years, ≥ 18 years). Potential interactions between the effect of age and health-status and between the effect of gender and health-status were assessed in the regression analyses.

In the analysis, the cephalometric variables were grouped according to bony origin of the structures (Fig. 2). Means and standard deviations were used as descriptive statistics and P-values equal to or below 0.05 were considered statistically significant.

The data were analyzed using Stata® 11.0 (StataCorp, College Station, TX). Output by Stata® from the regression analyses are provided in the Appendix I—see online supporting information for the manuscript.

RESULTS

The proportion of females in the HR group (68%) was not significantly higher than in the control group (53%) ($P = 0.091$). Further, the differences in mean age between HR group and controls were not statistically significant, irrespective of gender (Table I).

Supplementary Tables with the cephalometric data (eTables I–VI) can be viewed in the manuscript's supporting information available through the Wiley Online Library at http://onlinelibrary.wiley.com. The data are presented according to gender and age categories (<18 years, ≥ 18 years). In addition, P-values from the regression analyses are included as well as information on significant interactions between health (HR patient or control) and age, or between health and gender.

Cartilagineous Developed Bone

Both cranial base angles (n-s-ba and n-s-ar) were significantly increased in the HR group compared to the control group ($P = 0.001$) (eTable I—see supporting information online). In contrast, no significant differences in size of structures in the cranial base were found. A borderline significant interaction between the effect of health-status and the effect of gender was seen for both cranial base angles ($P = 0.057$, $P = 0.053$). The difference of cranial base angle between the HR group and the control group was larger for males than for females (eTable I—see supporting information online).

In the posterior cranial fossa, the angle, d-s-iop, the depth, d-p, and the length, p-iop were all significantly reduced in HR patients. The thickness of the skull at the cephalometric landmark iop was
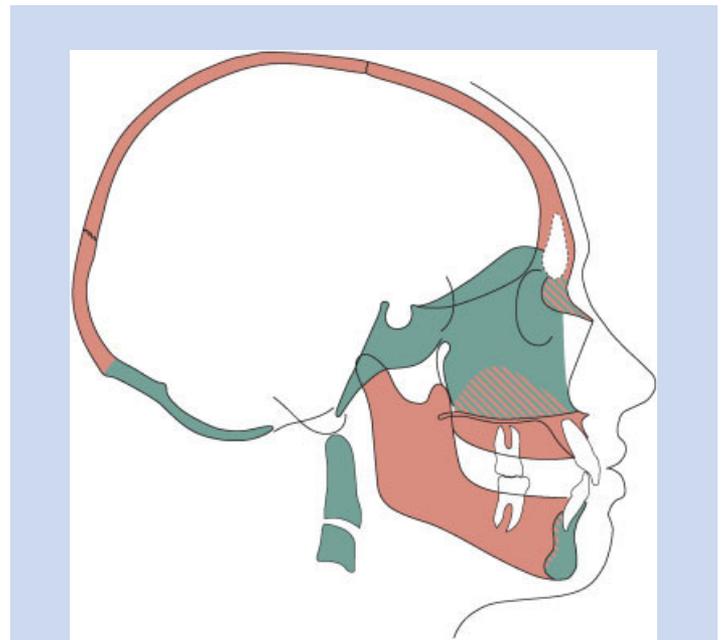
FIG. 2. Drawing of the skull with the bony origin of craniofacial structures marked schematically. The cranial base, the upper part of the nasal septum, and the caudal part of the occipital bone are cartilaginous developed (green). The nasal bone, the mandible, and vomer are of intramembranous origin developed upon a scaffold of cartilage (Meckel's cartilage, cartilaginous nasal capsule and septum) (red/green). All other cranial structures are intramembranous developed (red) [Kjaer et al., 1999]. [Color figure can be seen in the online version of this article, available at http://onlinelibrary.wiley.com/journal/10.1002/(ISSN)1552-4833]

significantly increased (eTable II—see supporting information online).

Intramembraneous Developed Bone

In the neurocranium the following lengths were significantly increased in the HR patients: n-br, s-fr, s-br, and at a lower level of significance also s-l. The length of the linear variable, ba-l was significantly reduced (eTable III—see supporting information online). A borderline significant interaction between the effect of health-status and the effect of gender was seen for the length, n-br ($P = 0.051$). The difference of the length, n-br between the HR group and the control group was much larger for males than for females.

The thickness of theca and the frontal prominence were significantly increased in the HR group (eTable IV—see supporting information online). A significant interaction between the effect of health-status and the effect of gender was seen for the parietal thickness ($P = 0.020$). The difference of the parietal thickness between HR patients and controls was much larger for males than for females. In addition, the frontal prominence (s-n-fr) was affected by a significant interaction between the effect of health-status and the effect of age. The prominence decreased with increasing age in both HR and control group, but the age dependence was significantly stronger in HR group ($P = 0.029$).

The anterior maxillary height (n-sp) was significantly reduced in the HR group, but none of the other maxillary variables were significantly affected compared to the control group (eTable V—see supporting information online). Posterior maxillary height (ptm-NL) was affected by interaction between the effect of health-status and the effect of age. The height increased with increasing age in both groups, but the age dependence of the posterior maxillary height was significantly stronger in HR group compared to control group ($P = 0.026$).

The length of the nasal bone (n-na) was significantly reduced in the HR group, but none of the mandibular variables were significantly affected by health-status (eTable VI—see supporting information online).

DISCUSSION

The results of the present study show that HR, in comparison with healthy controls, affects bony structures both of cartilaginous and of intramembraneous origin. Bony structures of cartilaginous origin seem primarily to be affected by differences in shape, i.e., deformation, while some structures of intra-membranous origin were found to be affected by differences in size (Fig. 3).

The present study is based on a higher number of patients with HR in comparison with other studies [Marks et al., 1965; Tracy and Campbell, 1968; Al-Jundi et al., 2009]. Furthermore, the genetic as well as the biochemical profile of the diseased individuals fulfilled well-defined diagnostic criteria of HR [Beck-Nielsen et al., 2010]. The diagnosis of HR in three patients was not genetically verified but they remained included as they fulfilled the biochemical inclusion criteria. We have not investigated whether these three HR patients had autosomal recessive HR caused by the newly discovered mutation in ENPP1 as this gene was not discovered at the time of genetic evaluation. Two of these three patients were a mother and her son, only one patient with sporadic HR and no genetic diagnosis could be suspicious of an ENPP1 mutation. The male:female ratio was not the same in the HR (1:2.12) and the control (1:1.14) groups, however the difference was not significant.

This gender discrepancy was in accordance with the dominant X-linked inheritance of the disease, and a predominant female group is characteristic in research regarding HR [Al-Jundi et al., 2009; Gauche et al., 2009]. The youngest age group (<7 years of age) was only present in the HR group. For ethical reasons, the children in the control group were only represented by profile radiographs taken for orthodontic treatment purposes. As such radiographs are rarely indicated in relation to the treatment of the very young children, this age group was not represented in the control group. The statistical models were designed to analyze the effect of gender and age on the influence of HR. This choice of models aimed to compensate for the gender and age discrepancies between the HR group and the control group.

Except for the parietal thickness of theca, the influence of gender on the craniofacial morphology was almost the same in HR patients as in healthy controls. This is in agreement with the conclusion from the medical survey of our HR patients: Compared to females, males tended to be skeletally and biochemically more severely affected, but the differences did not reach statistical significance [Beck-Nielsen et al., 2010].

Cartilaginous Developed Bone

The shape of the cranial base was affected by flattening, while the size of the anterior as well as the posterior cranial base was unaffected. This is in agreement with earlier findings [Al-Jundi et al., 2009]. The depth of the posterior cranial fossa was reduced, but no significant difference of the anterior–posterior length of the fossa was seen. The differences in shape of the posterior-inferior part of the cranium could be described as an upward compression of the structures around foramen magnum, including a more cranial position of the inferior part of clivus (basion) which would also add to the increased cranial base angle (n-s-ba). The reduced height of the posterior cranial fossa indicates a reduced volumen of the fossa, and this is in agreement with results from a study based on three-dimensional imaging (computed tomographic or magnetic resonance imaging) [Tubbs et al., 2004]. A small posterior
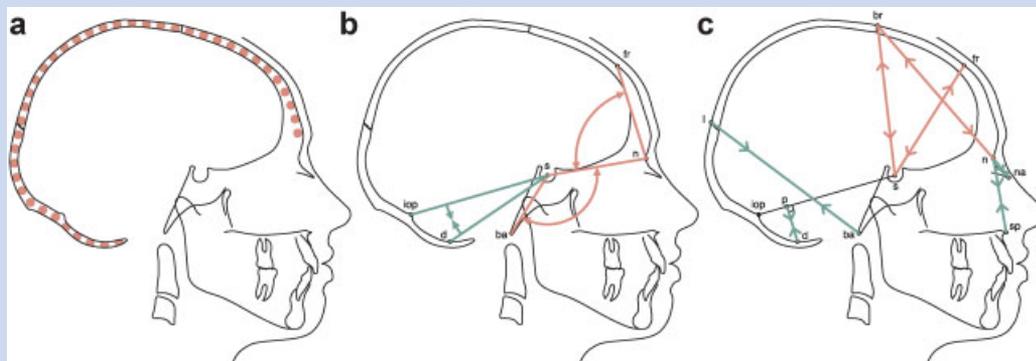
FIG. 3. Cranial morphology of HR patients compared to controls. A graphic summary of the significant differences. a: Increased thickness of theca, red dotted line. b: Increased angles (n-s-ba, s-n-fr), red lines; decreased angle (d-s-iop), green lines. c: Increased dimensions (s-br, s-fr, n-br), red arrows; decreased dimensions (ba-l, d-p, n-na, n-sp), green arrows. [Color figure can be seen in the online version of this article, available at http://onlinelibrary.wiley.com/journal/10.1002/(ISSN)1552-4833]

cranial fossa reduces the available room for the development of rhombencephalon. This might be related to the increased prevalence of hindbrain herniation (Chiari I malformation) reported in children with HR and other types of rickets [Caldemeyer et al., 1995; Tubbs et al., 2004].

Spranger et al. [1982] mentions the bowed legs of patients with nutritional rickets as an example of a deformation (i.e., an abnormal form, shape, or position of a part of the body caused by mechanical forces). In a similar way, the increased cranial base angle (n-s-ba) and the reduced depth of the posterior cranial base in HR might be explained as a deformation of poorly mineralized bony structures caused by the weight of the brain and/or the weight of the thickened skull. The same interpretation has been proposed in relation to patients with osteogenesis imperfecta (OI) which is a dysplasia (i.e., an abnormal organization of cells into tissue and its morphological result) of connective tissue and which affects all bony structures. In the severe types of OI as well as in patients with HR, the cranial base angle is increased but the size of the cranial base is unaffected [Waltimo-Siren et al., 2005]. Achondroplasia is a cartilaginous dysplasia affecting the formation of bony structures of cartilaginous origin. In this condition, both shape and size of the cranial base are affected, the length of the posterior cranial base being reduced in addition to a reduced cranial base angle [Cohen et al., 1985]. The affection of the cartilaginous developed cranial base seems to be a deformation, i.e., abnormal form, in both HR, i.e., deficient bone mineralization, and in OI, i.e., connective tissue dysplasia. In contrast, achondroplasia, i.e., cartilaginous dysplasia, seems to have greater impact upon the formation of the cranial base, affecting both shape and size of the structure.

Intramembraneous Developed Bone

In HR patients compared to controls, the morphology of the skull was abnormal as the result of an increased frontal bossing, an increased height of the anterior part of neurocranium, and a flattening of the parietal area. The finding of increased frontal prominence is in agreement with former reports of frontal bossing [Marks et al., 1965; Tracy and Campbell, 1968]. In addition, a significant increase in the thickness of the skull was found; both in the parietal and frontal part, both being of intramembraneous origin, and in the lower occipital part, which is of cartilaginous origin. The morphological differences found in the neurocranium in HR patients could be described partly as deformation and partly as a different size of bony structures. The total neurocranium lengths (n-l, n-opi) were not affected, which is in contrast to the results from anthropological studies where increased head circumference has been reported [Pronicka et al., 2004; Beck-Nielsen et al., 2010] and to the reporting of an increased risk of sagittal craniosynostosis with dolichocephaly [Currarino, 2007]. Profile radiographs are only suitable for reporting two-dimensional, sagittal dimensions, and differences in transverse dimensions of the skull, which have not been assessed in the present study, might explain this disagreement. Furthermore, the anthropological measurement of the head circumference includes the increased frontal prominence, which was not included in the cranial lengths used in this study.

The reduced anterior maxillary height might indicate some affection of the sutural growth between the maxilla and the cranial base. Similarly, reduced posterior height was found in younger individuals, but this finding disappeared with increasing age. Otherwise, the intramembranous developed maxilla was not affected in its sagittal position or in the anterior-posterior size of the bony structure.

The reduced length of the nasal bone, which is of intramembraneous origin, is an interesting finding. The nasal bone length was not related to gender or age. This is remarkable, since the remaining linear measurements of the craniofacial structures, were greatest among males and increased by age. Animal studies have shown the same affection of the nasal bone in HYP mice, a murine homologue of the PHEX-mutation in human [Mostafa et al., 1982; Iorio et al., 1980]. The reduced length of the nasal bone has also been reported in patients with achondroplasia [Cohen et al., 1985], cleft lip and palate [Nielsen et al., 2005], and hypohidrotic ectodermal dysplasia [Lexner et al., 2007]. Achondroplasia and HR are diseases of different origin, but they both affect the development of the cartilaginous developed long bones. In addition, both conditions are characterized by reduced length of the nasal bone, which is of intramembraneous origin. This might be related to a primary affection of the cartilaginous nasal capsule, which is the scaffold of the nasal bone.

When comparing HR patients and healthy controls, no significant differences in shape, position, or size of the mandible were found. This is in agreement with Tracy and Campbell [1968] but in contrast to the findings in Jordanian children with HR (2−16 years of age) in whom reduced mandibular dimensions and a relatively prognathic mandible was seen [Al-Jundi et al., 2009]. These discrepancies might be explained by the differences in age range, the diagnostic criteria for inclusion of the diseased individuals, and the sample size. According to our study, Meckel cartilage apparently does not disturb the adjacent bone formation of the mandible which is in contrast to the suggested impact of the cartilaginous nasal capsule on the development of the nasal bone. The same findings are reported in patients with achondroplasia. The early (prenatal) disappearance of Meckel cartilage might explain the normal mandible in both achondroplasia and HR [Cohen et al., 1985].

CONCLUSION

In patients with HR, the craniofacial bones of cartilaginous as well as of intramembranous origin are affected. The cranial base, which is of cartilagineous origin, was flattened and the depth of the posterior cranial fossa was reduced. This is suggested to be the result of deformation similarly to the deformation of the long bones in HR patients. The neurocranium, which is of intramembraneous origin, was expanded anteriorly with increased height and frontal bossing. In addition, the thickness of the skull was increased and this for both the upper part, which is of intramembranous origin, and the lower part, being of cartilaginous origin. The thickened skull indicates interference with the bone-remodeling processes in patients with HR and needs further elucidation. The nasal bone was reduced in length, but not influenced by gender or age. The size and morphology of the nasal bone needs further investigation.

REFERENCES

Al-Jundi SH, Dabous IM, Al-Jamal GA. 2009. Craniofacial morphology in patients with hypophosphataemic vitamin-D-resistant rickets: A cephalometric study. J Oral Rehabil 36:483–490.

Axelsson S, Kjaer I, Bjornland T, Storhaug K. 2003. Longitudinal cephalometric standards for the neurocranium in Norwegians from 6 to 21 years of age. Eur J Orthod 25:185–198.

Baroncelli GI, Angiolini M, Ninni E, Galli V, Saggese R, Giuca MR. 2006. Prevalence and pathogenesis of dental and periodontal lesions in children with X-linked hypophosphatemic rickets. Eur J Paediatr Dent 7:61–66.

Beck-Nielsen SS, Brock-Jacobsen B, Gram J, Brixen K, Jensen TK. 2009. Incidence and prevalence of nutritional and hereditary rickets in southern Denmark. Eur J Endocrinol 160:491–497.

Beck-Nielsen SS, Brusgaard K, Rasmussen LM, Brixen K, Brock-Jacobsen B, Poulsen MR, Vestergaard P, Ralston SH, Albagha OM, Poulsen S, Haubek D, Gjørup H, Hintze H, Andersen MG, Heickendorff L, Hjelmborg J, Gram J. 2010. Phenotype presentation of hypophosphatemic rickets in adults. Calcif Tissue Int 87:108–119.

Bolino A, Devoto M, Enia G, Zoccali C, Weissenbach J, Romeo G. 1993. Genetic mapping in the Xp11.2 region of a new form of X-linked hypophosphatemic rickets. Eur J Hum Genet 1:269–279.

Bjørk A. 1975. Kæbernes relation til det øvrige kranium. In: Lundström I, (editors). Nordisk Lärobok i Ortodonti. Stockholm: Sveriges Tandläkarförbunds Förlagsförening.

Caldemeyer KS, Boaz JC, Wappner RS, Moran CC, Smith RR, Quets JP. 1995. Chiari I malformation: Association with hypophosphatemic rickets and MR imaging appearance. Radiology 195:733–738.

Caspersen LM, Kjaer I, Sonnesen L. 2010. How does occipitalization influence the dimensions of the cranium? Orthod Craniofac Res 13: 162–168.

Cohen MM Jr, Walker GF, Phillips C. 1985. A morphometric analysis of the craniofacial configuration in achondroplasia. J Craniofac Genet Dev Biol 1:139–165.

Currarino G. 2007. Sagittal synostosis in X-linked hypophosphatemic rickets and related diseases. Pediatr Radiol 37:805–812.

Dahlberg G. 1940. Statistical methods for medical and biological students. New York: Interscience Publications.

Gauche C, Walrant-Debray O, Nguyen TM, Esterle L, Garabedian M, Jehan F. 2009. PHEX analysis in 118 pedigrees reveals new genetic clues in hypophosphatemic rickets. Hum Genet 125:401–411.

Houston WJB. 1983. The analysis of errors in orthodontic measurements. Am J Orthod 83:382–390.

Hyp Consortium. 1995. A gene (*PEX*) with homologies to endopeptidases is mutated in patients with X-linked hypophosphatemic rickets. The HYP Consortium. Nat Genet 11:130–136.

Iorio RJ, Murray G, Meyer RA Jr. 1980. Craniometric measurements of craniofacial malformations in mice with X-linked, dominant hypophosphatemia (vitamin D-resistant rickets). Teratology 22:291–298.

Kjaer I, Keeling JW, Hansen BF. 1999. The prenatal human cranium - normal and pathologic development. Copenhagen: Munksgaard.

Levy-Litan V, Hershkovitz E, Avizov L, Leventhal N, Bercovich D, Chalifa-Caspi V, Manor E, Buriakovsky S, Hadad Y, Goding J, Parvari R. 2010. Autosomal-recessive hypophosphatemic rickets is associated with an inactivation mutation in the ENPP1 gene. Am J Hum Genet 86:273–278.

Lexner MO, Bardow A, Bjørn-Jørgensen J, Hertz JM, Almer L, Kreiborg S. 2007. Anthropometric and cephalometric measurements in X-linked hypohidrotic ectodermal dysplasia. Orthod Craniofac Res 10:203–215.

Marks SC, Lindahl RL, Bawden JW. 1965. Dental and cephalometric findings in vitamin D resistant rickets. J Dent Child 32:259–265.

McNamara JA Jr. 1984. A method of cephalometric evaluation. Am J Orthod 86:449–469.

Mostafa YA, El-Mangoury NH, Meyer RA Jr, Iorio RJ. 1982. Deficient nasal bone growth in the X-linked hypophosphataemic (HYP) mouse and its implication in craniofacial growth. Arch Oral Biol 27:311–317.

Nielsen BW, Mølsted K, Skovgaard LT, Kjaer I. 2005. Cross-sectional study of the length of the nasal bone in cleft lip and palate subjects. Cleft Palate Craniofac J 42:417–422.

Pereira CM, de Andrade CR, Vargas PA, Coletta RD, de Almeida OP, Lopes MA. 2004. Dental alterations associated with X-linked hypophosphatemic rickets. J Endod 30:241–245.

Pronicka E, Popowska E, Rowinska E, Arasimowicz E, Syczewska M, Jurkiewicz D, Lebiedowski M. 2004. Anthropometric characteristics of X-linked hypophosphatemia. Am J Med Genet Part A 126A:141–149.

Seow WK. 2003. Diagnosis and management of unusual dental abscesses in children. Aust Dent J 48:156–168.

Solow B. 1966. The pattern of craniofacial associations. Copenhagen: Department of Orthodontics, The Royal Dental College.

Spranger J, Benirschke K, Hall JG, Lenz W, Lowry RB, Opitz JM, Pinsky L, Schwarzacher HG, Smith DW. 1982. Errors of morphogenesis: Concepts and terms. Recommendations of an international working group. J Pediatr 100:160–165.

Tracy WE, Campbell RA. 1968. Dentofacial development in children with vitamin D resistant rickets. J Am Dent Assoc 76:1026–1031.

Tubbs RS, Webb D, Abdullatif H, Conklin M, Doyle S, Oakes WJ. 2004. Posterior cranial fossa volume in patients with rickets: Insights into the increased occurrence of Chiari I malformation in metabolic bone disease. Neurosurgery 55:380–383.

Waltimo-Siren J, Kolkka M, Pynnonen S, Kuurila K, Kaitila I, Kovero O. 2005. Craniofacial features in osteogenesis imperfecta: A cephalometric study. Am J Med Genet Part A 133A:142–150.

Winters RW, Graham JB, Williams TF, McFalls VW, Burnett CH. 1958. A genetic study of familial hypophosphatemia and vitamin D-resistant rickets with a review of the literature. Medicine 37:97–142.

H. Gjørup
I. Kjaer
L. Sonnesen
S. S. Beck-Nielsen
D. Haubek

Morphological characteristics of frontal sinus and nasal bone focusing on bone resorption and apposition in hypophosphatemic rickets

Authors' affiliations:

H. Gjørup, Center for Oral Health in Rare Diseases, Aarhus University Hospital, Aarhus, Denmark
I. Kjaer, L. Sonnesen, Faculty of Health Sciences, Department of Orthodontics, Institute of Odontology, University of Copenhagen, Copenhagen, Denmark
H. Gjørup, D. Haubek, Department of Dentistry, Faculty of Health, Aarhus University, Aarhus, Denmark
S. S. Beck-Nielsen, Department of Pediatrics, Hospital of Southwest Denmark, Esbjerg, Denmark
S. S. Beck-Nielsen, Institute of Clinical Research, University of Southern Denmark, Odense, Denmark

Correspondence to:

H. Gjørup
Center for Oral Health in Rare Diseases
Department of Maxillofacial Surgery
Aarhus University Hospital
Nørrebrogade 44
DK-8000 Aarhus, Denmark
E-mail: hangjo@rm.dk

Structured Abstract

Objectives – To characterize the size and the morphology of the frontal sinus (i.e., structure evolved by bone resorption) and the nasal bone (i.e., structure evolved by bone formation) in adults with hypophosphatemic rickets (HR) compared with controls.

Setting and sample population – Thirty-six patients with HR (12 males and 24 females) aged 21–74 years were included. The control group comprised 49 healthy individuals (23 males and 26 females) aged 20–79 years.

Material and methods – Profile cephalograms were obtained and the following measurements were included: height and width of the frontal sinus; length, width, and area of the nasal bone. The morphology of the nasal bone was assessed. Linear regression analyses were used to compare HR patients with controls.

Results – In HR patients, the size of the frontal sinus was unaffected ($p = 0.406$ to $p = 0.862$). The proximal width of the nasal bone, and the ratio between the proximal width and the axial length of the nasal bone were increased in HR patients ($p < 0.05$).

Conclusions – The size of the frontal sinus was unaffected, indicating a normal ability of bone resorption within the bone. The morphology of the nasal bone was abnormal indicating a disturbance in bone formation during growth. The disturbances in nasal bone modeling were mainly expressed in the proximal part supported by structures of cartilaginous origin.

Key words: bone formation; bone resorption; frontal sinus; hypophosphatemic rickets; nasal bone

Introduction

Hypophosphatemic rickets (HR) is a rare disease characterized by insufficient mineralization of the bones due to abnormal renal wasting of phosphate (1). The most predominant type of HR is inherited in a dominant X-linked fashion, caused by mutations in the gene encoding for the phosphate-regulating endopeptidase homolog, X-linked (*PHEX,* MIM 300550) (XLHR, MIM 307800) (2). XLHR is a fibroblast-growth-factor-23 (FGF23)-associated HR, and FGF23 is a potent phosphaturetic factor, being the principal regulatory hormone of the phosphate homeostasis. In addition, FGF23 is suggested to have a direct effect on bone cells (3).

The skeletal symptoms of HR include impact upon cranial bones in humans (1, 4–8), and in animals (9, 10). In a cephalometric study, including 53 individuals with X-linked HR, we recently reported an increased thickness of the theca compared with controls (11). During normal development of the skull, the sutural growth of the flat bones is combined with internal (i.e., endosteal) resorption and external (i.e., ectocranial and endocranial) apposition of bone (12). The increased thickness of theca in the HR patients indicates a disturbance in the bone modeling of the skull, but the former study (11) did not reveal if it was a matter of excess bone formation (apposition) or lack of bone resorption. Generally, high levels of FGF23 cause hypophosphatemia, and impair bone modeling (i.e., the reshaping of bone by the independent action of osteoblasts and osteoclasts during the development of bony structures) as well as bone remodeling (i.e., resorption of bone tissue and simultaneous deposition of new bone by coupling between bone cells), and based on animal models of HR, the disturbances in bone modeling and remodeling might be explained by both an alteration in osteoblast function and a reduced number of osteoclasts (13).

All anatomical structures in a developmental field are evolved from the same origin (14). In a specific developmental field (e.g., the nasofrontal field), the morphology of some osseous structures may evolve primarily by bone resorption and oth-

ers primarily by apposition. In the nasofrontal field, the frontal sinus is a structure not present in newborns. The frontal sinus develops by resorption of bone and appears radiographically around the age of five (15). The final size of the frontal sinus varies considerably (16). The growth of the nasal bone is extensive from 2–17 years of age, and the growth occurs both in the nasofrontal suture and appositional at the nasal tip along with a bone modeling occurring at the superior and the inferior borders (17). Thus, in this study, the frontal sinus and the nasal bone were chosen as the structures for studying bone resorption and formation, respectively.

Focusing on bone resorption and apposition, the aim was to analyze the size of the frontal sinus and evaluate the morphology and the size of the nasal bone, in patients with XLHR compared with healthy controls. Furthermore, the aim was to examine the interrelationship between the nasal bone morphology and the severity of general skeletal impact of HR.

Materials and methods
Study population

A total of 36 adults (age > 18 years.) with X-linked HR participated in this study. The HR diagnosis was based on biochemical analyses and was genetically verified (1). In three cases, the genetic verification was not possible. According to the criteria of skeletal impact of HR defined by Beck-Nielsen et al. (1), the skeletal impact in 14 HR patients was categorized as 'mild', and in 22 patients as 'severe' impact. The control group consisted of 49 healthy adults with a minimum of 24 permanent teeth and with a neutral occlusion or only minor deviations of the morphological occlusion. In both groups, the distribution according to gender was tabulated (Table 1).

Methods

Standardized profile radiographs were obtained as described by Solow (18), using the digital radiographic equipment Planmeca Promax© (Planmeca Oy, Helsinki, Finland). The sensor-focus distance

Table 1. **Number of HR patients and controls according to gender**

	HR		Controls	
	Female	Male	Female	Male
N	24	12	26	23
Mean age (SD)	41.2 (14.6)	42.4 (18.7)	42.3 (15.4)	39.5 (15.9)
Age range	21.0–74.5	18.8–73.2	23.0–74.5	20.7–72.6

Age in years.

was 1.50 m and the enlargement factor 1.13. During exposure, the head of the patient was fixed in a rigid cephalostat, and the participants were instructed to keep their teeth in occlusion. The head posture was adjusted to the best fit of the borders of the X-ray sensor.

The analysis of the radiographs was performed using software for cephalometric analysis, Pordios® (Institute of Orthodontic Computer Science, Aarhus, Denmark). The first author performed the digitizing of all the radiographs after randomization in order to blind the observer to the health status of the individuals.

The structures which had to be analyzed (i.e., the frontal sinus and the nasal bone) were both located in the nasofrontal developmental field (Fig. 1).

Cephalometric analysis, the frontal sinus

The landmarks for the analysis of the frontal sinus were as follows: Sella (S), the midpoint of the sella turcica; Nasion (N), the most anterior point of the nasofrontal suture; Glabella (Gla), the most prominent point above the supraorbital ridge; the most inferior (Sl), and the most superior (Sh) points of the contour of the frontal sinus. In addition, posterior (Spo^) and anterior (Sa^) landmarks were defined on the contour of the sinus at the level of the greatest transverse dimension perpendicular to the axis of the frontal sinus (Sl-Sh). Posterior (Spo) and anterior (Sa) landmarks were defined as the intersection between the line S-Gla and the contour of the frontal sinus (Fig. 2).

The projection height of the frontal sinus perpendicular to the line S-N (Sh-Sl^), the absolute
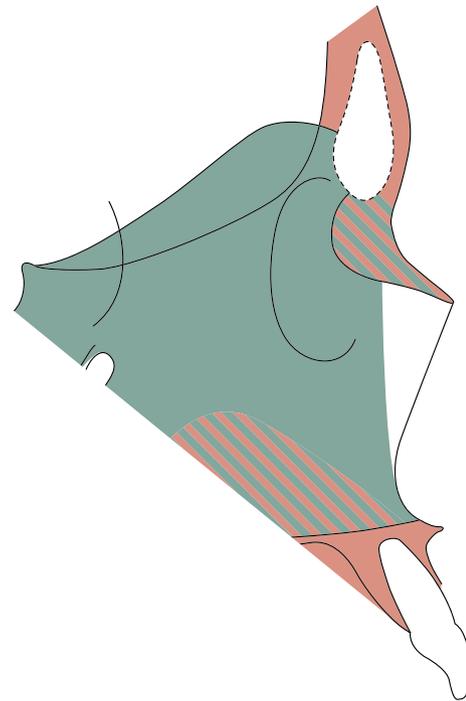
Fig. 1. Drawing of the fronto-nasal field. The bony origins of osseous structures are marked schematically. The cranial base and the upper part of the nasal septum are cartilaginous developed (green). The nasal bone and vomer are structures of intramembranous origin developed upon a scaffold of cartilage (the cartilaginous nasal capsule and the nasal septum) (red/green). Only the proximal part of the nasal bone is supported by structures of cartilaginous origin. The other bony structures are intramembranous developed (red) (14). The drawing shows the fronto-nasal field as a section of Fig. 2 in the former report by Gjørup et al. (11).

height of the frontal sinus (Sh-Sl), the width of sinus (Spo^-Sa^; Spo-Sa), and the angle S-N-Gla were calculated by the software in accordance with the definitions by Brown et al. (15), Ertürk (19), and Dostalova et al. (20).

Cephalometric analysis, the nasal bone

The main landmarks for the analysis of the nasal bone were as follows: Sella (S); Nasion (N); and Nasal-apex (Na): the most anterior point of the nasal bone (Fig. 3). The length of the nasal bone and the angulation of the nasal bone in relation to the cranial base (S-N) were measured in accordance with the definition by Solow (18). The nasal bone morphology was assessed by measuring the transversal dimensions of the nasal bone by lines perpendicular to the axis of the nasal bone. The axis of the nasal bone was defined by the midpoint of a line N-N^ (Nmi) and Na. The point N^ was

defined as the intersection of the lower border of the nasal bone and a perpendicular line to N-Na through N. N-N^ was regarded as a constructed fronto-nasal suture. Perpendicular to the nasal axis, lines were constructed with a distance of 3 mm between lines. The lines were numbered from 0 to 11: proximally, line '0' was the baseline
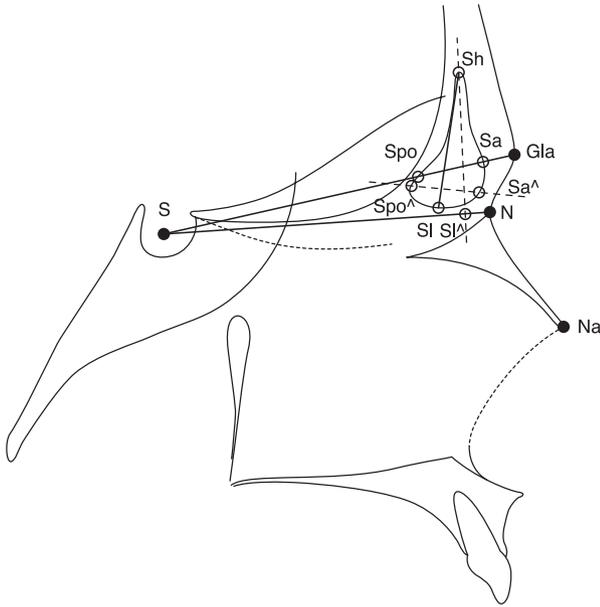
Fig. 2. Landmarks and cephalometric variables. The frontal sinus: Sh-Sl: the absolute height of the sinus; Spo^-Sa^: the greatest anterior–posterior width perpendicular to the axis (Sh-Sl); Spo-Sa: the anterior–posterior width at the line S-Gla; Sh-Sl^: the projection height, *that is*, the distance between Sh and Sl^ (i.e., the projection of Sh on S-N line). The nasal bone: N-Na: the length of the bone; S-N-Na: the inclination (degree) of the nasal bone (N-Na) in relation to the anterior cranial base (S-N).

passing through N (L0-N) and distally, line '11' was near the apex of the nasal bone (Na). The intersections between the perpendicular line and the upper and lower border were used as landmarks (U1-U11 and L0-L11, respectively). The distances from the N-Na line to the upper and lower border, and the transversal dimensions (L0-N, L1-U1, L2-U2, etc.) were calculated by the software. In addition, the ratio between the length of the basal line and the length of the nasal axis was calculated (base/axis: L0-N/Nmi-Na), and the area of the polygon defined by the multiple landmarks on the upper and the lower borders of the nasal bone was calculated. The ratio (L0-N / Nmi-Na) was defined as 'low' when below 0.5 and 'high' when above 0.5.

Reliability

To test the intra-examiner reliability, the first author digitized 22 randomly selected radiographs twice. The radiographs selected for redigitizing were included in the overall randomization of radiographs in order to blind the observer to whether the radiographs were read before. Except for three of the 11 variables describing the transversal dimension of the nasal bone, the differences for none of the variables were significantly different from zero ($p > 0.05$). For each of the cephalometric variables, the random error (S) was calculated as described by Dahlberg (21). S ran-

Fig. 3. Analysis of the morphology of the nasal bone. N-N^: line perpendicular to line N-Na. Nmi: the midpoint of the line N-N^; Nmi-Na: the axis of the nasal bone; N-L0: the base of the nasal bone perpendicular to the axis (Nmi-Na). Line numbers 1–11 are perpendicular to the axis (Nmi-Na), with 3-mm interline distance, and crossing the upper and lower border of the nasal bone in U1-U11 and L1-L11, respectively.
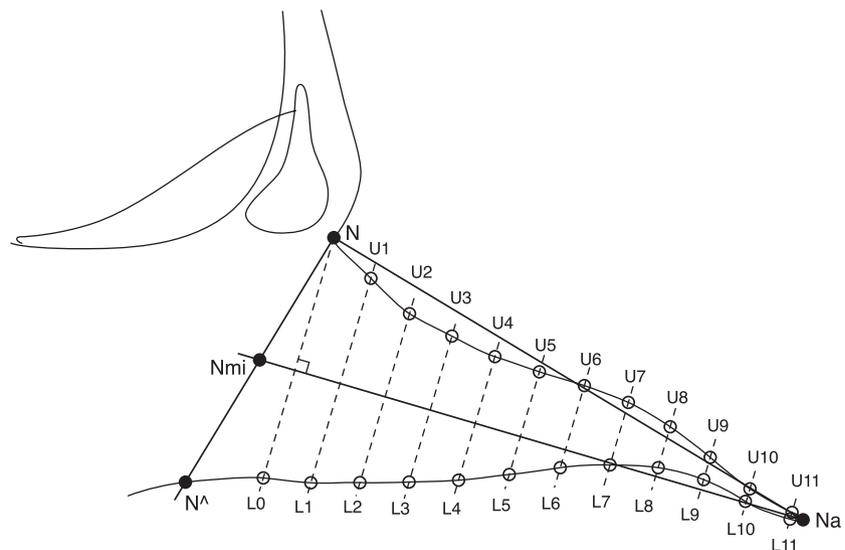
ged from 0.01 to 2.29 in the case of variables of the nasal bone and from 0.64 to 4.38 in the case of variables of the frontal sinus. The coefficient of reliability (R) was estimated according to Houston (22). In the case of variables describing the transverse dimensions of the nasal bone, R ranged from 0.74 to 0.97, and in the case of the other variables, R ranged from 0.92 to 0.99.

Statistical analyses

Irrespective of age, the gender distribution in HR group and in control group was compared by the two-sided chi-squared test. For each gender, the age distribution in the two groups was compared with the unpaired t-test. In both the HR group and the control group, the cephalometric measurements underwent a visual examination for normality using Q-Q plots and histograms, and a normal distribution was found in both groups. The effect of the health status (i.e., HR or control), age, and gender upon the cephalometric measurements was assessed by a linear regression analysis. To allow for familiar dependence, the regression estimates were adjusted for clustering. Potential interactions between the effect of the age and the health status and between the effect of the gender and the health status were assessed in the regression analysis.

The cephalometric data are presented according to the gender. Means and standard deviations were used as descriptive statistics and p-values equal to or below 0.05 were considered statistically significant.

The proportion of high-ratio base/axis (L0-N/ Nmi-Na) according to skeletal severity impact was compared by a two-sided chi-squared test.

Data analysis was performed using STATA® 11.0 (StataCorp, College Station, TX, USA).

Ethics

The study was approved by the Regional Scientific Ethical Committees for Southern Denmark (M-2678-05) and by the Danish Data Protection Agency (2009-41-3613). Written informed consent was obtained from all patients before entering the study.

Results

The distribution of the participants according to the health (HR patients and controls) and the gender is presented in Table 1. The proportion of females in the HR group (67%) did not significantly exceed the proportion of females in the control group (53%) ($p = 0.208$). Irrespective of gender, the mean age of the HR group and the control group was not significantly different.

The height and width of the frontal sinus were not significantly different in HR patients and controls ($p = 0.406$ to $p = 0.863$) (Table 2). Five HR patients (13.9%) and 3 controls (6.1%) had no visible frontal sinus, but this difference was not statistically significant ($p = 0.116$). According to the regression analysis, the cephalometric variables of the frontal sinus were not significantly affected by age.

Hypophosphatemic rickets patients showed, in comparison with controls, a tendency toward a reduced mean length of the nasal bone and an increased mean area of the nasal bone was found, but this did not reach a significant level (Table 2). Regression analysis with the nasal bone length (N – Na) as outcome variable, revealed a negative regression-coefficient for the effect of HR (coefficient = −1.73; 95% CI: −4.94, 0.48), which indicated a reduced nasal bone length in HR patients. Proximal, the width of the nasal bone was greater in HR patients compared with controls. The significant differences were restricted to the four proximal lines, the differences in width being: L0: 1.06 ($p = 0.014$), L1: 1.04 ($p = 0.005$), L2: 0.081 ($p = 0.002$), and L3: 0.59 ($p = 0.007$). The morphology of the nasal bone was illustrated by the mean distances from the line N-Na to the upper and the lower border of the nasal bone (Fig. 4). In addition, examples of the radiographic appearance of the nasal bone in HR patients and in controls have been depicted (Fig. 5). According to the regression analysis, the cephalometric variables of the nasal bone were not significantly affected by age.

The morphology of the nasal bone was expressed by the ratio base/axis. This ratio was significantly increased in HR patients compared

Table 2. Descriptive statistics (means and standard deviations) of cephalometric measurements in the fronto-nasal field of HR patients according to gender and compared with healthy controls

	Males				Females				Adjusted comparison of HR and control p-value
	Control		HR		Control		HR		
	N = 23		N = 12		N = 26		N = 24		
Variable name	Mean	SD	Mean	SD	Mean	SD	Mean	SD	
Frontal sinus									
Spo^-Sa^ (mm)	12.67	4.42	13.16	5.17	9.96	3.36	10.07	5.52	0.815
Sh-Sl^ (mm)	27.12	8.50	23.94	10.42	26.02	9.47	23.63	13.60	0.406
Sh-Sl (mm)	28.16	8.71	27.21	11.56	28.90	10.67	25.59	13.94	0.517
Spo-Sa (mm)	13.89	4.94	15.18	7.11	10.49	4.96	10.09	6.21	0.863
Nasal bone									
N_Na (mm)	27.12	3.97	24.37	4.90	25.24	4.14	24.15	3.39	0.122
NNa_NS (degree)	117.72	6.08	117.03	4.57	114.97	5.75	114.23	6.33	0.543
Base/axis (ratio)	0.45	0.07	0.58	0.12	0.45	0.09	0.52	0.12	0.010*
Nasal area (mm^2)	98.94	27.06	103.97	25.05	90.29	26.38	94.76	25.68	0.440

p-values are from the regression analysis after adjustment for the effect of gender, age, and clustering.
*p-value <0.05.

with controls (Table 2). In HR patients with severe skeletal impact, the percentage of 'high' ratio base/axis was almost twice that of the mildly affected group (Table 3).

Discussion

Detailed analyses of nasal bone morphology have not previously been extensively reported in the literature. In this study, we report abnormal nasal bone morphology (eaglebeak-like) in HR patients, primarily because of an increased proximal width of the nasal bone.

Despite the rarity of the HR disease, the number of patients was relatively high and the number equals or exceeds the number of patients included in previous cephalometric HR studies (4, 5, 7). Furthermore, the patients of our study have been uniformly diagnosed, and except for three cases, the diagnosis was genetically verified. In the group of patients with HR, the male:female ratio was 1:2, which was in accordance with the X-linked inheritance of the disease, but not significantly different from the apparently equal gender distribution in the control group (Table 1). In the

analyses of the study, we adjusted for the potential effect of the gender. The analysis of 3-dimensional (3D) anatomical structures (the frontal sinus and the nasal bones) was performed on 2-dimensional (2D) radiographs, which to some extent limits the interpretation of the results. The advantage of 2D-methods is the comparability with previous studies where 2D methods traditionally have been used in cephalometric studies of craniofacial structures [e.g., Jensen and Kreiborg (23), Ruf and Pancherz (16), Lexner et al. (24), Al-Jundi et al. (7)].

The frontal sinus and bone resorption

In this study, the size of the frontal sinus varied considerably in both groups (i.e., HR patients and controls), but the differences between the groups were not statistically significant (Table 2). These findings of size variation are in accordance with a previous study regarding variations in sinus development in healthy children (15). In HR patients, the unaffected resorption during development of the frontal sinus indicates a normal osteoclast formation and function within the frontal bone. Only three of 36 HR patients

Females

Line[a]		0	1	2	3	4	5	6	7	8	9	10	11
N[b]	CTR	26	26	26	26	26	26	25	20	15	7	5	1
	HR	24	24	24	24	24	24	24	17	12	2	1	0

Males

Line[a]		0	1	2	3	4	5	6	7	8	9	10	11
N[b]	CTR	23	23	23	23	23	23	22	22	19	11	5	1
	HR	12	12	12	12	12	11	11	9	6	2	2	0
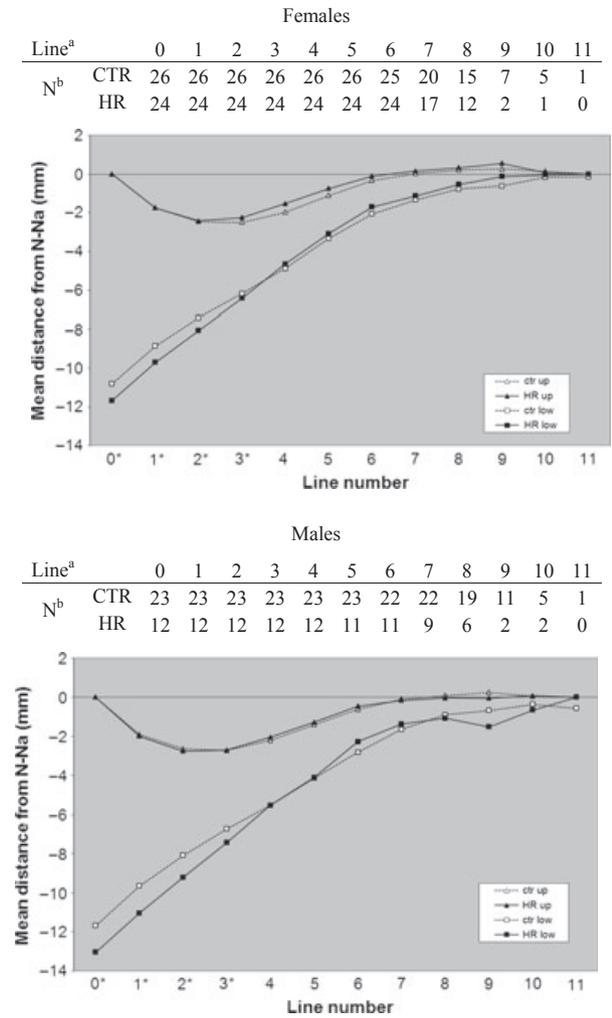
Fig. 4. Morphology of the nasal bone in HR patients and controls (ctr) according to gender. Mean distances from the line N-Na to the upper (up) and the lower (low) border of the nasal bone measured at perpendicular lines (No. 0–11) to the axis of the nasal bone. [a]Line number of perpendicular lines to the nasal axis. 0 = N-L0, 1 = U1-L1, 2 = U2-L2, etc. [b]N are numbers of assessable measurements for the variable. *Line numbers with significant difference in width of nasal bone, HR patients in comparison with controls adjusted for the effect of gender, age, and clustering.

did not have a frontal sinus at all. In contrast, patients with cleidocranial dysplasia (CCD, MIM 119600) generally have a missing or hypoplastic frontal sinus (23). This indicates an impaired osteoclast function in CCD although a runt-related transcription factor 2 gene (*RUNX2*, MIM 600211) association with osteoclast function has not yet been reported.

In adults in contrast to growing children, the effect of age upon the size of osseous structures, for example, the frontal sinus, was supposed to be the same in all age groups of this study. This might be in contradiction with the knowledge

on post-menopausal osteoporosis in women and the age-related bone loss in both men and women which induce increasing bone loss with increasing age, especially in women. However, the post-menopausal and the age-related remodeling primarily impact the internal trabecular bone (25). Thus, it can be justified to include all age groups in this study of macroscopic dimensions of bony structures.

The nasal bone and bone formation

According to this study, the morphology of the nasal bone in HR patients was abnormal because of an extensive proximal width of the bone (Table 2, Figs 4 and 5). Further, the degree of abnormal morphology of the nasal bone seemed to be related to the severity of the general skeletal impact of HR (Table 3). The age had no or minimal impact on the size and the morphology of the nasal bone. This indicates that the changes in morphology occur primarily during early childhood or even earlier in fetal development. Prenatally, the nasal bone develops bilaterally in the mesenchyme in close relation to the chondral nasal capsule. The osseous structure develops directly from the mesenchymal cells using the chondral nasal capsule as a scaffold (26). Later in the post-natal development, the proximal part of the nasal bone remains surrounded by bony structures of cartilaginous origin (i.e., structures of the ethmoid bone), but the apical part of the nasal bone develops without the support from bony structures of cartilaginous origin (Fig. 1). In the adult HR patients, the mean nasal bone length was reduced in both genders in comparison with controls, although the difference did not reach the level of statistical significance (Table 2). In our former report, which included children (11), the nasal bone length was significantly reduced, and the same has been reported in an animal study (10). It remains unanswered, if the significant difference in the former report was caused by an inaccuracy in the statistical analysis not adjusting for the different dimensional effects of the age depending on the age group (e.g., growing children vs. mature adults). More likely, the
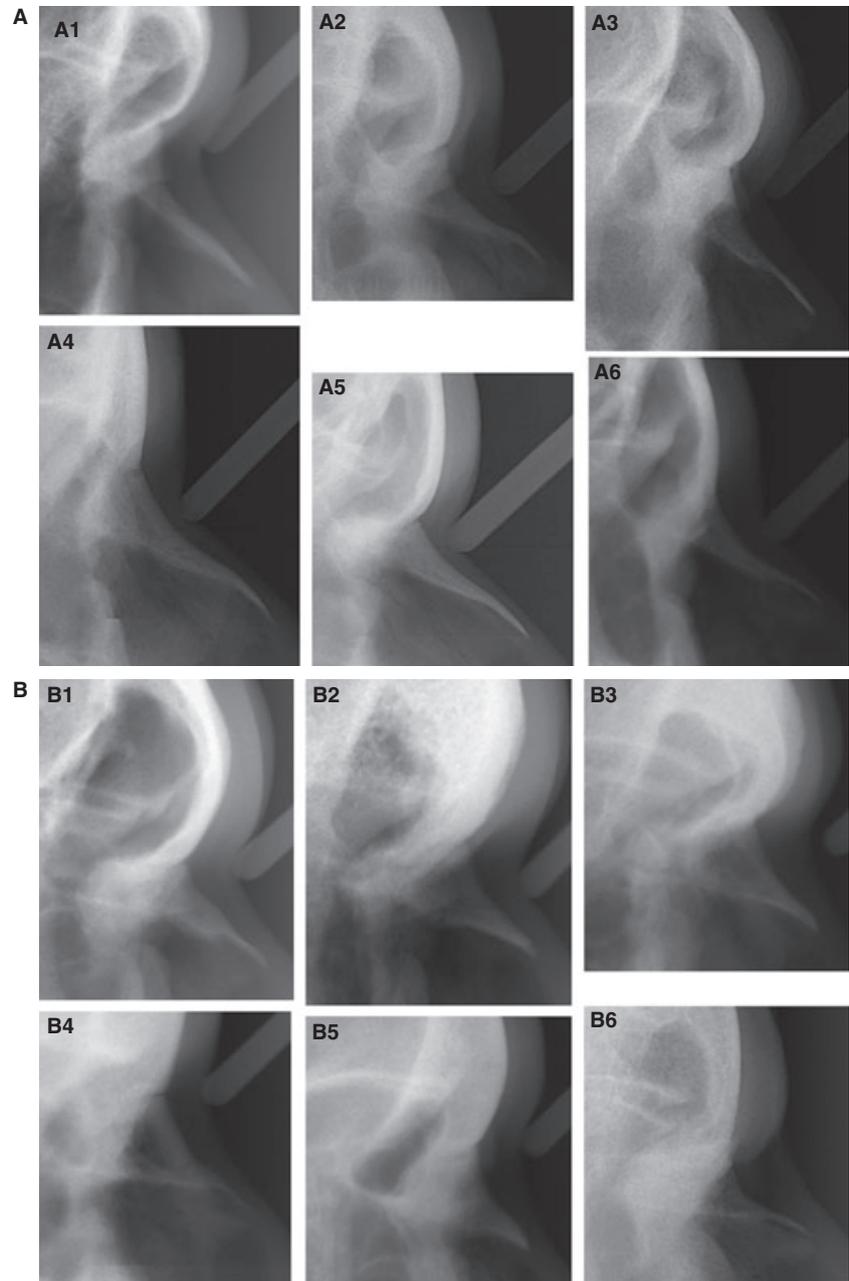
Fig. 5. Radiographic appearance of the nasal bone. A: Examples from healthy controls. B: Examples from HR patients. A1: male 21 years; A2: female 40 years; A3: male 53 years; A4: female 51 years; A5: female 39 years; A6: female 45 years; B1: female 40 years; B2: male 23 years; B3: male 33 years; B4: female 23 years; B5: female 49 years; B6: female 65 years.

non-significant difference in the nasal bone length was caused by the reduced sample size of the present report, which was indicated by the negative regression-coefficient for the effect of HR and the 95% confidence interval hardly exceeding zero. In other diseases, a reduced size of the nasal bone has been reported, for example, in 51 patients with achondroplasia in whom the reduced size has been related to abnormalities in the cartilaginous developed nasal septum (27). The reporting of a reduced length of the nasal bone in 20 patients with cleft lip indicates

alternative, intrinsic, and non-cartilaginous related factors of importance in the development of the nasal bone (28). In HR patients, the eagle-beak-like appearance of the nasal bone reflected increased bone formation in the proximal part, which was supported by structures of cartilaginous origin, and the morphological results could be interpreted as disturbances in modeling with a net gain of bone in the proximal part. Alterations in some unknown signaling from the cartilaginous scaffold might explain the disturbances in bone modeling of the proximal part, which

Table 3. Relation between the skeletal severity and the ratio nasal base/nasal axis (N-L0/Nmi-Na) in 36 HR patients. The number (%) in the low-ratio group compared with the high-ratio group according to the skeletal severity

| Nasal base/axis | N | Skeletal severity | | p-value |
		Mild	Severe	
Low	16	9 (56)	7 (44)	0.056
High	20	5 (25)	15 (75)	

Low: ratio base/axis <0.5; High: ratio base/axis >0.5.
p-value from chi-squared test.

develops supported by the scaffold. Apparently, the modeling of the apical part of the nasal bone, which is not supported by these structures, had another character. The mechanisms behind the increased width of the proximal part of the nasal bone might be identical with the mechanisms responsible for the increased thickness of the theca, which develops with the meninges as a scaffold. The knowledge of impaired osteoclastogenesis in FGF23–associated HR (13) supports the suggestions of disturbances in the modeling of bone, although the reason for the apparent differences according to the presence of a supporting scaffold remains unclear.

Conclusions

In comparison with healthy controls, the size of the frontal sinus was unaffected in HR patients, indicating normal ability of the osteoclasts to perform internal resorption of the frontal bone.

The morphology of the nasal bone was abnormal (eaglebeak-like appearance) which indicated an overall impact upon bone formation, and the increased width of the proximal part was an indication of impaired bone modeling in bony

tissue supported by cartilage during growth. Furthermore, the degree of abnormal morphology of the nasal bone tended to correlate with the severity of the general skeletal impact of HR.

Clinical Relevance

In patients with hypophosphatemic rickets, the abnormal morphology of the nasal bone was a radiological sign of disturbances in bone formation. In the usage of profile cephalograms for orthodontic treatment planning, the clinician's awareness of the morphology of the nasal bone as well as other cranial structures is advocated, as the morphology of bony structures might reflect abnormalities in bone metabolism and indicate a general disease, for example, hypophosphatemic rickets.

Conflict of interest

The authors declare that they have no conflict of interest.

References

1. Beck-Nielsen SS, Brusgaard K, Rasmussen LM, Brixen K, Brock-Jacobsen B, Poulsen MR et al. Phenotype Presentation of Hypophosphatemic Rickets in Adults. *Calcif Tissue Int* 2010;87:108–19.

2. Hyp Consortium. A gene (PEX) with homologies to endopeptidases is mutated in patients with X-linked hypophosphatemic rickets. The HYP Consortium. *Nat Genet* 1995;11:130–6.

3. Shimada T, Kakitani M, Yamazaki Y, Hasegawa H, Takeuchi Y, Fujita T et al. Targeted ablation of FGF23 demonstrates an essential physiological role of FGF23 in phosphate and vitamin D metabolism. *J Clin Invest* 2004;113:561–8.

4. Marks SC, Lindahl RL, Bawden JW. Dental and cephalometric findings in vitamin D resistant rickets. *J Dent Child* 1965;32:259–65.

5. Tracy WE, Campbell RA. Dentofacial development in children with vitamin D resistant rickets. *J Am Dent Assoc* 1968;76:1026–31.

6. Currarino G. Sagittal synostosis in X-linked hypophosphatemic rickets and related diseases. *Pediatr Radiol* 2007;37:805–12.

7. Al-Jundi SH, Dabous IM, Al-Jamal GA. Craniofacial morphology in patients with hypophosphataemic vitamin-D-resistant rickets: a cephalometric study. *J Oral Rehabil* 2009;36:483–90.

8. Pronicka E, Popowska E, Rowinska E, Arasimowicz E, Syczewska M, Jurkiewicz D et al. Anthropometric characteristics of X-linked hypophosphatemia. *Am J Med Genet A* 2004;126A:141–9.

9. Iorio RJ, Murray G, Meyer RA Jr. Craniometric measurements of craniofacial malformations in mice with X-linked, dominant hypophosphatemia (vitamin D-resistant rickets). *Teratology* 1980;22:291–8.

10. Mostafa YA, El-Mangoury NH, Meyer RA Jr, Iorio RJ. Deficient nasal bone growth in the X-linked hypophosphataemic (HYP) mouse and its implication in craniofacial growth. *Arch Oral Biol* 1982;27:311–7.

11. Gjorup H, Kjaer I, Sonnesen L, Haubek D, Beck-Nielsen SS, Hintze H et al. Craniofacial morphology in patients with hypophosphatemic rickets: a cephalometric study focusing on differences between bone of cartilaginous and intramembranous

origin. *Am J Med Genet A* 2011;155A:2654–60.

12. Enlow DH, Hans MG. The neurocranium. In: Enlow DH, Hans MG, editor. . *Facial Growth. Handbook in Facial Growth*. Philadelphia: Saunders; 1996. pp. 99–110.

13. Lu Y, Feng JQ. FGF23 in skeletal modeling and remodeling. *Curr Osteoporos Rep* 2011;9:103–8.

14. Kjaer I. Orthodontics and foetal pathology: a personal view on craniofacial patterning. *Eur J Orthod* 2010;32:140–7.

15. Brown WA, Molleson TI, Chinn S. Enlargement of the frontal sinus. *Ann Hum Biol* 1984;11:221–6.

16. Ruf S, Pancherz H. Development of the frontal sinus in relation to somatic and skeletal maturity. A cephalometric roentgenographic study at puberty. *Eur J Orthod* 1996;18:491–7.

17. Lestrell PE, Engstrom C, Chaconas SJ. A longitudinal study of the human nasal bone in Norma Lateralis: size and shape considerations. In: Dixon AD, Sarnat BG, Hoyte DAN, editors. *Fundamentals of Bone Growth: Methodology and Applications*. London: CRC Press. Inc.; 1991. pp. 547–64.

18. Solow B. *The Pattern of Craniofacial Associations [Thesis]*. Copenhagen: The Royal Dental College; 1966.

19. Erturk N. Teleroentgen studies on the development of the frontal sinus. *Fortschr Kieferorthop* 1968;29:245–8.

20. Dostalova S, Sonka K, Smahel Z, Weiss V, Marek J. Cephalometric assessment of cranial abnormalities in patients with acromegaly. *J Craniomaxillofac Surg* 2003;31:80–7.

21. Dahlberg G. *Statistical Methods for Medical and Biological Students*. London: Georges Allen and Unwin; 1940.

22. Houston WJB. The analysis of errors in orthodontic measurements. *Am J Orthodont* 1983;83:382–90.

23. Jensen BL, Kreiborg S. Craniofacial growth in cleidocranial dysplasia–a roentgencephalometric study. *J Craniofac Genet Dev Biol* 1995;15:35–43.

24. Lexner MO, Bardow A, Bjorn-Jorgensen J, Hertz JM, Almer L, Kreiborg S. Anthropometric and cephalometric measurements in X-linked hypohidrotic ectodermal dysplasia. *Orthod Craniofac Res* 2007;10:203–15.

25. Feng X, McDonald JM. Disorders of boneremodeling. *Ann Rev Pathol Mech Dis* 2011;6:121–45.

26. Sandikcioglu M, Molsted K, Kjaer I. The prenatal development of the human nasal and vomeral bones. *J Craniofac Genet Dev Biol* 1994;14:124–34.

27. Cohen MM Jr, Walker GF, Phillips C. A morphometric analysis of the craniofacial configuration in achondroplasia. *J Craniofac Genet Dev Biol Suppl* 1985;1:139–65.

28. Nielsen BW, Molsted K, Skovgaard LT, Kjaer I. Cross-sectional study of the length of the nasal bone in cleft lip and palate subjects. *Cleft Palate Craniofac J* 2005;42:417–22.

Upper spine morphology in hypophosphatemic rickets and healthy controls: a radiographic study

Hans Gjørup*,**, Liselotte Sonnesen***, Signe S. Beck-Nielsen****,***** and Dorte Haubek**

*Section of Oral Health in Rare Diseases, Department of Maxillofacial Surgery, Aarhus University Hospital, **Department of Dentistry, Health, Aarhus University, ***Department of Orthodontics, Institute of Odontology, Faculty of Health Sciences, University of Copenhagen, ****Department of Pediatrics, Hospital of Southwest Denmark, Esbjerg, and *****Institute of Clinical Research, University of Southern Denmark, Odense, Denmark

Correspondence to: Hans Gjørup, Section of Oral Health in Rare Diseases, Department of Maxillofacial Surgery, Aarhus University Hospital, Noerrebrogade 44, DK-8000, Aarhus, Denmark. E-mail: hangjo@rm.dk

SUMMARY

BACKGROUND/OBJECTIVES: The aim of this study was to describe upper spine morphology in adult patients with hypophosphatemic rickets (HR) compared with controls to assess differences in spine morphology in terms of severity of skeletal impact and to study associations between spine morphology and craniofacial morphology.

MATERIAL/METHODS: The study population comprised 36 HR patients and 49 controls. The atlas and axis dimensions were measured on cephalograms, and the differences between the groups were estimated by regression analysis. The upper spine morphology was visually assessed to estimate the prevalence of cervical vertebral anomalies.

RESULTS: The dimensions of the atlas and the axis were larger in HR patients than in controls ($P \leq 0.001$), and fusions (FUS) occurred more often in HR patients (39%) than in controls (6%; $P \leq 0.001$). In HR patients, the length of the atlas correlated positively ($P = 0.008$) and the height of the dens correlated negatively ($P = 0.043$) with the severity of skeletal impact. The height of the posterior arch of the atlas and the length of the axis correlated negatively with the cranial base angle ($P \leq 0.017$), and the vertical dimensions of the atlas correlated positively with the thickness of the occipital skull ($P \leq 0.015$). The length of the atlas correlated positively with mandibular prognathism ($P = 0.042$). FUS correlated positively with the frontal and parietal thickness ($P = 0.034$ and $P = 0.003$, respectively).

CONCLUSIONS: The dimension of the atlas and the axis and the prevalence of the FUS were increased in HR patients compared with controls. Upper spine dimensions were associated with craniofacial dimensions, primarily in relation to the posterior cranial fossa.

Introduction

Hypophosphatemic rickets (HR) is a rare disease characterized by insufficient mineralization of the bones due to abnormal renal wasting of phosphate (Beck-Nielsen *et al.*, 2010). The predominant type of HR is inherited in a dominant X-linked fashion, and it is caused by mutations in the gene encoding for the phosphate-regulating endopeptidase homolog, X-linked (*PHEX*, MIM 300550; XLHR, MIM 307800; Hyp Consortium, 1995; Beck-Nielsen *et al.*, 2012).

A recent cephalometric study of 53 individuals with X-linked HR showed an affection of cranial bones of enchondral and of intramembranous origin. In comparison with controls, the cranial base angle was increased and the depth of the posterior cranial fossa was reduced. This was suggested to be the result of bone deformation. In contrast, the maxilla and the mandible were unaffected (Gjørup *et al.*, 2011).

Cephalograms are used routinely by orthodontists to analyse craniofacial structures. Such cephalograms also depict the upper cervical vertebrae (C). The cervical vertebrae belong to the cerebellar and cervical spine field (Kjaer *et al.*, 1994; Kjaer, 1999; Lomholt *et al.*, 2003; Kjaer, 2010). Cervical vertebral anomalies (CVA) include posterior arch deficiencies (PAD) and fusions (FUS; Farman *et al.*, 1979; Sandham, 1986). The presence of FUS between C2 and C3 (14%) and PAD of C1 (5%) are considered normal morphological variations (Sonnesen and Kjaer, 2007b). In comparison with controls, the occurrence of CVA is, however, more frequent in a number of syndromes and pathological conditions such as cleft palate (Sandham, 1986; Uğar and Semb, 2001), mandibular hypoplasia (Sonnesen *et al.*, 2007), and obstructive sleeping apnea (Sonnesen *et al.*, 2008). In addition, the occurrence of CVA is frequent in non-syndromic individuals with extreme skeletal malocclusions such as deep bite, mandibular overjet, maxillary overjet, and open bite (Sonnesen and Kjaer, 2007a,b; Sonnesen and Kjaer, 2008a,b). Furthermore,

the vertical dimension of the dorsal arch of the atlas is associated with the growth direction of the mandible, which is a factor that influences the maxillofacial morphology and dental occlusion (Huggare, 1989; Huggare, 1991).

According to the scientific community, it is unknown if the morphology and the dimensions of the upper cervical vertebrae are affected in patients with HR. Morphological deviations observed in the bony structures of the cranial part of the cerebellar and cervical spine field in HR patients have given rise to the hypothesis that additional deviations may exist in the morphology and dimensions of the upper cervical vertebrae (Caspersen *et al*., 2010). It has also been hypothesized that the severity of the general skeletal impact in HR patients may be reflected in the degree of such morphological alterations. Furthermore, the existence of a relationship between the morphology of the cervical vertebrae and the craniofacial morphology has been hypothesized.

The aim of this study was to characterize the size and morphology of the upper cervical vertebrae in adult patients with HR compared with healthy controls and to elucidate if the upper spine morphology was related to the severity of the skeletal impact in these patients. The study also explored the relationship between the morphology of the cervical vertebrae and 1. the dimensions of the posterior cranial fossa, 2. the maxillofacial morphology, and 3. the thickness of theca.

Materials and methods

Study population

The study population included a control group of 49 healthy individuals and a group of 36 patients with HR in whom X-linked disease was verified in 33 cases (Beck-Nielsen *et al*., 2012; Table 1). The recruitment and diagnostic methods of the HR patients have been described in detail in a previous report (Gjørup *et al*., 2011).

The size of the control group was based on power calculations after the recruitment of all HR patients as previously described (Gjørup *et al*., 2011). It was estimated to yield sufficient power (80%) to identify relevant differences at the 5% level of significance. The controls were recruited among patients, students, and employees at Aarhus University and

Aarhus University Hospital, Denmark. The inclusion criteria for the control group were 1. Scandinavian ethnicity, 2. no chronic diseases except for allergies, 3. a minimum of 24 permanent teeth, 4. normal, or only minor deviations from normal occlusion, 5. no history of orthodontic treatment, and 6. no craniofacial anomaly.

The analyses of this study were based on adult participants ($n = 85$; Table 1). According to the definition of skeletal severity score by Beck-Nielsen *et al*. (2010), the skeletal impact was categorized as 'mild' in 14 HR patients and as 'severe' in 22 HR patients.

Methods

Measurements of osseous structures in the cerebellar and cervical spine field (Figure 1), visual assessment of the upper five cervical vertebrae (C1–C5), measurements of the cranial base as well as the position of the maxilla and the mandible in relation to the cranial base, and the thickness of theca were evaluated on standardized lateral cephalograms. The cephalograms were obtained with the digital radiographic equipment Planmeca Promax© (Planmeca Oy, Helsinki, Finland). All radiographs included the upper five cervical vertebrae (C1–C5). The sensor-focus distance was 1.50 m and the enlargement factor was 1.13. During exposure, the participant's head was fixed in a rigid cephalostat, and the participant was instructed to keep the teeth in occlusion. The head posture was adjusted to the best fit of the borders of the X-ray sensor.

The analysis of the cephalograms was performed using software for cephalometric analysis, Pordios® (Institute of Orthodontic Computer Science, Aarhus, Denmark). The digitizing of all radiographs was performed by HG after randomization of the radiographs in order to blind the observer to the status of the individuals (i.e. HR patients or controls).

Cervical vertebrae: size and morphology

The landmarks of the atlas and the axis were defined according to Huggare (1991) (Figure 2). The landmarks were digitized directly on the cephalograms, and the dimensions of the atlas and the axis were calculated accordingly (Huggare, 1991).

Deviations in the morphology of the upper cervical vertebrae (C1–C5) were visually assessed as a PAD, which was subclassified as 'partial clefting' or 'dehiscence', or a FUS, which was subclassified as 'fusion' (Fus), 'block fusion' (Blo), or 'occipitalization' (Occ) (Sandham, 1986; Figure 3). The assessment was performed by HG according to the following criteria: 1. All the assessments were checked by LS in a blinded fashion. 2. When more than one cephalogram was available in one participant, the morphological deviations had to be present on all cephalograms. 3. If there was any doubt about the assessment of the cervical vertebral column, the vertebral column was registered as 'no morphological deviations'.

Table 1 Number and age (yrs) of hypophosphatemic rickets (HR) patients and controls according to gender.

	HR patients		Controls	
	Females	Males	Females	Males
N	24	12	26	23
Mean age (SD)	41.2 (14.6)	42.4 (18.7)	42.3 (15.4)	39.5 (15.9)
Age range	21.0–74.5	18.8–73.2	23.0–74.5	20.7–72.6
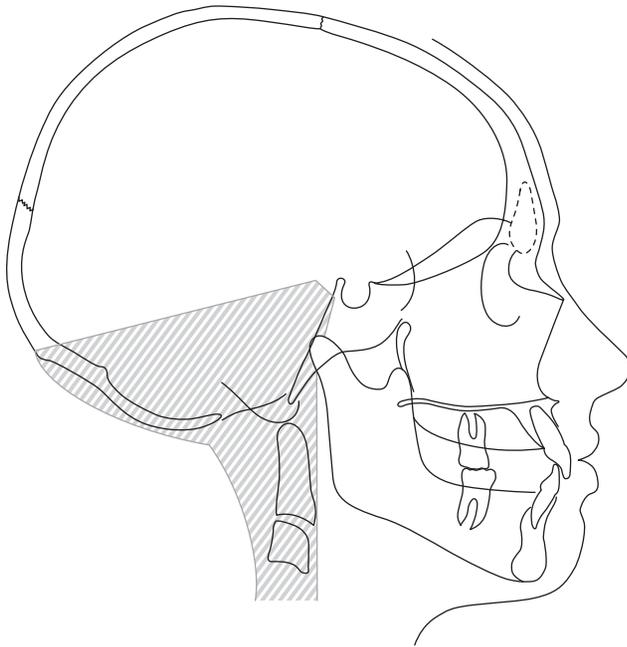
Figure 1 Schematic illustration of the cerebellar and cervical spine field (Kjaer *et al*., 1994; Kjaer *et al*., 1999; Kjaer, 2010). A modified version of the illustration by Kjaer (2010).
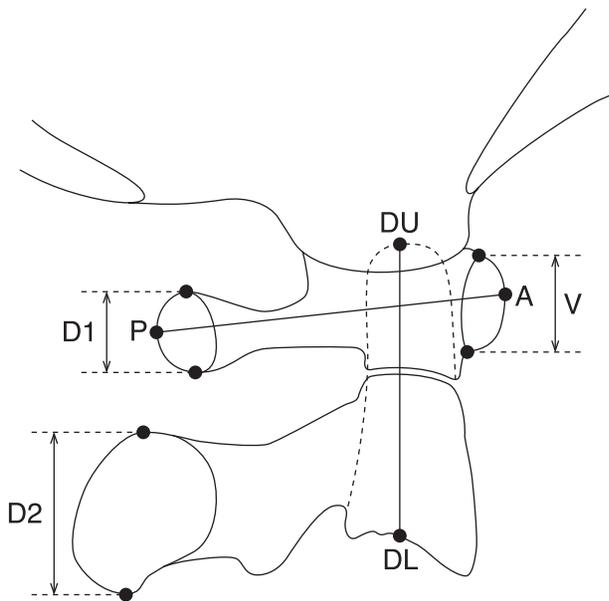
Figure 2 Reference points and variables of the atlas and the axis. Atlas: V, the height of the anterior tubercle; D1, the height of the dorsal arch; A-P, the length of the atlas. Axis: D2, the height of the dorsal arch; DU-DL, the height of the dens.

Craniofacial structures: size and morphology

The cephalometric measurements of the posterior cranial fossa, the maxillofacial region (i.e. the maxilla and the mandible), and the theca comprised six linear and six angular variables, which were calculated by the software after digitizing of the cephalometric landmarks (Figure 4). The variables were defined according to definitions by Solow (1966), Bjørk (1975), Axelsson *et al*. (2003), and Caspersen *et al*. (2010).

Reliability

The reliability of the variables describing the craniofacial measurements and the size of the atlas and the axis was assessed in 22 randomly selected radiographs digitized twice by HG. The radiographs selected for re-digitizing were included in the overall randomization of radiographs. For each of the linear measurements of the atlas and the axis, no systematic error was found. The method error ranged from 0.03 to 0.83 (Dahlberg, 1940), and the reliability coefficient ranged from 0.97 to 0.99 (Houston, 1983). The reliability of the craniofacial measurements has previously been reported (Gjørup *et al*., 2011). The reliability of the visual assessment of the morphological characteristics of the cervical vertebrae has also previously been reported ($\kappa = 0.82$; Sonnesen *et al*., 2007).

Statistical analyses

A two-sided chi-square test was used to compare the gender distribution in the HR group and the control group. For each gender, the age distributions in the two groups were compared with unpaired *t*-test.

Measurements of the atlas and the axis according to health status (i.e. HR patient or control) were compared by linear regression analysis adjusted for the effect of age and gender. To allow for familiar dependence, the regression estimates were adjusted for clustering. Potential interactions between the effect of age and health status and between the effect of gender and health status were assessed. The presence of FUS and PAD in HR patients in comparison with controls was evaluated by chi-squared test for the whole group of participants with and without HR.

In the group of HR patients, the associations between the linear variables of the cervical column and the severity of the skeletal impact were assessed by linear regression analysis with adjustment for the effect of age, gender, and clustering. In addition, the association between the categorical variables of the cervical column and the severity of the skeletal impact was evaluated by chi-squared test.

In the whole group of participants (i.e. HR patients and controls), associations between the linear measurements of the cervical column and the cephalometric variables of the craniofacial structures were assessed by linear regression analysis with adjustment for the effect of health, gender, and clustering. In the same group, the association between CVA and the cephalometric variables of craniofacial structures were evaluated by logistic regression analysis with adjustment for the effect of health, gender, age, and clustering. Potential interactions between the effect of the
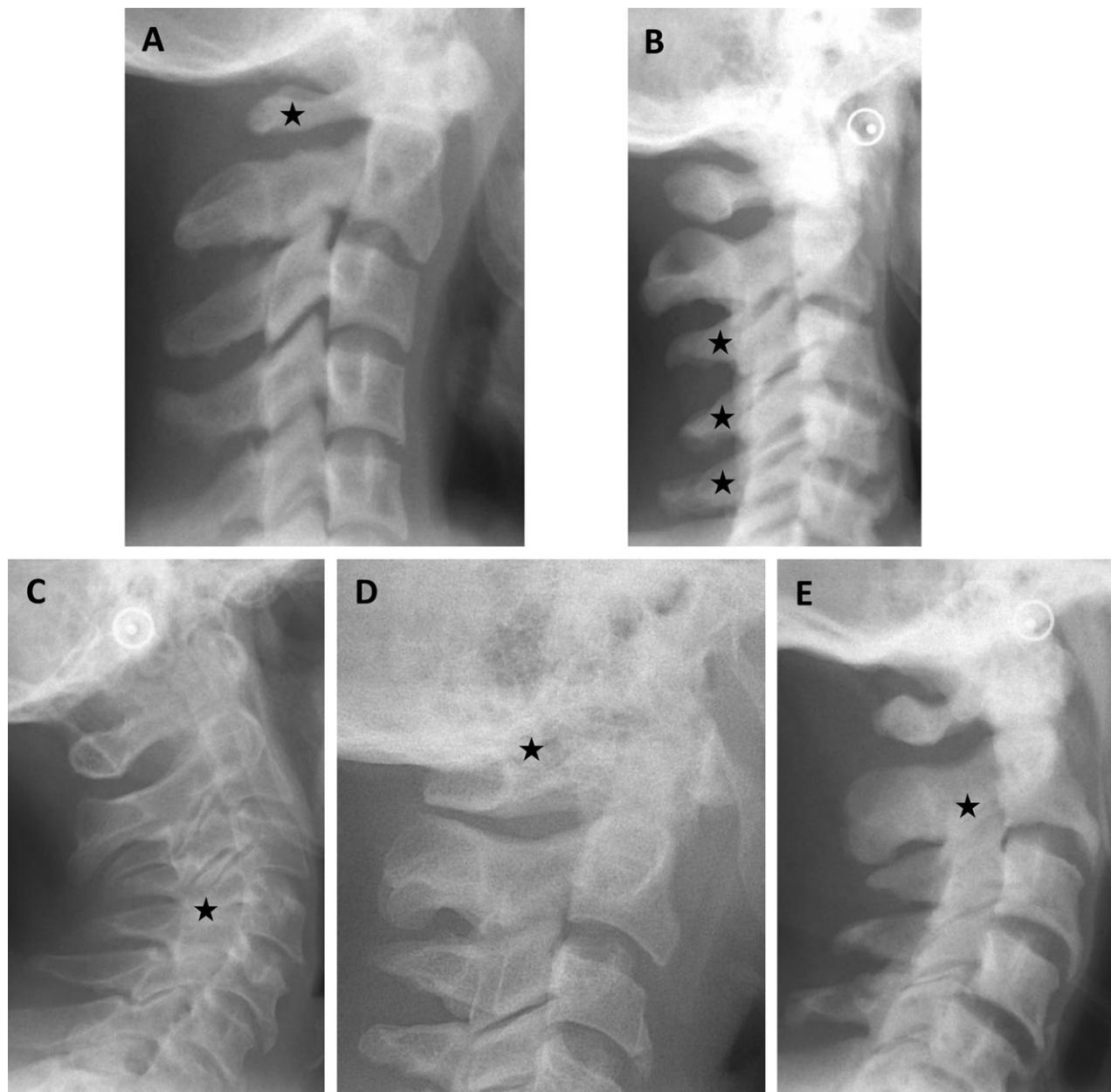
Figure 3 Posterior arch deficiences (PAD) and fusions (FUS) of the cervical vertebrae in hypophosphatemic rickets patients illustrated on radiographs: A, partial cleft of C1; B, dehiscence of the posterior arch of C3-4–5; C, fusion of C3-4-5; D, occipitalization; E, fusion of C2-3. Stars indicate the location of PAD and FUS.

cephalometric variable and health and gender, respectively, were assessed.

The data were analysed using Stata® 11.0 (StataCorp, College Station, Texas, USA). *P* values equal to or below 0.05 were considered statistically significant.

Results

The proportion of females was not higher in the HR group (67%) than in the control group (53%; *P* = 0.208). The mean age in the HR group [41.6 (standard deviation 2.6) years] did not significantly deviate from that of the control group [41.0 (standard deviation 2.2) years; Table 1].

Cervical vertebrae and craniofacial structures: HR patients versus controls

The height and the length of the atlas and the height of the posterior arch of the axis were larger in HR patients than in controls (*P* ≤ 0.001; Table 2). In addition to the adjusted comparison, Table 2 presents descriptive statistics (i.e. means and standard deviation) according to status (HR patients or
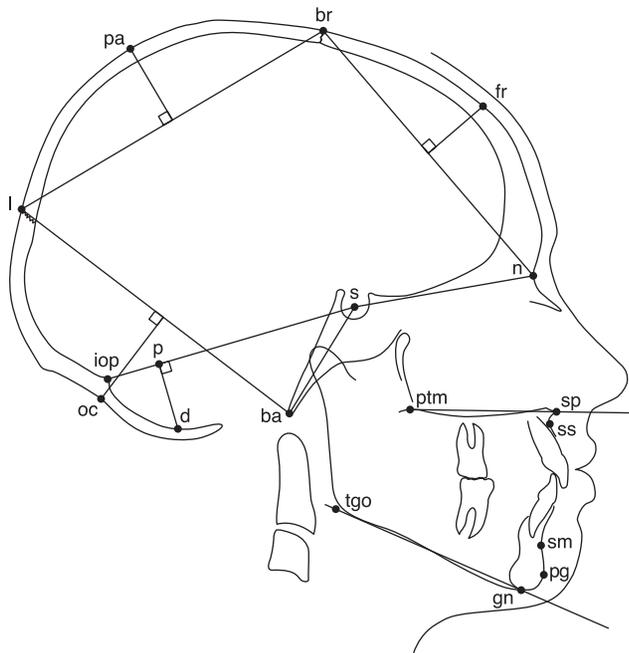
Figure 4 Craniofacial variables: n-s-ba, cranial base angle; s-ba, length of the posterior cranial base; thi-oc, occipital thickness of the theca; thi-pa, parietal thickness of the theca; thi-fr, frontal thickness of the theca; d-s-iop, angle point d-sella-internal occipital protuberance; s-iop, length of the posterior cranial fossa; d-p, height of the posterior cranial fossa; s-n-ss, maxillary prognathism; s-n-pg, mandibular prognathism; ss-n-sm, ANB-angle; and ss-n-pg, sagittal jaw relation.

Table 2 Dimensions [means and standard deviations (SD) in millimetres] of atlas and axis in 36 hypophosphatemic rickets (HR) patients and 49 controls.

		HR patients			Controls			Adjusted comparison HR versus control
		n	Mean	SD	n	Mean	SD	P value
Axis	Height V	36	12.10	1.38	48	11.43	1.17	<0.001
	Height D1	36	13.27	1.96	49	11.70	1.94	<0.001
	Length A-P	36	54.34	3.31	49	52.81	4.44	0.001
Atlas	Height D2	36	19.58	3.39	49	16.94	2.90	<0.001
	Dens DU-DL	36	38.12	2.65	49	38.96	3.09	0.392

Comparison between groups adjusted for the effect of gender, age, and clustering. P value, linear regression analysis.

controls). In HR patients, the cranial base angle was increased, the depth of the posterior cranial fossa was decreased, and the thickness of the occipital and the frontal theca was increased compared with controls ($P \leq 0.038$; Table 3).

The prevalence of FUS was increased in HR patients compared with controls and occipitalization of the axis was the dominant finding ($P < 0.001$; Table 4).

Associations between cervical vertebral column and severity of skeletal impact in HR

The length of the atlas was positively ($P = 0.043$) and the height of the dens was negatively ($P = 0.008$) associated with the severity of skeletal impact in HR patients (Table 5). No significant associations between CVA (i.e. FUS or PAD) and the severity of skeletal impact were found in HR patients.

Associations between cervical vertebral column and craniofacial structures

In the whole group of HR patients and controls, the height of the posterior arch of the atlas (D1) and the length of the axis (A-P) correlated negatively with the cranial base angle (n-s-ba; D1: $P = 0.017$; A-P: $P = 0.008$); D1 correlated positively with the length of the posterior cranial base (s-ba: $P = 0.009$) and negatively with the length of the posterior cranial fossa (s-iop: $P = 0.037$; Table 6). The anterior (V) and posterior height of the atlas (D1) correlated positively with the thickness of the occipital theca (V: $P = 0.015$; D1: $P = 0.001$; Table 6). The height of the posterior arch of the axis (D2) was correlated positively with the depth of the posterior cranial base (d-s-iop: $P = 0.004$; P-d: $P = 0.013$; Table 6). Furthermore, the length of the atlas correlated positively with the degree of mandibular prognathism ($P = 0.042$; Table 3). The height of the posterior arch of the axis (D2) was affected by the interaction between the effect of the sagittal jaw relation and the effect of health (ss-n-sm, $P = 0.003$; ss-n-pg, $P = 0.015$); and a significant correlation between the height of the axis (D2) and the sagittal jaw relation was present only in healthy controls.

In the whole group of HR patients and controls, the only association identified between the CVA and the craniofacial structures was that of a positive association between the FUS and the frontal and parietal thickness ($P = 0.034$ and $P = 0.003$, respectively). In controls as opposed to HR patients, PAD was associated with the length of the posterior cranial fossa (s-iop, $P = 0.033$). In females as opposed to males, FUS was associated with the occipital thickness (thi-oc, $P = 0.001$). Neither PAD nor FUS were significantly affected by the interaction between the effect of any other cephalometric variable and health or gender, respectively.

Discussion

This radiological study has revealed increased dimensions of the atlas and the posterior arch of the axis as well as more occipitalizations in HR patients compared with controls. In HR patients, the vertebral dimensions were related to the severity of the skeletal impact. This study also demonstrated an association between the dimensions of the upper cervical vertebrae and the dimensions of the posterior cranial fossa.

Table 3 Craniofacial measurements [means and standard deviations (SD) in millimetres or degrees] in 36 hypophosphatemic rickets (HR) patients and 49 controls. d-p, height of the posterior cranial fossa; d-s-iop, angle point d-sella-internal occipital protuberance; n-s-ba, cranial base angle; s-ba, length of the posterior cranial base; s-iop, length of the posterior cranial fossa; s-n-ss, maxillary prognathism; s-n-pg, mandibular prognathism; ss-n-sm, ANB-angle; and ss-n-pg, sagittal jaw relation; thi-oc, occipital thickness of the theca; thi-fr, frontal thickness of the theca; thi-pa, parietal thickness of the theca.

		HR patients			Controls			Adjusted comparison HR versus control
		n	Mean	SD	n	Mean	SD	P value
Cranial base	n-s-ba (degree)	24	133.79	5.68	26	132.52	5.73	0.038
	s-ba (mm)	24	45.48	2.84	26	45.70	2.65	0.548
Posterior cranial base	d-p (mm)	24	30.03	3.50	25	35.30	3.55	<0.001
	d-s-iop (degree)	24	21.17	2.79	25	25.74	3.33	<0.001
	s-iop (mm)	24	106.56	4.83	25	105.56	4.78	0.256
Theca	thi-oc (mm)	24	6.21	1.99	25	4.64	1.46	0.010
	thi-pa (mm)	18	9.68	2.25	24	8.93	1.51	0.052
	thi-fr (mm)	18	10.83	2.79	25	8.28	1.46	<0.001
Maxilla and mandible	s-n-ss (degree)	24	82.89	3.56	26	82.16	3.02	0.883
	s-n-pg (degree)	24	80.01	3.98	26	79.48	2.98	0.922
	ss-n-sm (degree)	24	2.88	2.84	26	2.68	2.05	0.792
	ss-n-pg (degree)	24	4.09	2.21	26	3.59	1.73	0.922

Comparison between groups adjusted for the effect of gender, age and clustering. P value, linear regression analysis.

Table 4 Distribution of cervical vertebral anomalies in 36 hypophosphatemic rickets (HR) patients and 49 healthy controls according to type of posterior arch deficiencies (PAD) and fusions (FUS).

	HR patients		Controls		Chi^2
	n	%	n	%	P value
PAD	6	16.7	9	18.4	NS
Partial*	2	5.6	4	8.2	NS
Dehis**	4	11.1	5	10.2	NS
FUS	14	38.9	3	6.1	<0.001
Fus***	1	2.8	3	6.1	NS
Blo****	1	2.8	0	0	NS
Occ*****	13	36.1	0	0	<0.001

Chi-squared test comparing controls and HR patients. One HR patient had both fusion of C2-C3 and occipitalization; two controls had both PAD and FUS.
% is the percentage of the total number in the group.
*Partial cleft of posterior arch; **dehiscence of posterior arch; *** fusion between C2-C3; **** block fusion of C3-C4-C5; ***** occipitalization, i.e. fusion of atlas and cranial base; NS, not significant: P value > 0.05.

Table 5 Length and height (in millimetres) of atlas and axis in 36 adult hypophosphatemic rickets patients according to severity of skeletal impact as defined by Beck-Nielsen *et al*. (2010). SD, standard deviation.

	Mild (n = 14)		Severe (n = 22)		Adjusted comparison Mild versus severe
	Mean	SD	Mean	SD	P value
Height V	11.44	1.08	12.52	1.41	0.113
Height D1	12.69	1.18	13.63	2.28	0.384
Length A-P	52.74	2.53	55.36	3.39	0.043
Height D2	18.59	3.71	20.20	3.09	0.419
Dens	38.39	2.20	37.95	2.94	0.008

P values, linear regression analysis with adjustment for the effect of gender, age, and clustering.

patients. We did not match controls according to gender and age during recruitment. However, the age and gender differences between the two groups were not significant and potential inaccuracies were adjusted for in the statistical analysis. Thus, the control group was considered to be appropriate for this study.

The analyses of the cervical structures were performed on two-dimensional (2D) radiographs. The difficulty of determining deviations in the upper spine morphology on the basis of a single lateral cephalogram has previously

The number of HR patients in this study was relatively high in spite of the fact that HR is a rare disease, and we included more patients than previous cephalometric HR studies (Marks *et al*., 1965; Tracy and Campbell, 1968; Al-Jundi *et al*., 2009). Another strength of this study is its clearly defined diagnostic criteria of HR and the detection of a disease-causing gene mutation in 33 of the 36 HR

Table 6 Analysis of associations between linear variables of the cervical column (C1 and C2) and cephalometric variables of the cerebellar and cervical spine field in 36 hypophosphatemic rickets (HR) patients and 49 controls. d-p, height of the posterior cranial fossa; d-s-iop, angle point d-sella-internal occipital protuberance; n-s-ba, cranial base angle; s-ba, length of the posterior cranial base; s-iop, length of the posterior cranial fossa; thi-oc, occipital thickness of the theca.

C1 and C2 (mm)	s-ba (mm)		n-s-ba (degree)		thi-oc (mm)		d-s-iop (degree)		d-p (mm)		s-iop (mm)	
	Co	P	Co	P	Co	P	Co	P	Co	P	Co	P
Height V	0.01	0.755	−0.01	0.554	0.10	0.015	0.05	0.123	0.03	0.382	−0.01	0.551
Height D1	0.16	0.009	−0.06	0.017	0.30	0.001	0.11	0.071	0.06	0.23*	−0.07	0.037
Length A-P	0.20	0.118	−0.14	0.008	−0.02	0.95*	0.20	0.092	0.15	0.072	−0.03	0.705
Height D2	0.15	0.158	−0.07	0.159	0.30	0.240	0.23	0.004	0.18	0.013	0.03	0.653
Dens	−0.03	0.772	−0.02	0.628	0.12	0.445	0.14	0.057	0.11	0.062	0.05	0.301

P values, linear regression analysis of the association between cervical column variables and cephalometric variables with adjustment for the effect of health, gender, and clustering.
Co, regression coefficient of the cephalometric variable in relation to the cervical column variable.
*Significant interaction between the cephalometric variable and health (HR patient or control).

been discussed (Massengill *et al*., 1997; Koletsis and Halazonetis, 2010; Bebnowski *et al*., 2012). These studies found that some FUS observed on 2D radiographs were likely to be 'pseudo-FUS', and they therefore recommended to use a more reliable method such as computed tomography (CT) or cone-beam CT (CBCT). However, in a recent study of CVA in patients with obstructive sleeping apnea, the agreement between the occurrence of CVA as determined by lateral cephalograms and CBCTs was good (k = 0.64; Sonnesen *et al*., 2013). In this study, the lateral cephalograms were obtained before CBCT was generally used. In order to minimize false-positive findings on 2D, clearly defined criteria were set up in this study. We, therefore, expect that our 2D results provide useful and reliable results about dimensional and morphological deviations.

The increased dimensions of the atlas and the posterior arch of the axis may be associated with the increased thickness of the theca, which has been reported previously (Gjørup *et al*., 2011). The increment in size of the atlas and the axis as well as the theca may reflect disturbances in the normal balance between bone resorption and bone formation. Calcification of ligaments is common in adult HR patients (Polisson *et al*., 1985; Beck-Nielsen *et al*., 2010), and this kind of calcification might also be the result of disturbances in bone cell functioning.

In this study, the length of the atlas and the height of the dens were related to HR severity. Thus, the atlas was longer and the dens were shorter in severely than in less severely affected HR patients (Table 5). The differences in the severity of skeletal impact depending on the subunits of the vertebral unit (e.g. vertebral body or posterior arch) might reflect the differentiated development of the vertebrae, which originate from the embryological sclerotomes. The cells of a specific region of the sclerotome (e.g. the future vertebral body that surround the notochord) are controlled by distinct genes, which determine the characteristics of the

region (Schoenwolf, 2009), and it could be hypothesized that the regional characteristics also determine the susceptibility and reaction to pathological conditions like HR.

CVA was a relatively frequent finding in HR patients, and FUS (39%) was more common than PAD (17%). Comparable differences have been reported in patients with severe skeletal malocclusions (FUS 42–61%; PAD 6–13%; Sonnesen and Kjaer, 2007a,b; Sonnesen and Kjaer, 2008a,b). In patients with cleft deformities (cleft lip, cleft palate, or combined), whose maxillofacial morphology is severely affected, PAD (8–17%) was more frequent than FUS (0–12%; Sandham, 1986; Uğar and Semb, 2001). The differences in the prevalence and pattern of CVA may reflect the different pathogenesis of the conditions.

The analyses of the correlations between the dimensions of the upper cervical column and the cranial structures included all participants (HR patients and controls). Except from one pair of variables (D1/P-D), no significant interactions between cephalometric variables and health status were found in the statistical analyses. This indicated that the same interrelationship existed between the variables irrespective of participant's health status. This finding of a significant correlation between the height of the dorsal arch of the atlas and the length of both the posterior cranial base and the posterior cranial fossa is in accordance with a previous study, which reported a significant correlation between the height of the dorsal arch of the atlas and the length of the posterior cranial base in healthy adults (Huggare, 1991). In addition, both the height of the arch and the length of the atlas correlated positively with the flexure of the cranial base (inversely related to the cranial base angle). These positive correlations indicate a close connection between the osseous structures of the cerebellar and the cervical spine field (Figure 1). This finding supports the idea of a common embryological origin initiated by notochordal induction of sclerotome formation in the somites, which develop into the

cervical spine and the osseous structures of the posterior cranial fossa (Kjaer, 1998).

A previous report on the association between the height of the posterior arch of the atlas and the forward growth of the mandible (Huggare, 1989) is supported by our finding of the positive correlation between the length of the atlas and the mandibular prognathism. In contrast, this study found no association between FUS and jaw relationship, which has been reported in patients with skeletal malocclusions (Sonnesen and Kjaer, 2007a; Sonnesen and Kjaer, 2008a,b). It has been suggested that a probable interrelationship between the upper spine morphology and the maxillofacial morphology is rooted in the neural tube origin of the neural crest cells, which migrate anteriorly from the neural tube region to become involved in the development of the foetal face (Kjaer, 1998; Sonnesen and Kjaer, 2007a,b; Sonnesen and Kjaer, 2008a,b). In this study, the absence of an interrelationship between CVA and maxillofacial morphology may be related to the fact that the participants had a fairly normal maxillofacial morphology (Table 3), and thus, severe deviations in maxillofacial morphology were not present in the study population. A previous study based on human skulls concluded that occipitalizations were associated with deviations in the neighbouring structures (i.e. the cerebellar region) and not with deviations in the maxillofacial morphology (Caspersen et al., 2010). In this study, a high number of HR patients had occipitalizations, but no associations were found between FUS and deviations in neither the neighbouring nor the maxillofacial structures. In contrast, a significant association was found between FUS and the thickness of the frontal and the occipital theca.

The results of this study illustrate the importance of awareness of all structures of the cephalogram when it is used by orthodontists for routine cephalometric analyses. Cephalograms depict the upper cervical vertebrae, and CVA or a deviating dimension of the vertebrae in addition to other symptoms may indicate general pathology, e.g. HR.

Conclusions

The dimensions of the atlas and the axis were increased in HR patients compared with healthy controls, and HR patients had a high prevalence of FUS of the upper spine. Dimensions of the atlas and the axis were also associated with the severity of skeletal impact in HR patients. Furthermore, the analyses of the whole study population revealed associations between upper spine morphology and craniofacial morphology mainly in the form of an association with the morphology of the cranial part of the cerebellar and cervical spine field. This may indicate an association between dysmorphological traits of osseous structures belonging to the same developmental field.

References

Al-Jundi S H, Dabous I M, Al-Jamal G A 2009 Craniofacial morphology in patients with hypophosphataemic vitamin-D-resistant rickets: a cephalometric study. Journal of Oral Rehabilitation 36: 483–490

Axelsson S, Bjørnland T, Kjaer I, Heiberg A, Storhaug K 2003 Dental characteristics in Williams syndrome: a clinical and radiographic evaluation. Acta Odontologica Scandinavica 61: 129–136

Bebnowski D, Hänggi M P, Markic G, Roos M, Peltomäki T 2012 Cervical vertebrae anomalies in subjects with class II malocclusion assessed by lateral cephalogram and cone beam computed tomography. European Journal of Orthodontics 34: 226–231

Beck-Nielsen S S, Brixen K, Gram J, Brusgaard K 2012 Mutational analysis of PHEX, FGF23, DMP1, SLC34A3 and CLCN5 in patients with hypophosphatemic rickets. Journal of Human Genetics 57: 453–458

Beck-Nielsen S S et al. 2010 Phenotype presentation of hypophosphatemic rickets in adults. Calcified Tissue International 87: 108–119

Bjørk A 1975 Kæbernes relation til det øvrige kranium. In: Lundström I (ed.). Nordisk Lärobok i Ortodonti. Sveriges Tandläkarförbunds Förlagsförening, Stockholm, pp. 69–110

Caspersen L M, Kjaer I, Sonnesen L 2010 How does occipitalization influence the dimensions of the cranium? Orthodontics and Craniofacial Research 13: 162–168

Dahlberg G 1940 Statistical methods for medical and biological students. Georges Allen and Unwin, London

Farman A G, Nortjé C J, Joubert J J 1979 Radiographic profile of the first cervical vertebra. Journal of Anatomy 128: 595–600

Gjørup H et al. 2011 Craniofacial morphology in patients with hypophosphatemic rickets: a cephalometric study focusing on differences between bone of cartilaginous and intramembranous origin. American Journal of Medical Genetics Part A 155A: 2654–2660

Houston W J 1983 The analysis of errors in orthodontic measurements. American Journal of Orthodontics 83: 382–390

Huggare J 1989 The first cervical vertebra as an indicator of mandibular growth. European Journal of Orthodontics 11: 10–16

Huggare J 1991 Association between morphology of the first cervical vertebra, head posture, and craniofacial structures. European Journal of Orthodontics 13: 435–440

Hyp Consortium 1995 A gene (PEX) with homologies to endopeptidases is mutated in patients with X-linked hypophosphatemic rickets. The HYP Consortium. Nature Genetics 11: 130–136

Kjaer I 1998 Neuro-osteology. Critical Reviews in Oral Biology and Medicine 9: 224–244

Kjaer I 1999 Developmental fields in the cranium. In: Kjaer I (ed.). The prenatal human cranium. Munksgaard, Copenhagen, pp. 155–162

Kjaer I. 2010 Orthodontics and foetal pathology: a personal view on craniofacial patterning. European Journal of Orthodontics 32: 140–147

Kjaer I, Keeling J W, Graem N 1994 Cranial base and vertebral column in human anencephalic fetuses. Journal of Craniofacial Genetics and Developmental Biology 14: 235–244

Kjaer I, Keeling J W, Hansen B F 1999 The prenatal human cranium - normal and pathologic development. Munksgaard, Copenhagen

Koletsis D D, Halazonetis D J 2010 Cervical vertebrae anomalies in orthodontic patients: a growth-based superimpositional approach. European Journal of Orthodontics 32: 36–42

Lomholt J F, Nolting D, Hansen B F, Stoltze K, Kjaer I 2003 The prenatal development and osseous growth of the human cerebellar field. Orthodontics and Craniofacial Research 6: 143–154

Marks S C, Lindahl R L, Bawden J W 1965 Dental and cephalometric findings in vitamin D resistant rickets. Journal of Dentistry for Children 32: 259–265

Massengill A D, Huynh S L, Harris J H Jr 1997 C2-3 facet joint "pseudofusion": anatomic basis of a normal variant. Skeletal Radiology 26: 27–30

Polisson R P *et al.* 1985 Calcification of entheses associated with X-linked hypophosphatemic osteomalacia. The New England Journal of Medicine 313: 1–6

Sandham A 1986 Cervical vertebral anomalies in cleft lip and palate. The Cleft Palate Journal 23: 206–214

Schoenwolf G C 2009 Development of the musculoskeletal system. In: Schoenwolf G C, Bleyl S B, Brauer P R, Francis-West P H (eds). Larsen's human embryology, 4th edn, Churchil Livingstone Elsevier, Philadelphia

Solow B 1966 The pattern of craniofacial associations. Department of Orthodontics, The Royal Dental College, Copenhagen

Sonnesen L, Jensen K, Petersson A, Petri N, Berg S, Svanholt P 2013 Cervical vertebral column morphology in patients with obstructive sleep apnoea assessed using lateral cephalograms and cone beam CT. A comparative study. Dento Maxillo Facial Radiology 42: 20130060

Sonnesen L, Kjaer I 2007a Cervical column morphology in patients with skeletal class III malocclusion and mandibular overjet. American Journal of Orthodontics and Dentofacial Orthopedics. 132: 427.e7–e12

Sonnesen L, Kjaer I 2007b Cervical vertebral body fusions in patients with skeletal deep bite. European Journal of Orthodontics 29: 464–470

Sonnesen L, Kjaer I 2008a Anomalies of the cervical vertebrae in patients with skeletal class II malocclusion and horizontal maxillary overjet. American Journal of Orthodontics and Dentofacial Orthopedics. 133: 188.e15–e20

Sonnesen L, Kjaer I 2008b Cervical column morphology in patients with skeletal open bite. Orthodontics and Craniofacial Research 11: 17–23

Sonnesen L, Pedersen C E, Kjaer I 2007 Cervical column morphology related to head posture, cranial base angle, and condylar malformation. European Journal of Orthodontics 29: 398–403

Sonnesen L, Petri N, Kjaer I, Svanholt P 2008 Cervical column morphology in adult patients with obstructive sleep apnoea. European Journal of Orthodontics 30: 521–526

Tracy W E, Campbell R A 1968 Dentofacial development in children with vitamin D resistant rickets. Journal of the American Dental Association (1939) 76: 1026–1031

Uğar D A, Semb G 2001 The prevalence of anomalies of the upper cervical vertebrae in subjects with cleft lip, cleft palate, or both. The Cleft Palate-Craniofacial Journal 38: 498–503

A radiological study on intra- and extra-cranial calcifications in adults with X-linked hypophosphatemic rickets and associations with other mineralizing enthesopathies and childhood medical treatment

H. Gjørup[1,3]

I. Kjaer[2]

S. S. Beck-Nielsen[4,5]

M. R. Poulsen[6]

D. Haubek[3]

[1] Section of Oral Health in Rare Diseases, Department of Maxillofacial Surgery, Aarhus University Hospital, Aarhus, Denmark

[2] Department of Orthodontics, Institute of Odontology, Faculty of Health Sciences, University of Copenhagen, Copenhagen, Denmark

[3] Section for Paediatric Dentistry, Department of Dentistry, Health, Aarhus University, Aarhus, Denmark

[4] Department of Pediatrics, Hospital of Southwest Denmark, Esbjerg, Denmark

[5] Institute of Clinical Research, University of Southern Denmark, Odense, Denmark

[6] Department of Diagnostic Radiology, Odense University Hospital, Odense, Denmark

Correspondence to:

Hans Gjørup

Section of Oral Health in Rare Diseases, Department of Maxillofacial Surgery

Aarhus University Hospital

Nørrebrogade 44

DK-8000 Aarhus, Denmark

Structured abstract

Objectives - The purpose was to: 1) explore radiological signs of intracranial calcifications and of nuchal ligament calcifications in adult patients with hypophosphatemic rickets (HR) compared with controls, 2) correlate signs of cranial calcifications in HR patients with the presence of other extra-cranial enthesopathies, to the severity of skeletal HR impact, and to medical treatment during childhood.

Setting and Sample Population - Lateral and postero-anterior cephalograms from 36 adult HR patients and 49 adult controls and X-rays from spine, pelvis, knees and ankles from 31of the 36 HR patients were included.

Methods - Radiological signs of intracranial calcifications and of nuchal-ligament-calcifications in HR patients were compared with controls by Fischer's exact test. In HR patients, the presence of cranial calcifications was correlated to the presence of other enthesopathies, to the severity of skeletal HR impact, and to medical treatment by Fischer`s exact or chi-squared test.

Results - Six (17%) HR patients revealed major signs of intracranial calcifications. Nuchal ligament calcifications were common in HR patients compared with controls (*p*=0.018). Enthesopathy was present at 0-24 sites per HR patient (median 2). Intracranial calcifications trended to correlate positively with vertebral enthesopathies (*p*=0.059). Nuchal calcifications correlated positively with the severity of skeletal HR impact (*p*=0.040). Vertebral enthesopathies correlated negatively with medical treatment (*p*=0.008).

Conclusion - On lateral cephalograms, more HR patients than controls showed nuchal ligament calcifications, and some HR patients showed intracranial calcifications. Severely affected HR patients often had nuchal ligament calcifications. Medically treated HR patients had few vertebral enthesopathies.

2

Keywords - Hypophosphatemic rickets, cranium, enthesopathy, extra-skeletal calcifications, radiology

Clinical relevance

The finding of unusual calcifications in relation to the cranium calls for attention by clinicians obtaining cephalograms. These findings may indicate a pathological condition and, in addition to a number of other diseases, HR should be considered. Future studies to assess these findings in other metabolic bone diseases, e.g., nutritional rickets, other subtypes of hereditary rickets, or osteogenesis imperfecta, are warranted.

Introduction

Hypophosphatemic rickets (HR) is a rare disease characterized by an insufficient mineralization of the bones due to abnormal renal phosphate wasting (1). The most predominant type of HR is inherited in a dominant X-linked fashion caused by mutations in the gene encoding for the phosphate regulating endopeptidase homolog, X-linked (*PHEX*, MIM 300550) (XLHR, MIM 307800) (2). Less predominant types of HR include autosomal dominant HR caused by a mutation in the gene encoding for fibroblast growth factor 23 *(FGF23,* MIM 605380*) (*ADHR, MIM 193100) (3) and autosomal recessive HR caused by a mutation in the gene encoding for dentin matrix acidic phosphoprotein 1 (*DMP1,* MIM 600980) (ARHR, MIM 241520) (4). XLHR, ADHR, and ARHR are fibroblast-growth-factor-23 (FGF23)-associated HR. FGF23 is a potent phosphaturetic factor, being the principal regulatory hormone of the phosphate homeostasis. In addition, FGF23 is suggested to have a direct effect on the bone cells (5).

HR affects the cranium in humans (1, 6-10), and in HYP mice (the murine model of XLH) (11, 12). Furthermore, HR patients have dental abnormalities (13-15), and endodontically affected teeth are common in adults with HR (16). In addition to skeletal and dental affection, mineralizing enthesopathy (i.e., the calcification of joint capsules, tendons, and ligament insertions) has been reported in HR patients (1, 17, 18). In animal models of HR, a mineralizing enthesopathy has also been demonstrated where it appears as an expansion of mineralizing fibrocartilage in the tendons and the ligaments (19, 20).

A recent cephalometric study on 53 individuals with X-linked HR showed a different morphology of the cranial base compared to controls, and that the skull thickness was increased (21). Another study based on profile radiographs (i.e., cephalograms) of adults from the same HR population focused on the dimensions and the morphology of selected osseous structures adjacent to the anterior cranial fossa. Deviations in the morphology and the dimensions of the nasal bone were

described (22). A succeeding study of the same adult population focused on the osseous structures adjacent to the posterior cranial fossa and revealed deviations in the morphology and the dimensions of the upper cervical vertebrae (23).

On cranial radiographs, intracranial calcifications are generally reported as incidental findings, normally described as a physiological phenomenon (24-26). The potential sites of calcification include the fibrous dura mater sheets, which include the falx cerebri. Extensive calcification of the falx cerebri is a rare condition, which in some cases has been associated with pathology (27-29). In addition to intracranial structures, the lateral cephalogram includes a number of extra-cranial structures related to the cranium, e.g., the attachment site of the nuchal ligament. The nuchal ligament, which is the uppermost ligament of the spine, attaches to the posterior surface of the occipital bone at the external occipital protuberance and the occipital crest. In the present study, it is hypothesized that extraordinary calcification of both the extra-skeletal nuchal ligament and intracranial fibrous structures (e.g., the dura mater) are present in HR patients, which would be in line with the previously reported calcification of other fibrous structures (i.e., mineralizing enthesopathy) in these patients (1, 17, 18).

The primary purpose of the present study was to reveal the presence of intracranial and extra-cranial calcifications on cephalograms in adult HR patients compared with adult controls. The second purpose was to assess the association between the presence of intra- and extra-cranial calcifications and a) the presence of mineralizing enthesopathy at other extra-skeletal sites, b) the severity of skeletal HR impact, and c) the medical treatment during childhood.

Material and methods

Study population and radiographic material

The study population comprised a HR group of 36 adult patients with HR (age>18 yrs.) and a control group of 49 healthy adults (Table 1). A detailed description of the recruitment of the participants has previously been published (1, 21, 23). In the HR group, the diagnosis of HR was confirmed biochemically, and the diagnosis was genetically verified in 33 of the 36 HR patients (92%) (30).

The study material comprised standardized profile radiographs (lateral cephalograms) and standardized postero-anterior radiographs (PA cephalograms) of the cranium. Lateral cephalograms were obtained in all participants, and PA cephalograms were obtained in all participants except in two HR patients and two controls. The radiographs were obtained as described by Solow (31) with minor modifications according to the digital radiographic equipment. The equipment was Planmeca Promax© (Planmeca Oy, Helsinki, Finland). The sensor-focus distance was 1.50 meter and the enlargement factor 1.13. During the exposure, the head of the patient was fixed in a rigid cephalostat, and the participants were instructed to keep their teeth in occlusion. During the exposure for the lateral cephalogram, the head posture was adjusted to the best fit of the borders of the X-ray sensor. During the exposure for the PA cephalogram, the head was postured with the Frankfort plane horizontal.

In addition, X-rays of the ankles, knees, pelvis, including the hips, and the lumbar spine (postero-anterior projections) were obtained in 31 of the 36 HR patients. Similar X-rays were not available in the control group.

Intracranial and extra-cranial calcifications

According to intra- and extra-cranial calcifications, the lateral cephalograms underwent visual assessment to reveal unusual radiopacities, which indicate a calcification of intracranial or extra-cranial structures. This assessment was performed by the first author in a blinded fashion according to the information on group (HR or control group). Diffuse and indistinct radiopacities above the

anterior cranial base and close to the inside of the frontal bone were recorded as present or absent. The radiopacities were sub-classified as minor or major based on a subjective assessment of their extent and clearness. In patients with radiopacities present on the lateral cephalogram, a supplementary assessment was performed on the PA cephalogram to locate the radiopacities in the transverse plane. On the PA cephalogram, the radiopacities were characterized as 1) widespread in the neurocranium on both sides of the midline, 2) localized on one side of the midline, or 3) localized in the midline. Unusual radiopacities at the cranial end of the nuchal ligament indicated an extra-cranial calcification of the ligament. The radiopacities were recorded as present or absent.

The presence of mineralizing enthesopathy of ligaments and tendons in relation to the vertebral column, the ankles, the knees, and the hips was assessed from the evaluation of X-rays of the structures. This assessment was performed by the author MRP. Mineralizing enthesopathies were defined as bone proliferation at sites of ligament attachments or calcification of ligaments. The total number of sites with mineralizing enthesopathy and a grouping according to the number of sites (0-1; 2-6, and ≥7) was recorded. In addition, vertebral enthesopathy (i.e., a mineralizing enthesopathy of the collateral ligaments of the vertebral column) was recorded as present or absent.

Medical treatment during childhood

The medical treatment history during childhood (age 0-18 years) was obtained by a review of the medical files and confirmed by interview. "Continued treatment" was defined as treatment with both calcitriol and phosphate initiated at least from 4 years of age and continued without significant interruptions until 18 years of age. "Periodical treatment" was defined as treatment with a total duration of less than 10 years. "No treatment" was defined as treatment with a total duration of less than one year.

The study was approved by The Regional Scientific Ethical Committee of Southern Denmark (ID: M-2678-05).

Statistical analysis

Concerning study population, the gender distribution in the HR group and in the control group was compared by the two-sided chi-squared test. For each gender, the age distribution in the two groups was compared with the unpaired t-test.

The prevalence of the HR patients with intracranial calcifications was compared with controls by the Fischer's exact test. The prevalence of the HR patients with nuchal ligament calcifications was compared with controls by the Fischer's exact test and by the logistic regression analysis adjusted for the effect of age, gender, and family clustering.

In the group of HR patients, the associations between the presence of vertebral enthesopathies and intracranial calcifications respectively nuchal ligament calcifications were assessed by the Fischer`s exact test. The associations between the enthesopathy grouping (total sites: 0-1, 2-6, and ≥7) and intracranial calcifications respectively nuchal ligament calcifications were assessed by the Fischer`s exact test. Furthermore, the associations between intracranial or nuchal ligament calcifications and the total number of sites with mineralizing enthesopathy were assessed by logistic regression analysis adjusted for the effect of age, gender, and family clustering.

In the group of HR patients, the prevalence of the patients with intracranial calcifications was compared in terms of the severity of the skeletal HR impact by the Fischer's exact test. The prevalence of patients with nuchal ligament calcifications and the prevalence of patients with vertebral enthesopathies were compared in terms of the severity of skeletal HR impact by the two-sided chi-squared test.

In the group of HR patients, the prevalence of patients with signs of intracranial calcifications and the prevalence of patients with signs of nuchal ligament calcifications were compared in terms of the childhood medical treatment by Fischer's exact test.

Data analysis was performed using Stata® 11.0 (StataCorp, College Station, TX). *P*-values equal to or below 0.05 were considered statistically significant.

Results

Study population

With regards to age and gender, no significant differences were found between the HR group and the control group (Table 1).

Intracranial and extra-cranial calcifications

The visual assessment of the lateral cephalograms revealed major intracranial radiopacities in six of 36 HR patients (16.7%), and minor radiopacities in three of 49 controls (6.1%) (Fig. 1-3 and Table 2). A supplementary assessment of the PA cephalograms was possible in five of the six HR patients with radiopacities visible on the lateral cephalograms. The assessment revealed three cases with widespread diffuse radiopacities on both sides of the midline (Fig. 2A, 2D, and 2F). The PA cephalograms of the three controls with radiopacities present on the lateral cephalograms did not provide additional information regarding the location of the radiopacities in the transversal plane.

Calcification of the nuchal ligament was visible in 18 of 36 HR patients (50%) and in 10 of 44 controls (23%) (Fig. 4 and Table 2). According to the comparison adjusted for the effect of the gender, the age, and the clustering, this difference between the groups was significant (p=0.018). The nuchal ligament calcifications were present in only one of the six HR patients with intracranial radiopacities (Table 3).

Mineralizing enthesopathy

The total number of sites with mineralizing enthesopathy was 0-24 sites per HR patient (median 2; 0-1: 12 patients; 2-6: 9 patients; ≥7: 10 patients). Thirteen of 31 HR patients (42%) had at least one site with vertebral enthesopathy.

In exception of one patient, all patients with intracranial calcifications had vertebral enthesopathy (Table 3), but this association was not statistically significant (p=0.059, Table 4). According to the regression analysis, the total number of sites with mineralizing enthesopathy was associated with the presence of intracranial calcifications (p=0.018). The presence of nuchal ligament calcifications was not significantly associated with mineralizing enthesopathy at other skeletal sites (Table 4).

Severity of skeletal impact

According to the definition by Beck-Nielsen and coworkers (1), the skeletal impact was categorized as "mild" in 14 HR patients and "severe" in 22 of the HR patients in this study. The intracranial radiopacities were identified in four of 14 mildly affected (28.9%) and in two of 22 severely affected HR patients (9.1%). The calcification of the nuchal ligament was identified in four of 14 mildly affected (29%) and in 14 of 22 severely affected HR patients (64%). The vertebral enthesopathy was identified in four of 13 mildly affected (30.8%) and in nine of 18 severely affected HR patients (50%). According to the statistical analysis, the severity of skeletal impact was associated with nuchal ligament calcification (p=0.040), but not with intracranial calcifications (p=0.181) or vertebral enthesopathy (p=0.284).

Medical treatment

In the group of 36 adult HR patients, 12 patients (33%) had continuous; two patients (6%) had sporadic, and 22 patients (61%) had no treatment during childhood.

The six HR patients with intracranial calcifications were all untreated during childhood (Table 3). However, the occurrence of neither intracranial nor nuchal ligament calcifications was significantly associated with childhood treatment (p≥0.226). This was in contrast to the presence of vertebral enthesopathy, which correlated negatively with childhood treatment (p=0.008) (Table 5).

11

Discussion

According to the present radiographic study, calcifications in the nuchal ligament were common in HR patients, and the presence of the nuchal ligament calcifications was positively correlated with the severity of skeletal HR impact. In addition, radiological signs of intracranial calcifications were revealed in some HR patients, all being non-treated during childhood. The intracranial calcifications showed a tendency to be correlated with mineralizing enthesopathy at other skeletal sites. Furthermore, the presence of vertebral enthesopathies was negatively correlated with childhood treatment. These findings are new and not previously described in the literature.

Intra- and extra-cranial calcifications

On the lateral cephalograms, radiological signs of intracranial calcifications were a dominant finding in six of the 36 HR patients (17%). In contrast, only three of 49 controls (6%) showed signs of intracranial calcifications, and the signs were discrete. In three of the six HR patients (50%) (Fig. 3A, 3D, and 3F), the supplementary assessment of the frontal cephalograms revealed widespread and diffuse radiopacities inside the neurocranium on both sides of the midline. Sporadic cases with calcification of the falx cerebri or of other parts of the meninges have previously been reported in otherwise healthy patients, as well as in a patient with a tertiary hyperparathyroidism (27-29). According to the PA cephalograms of the previously mentioned three HR patients (Fig. 3A, 3D, and 3F), the radiopacities were not located in the midline. Thus, they did not represent calcification of the falx cerebri. Instead, they indicated calcification of the dura mater or atypical osteoid formation on the inside of the frontal bone. Five of six HR patients (83%) with signs of intracranial calcifications did not show signs of nuchal ligament calcifications (Table 3). In contrast, there was a tendency towards a positive correlation between the presence of intracranial calcifications and the presence of mineralizing enthesopathy at other skeletal sites (Table 4). This might indicate different mechanisms behind the intracranial and the nuchal ligament calcifications.

Extra-cranial calcifications in the nuchal ligament were frequent findings in HR patients (Table 2). The presence of nuchal ligament calcifications adjacent to the surface of the occipital bone adds information to the previous reporting of a high prevalence of mineralizing enthesopathy in HR patients (17-19). However, the present study did not show a significant association between the presence of nuchal ligament calcifications and the presence of other sites with mineralizing enthesopathy. Previous HYP mice studies have revealed mineralizing fibrocartilage in ligaments and tendons, and it has been suggested to be due to a direct action of FGF23 on the fibrochondrocytes (19, 20) . Thus, it could be hypothesized that the present nuchal ligament calcifications represent mineralized fibrocartilage produced by fibrochondrocytes due to a direct FGF23-action.

Severity of skeletal impact and childhood treatment

The presence of the extra-cranial calcifications in the nuchal ligament was correlated positively with the severity of skeletal HR impact (p=0.040), whereas the intracranial calcifications and the vertebral enthesopathy were not ($p{\geq}0.181$). This difference is an additional indication of different mechanisms behind the formation of intracranial, nuchal ligament, and other extra-skeletal calcifications. The positive correlation between childhood treatment and the absence of vertebral enthesopathy might be interpreted as a positive effect of the current treatment method ($p{\geq}0.008$; Table 5). In contrast, the presences of intracranial calcifications or nuchal ligament calcifications were not associated with childhood treatment (Table 5). This may be an indication of shortcomings or insufficient strategy in the current treatment approach. Future treatment strategies based on a direct modification of the FGF23-activity are believed to be more effective, e.g., by restraining the presence of mineralizing enthesopathy (32). This effect might include a reduction in the atypical calcification of the nuchal ligament as well as calcification of ligaments at other skeletal sites.

According to a previous cephalometric study, the cranial base is flattened in HR patients (21). This may be seen as a deformation of hypomineralized cranial bone in line with the deformation of the lower extremities, which is one of the characteristics of HR (1, 2). Thus, the cephalogram may demonstrate the previously described paradox in the presence of both extra-skeletal calcifications (e.g., nuchal ligament calcifications) and bone hypomineralization (e.g., cranial base deformation) in HR patients (19, 20).

In studies on rare diseases, it is an ever-standing challenge to achieve a reasonable sample size. The previously published cephalometric HR studies included up to 22 HR patients (6, 7, 9). The present study, which include 36 patients, add further to the total number of reported HR cases dealing with an assessment of cranial deviations. Furthermore, this study was strengthened by clearly defined diagnostic criteria of HR, in addition to the detection of a disease-causing gene mutation in 33 of the 36 HR patients (92%).

Conclusions

Calcifications of the nuchal ligament were common in HR patients, but they were not associated with mineralizing enthesopathy at other extra-skeletal sites. Some HR patients showed evidence of intracranial calcifications, supposedly in the dura mater. The presence of the intracranial calcifications showed a trend towards a positive correlation with other types of mineralizing enthesopathy. The nuchal ligament calcifications were positively correlated with the severity of the skeletal HR impact. The medical treatment during childhood was associated with the presence of vertebral enthesopathy, but not with intracranial or nuchal ligament calcifications.

References

(1) Beck-Nielsen SS, Brusgaard K, Rasmussen LM, Brixen K, Brock-Jacobsen B, Poulsen MR, et al. Phenotype presentation of hypophosphatemic rickets in adults. *Calcif Tissue Int* 2010;87:108-19.

(2) Hyp Consortium. A gene (PEX) with homologies to endopeptidases is mutated in patients with X-linked hypophosphatemic rickets. The HYP Consortium. *Nat Genet* 1995;11:130-6.

(3) ADHR Consortium. Autosomal dominant hypophosphataemic rickets is associated with mutations in FGF23. *Nat Genet* 2000;26:345-8.

(4) Lorenz-Depiereux B, Bastepe M, Benet-Pages A, Amyere M, Wagenstaller J, Muller-Barth U, et al. DMP1 mutations in autosomal recessive hypophosphatemia implicate a bone matrix protein in the regulation of phosphate homeostasis. *Nat Genet* 2006;38:1248-50.

(5) Shimada T, Kakitani M, Yamazaki Y, Hasegawa H, Takeuchi Y, Fujita T, et al. Targeted ablation of FGF23 demonstrates an essential physiological role of FGF23 in phosphate and vitamin D metabolism. *J Clin Invest* 2004;113:561-8.

(6) Marks SC, Lindahl RL, Bawden JW. Dental and cephalometric findings in vitamin D resistant rickets. *J Dent Child* 1965;32:259-65.

(7) Tracy WE, Campbell RA. Dentofacial development in children with vitamin D resistant rickets. *J Am Dent Assoc* 1968 May;76(5):1026-31.

(8) Currarino G. Sagittal synostosis in X-linked hypophosphatemic rickets and related diseases. *Pediatr Radiol* 2007;37:805-12.

(9) Al-Jundi SH, Dabous IM, Al-Jamal GA. Craniofacial morphology in patients with hypophosphataemic vitamin-D-resistant rickets: a cephalometric study. *J Oral Rehabil* 2009;36:483-90.

(10) Pronicka E, Popowska E, Rowinska E, Arasimowicz E, Syczewska M, Jurkiewicz D, et al. Anthropometric characteristics of X-linked hypophosphatemia. *Am J Med Genet A* 2004;126A:141-9.

(11) Iorio RJ, Murray G, Meyer RA, Jr. Craniometric measurements of craniofacial malformations in mice with X-linked, dominant hypophosphatemia (vitamin D-resistant rickets). *Teratology* 1980;22:291-8.

(12) Mostafa YA, El-Mangoury NH, Meyer RA, Jr., Iorio RJ. Deficient nasal bone growth in the X-linked hypophosphataemic (HYP) mouse and its implication in craniofacial growth. *Arch Oral Biol* 1982;27:311-7.

(13) Pereira CM, de Andrade CR, Vargas PA, Coletta RD, de Almeida OP, Lopes MA. Dental alterations associated with X-linked hypophosphatemic rickets. *J Endod* 2004;30:241-5.

(14) Larmas M, Hietala EL, Simila S, Pajari U. Oral manifestations of familial hypophosphatemic rickets after phosphate supplement therapy: a review of the literature and report of case. *ASDC J Dent Child* 1991;58:328-34.

(15) Chaussain-Miller C, Sinding C, Wolikow M, Lasfargues JJ, Godeau G, Garabedian M. Dental abnormalities in patients with familial hypophosphatemic vitamin D-resistant rickets: prevention by early treatment with 1-hydroxyvitamin D. *J Pediatr* 2003;142:324-31.

(16) Andersen MG, Beck-Nielsen SS, Haubek D, Hintze H, Gjorup H, Poulsen S. Periapical and endodontic status of permanent teeth in patients with hypophosphatemic rickets. *J Oral Rehabil* 2012;39:144-50.

(17) Reid IR, Hardy DC, Murphy WA, Teitelbaum SL, Bergfeld MA, Whyte MP. X-linked hypophosphatemia: a clinical, biochemical, and histopathologic assessment of morbidity in adults. *Medicine (Baltimore)* 1989;68:336-52.

(18) Polisson RP, Martinez S, Khoury M, Harrell RM, Lyles KW, Friedman N, et al. Calcification of entheses associated with X-linked hypophosphatemic osteomalacia. *N Engl J Med* 1985;313:1-6.

(19) Liang G, Katz LD, Insogna KL, Carpenter TO, Macica CM. Survey of the enthesopathy of X-linked hypophosphatemia and its characterization in Hyp mice. *Calcif Tissue Int* 2009;85:235-46.

(20) Karaplis AC, Bai X, Falet JP, Macica CM. Mineralizing enthesopathy is a common feature of renal phosphate-wasting disorders attributed to FGF23 and is exacerbated by standard therapy in hyp mice. *Endocrinology* 2012;153:5906-17.

(21) Gjørup H, Kjaer I, Sonnesen L, Haubek D, Beck-Nielsen SS, Hintze H, et al. Craniofacial morphology in patients with hypophosphatemic rickets: a cephalometric study focusing on differences between bone of cartilaginous and intramembranous origin. *Am J Med Genet A* 2011;155A:2654-60.

(22) Gjørup H, Kjaer I, Sonnesen L, Beck-Nielsen SS, Haubek D. Morphological characteristics of frontal sinus and nasal bone focusing on bone resorption and apposition in hypophosphatemic rickets. *Orthod Craniofac Res* 2013;16:246-55.

(23) Gjørup H, Sonnesen L, Beck-Nielsen SS, Haubek D. Upper spine morphology in hpophosphatemic rickets and healthy controls: A radiographic study. *Eur J Orthod 2013* [Epub ahead of print].

(24) Daghighi MH, Rezaei V, Zarrintan S, Pourfathi H. Intracranial physiological calcifications in adults on computed tomography in Tabriz, Iran. *Folia Morphol* 2007;66:115-9.

(25) Kieffer SA, Gold LH. Intracranial physiologic calcifications. *Semin Roentgenol* 1974;9:151-62.

(26) Saldino RM, Di CG. Tentorial calcification. *Radiology* 1974;111:207-10.

(27) Debnath J, Satija L, George RA, Vaidya A, Sen D. Computed tomographic demonstration of unusual ossification of the falx cerebri: a case report. *Surg Radiol Anat* 2009;31:211-3.

(28) Tubbs RS, Kelly DR, Lott R, Salter EG, Oakes WJ. Complete ossification of the human falx cerebri. *Clin Anat* 2006;19:147-50.

(29) Dorenbeck U, Leingartner T, Bretschneider T, Kramer BK, Feuerbach S. Tentorial and dural calcification with tertiary hyperparathyroidism: a rare entity in chronic renal failure. *Eur Radiol* 2002;12:S11-S13.

(30) Beck-Nielsen SS, Brixen K, Gram J, Brusgaard K. Mutational analysis of PHEX, FGF23, DMP1, SLC34A3 and CLCN5 in patients with hypophosphatemic rickets. *J Hum Genet* 2012;57:453-8.

(31) Solow B. The pattern of craniofacial associations Department of Orthodontics, The Royal Dental College, Copenhagen; 1966.

(32) Lee JY, Imel EA. The changing face of hypophosphatemic disorders in the FGF-23 era. *Pediatr Endocrinol Rev* 2013;10 Suppl 2:367-79.

Fig. 1. Lateral cephalograms of the six HR patients with major radiopacities posterior to the frontal bone. The radiopacities are situated intra-cranially and represent supposedly calcifications of dura mater structures. The arrows point at the radiopacities.

Fig. 2. PA cephalograms of five of the six HR patients depicted in Fig. 1. Radiographs A, D, and F: The radiopacities are widespread in the neurocranium on both sides of the midline. Radiograph B and E: The radiopacities are not visible.

Fig. 3. Lateral cephalograms of the three controls with minor radiopacities posterior to the frontal bone. The radiopacities are situated intra-cranially. The arrows point at the radiopacities.

Fig. 4. Lateral cephalograms of HR patients with examples of the radiopacities, which are described as nuchal ligament calcifications. The arrows point at the radiopacities.

Table 1. The number and the age in years according to the group (HR patients or controls) and the gender

	HR patients		Controls	
	Females	Males	Females	Males
N	24	12	26	23
Mean age (SD)	41.2 (14.6)	42.4 (18.7)	42.3 (15.4)	39.5 (15.9)
Age range	21.0-74.5	18.8-73.2	23.0-74.5	20.7-72.6

Table 2. The distribution of intra- and extra-cranial radiopacities on lateral cephalograms of 36 adult HR patients in comparison with 49 adult controls

Calcifications	HR patients N=36		Controls N=49		
	n	%	n	%	p [*]
Intracranial major	6	16.7	0	0	0.159 [**]
Intracranial minor	0	0	3	6.1	
Extra-cranial (the nuchal ligament)	18	50	10 [a]	23	0.018

N is the total number in the group

n is the number of individuals with the specified type of radiopacity

[*] *p*-values, Ficher's exact test

[**] comparison including major and minor signs of intracranial calcifications

[a] N=44.

Table 3. Characteristics regarding gender, age, treatment, skeletal severity, nuchal ligament calcifications, and vertebral enthesopathy in the six HR patients and the three controls with intracranial calcifications in relation to the inside of the frontal bone

	Subject	Gender	Age yrs	Treatment 0-18 yrs[a]	Skeletal severity[b]	Intracranial calcification[c]	Nuchal calcification[d]	Vertebral enthesopathy[e]
	1A	f	53.7	0	x	xx	0	x
	1B	f	74.5	0	x	xx	0	0
HR	1C	f	65.5	0	xx	xx	0	x
patients	1E	f	48.8	0	x	xx	0	x
	1D	f	43.2	0	x	xx	0	x
	1F	m	67.5	0	xx	xx	x	x
	3A	m	30.9	-	-	x	0	-
Controls	3B	f	78.5	-	-	x	0	-
	3C	m	27.9	-	-	x	0	-

Subject refers to cephalograms depicted in Fig. 1 and Fig. 3

[a] Treatment with phosphate and activated vitamin D in childhood. "0" no treatment

[b] The severity of the skeletal impact in HR patients (Beck-Nielsen et al., 2010). "x" mild affection, "xx" severe affection

[c] The presence of intracranial radiopacities: "0" none, "x" minor, "xx" major

[d] The presence of nuchal ligament calcifications is marked with "x"

[e] The presence of one or more sites with mineralizing enthesopathy of the collateral ligaments of the vertebral column.

Table 4. The association between intracranial or nuchal ligament calcifications and the presence of mineralizing enthesopathies related to other sites of the skeleton in 31 of 36 adult HR patients

	Intracranial calcifications			Nuchal ligament calcifications		
	Yes N=6	No N=25	p^*	Yes N=15	No N=16	p^*
Enthesopathy vertebral[**] (n=13)	5 (85%)	8 (32%)	0.059	6 (40%)	7 (44%)	>0.999
Enthesopathy all[***]						
0-1 (n=12)	1 (17%)	11 (44%)	0.226 [0.018]	6 (40%)	6 (38%)	>0.999 [0.289]
2-6 (n=9)	1 (17%)	8 (32%)		4 (27%)	5 (31%)	
≥ 7 (n=10)	4 (67%)	6 (24%)		5 (33%)	5 (31%)	

Values are number and percentage of patients in the group with the specified type of mineralizing enthesopathy

N is the total number in the group

[*] *p*-values in Ficher`s exact test. The values in brackets are *p*-value from logistic regression analysis with the assessment of the association between intracranial or nuchal ligament calcifications and the total number of sites with mineralizing enthesopathies adjusted for the effect of age, gender, and family clustering

[**] One or more sites of the vertebral column with mineralizing enthesopathy (n is the number of HR patients with this assessment)

[***] All extra-skeletal sites with mineralizing enthesopathy grouped according to the number of sites (n is the number of HR patients in the group).

Table 5. The association between the medical treatment in childhood (3-18 years of age) and intracranial calcifications, nuchal ligament calcifications, or vertebral enthesopathy in 36 adult HR patients

Treatment[*]	Intracranial calcifications			Nuchal ligament calcifications			Vertebral enthesopathy[***]		
	Yes	No	p[**]	Yes	No	p[**]	Yes	No	p[**]
	N=6	N=30		N=18	N=18		N=13	N=18	
No (n=22)	6 (100)	16 (53)		9 (50)	13 (72)		12 (92)	8 (44)	
Periodic (n=2)	0	2 (7)	0.226	1 (6)	1 (6)	0.376			0.008
Yes (n=12)	0	12 (40)		8 (44%)	4 (22)		1 (8)	10 (56)	

N is the total number in the group

Figures are absolute numbers in the group, and percentages are given in parentheses

[*] The treatment characteristics (phosphate and activated vitamin D): "no treatment", "periodic treatment", or "yes", i.e., continuous treatment during childhood

[**] p-values in Fischer's exact test

[***] Radiographs of the vertebral column were obtained in 31 patients. Five assessments were missing.

Fig. 1

Fig. 2

Fig. 3

Fig. 4